

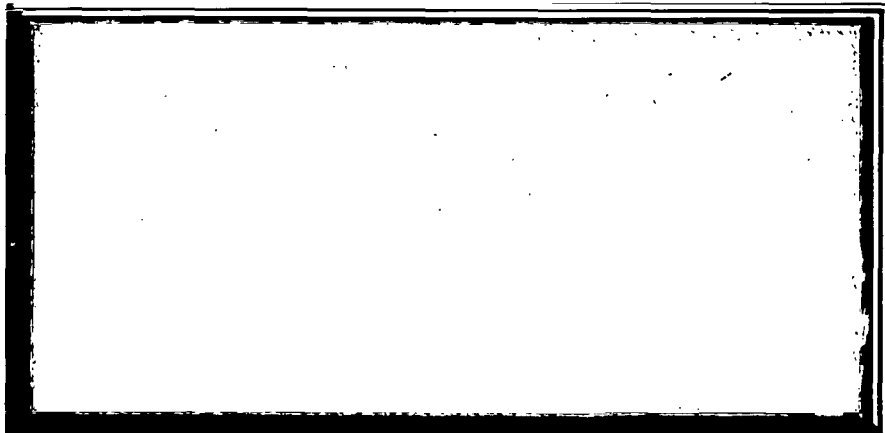
NASA CR-54257
~~NAS 2-1566~~

~~RE 638~~ ~~1-12-81~~

RE-ENTRY  SYSTEMS
DEPARTMENT

Philadelphia, Pa.

~~PERMANENT REFERENCE~~
~~PERMANENT REFERENCE~~



TECH LIBRARY KAFB, NM
0069469

~~NAS 2-1566~~



FINAL REPORT

“ANALYTICAL COMPARISONS OF

ABLATIVE NOZZLE MATERIALS”

June 20, 1963 to
November 20, 1964

Submitted Per: Contract NAS3-2566

To: NASA
LEWIS RESEARCH CENTER
CLEVELAND, OHIO

GENERAL  ELECTRIC
REENTRY SYSTEMS DEPARTMENT
3198 Chestnut Street, Philadelphia 4, Penna.

FINAL REPORT

ANALYTICAL COMPARISONS
OF
ABLATIVE NOZZLE MATERIALS

do not know

Prepared for

NATIONAL AERONAUTICS AND SPACE ADMINISTRATION

July 1, 1965

CONTRACT NAS 3-2566

Technical Management
NASA Lewis Research Center
Cleveland, Ohio
Liquid Rocket Technology Branch
E. A. Edelman

GENERAL ELECTRIC COMPANY
Re-entry Systems Department
3198 Chestnut Street
Philadelphia, Pennsylvania

NOTICE

This report was prepared as an account of Government sponsored work. Neither the United States, nor the National Aeronautics and Space Administration (NASA), nor any person acting on behalf of NASA:

- A.) Makes any warranty or representation, expressed or implied, with respect to the accuracy, completeness, or usefulness of the information contained in this report, or that the use of any information, apparatus, method, or process disclosed in this report may not infringe privately owned rights; or
- B.) Assumes any liabilities with respect to the use of, or for damages resulting from the use of any information, apparatus, method or process disclosed in this report.

As used above, "person acting on behalf of NASA" includes any employee or contractor of NASA, or employee of such contractor, to the extent that such employee or contractor of NASA, or employee of such contractor prepares, disseminates, or provides access to, any information pursuant to his employment or contract with NASA, or his employment with such contractor.

Requests for copies of this report should be referred to

National Aeronautics and Space Administration
Office of Scientific and Technical Information
Attention: AFSS-A
Washington, D. C. 20546

Abstract

A Reaction Kinetics Ablation Program was developed to analytically predict the ablation performance of rocket nozzle heat protection materials. The program was written in FORTRAN IV and made compatible with the NASA Lewis computation facilities.

The program can be used to predict the thermal degradation of a wide variety of materials exposed to an external source of heat. The program includes the effects of mass addition on heat transfer, the calculation of internal gas pressure and internal material stresses and a number of other options for surface or char removal.

The comparative performance of phenolic nylon, phenolic graphite and phenolic refracil as rocket nozzle heat protection materials was investigated. The results are reported for these materials exposed to the heating environment produced by the propellant combinations of hydrogen/oxygen and N_2O_4 /UDMH- N_2H_4 (50-50).

Acknowledgement

This program is managed by the Liquid Technology Office, Lewis Research Center, D. Bachkin and E.A. Edelman, Project Managers, and is monitored by F. Compitello in the Research, Propulsion, Liquid Office at OART.

Contribution to the technical context of this report were made by a number of individuals at General Electric Company-MSD. Overall technical direction was handled by F.E. Schultz, Consultant, System Simulation and Energy Management, Re-entry Systems Department. Project Engineer was P. B. Cline. The detailed activities were supported by the following:

Thermodynamic Considerations	Dr. S. Scala, P. Wells
Numerical Analysis	P. Gordon
Stress Considerations	E. Menkes
Computer Programming	C. Grebey

TABLE OF CONTENTS

	Page
Abstract	i
Acknowledgment	iii
Introduction	1
Summary	3
Conclusions and Recommendations	5
Discussion	7

Derivation of Thermodynamic Equations - Appendix A

Introduction	A-1
Physical Model	A-2
Equation of State	A-3
Diffusion Velocities	A-5
Momentum Equation	A-6
Continuity Equations	A-7
Energy Equation	A-11
Discussion	A-19
Boundary Conditions	A-26
Front Face Recession	A-28
Nomenclature	A-30
References	A-33

Numerical Analysis - Appendix B

Introduction	B-1
Physical Problem	B-3
Difference Equation for Heat Conduction Equation	B-13
Numerical Solution of Energy Equation and Boundary Conditions	B-33
Calculation of Density	B-53
Initial Temperature Distribution	B-65
Spacing Parameter	B-69
Procedure for Obtaining Solution	B-83
Accuracy of Program	B-85
Pressure Option	B-91
Derivation of Final Form of Partial Differential Equation (Appendix B1)	B1-1
Space Transformations Used in the Program (Appendix B2)	B2-1
Iteration Procedure (Appendix B3)	B3-1

TABLE OF CONTENTS (Cont)

	Page
Formulas Used in Numerical Approximations (Appendix B4)	B4-1
Thin Skin Option (Appendix B5)	B5-1
Terminology and Definitions (Appendix B6)	B6-1
References (Appendix B7)	B7-1
Derivation of Stress Equations - Appendix C	
Introduction	C-1
Previous Effort	C-2
Methods of Analysis	C-3
Nomenclature	C-18
References	C-21
Program Structure - Appendix D	
Introduction	D-1
User's Manual - Appendix E	
Problem Description	E-1
Flow Chart of the One Dimensional Heat Conduction Program	E-2
General Description of Input for this Problem	E-7
Sample Input Format	E-33
Restrictions	E-37
Timing	E-39
General Considerations	E-40
Error Messages	E-45
Sample Output Format	E-49
Material Properties - Appendix F	
Table F1 Approximate Material Properties for Use with REKAP for Rocket Nozzles	F-3
Application and Results - Appendix G	
References	G-3
Table G1 Summary of Material Performance	G-4
Table G2 Summary of Temperature Response	G-5

LIST OF FIGURES

Figure		Page
A1	Schematic of a Degrading Plastic and Corresponding Profile	A-36
A2	Mass Transfer Regimes for Ablating Graphite	A-37
A3	Normalized Ablation Rate of Graphite Over the Entire Range of Surface Temperature	A-38
C1	Characteristics of a Charring Ablator	C-23
C2	Mechanisms Contributing to the Surface Recession of Charring Ablators	C-24
C3	Thick Cylinder Geometry	C-25
C4	General Shell of Revolution	C-26
C5	Shear Stiffness of an Inhomogeneous Shell	C-27
C6	Conical Shell	C-28
F1	Phenolic Nylon	F-4
F2	Phenolic Refrasil	F-5
F3	Graphite Phenolic	F-6
F4	Carbon Phenolic	F-7
F5	Pyrolytic Graphite	F-8
F6	Phenolic Nylon	F-9
F7	Phenolic Refrasil	F-10
F8	Phenolic Graphite	F-11
G1	Temperature Response of Tungsten Calorimeter Within Small NASA Lewis Test Nozzle	G-8
G2	Temperature Response of Phenolic Graphite	G-9
G3	Temperature Response of Phenolic Nylon PROPELLENT: HYDROGEN- OXYGEN	G-10

LIST OF FIGURES (Cont)

Figure		Page
G4	Temperature Response of Phenolic Refrasil PROPELLENT: HYDROGEN-OXYGEN	G-11
G5	Temperature Response within Phenolic Nylon	G-12
G6	Temperature Response of Phenolic Nylon	G-13
G7	Temperature Response of Phenolic Silica	G-14

Introduction

The containment of the hot exhaust gases within a rocket nozzle presents an interesting and difficult thermodynamic problem. The temperature of the exhaust gases exceed all but the highest melting temperature materials. Therefore, it is necessary to provide some method for the thermal protection of the wall materials. With liquid propellant rocket engines, the fuel is commonly used as a coolant to maintain the wall temperature within acceptable bounds. However, the regenerative cooled nozzles are complex and difficult to manufacture, since the cooling passages must be fabricated into the walls of the nozzle. The wall thickness between the coolant and exhaust gas side must be held to a minimum, particularly for the high heat transfer rates experienced with hydrogen/fluorine.

Solid propellant rockets do not have a liquid fuel for a coolant. Therefore, another approach is desirable; one solution is to utilize an ablative heat protection system. An ablative system is one in which the wall material degrades due to being thermally heated. The degradation could involve melting, vaporization, sublimation or the pyrolysis of the material in depth. Within the degradation process, thermal energy is absorbed; in addition there is a reduction in the convective heat transfer to the surface due to the injection of mass into the boundary layer. These ablative heat protection systems may be composited of any number of materials, however, some of the more common ones are the carbons and graphites, plastics and resin impregnated materials.

The evaluation of these ablative heat protection systems has to a large extent been done empirically by actually building test nozzles and firing them. This method, although direct and accomplishes the goal of determining the performance of a given material, has the disadvantage of being costly and does not lend itself to the rapid evaluation of a number of materials in various environments. This type of trade-off activity is best done analytically. Various techniques have been investigated and used for predicting the performance of ablative materials in a heating environment. One approach is to determine the value of a quantity referred to as the effective heat of ablation from an experimental program and then apply this value to other applications. This approach is somewhat questionable if the environment is to change. A second approach is to consider the problem of material degradation in a heating environment in detail and develop analytical equations which will describe the various mechanisms and energy absorption processes taking place. This latter approach is the one considered within this report.

The Re-entry Systems Department of the General Electric Company had found that it was possible to predict the thermodynamic and chemical processes which take place when an ablative heat protection material was heated. This type of technology has been applied to the design of heat shield systems for re-entry vehicles. It was therefore the goal of this contract to develop a tool which could be used by NASA for future evaluation of rocket nozzle heat protection systems.

1. Develop a Reaction Kinetics Ablation Program (REKAP) for the purpose of predicting the performance of ablative materials and ablative systems in rocket engine environments.

2. Establish the material properties required by the REKAP Program for the evaluation of the ablative performance of a number of materials.
3. Demonstrate the usefulness of the program to predict the performance of rocket nozzle heat protection systems.
4. Modify the program as necessary to make it compatible with NASA Lewis' computing equipment.
5. Provide liaison and technical assistance to the responsible people at NASA Lewis in the use of the REKAP program.

A Reaction Kinetics Ablation Program was developed and was utilized to investigate the ablative performance of phenolic nylon, phenolic refrasil and phenolic graphite exposed to the heating environments associated with the propellant combinations of hydrogen/oxygen and N_2O_4 /UDMH- N_2H_4 . The results and discussion are included in Appendix G.

The derivation of the governing equations and the discussion of the entire program including the material properties is included in the seven appendices following the discussion.

Summary

A one-dimensional Reaction Kinetics Ablation Program was developed which would calculate the degradation and surface recession of a wide variety of materials. Five methods have been included for the control of the front face surface recession: no melting, specified char length, graphite sublimation, refracil and fixed melting temperature. The program includes the oxidation and sublimation of graphite, the effects of mass addition on heat transfer, the melting or vaporization of surface material, the calculation of internal gas pressure and the calculation of pressure, and thermally induced stresses. Although the equations describing the oxidation and sublimation of an ablative heat protection material are correlated only for graphite or carbonaceous chars exposed to air; they are general and may be applied to other materials provided the appropriate constants are available. The following assumptions were made during the development of the program:

1. Darcy's Law gives an adequate representation of the flow of ablation gases through the porous char.
2. The decomposition of the plastic material may be analytically expressed by the Arrhenius rate equation.
3. The ablation gases do not react with the char to change its final density.
4. The solid and the gases at a given point are in intimate contact and that their temperatures are equal.
5. The char material is an elastic, isotropic, nonhomogeneous porous material.

The above, are the major underlying assumptions for the equations derived in Appendices A and C. The general equations derived can be simplified still further by several additional assumptions such as:

1. The ablation gases are in local thermochemical equilibrium.
2. The problem of interest can be reduced to a one-dimensional situation.
3. The gas passing through a given element in a given period is the gas produced by all elements interior to the studies element during the same time period.
4. The mechanical work terms are negligible in comparison to the thermal terms in the energy equation.

The validity of some of the assumptions can only be determined upon examining the particular problem under investigation; for an example, if there is an extensive amount of axial heat conduction, the assumption of one dimensional heat transfer and the flow of gases may not hold. A detailed discussion of each of the above assumptions is included in Appendix A or C.

The capabilities and limitations of the developed REKAP program are:

1. The nozzle heat protection system can be composed of 10 layers each being a different material, however, the thermal degradation is limited to the first layer.
2. The time varying heating environment (recovery temperature or enthalpy, convective film coefficient and hot gas radiation) must be provided.
3. The initial temperature and density distribution must be uniform throughout all layers; normally that of the virgin material.
4. The surface loss mechanism of materials due to oxidation and sublimation has been calibrated only for graphitic materials within air.
5. Heat loss from the backface may be specified either by temperature or heat flux.
6. The program will calculate the temperature distribution throughout the 10 layers, material density and ablation gas density as a function of time and position within a flat or cylindrical body. The flow of gases and thermal energy is limited to one dimension.
7. Surface recession by melting and vaporization is included within the program.

Although these limitations are now in the basic program, any of them can be eliminated without introducing major changes into the program except for extending the program to three dimensions.

The computed surface recession, char thickness and temperature response for three small NASA Lewis hydrogen/oxygen test nozzles were in fair agreement with the experimental data when the proper driving temperatures were used. The initial results were calculated using the combustion gases recovery temperature. An analysis of calorimeter data was made and it was found that 3100°F was a more realistic driving temperature. The surface recession and char thickness of 2 test runs using N_2O_4 and UDMH- N_2H_4 as the propellants were also compared and found to be in reasonable agreement.

The material properties for phenolic nylon, phenolic refracil, phenolic graphite, phenolic carbon and pyrolytic graphite are given in Appendix F.

Conclusions and Recommendations

The performance of thermal protection systems for rocket nozzles can be analytically evaluated. A 7094 computer program was developed which can be used to study a number of material systems exposed to a wide variety of heating environments quickly and inexpensively.

The computed material degradation and temperature response cannot be any better than the heating environment and the thermochemical properties provided to the program. The parameters which have been found to be the most important are the thermal conductivity, primarily that of the char, and the recovery temperature or enthalpy. This is not to imply that the other parameters are not important but that the degradation and temperature response is less sensitive to them.

The results of the analysis of phenolic nylon, phenolic refrasil and phenolic graphite indicated that for a 17 to 20 second exposure that phenolic refrasil had the least surface recession, followed by phenolic graphite and then phenolic nylon. The predicted surface recession for phenolic nylon was 0.0514 inches after only a 17.3 second exposure to a heating environment produced by the combustion of hydrogen/oxygen in the small NASA Lewis rocket nozzle test chamber.

In addition to the surface recession the temperature response and char growth were computed; however, as a measure of the performance of a material within a rocket nozzle it is felt that the recession rate is the most important.

Having developed an analytical method for the prediction of the performance of heat protection systems, it is recommended that the usefulness of the program be increased by completing the following tasks:

1. Include a rocket nozzle heat transfer calculation procedure within the program. Therefore, the changes in operating pressure, characteristic velocity and geometry would be reflected in the heat transfer to the nozzle walls.
2. Modify the program to calculate charring in more than one layer. This would simplify the calculations for nozzle inserts.
3. Extend the surface reaction option to include more than just the oxidation of graphite in air.
4. A detailed investigation should be made of the effects of curtain cooling and its influence on the recovery temperature or enthalpy and the convective film coefficient.
5. The material properties for the actual material with which NASA Lewis is working should be determined.

6. Develop a multi-dimensional REKAP program which will compute the axial heat conduction as well the radial heat transfer. Included within this program could be a liquid layer routine which would account for the absorption and blocking of the heat transfer due to the flow of a liquid layer along the walls of a rocket nozzle.

The final program resulting from the completion of these tasks would be one which would do the complete evaluation of the thermal protection system of a rocket nozzle including the combustion chamber, throat and nozzle skirt at one time.

Discussion

The discussion of the various aspects of the work done on this contract are included in the seven appendices which follow. The derivation and discussion of the governing thermodynamic equations and boundary conditions are included in Appendix A. The numerical considerations required for solving the equation is discussed in detail in Appendix B. The derivation and discussion of the stresses produced by temperature and pressure gradients within a heat protection material is described in Appendix C. A description and flow diagram of each of the subroutines in the REKAP program is given in Appendix D. The user's manual giving detailed instruction on the use of program is given in Appendix E. A listing of the thermochemical properties for phenolic nylon, phenolic refrasil, phenolic graphite, phenolic carbon and pyrolytic graphite is included in Appendix F. A discussion of the data generated on this contract is also included. The last section (Appendix G) describes the application and the performance results obtained from the REKAP analysis of phenolic graphite, phenolic refrasil and phenolic nylon exposed to the heating environment produced by hydrogen/oxygen and N_2O_4 /UDMH- N_2H_4 .

APPENDIX A

DERIVATION OF THE THERMODYNAMIC EQUATIONS

INTRODUCTION

In this appendix, the thermal energy equation is derived for a thermosetting plastic. Consideration is given first to the general three-dimensional case. Simplifications are then introduced to obtain an equation which reasonably satisfies the physical model.

The philosophy of this derivation is to start from fundamental physical principles and to utilize the concepts of continuum mechanics to proceed in a step-by-step fashion, listing all assumptions.

Figure A1 shows a cross section of the ablation model considered in this study. Initially, the outer boundary coincides with the broken line as indicated. The ambient temperature is low enough so that no chemical reactions occur within the plastic. Furthermore, the outer boundary temperature is the same as its surroundings and, therefore, radiation to or from the front face is zero.

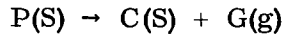
Convective and radiative heat fluxes (arbitrary with time) are impressed on the outer boundary. As a consequence of thermal conduction, laminates of the plastic near the outer boundary increase in temperature and the front face begins to radiate heat. In time, the hotter laminates undergo a chemical reaction which converts the virgin plastic into hydrocarbon gas and a porous char residue.

The gas pressure within the porous char increases as the virgin material undergoes chemical reaction. As a consequence, a pressure profile is established throughout the porous region causing the gas to flow to adjacent pores of lower pressure. In general, the gas flow will be to the outer boundary and result in thermal energy being introduced due to friction. Heat transfer will occur between char and gas if their respective temperatures are different. Varying temperature or pressure changes, or any combination of these two conditions, can result in chemical changes in the gas (cracking or recombination), which will absorb or generate thermal energy. As the gas passes the outer boundary, a portion of the convective heat flux is blocked. As more and more heat enters the front face, reacting laminates will completely de-gas, thus forming a char layer while moving the reaction zone deeper into the body. And, of course, the outer boundary moves as a result of structural failure, oxidation, or both. If the outer boundary temperature becomes high enough, the char layer will either melt or be vaporized.

The problem at hand is to derive a mathematical expression that reasonably satisfies the physical model described and is applicable to any point within the boundary. Furthermore, the expression must be amenable to programming on the IBM 7094 Digital Computer for the solution of practical problems. The problem is formidable but not impossible.

Physical Model

The physical model is that of a multicomponent flow of chemically reacting gases through a porous media which is itself undergoing chemical reactions. The ablation material consists of unreacted solid (denoted by subscript p), which decomposes to a porous solid (subscript C) and gaseous products of reaction (subscript g). The decomposition process can be schematically represented as:



Before decomposition begins, the ablation material consists solely of unreacted solid. After the process has gone to completion, only solid and gaseous products of reaction exist.

All densities are based on the same unit reference volume of the mixture (solid and gas). Consequently, as the decomposition proceeds at a given location, ρ_p decreases from some initial value to zero while P_C is simultaneously increasing from zero to some final value.

The gaseous ablation products are formed by the decomposition of the unreacted solid material. They are a mixture of many different chemical species which flow and diffuse through the porous solid. The various species may react with one another in the gas phase resulting in the familiar "cracking" effect. They may also react with the surrounding solid material, causing a reduction (or increase) in solid density.

In order to validly apply continuum theory to a porous media, all quantities are presumed to be suitably averaged over a small area - small with respect to the macroscopic dimensions of the material but large with respect to pore size. It is assumed that the ratio of pore area to total area is the same as that of pore volume to total volume, the latter quantity being the definition of porosity.

The solid species remain stationary as the displacements due to thermal expansion, a stress field and/or changes in molecular structure are generally negligible. All species are considered to be pure substances. External body forces (e.g. gravity) have been neglected as they are small for all practical applications.

Equations of State

The caloric equation of state for each solid specie is assumed to be of the form:

$$e_p = e_p(T) \qquad e_c = e_c(T)$$

Thus, for any process:

$$e_p = \int_{T_R}^T C_{vp} dT + \left(e_{F_p} \right)_{T_R} \quad (1)$$

$$e_c = \int_{T_R}^T C_{vc} dT + \left(e_{F_c} \right)_{T_R} \quad (2)$$

The internal energy accounts for thermal and chemical energy. The solid species do not have a thermal equation of state as their densities are determined by the application of non-equilibrium reaction kinetics.

The gaseous products are assumed to be a mixture of chemical reacting perfect gases. Thus, the thermal and caloric equations of state for each specie are:

$$P_i = \rho_i \frac{R}{M_i} T \quad (3)$$

$$e_i = \int_{T_R}^T C_{vi} dT + \left(e_{Fi} \right)_{T_R} \quad (4)$$

$$h_i = \int_{T_R}^T C_{pi} dT + \left(e_{Fi} \right)_{T_R} \quad (5)$$

Note that P_i and ρ_i are partial quantities which are based on a reference volume of the entire mixture (solid plus gas).

For the gaseous mixture as a whole, we have (assuming Dalton's Law of Partial Pressures is valid):

$$P = \rho \frac{R}{M_g} T \quad (6)$$

$$M_g = \frac{1}{\sum_i K_i \frac{\rho_i}{M_i}} \quad K_i = \frac{\rho_i}{\rho} \quad (7)$$

$$e_g = \sum_i K_i e_i \quad (8)$$

$$h_g = \sum_i K_i h_i \quad (9)$$

Note that these assumptions imply that pressure, stress, chemical reactions, etc. have a negligible effect on the specific internal energy of each species. Obviously, they do affect the amount of each species present at a given location and thus they do effect the total energy.

Diffusion Velocities

In the flow of multicomponent gases, diffusion currents are generated by gradients in concentration, pressure and temperature. For the present problem, pressure and thermal diffusion effects should be small and so they are neglected. The velocity of the i th species relative to a fixed coordinate system is defined as \vec{V}_i . The mass-averaged or observable velocity of the total gas flow is defined as:

$$\vec{V} = \frac{1}{\rho_g} \sum_i \rho_i \vec{V}_i$$

The diffusional velocity of the i th species (\vec{V}_{d_i}) is defined as the velocity of the i th species relative to the mass-averaged velocity.

$$\vec{V}_{d_i} = \vec{V}_i - \vec{V}$$

Note that:

$$\sum_i \rho_i \vec{V}_{d_i} = \sum_i \rho_i \vec{V}_i - \sum_i \rho_i \vec{V}$$

$$\therefore \sum_i \rho_i \vec{V}_{d_i} = \rho_g \vec{V} - \rho_g \vec{V} = 0$$

To summarize, the absolute velocity of the i th species is given by the vector sum of the mean flow velocity and the diffusional velocity of the i th species, and the mass averaged diffusional velocity is zero.

$$\vec{V}_i = \vec{V} + \vec{V}_{d_i}$$

$$\sum_i \rho_i \vec{V}_{d_i} = 0 \quad (10)$$

For ordinary concentration diffusion in a multicomponent gas, a first order approximation for \vec{V}_{d_i} is that it depends linearly upon the concentration gradients of all species. For a mixture of perfect gases (p. 569, Reference 4):

$$\rho_i \vec{V}_{d_i} = \frac{n}{\rho_g} \sum_{j \neq i} M_i M_j P_{ij} \nabla X_j$$

Use of this equation results in a formidable mathematical problem to determine the composition of the mixture. Also, since we are dealing with transport phenomena in a porous

media, its accuracy is not assured. It has been noted by Von Karman (Ref. 1) that "... the process in a multicomponent mixture is so complicated that one mostly uses an approximation by considering the diffusion between one appropriately chosen component and the mixture of the rest replaced by a homogeneous gas of average characteristics", i.e., an effective binary mixture insofar as diffusion is concerned.

With this approximation, the diffusion velocity is related to the mass concentration by Fick's Law:

$$\rho_i \vec{V}_{d_i} = - \rho_g D_{12} \nabla K_i \quad (11)$$

The concept of an effective binary mixture would be a useful starting point in accounting for the effects of diffusion. Probably the largest error in this approximation is that the diffusion coefficient for each specie is the same.

Momentum Equation

Experimental evidence for the flow of a gas through a porous media indicates that the usual momentum equation of fluid mechanics does not apply (e.g. Reference 9). Consequently, it must be replaced by an empirical relationship between velocity and pressure. For the flow of a homogeneous gas through a porous media at low velocities, Darcy's Law is reasonably accurate (Reference 9). Very little is known about the present case of chemically reacting flow through a media of variable porosity. It will be assumed that Darcy's Law gives an adequate representation for the present problem, although other forms could be used if desired. Thus:

$$\vec{V} = - \nabla \frac{k}{\mu} P \quad (12)$$

where k is the permeability of the charring material and μ is the viscosity of the ablation gases. These quantities are normally determined by experiments.

Continuity Equations

The principal of conservation of mass as applied to the i th gaseous specie within a stationary control volume says that the rate at which mass is accumulated within the volume equals the rate at which mass is transported out by convection and diffusion plus the net rate of production due to chemical reaction. The mathematical statement of this is:

$$\frac{d}{dt} \int_V \rho_i dV = - \int_A \rho_i \left(\vec{V} + \vec{V}_{d_i} \right) \cdot \vec{n} dA + \int_V \dot{W}_i dV \quad (13)$$

Here, \dot{W}_i is the net amount of specie i produced per unit volume per unit time. Note that \dot{W}_i includes the formation of the species from the unreacted solid as well as any further gas phase or gas-solid phase reactions that might occur.

The surface integral involved in (13) can be transformed into a volume integral by means of the Divergence Theorem*:

$$\int_A \rho_i \left(\vec{V} + \vec{V}_{d_i} \right) \cdot \vec{n} dA = \int_V \nabla \cdot \rho_i \left(\vec{V} + \vec{V}_{d_i} \right) dV$$

The order of integration and differentiation can be interchanged* so that:

$$\frac{d}{dt} \int_V \rho_i dV = \int_V \frac{\partial \rho_i}{\partial t} dV$$

Substituting these relations into (13) yields:

$$\int_V \left[\frac{\partial \rho_i}{\partial t} + \nabla \cdot \rho_i \left(\vec{V} + \vec{V}_{d_i} \right) - \dot{W}_i \right] dV = 0$$

Since the volume is arbitrary, the integrand must be identically zero. Thus, the species continuity equation is:

$$\frac{\partial \rho_i}{\partial t} + \nabla \cdot \rho_i \left(\vec{V} + \vec{V}_{d_i} \right) = \dot{W}_i \quad (14)$$

* It is assumed that all functions are continuous and continuously differentiable and that the region is simply connected (Reference 6).

Summing this equation over all gaseous species and noting that

$$\sum_i \rho_i \vec{V}_{d_i} = 0: \sum_i \rho_i = \rho_g : \sum_i \dot{W}_i = \dot{W}_g$$

results in the continuity equation for the gas:

$$\frac{\partial \rho_g}{\partial t} + \nabla \cdot \rho_g \vec{V} = \dot{W}_g \quad (15)$$

Now, gas phase reactions do not change the total mass of gas present; rather, they redistribute the species. Therefore, $\dot{W}_g = \sum_i \dot{W}_i$ is the total rate at which gas is being produced by the decomposition of the unreacted material and by gas-solid phase reactions.

The continuity equations for the solid species are:

$$\frac{\partial \rho_p}{\partial t} = \dot{W}_p \quad (16)$$

$$\frac{\partial \rho_c}{\partial t} = \dot{W}_c \quad (17)$$

\dot{W}_p is the rate of depletion of the unreacted material due to decomposition. For charring ablation materials, the decomposition is irreversible and the rate at which it proceeds is generally limited by chemical kinetics. \dot{W}_p is deduced from TGA (thermogravimetric analysis) experiments and is often expressed analytically as a single nth order reaction with an Arrhenius "rate constant".

$$\dot{W}_p = -A (\rho_p)^n$$

$$A = A_o \exp \left(- \frac{E}{RT} \right)$$

\dot{W}_c is the rate at which char is formed from the decomposition of the unreacted material (generally a known fraction of \dot{W}_p) plus gas-solid phase reactions. There is no overall production of mass so that:

$$\dot{W}_p + \dot{W}_c + \dot{W}_g = 0 \quad (18)$$

It is useful to separate out the mass production rates due to the decomposition, the gas phase reactions, and the gas-solid phase reactions. This can be done by introducing some new quantities.

$$\dot{W}_c = -f_c \dot{W}_p + \dot{W}_c'' \quad (19)$$

$$\dot{W}_g = -(1-f_c) \dot{W}_p + \dot{W}_g'' \quad (20)$$

Here f_c denotes the fraction of unreacted material which forms char (not necessarily constant) and the superscript double prime denotes gas-solid phase reactions only. The first part of these equations state that char and gas are produced from the decomposition of the unreacted material, while the second part accounts for additional formation due to gas-solid phase reactions. Note that

$$\dot{W}_g'' = -\dot{W}_c'' \quad (21)$$

which follows from (18).

Finally, the species continuity equation can be expressed in terms of gas phase reactions only. Using $\rho_i = K_i \rho_g$ and the chain rule on (14) yields:

$$K_i \left[\frac{\partial \rho_g}{\partial t} + \nabla \cdot \rho_g \nabla \right] + \rho_g \left[\frac{\partial K_i}{\partial t} + \mathbf{V} \cdot \nabla K_i \right] + \nabla \cdot \left(\rho_g \mathbf{V}_{d_i} K_i \right) = \dot{W}_i$$

The first term in brackets equals \dot{W}_g by virtue of (15) and so:

$$\rho_g \left[\frac{\partial K_i}{\partial t} + \mathbf{V} \cdot \nabla K_i \right] + \nabla \cdot \left(\rho_g K_i \mathbf{V}_{d_i} \right) = \dot{W}_i' \quad (22)$$

Where:

$$\dot{W}_i' = \dot{W}_i - K_i \dot{W}_g \quad (23)$$

\dot{W}_i' is the net rate of production of the i th species minus the amount of the i th species formed by the decomposition of the unreacted material plus gas-solid phase reactions. Consequently, \dot{W}_i' is the net rate of production due to gas phase reactions only. Note that:

$$\sum_i \dot{W}_i' = 0$$

In general, the \dot{W}_i' are functions of temperature, pressure and composition and are determined from a knowledge of the exact chemical reactions (and these rates) which occur. For very slow reactions in the gas phase (i. e. , "frozen-flow"), the $\dot{W}_i' = 0$. For very fast reactions, the flow will be in local thermochemical equilibrium and the \dot{W}_i' are determined by imposing constraints on the composition (i. e. , equilibrium "constants").

Energy Equation

The energy equation is derived by applying the First Law of Thermodynamics to a stationary control volume within the material. This means that the time rate of change of the total energy within the volume equals the rate at which energy is transported into the volume minus the rate at which energy is being convected out plus the rate at which work is being done on the volume. The mathematical expression is

$$\begin{aligned} \frac{d}{dt} \int_V \left[\rho_p e_p + \rho_c e_c + \sum_i \rho_i \left(e_i + \frac{\vec{v} \cdot \vec{v}}{2} \right) \right] dV = - \int_A \vec{Q} \cdot \vec{n} dA \\ - \int_A \left[\sum_i \rho_i \vec{v} \left(e_i + \frac{\vec{v} \cdot \vec{v}}{2} \right) \cdot \vec{n} \right] dA + \int_A \vec{P} \cdot \vec{v} dA \end{aligned} \quad (24)$$

The energy flux vector \vec{Q} may be expressed in terms of contributions due to heat conduction, thermal radiation and diffusion (References 2-4):

$$\vec{Q} = \vec{q}_c + \vec{q}_R + \sum_i \rho_i \vec{v}_i h_i$$

It now remains to relate the heat flux vectors and the surface force per unit area to the variables of the problem. Since the solid and the gas are in intimate contact, it is assumed that the temperature of the gas equals that of the solid. The conduction heat flux vector is approximately linearly dependent upon the temperature gradients. For an isotropic material* this implies

$$\vec{q}_c = -K \nabla T$$

which is Fourier's Law.

For an isotropic material, the heat flux depends upon temperature gradients through a second order conductivity tensor. In rectangular cartesian coordinates, this is (p. 38, Reference 7):

$$\vec{q}_c = K_{ij} \frac{\partial T}{\partial x_j} \vec{e}_i \quad (25)$$

* Isotropic material - media whose structure and properties in the neighborhood of any point are the same relative to all directions through the point (p. 6, Ref. 7)

For example, the ablation material may be somewhat anisotropic due to fiber-type fillers in the solid material or because of the changes in composition. *

For the purposes of the present analysis, the material will be considered isotropic although it is noted that it would be easy to include (25) in the analysis should sufficient data be available to justify it. Thus, the conduction heat flux vector is related to the temperature by:

$$\vec{q}_c = -K \nabla T \quad (26)$$

Note that the conductivity will be a weighed average of the conductivities of all species that are present, both solid and gas.

In general, the radiation heat flux vector accounts for the net effect of emission, absorption and scattering of thermal radiation of all wavelengths within the material. It is usually assumed that scattering is negligible, the material is isotropic and that the optical properties do not depend on the wavelength. Even with these drastic assumptions, the calculation of \vec{q}_R is quite complex. Thus, for practical calculations, \vec{q}_R is usually neglected and the transport of thermal radiation is approximately accounted for by an increase in thermal conductivity with temperature.

The surface force per unit area can be related to the stresses by considering the forces acting on a small tetrahedron (p. 101, Reference 8).

$$\vec{P} = \vec{n} \cdot \underline{T}$$

\vec{n} is an outward unit normal and \underline{T} is a second order stress tensor whose components are σ_{ij} .

Note that this is a dot product of a vector with a tensor and the result is a vector which is different than \vec{n} , both in magnitude and direction. Using indicial notation, the surface force would be expressed as:

$$\vec{P} = \sigma_{ij} n_i \vec{e}_j$$

The required work term is:

$$\vec{P} \cdot \vec{V} = (\vec{V} \cdot \underline{T}) \cdot \vec{n}$$

The stress tensor may be separated into a hydrostatic pressure component (a scalar) and a viscous stress tensor.

$$\underline{T} = -P + \underline{\tau}$$

* An excellent example of an anisotropic material of current interest is pyrolytic graphite but since it does not decompose in depth it is not pertinent to the present problem.

For a linear isotropic fluid, the viscous stresses are linearly related to the velocity gradients. For the purposes of this analysis, the viscous stresses will be retained in the general form of $\underline{\tau}$. The final form of the work term is then:

$$\vec{P} \cdot \vec{V} = - (p \vec{V}) \cdot \vec{n} + (\vec{V} \cdot \underline{\tau}) \cdot \vec{n}$$

Substituting (26) and (27) into (24) and following exactly the same procedure as with the species continuity equation results in the differential energy equation:

$$\begin{aligned} \frac{\partial}{\partial t} \left[\rho_p e_p + \rho_c e_c + \sum_i \rho_i \left(e_i + \frac{\vec{V} \cdot \vec{V}}{2} \right) \right] + \nabla \cdot \left[\sum_i \rho_i \vec{V} \left(e_i + \frac{\vec{V} \cdot \vec{V}}{2} \right) \right] \\ + \nabla \cdot \left[\sum_i \rho_i \vec{V}_{d_i} h_i \right] = \nabla \cdot K \nabla T - \nabla \cdot \vec{q}_R - \nabla \cdot p \vec{V} + \nabla \cdot (\vec{V} \cdot \underline{\tau}) \end{aligned} \quad (28)$$

The various terms of the energy equation can be expanded and rearranged to a more convenient form. Adding the term $\frac{\partial p}{\partial t} + \nabla \cdot p \vec{V}$ to both sides of (28) and using Dalton's Law gives:

$$\begin{aligned} \frac{\partial}{\partial t} \left[\rho_p e_p + \rho_c e_c + \sum_i \rho_i \left(e_i + \frac{p_i}{\rho_i} + \frac{\vec{V} \cdot \vec{V}}{2} \right) \right] \\ + \nabla \cdot \left[\sum_i \rho_i \vec{V} \left(e_i + \frac{p_i}{\rho_i} + \frac{\vec{V} \cdot \vec{V}}{2} \right) \right] + \nabla \cdot \left[\sum_i \rho_i \vec{V}_{d_i} h_i \right] \\ = \nabla \cdot K \nabla T - \nabla \cdot \vec{q}_R + \frac{\partial p}{\partial t} + \nabla \cdot (\vec{V} \cdot \underline{\tau}) \end{aligned} \quad (29)$$

Noting that

$$h_i = e_i + \frac{p_i}{\rho_i} \quad ; \quad \rho_g = \sum_i \rho_i$$

and using the chain rule, (29) can be expanded to:

$$\begin{aligned} \left[\rho_p \frac{\partial e_p}{\partial t} + e_p \frac{\partial \rho_p}{\partial t} + \rho_c \frac{\partial e_c}{\partial t} + e_c \frac{\partial \rho_c}{\partial t} + \sum_i \left(\rho_i \frac{\partial h_i}{\partial t} + h_i \frac{\partial \rho_i}{\partial t} \right) \right. \\ \left. + \frac{\partial}{\partial t} \left(\rho_g \frac{\vec{V} \cdot \vec{V}}{2} \right) \right] + \left[\sum_i \left(\rho_i \left(\vec{V} + \vec{V}_{d_i} \right) \cdot \nabla h_i + h_i \nabla \cdot \rho_i \left(\vec{V} + \vec{V}_{d_i} \right) \right) \right] \\ + \nabla \cdot \rho_g \vec{V} \frac{\vec{V} \cdot \vec{V}}{2} = \nabla \cdot K \nabla T - \nabla \cdot \vec{q}_R + \frac{\partial p}{\partial t} + \nabla \cdot (\vec{V} \cdot \underline{\tau}) \end{aligned} \quad (30)$$

Noting that the temperature of the gas equals that of the solid, differentiating the caloric equations of state, (1), (2) and (5) yields:

$$\begin{aligned}\frac{\partial e_p}{\partial t} &= C_{v_p} \frac{\partial T}{\partial t} & \frac{\partial h_i}{\partial t} &= C_{p_i} \frac{\partial T}{\partial t} \\ \frac{\partial e_c}{\partial t} &= C_{v_c} \frac{\partial T}{\partial t} & \nabla h_i &= C_{p_i} \nabla T\end{aligned}$$

Substituting these relations into (30) and rearranging terms gives

$$\begin{aligned}& \left[\rho_p C_{v_p} + \rho_c C_{v_c} + \sum_i \rho_i C_{p_i} \right] \frac{\partial T}{\partial t} + \left[e_p \frac{\partial \rho_p}{\partial t} + e_c \frac{\partial \rho_c}{\partial t} + \sum_i h_i \left(\frac{\partial \rho_i}{\partial t} \right. \right. \\& \quad \left. \left. + \nabla \cdot \rho_i \left(\vec{V} + \vec{V}_{d_i} \right) \right) \right] + \left[\sum_i \rho_i C_{p_i} \left(\vec{V} + \vec{V}_{d_i} \right) \cdot \nabla T = \nabla \cdot K \nabla T - \nabla \cdot \vec{q}_R \right. \quad (31) \\& \quad \left. + \frac{\partial \rho}{\partial t} + \nabla \cdot (\vec{V} \cdot \vec{\tau}) - \left[\frac{\partial}{\partial t} \left(\rho_g \frac{\vec{V} \cdot \vec{V}}{2} \right) + \nabla \cdot \left(\rho_g \vec{V} \frac{\vec{V} \cdot \vec{V}}{2} \right) \right] \right]\end{aligned}$$

The second and eighth terms can be simplified by use of the continuity equations. Using (14), (16) and (17), the second term becomes

$$\left[\cdot \cdot \cdot \right] = e_p \dot{W}_p + e_c \dot{W}_c + \sum_i h_i \dot{W}_i$$

Using (23), this last term is:

$$\sum_i \dot{W}_i h_i = \sum_i \dot{W}'_i h_i + \dot{W}_g h_g$$

From (19), (20), and (21) we have:

$$\begin{aligned}\dot{W}_c &= -f_c \dot{W}_p + \dot{W}_c'' \\ \dot{W}_g &= -(1 - f_c) \dot{W}_p + \dot{W}_g'' \\ \dot{W}_g'' &= -\dot{W}_c''\end{aligned}$$

Combining these relations, the final form of the second term of (31) is:

$$[\dots] = -\dot{W}_p \left[(1 - f_c) h_g + f_c e_c - e_{vp} \right] + \sum_i \dot{W}_i' h_i - \dot{W}_c'' (h_g - e_c) \quad (32)$$

The eighth term of (31) can be expanded to:

$$[\dots] = \frac{\vec{V} \cdot \vec{V}}{2} \left[\frac{\partial \rho_g}{\partial t} + \nabla \cdot \rho_g \vec{V} \right] + \rho_g \left[\frac{\partial}{\partial t} \left(\frac{\vec{V} \cdot \vec{V}}{2} \right) + \vec{V} \cdot \nabla \left(\frac{\vec{V} \cdot \vec{V}}{2} \right) \right]$$

Using (15), the final form of the eighth term is:

$$[\dots] = \frac{\vec{V} \cdot \vec{V}}{2} \dot{W}_g + \rho_g \left[\frac{\partial}{\partial t} \left(\frac{\vec{V} \cdot \vec{V}}{2} \right) + \vec{V} \cdot \nabla \left(\frac{\vec{V} \cdot \vec{V}}{2} \right) \right] \quad (33)$$

Substituting (32) and (33) into (31) yields a final form of the energy equation.

Storage

$$\left(\rho_p C_{v_p} + \rho_c C_{v_c} + \rho_g \bar{C}_{p_g} \right) \frac{\partial T}{\partial t}$$

I

Decomposition

Cracking

Gas-solid phase reaction

$$- \dot{W}_p \left[(1 - f_c) h_g + f_c e_c - e_p \right] + \sum \dot{W}_i h_i - \dot{W}_c'' (h_g - e_c)$$

II

III

IV

Convection

Diffusion

$$\rho_g \bar{C}_{p_g} \vec{V} \cdot \nabla T + \sum_i \rho_i C_{p_i} \vec{V}_{d_i} \cdot \nabla T$$

V

VI

Heat Conduction

Thermal Radiation

Pressure

Kinetic Energy

$$= \nabla \cdot K \nabla T - \nabla \cdot \vec{q}_R + \frac{\partial P}{\partial t} + \frac{\vec{V} \cdot \vec{V}}{2} \dot{W}_g$$

VII

VIII

IX

X

$$+ \left[\nabla \cdot (\vec{V} \cdot \tau) - \rho_g \left\{ \frac{\partial}{\partial t} \left(\frac{\vec{V} \cdot \vec{V}}{2} \right) + \vec{V} \cdot \nabla \left(\frac{\vec{V} \cdot \vec{V}}{2} \right) \right\} \right] \quad (34)$$

XI

Summary of Equations

Energy Equation

$$\begin{aligned}
 & \left(\rho_p C_{v_p} + \rho_c C_{v_c} + \rho_g \bar{C}_{p_g} \right) \frac{\partial T}{\partial t} - \dot{W}_p \left[(1 - f_c) h_g + f_c e_c - e_p \right] \\
 & + \sum_i \dot{W}_i' h_i - \dot{W}_c'' (h_g - e_c) + \rho_g \bar{C}_{p_g} \vec{V} \cdot \nabla T + \sum_i \rho_i \vec{V}_{d_i} h_i \cdot \nabla T \\
 & = \nabla \cdot K \nabla T - \vec{q}_R + \frac{\partial P}{\partial t} + \frac{\vec{V} \cdot \vec{V}}{2} \dot{W}_g + \nabla \cdot (\vec{V} \cdot \underline{\tau}) \\
 & - \rho_g \left\{ \frac{\partial}{\partial t} \left(\frac{\vec{V} \cdot \vec{V}}{2} \right) + \vec{V} \cdot \nabla \left(\frac{\vec{V} \cdot \vec{V}}{2} \right) \right\}
 \end{aligned} \tag{35}$$

Species Continuity

$$\rho_g \left(\frac{\partial K_i}{\partial t} + \vec{V} \cdot \nabla K_i \right) + \nabla \cdot \left(\rho_i \vec{V}_{d_i} \right) = \dot{W}_i' \tag{36}$$

Continuity

$$\frac{\partial \rho_g}{\partial t} + \nabla \cdot \rho_g \vec{V} = - (1 - f_c) \dot{W}_p - \dot{W}_c'' \tag{37}$$

$$\frac{\partial \rho_p}{\partial t} = \dot{W}_p \tag{38}$$

$$\frac{\partial \rho_c}{\partial t} = - f_c \dot{W}_p + \dot{W}_c'' \tag{39}$$

The various terms of this equation are identified as:

- I energy storage
- II energy absorbed due to the decomposition of the solid
- III energy absorbed due to gas phase reactions (i.e. cracking)

- IV energy absorbed due to gas-solid phase reactions
- V energy transfer due to convection
- VI energy transfer due to diffusion
- VII energy transfer due to heat conduction
- VIII energy transfer due to thermal radiation
- IX rate of work associated with the pressure
- X kinetic energy associated with gas formation
- XI rate of work associated with the viscous stresses and kinetic energy

The "heat of decomposition" appears in term II.

$$h_{gf} = (1 - f_c) h_g + f_c e_c - e_{vp}$$

If the usual momentum equation could be used to simplify term XI, it would reduce to the familiar work of pressure forces plus the work of viscous forces (i.e. $V \cdot \nabla_p + \Phi$ where Φ is the dissipation function).

State

$$P = \rho_g \frac{R}{M_g} T \quad (40)$$

Momentum

$$\vec{V} = -\frac{k}{\mu} \nabla P \quad (41)$$

Diffusion (binary mixture approximation)

$$\rho_i \vec{V}_{d_i} = -\rho_g D_{12} \nabla K_i \quad (42)$$

Neglecting \mathcal{T} and q_R , there are $6 + 2(N-1)$ equations for the following physical variables (N is the total number of gaseous species):

$$T, \rho_p, \rho_c, \rho_g, P, \vec{V}, \vec{V}_{d_i}, K_i$$

These equations require that the following material properties ($10 + 4N$ in all) be known functions of the variables.

$$C_{v_p}, e_p, \dot{W}_p$$

$$C_{v_c}, e_c, f_c, \dot{W}_c''$$

$$C_{p_i}, h_i, \dot{W}_i', M_i$$

$$K, \frac{k}{\mu}, D_{12}$$

Discussion

The equations developed so far represent a quite general physical model of charring ablation. They account for the simultaneous transfer of energy and mass within a solid material of variable porosity which is decomposing. The ablation gases may be flowing, diffusing, reacting with themselves or reacting with the char and they are not necessarily in local thermochemical equilibrium.

It is generally desirable to invoke further physical assumptions in order to simplify the mathematical analysis and to reduce the number of required material properties, which are often not known. Several of these assumptions will now be discussed.

Two approaches will be described for the simplification of the general equations derived above. One approach to the problem is to simplify the gas chemistry while retaining the gas dynamical features. The ultimate end in this approach is to assume that the gas contains only a single specie. Note that this assumption does not exclude gas-solid phase reactions. Thus, we have $\vec{V}_{di} = 0$, $\dot{W}_i = 0$ and the species continuity equation is superfluous. Neglecting the radiant flux and using the definitions of \dot{W}_c (19) and \dot{W}_g (20), equations (35) - (39) simplify to:

Energy

$$\begin{aligned} & \left(\rho_p C_{vp} + e_c C_{vc} + \rho_g C_{pg} \right) \frac{\partial T}{\partial t} + \left(\dot{W}_p e_p + \dot{W}_c e_c + \dot{W}_g h_g \right) + (\rho_g C_{pg} \vec{V}) \cdot \nabla T \\ & = \nabla \cdot (K \nabla T) + \frac{\partial P}{\partial t} + \frac{\vec{V} \cdot \vec{V}}{2} \dot{W}_g + \nabla \cdot (\vec{V} \cdot \vec{\tau}) - e_g \left[\frac{\partial}{\partial t} \left(\frac{\vec{V} \cdot \vec{V}}{2} \right) + \vec{V} \cdot \nabla \left(\frac{\vec{V} \cdot \vec{V}}{2} \right) \right] \end{aligned} \quad (43)$$

Continuity

$$\frac{\partial \rho_g}{\partial t} + \nabla \cdot (e_g \vec{V}) = \dot{W}_g \quad (44)$$

$$\frac{\partial \rho_p}{\partial t} = \dot{W}_p \quad (45)$$

$$\frac{\partial \rho_c}{\partial t} = \dot{W}_c \quad (46)$$

$$\dot{W}_p + \dot{W}_c + \dot{W}_g = 0 \quad (47)$$

State

$$P = \rho \frac{R}{M} T \quad (48)$$

Momentum

$$\vec{V} = - \nabla \frac{k}{\mu} P \quad (49)$$

These equations were first derived by S. M. Scala. Scala distinguishes between the volume occupied by the gas and that by the solid, and so the correspondence between nomenclature is:

<u>Present Derivation</u>	<u>Scala</u>
ρ_p	$(1 - \epsilon) \rho'_p$
ρ_c	$(1 - \epsilon) \rho'_c$
ρ_g	$(\epsilon) \rho'_g$
p	$(\epsilon) p'$
τ	$(\epsilon) \tau_{ij}$
K	$\epsilon k_g + (1 - \epsilon) k_s$

ϵ is the porosity of the material, which is a variable.

The gas density used in the derivation of the equations described here is the weight of the gas in a given solid-gas volume divided by that volume. The gas density referred to within the REKAP program is the above density divided by the porosity of the material. Porosity is defined as:

$$\epsilon = \frac{\text{Actual Gas Volume}}{\text{Total Volume}} = \frac{\text{Void Volume}}{\text{Total Volume}}$$

The porosity is calculated at each time step by:

$$\epsilon = 1 - \tilde{\rho}_c \left(\frac{1}{\tilde{\rho}_c} - \frac{1}{\tilde{\rho}_{vp}} \right) - \frac{\rho_s}{\tilde{\rho}_{vp}}$$

The thermal conductivity of the gas (k_g) and thermal conductivity of the solid (K_s) are each based on their respective areas.

Where $\tilde{\rho}_c$ is the final density of the char based on the volume of the char (i.e. if the char is carbon then $\tilde{\rho}_c$ is equal to the density of carbon) and $\tilde{\rho}_{vp}$ is the initial density of the virgin plastic before heating or any charring has taken place.

Another approach, which is opposite in spirit to the previous one, is to simplify the gas dynamics and to deal with various limiting forms of the gas chemistry. Obviously, there are many possible ways of accomplishing this. We shall follow an approach which has been commonly used for engineering calculations. The key assumptions used in this simplification are that the gas is in local thermochemical equilibrium and that diffusion is negligible. This means that the gas composition is a known function of temperature and pressure. Finally, it is assumed that radiation can be accounted for as an increase in effective conductivity and that the mechanical work terms are negligible compared to the thermal terms in the energy equation. All of these are reasonably plausible engineering assumptions.

In the absence of diffusion, the species continuity equation (22) is:

$$\rho_g \left[\frac{\partial K_i}{\partial t} + \vec{V} \cdot \nabla K_i \right] = \dot{W}_i'$$

Since the composition is a known function of temperature and pressure, this implies:

$$\dot{W}_i' = \rho_g \left(\frac{\partial K_i}{\partial T} \right) \left[\frac{\partial T}{\partial t} + \vec{V} \cdot \nabla T \right] + \rho_g \left(\frac{\partial K_i}{\partial P} \right) \left[\frac{\partial P}{\partial t} + \vec{V} \cdot \nabla P \right]$$

Substituting this into the energy equation (34) and neglecting diffusion, radiation, and mechanical work terms we get:

$$\begin{aligned} & \left(\rho_p C_{v_p} + \rho_c C_{v_c} + \rho_g \bar{C}_{p_g} \right) \frac{\partial T}{\partial t} - \dot{W}_p \left[(1 - f_c) h_g + f_c e_c - e_p \right] \\ & + \rho_g \left(\sum_i h_i \frac{\partial K_i}{\partial T} \right) \left[\frac{\partial T}{\partial t} + \vec{V} \cdot \nabla T \right] + \rho_g \left(\sum_i h_i \frac{\partial K_i}{\partial P} \right) \left[\frac{\partial P}{\partial t} + \vec{V} \cdot \nabla P \right] \\ & - \dot{W}_c'' (h_g - e_c) + \left(\rho_g \bar{C}_{p_g} \vec{V} \right) \cdot \nabla T = \nabla \cdot K \nabla T \end{aligned} \quad (50)$$

The continuity equations (34) - (39), thermal equation of state (40) and the momentum equation (41) remain unchanged.

It is possible to simplify (50) even further by neglecting the gas density in comparison with the solid density, while retaining the mass flow rate term. This implies that as $\rho_g \rightarrow 0$, $\rho_g V$ remains finite so that $\vec{V} \rightarrow \infty$, i.e., the "residence time" is negligible. This means that the equation of state and the momentum equation are superfluous. The pressure is assumed to be uniform at its ambient value, which is not necessarily steady. The

continuity equations remain unchanged except the time derivative of the gas density in (37) is dropped. The energy equation (50) becomes:

$$\begin{aligned} & \left(\rho_p C_{v_p} + \rho_c C_{v_c} \right) \frac{\partial T}{\partial t} + \rho_g \vec{V} \left(\bar{C}_{p_g} + \sum_i h_i \frac{\partial K_i}{\partial T} \right) \cdot \nabla T = \nabla \cdot K \nabla T \\ & + \dot{W}_p \left[(1 - f_c) h_g + f_c e_c - e_p \right] + \dot{W}_c'' (h_g - e_i) \end{aligned} \quad (51)$$

Various forms of this equation in one dimension are the usual starting point for engineering calculations (e.f. References 10 - 13). The REKAP program, without the pressure option, is one such program neglecting the gas-solid phase reactions and by combining equations (37) - (39) and (51), the following equations result.

Energy:

$$\begin{aligned} & \left(\rho_p C_{v_p} + \rho_c C_{v_c} \right) \frac{\partial T}{\partial t} + \rho_g V \left(\bar{C}_{p_g} + \sum_i h_i \frac{\partial K_i}{\partial T} \right) \frac{\partial T}{\partial X} \\ & = \frac{\partial}{\partial X} \left(K \frac{\partial T}{\partial X} \right) + \left[\frac{\partial}{\partial t} (\rho_p + \rho_c) \right] \cdot \left[h_g + \frac{f_c}{1 - f_c} e_c - \frac{1}{1 - f_c} e_p \right] \end{aligned}$$

Continuity:

$$\rho_g V = - \int_{\text{backface}}^X \frac{\partial}{\partial t} (\rho_p + \rho_c) dX$$

Density:

$$\frac{\partial}{\partial t} (\rho_p + \rho_c) = - (1 - f_c) \dot{W}_p$$

The coordinate system used in Appendix B is opposite to the one used here so that the sign on $\dots dx$ and $\frac{\partial}{\partial X}$ is changed. The correspondence between nomenclature is:

<u>Present Derivation</u>	<u>REKAP Program</u>
$\rho_p + \rho_c$	ρ
$\frac{\rho_p C_{v_p} + \rho_c C_{v_c}}{\rho_p + \rho_c}$	C_p
$\rho_g V$	\dot{M}_g
$\sum_i h_i \frac{\partial K_i}{\partial T}$	H_{cg}
$h_g + \frac{f_c}{1 - f_c} e_c - \frac{1}{1 - f_c} e_p$	H_{gf}
$(1 - f_c) \dot{W}_p$	$\rho_{vp} \left(\frac{\rho - \rho_c}{\rho_{vp}} \right)^{n_1} Z e^{-E/RT}$

Summary of the Equations Solved in Appendix B

Normal REKAP Equations:

Energy:

$$\rho C_p \frac{\partial T}{\partial t} = \frac{\partial}{\partial X} \left(K \frac{\partial T}{\partial t} \right) + \dot{M}_g \left(\bar{C}_{p_g} + H_{c_g} \right) \frac{\partial T}{\partial X} + H_{gf} \frac{\partial \rho}{\partial t}$$

Continuity:

$$\dot{M}_g = - \int_x^{\text{backface}} \frac{\partial \rho}{\partial t} dX$$

Density:

$$\frac{\partial \rho}{\partial t} = - \rho_{vp} \frac{\rho - \rho_c}{\rho_{vp}} \frac{n}{Z} e^{-E/RT}$$

These are the equations that are solved in the non-pressure option of the program.

Pressure Option Equations:

Energy (Gas):

$$\begin{aligned} \rho_g C_p \frac{\partial T_g}{\partial t} = & - \rho_g C_p V \frac{\partial T}{\partial X} + \frac{\partial P}{\partial t} + \frac{\partial}{\partial X} \left(\epsilon K_g \frac{\partial T}{\partial X} \right) + \dot{Q}_{\text{transferred from gas}} \\ & + \dot{W}_g h_g + \frac{\partial}{\partial X} \left(\epsilon \tau_{ij} - V \right) - \rho_g V \frac{\partial V}{\partial t} - \rho_g V^2 \frac{\partial V}{\partial X} - \frac{\dot{W}_g V^2}{2} \end{aligned}$$

Energy (Solid):

$$\begin{aligned} (1 - \epsilon) \left(\rho_p C_{r_{vp}} + \rho_c C_{v_c} \right) \frac{\partial T_s}{\partial t} + \frac{\partial}{\partial X} \left[(1 - \epsilon) K_s \frac{\partial T_s}{\partial X} \right] \\ - \left(e_c \dot{W}_c + e_{vp} \dot{W}_{vp} \right) - \dot{Q}_{\text{transferred from gas}} \end{aligned}$$

If the temperature of the gas and the temperature of the adjacent solid material are the same, the above two equations may be added together.

$$\left[\rho_g C_p + (1 - \epsilon) \left(\rho_p C_{v_{vp}} + \rho_c C_{v_c} \right) \right] \frac{\partial T}{\partial t} = \frac{\partial T}{\partial t} \left\{ \left[\epsilon K_g + (1 - \epsilon) K_s \right] \frac{\partial T}{\partial X} \right\} \\ + \frac{\partial P}{\partial t} + h_g \dot{W}_g - (\rho_c \dot{W}_c + \rho_p \dot{W}_p) - \rho_g C_p V_g \frac{\partial T}{\partial X} + \frac{\partial}{\partial X} \left(\epsilon \tau_{ij} V \right) \\ - \rho_g V \frac{\partial V}{\partial X} - \rho_g V^2 \frac{\partial V}{\partial X} - \frac{V^2 \dot{W}_g}{2}$$

Continuity:

$$\frac{\partial \rho_g}{\partial t} + \frac{\partial(\rho_g V)}{\partial X} = \dot{W}_g$$

$$\frac{\partial \rho_g}{\partial t} = \dot{W}_g = - \dot{W}_s = \beta \rho_{vp} \left(\frac{\rho_s - \rho_c}{\rho_{vp}} \right)^n e^{-E/RT}$$

$$\frac{\partial \rho_{vp}}{\partial t} = \dot{W}_{vp}$$

$$\frac{\partial \rho_c}{\partial t} = \dot{W}_c$$

$$\dot{W}_s = \dot{W}_c + \dot{W}_{vp}$$

Momentum:

$$\bar{V} = \frac{\partial}{\partial X} \left(\frac{g \bar{R} T}{\mu} \frac{R}{\epsilon} \rho_g \right)$$

which was obtained by substituting the Equation of State in the momentum equation (12).

Boundary Conditions:

The boundary conditions that are of concern here are those describing the material heat input or removal from the front and back face and the surface recession at the heated face. The heating of the material can be described by three methods: front face temperature (T_w), front face heat flux (\dot{q}_c and/or \dot{q}_{hgr}), and front face convective film coefficient ($\dot{q}_c/\Delta h$ or $\dot{q}_c/\Delta T$).

Each of these quantities can be a function of time. The convective film coefficient option is the one most commonly used for the analysis of rocket engines, however, for some propellant combinations, it is necessary to account for the radiation (\dot{q}_{hgr}) from the exhaust gases. The program includes the capability of combining the radiative flux and the convective heat transfer by taking a thermal balance at the front face. The thermal balance is described by:

$$\dot{q}_{net} = \dot{q}_c + \dot{q}_{hgr} - \dot{q}_{rr} - \dot{q}_b = K_w \frac{\partial T}{\partial X}$$

The convective heat flux (\dot{q}_c) is determined either from program input which is a function of time or it is calculated from:

$$\begin{aligned} \dot{q}_c &= \frac{\dot{q}_c}{\Delta h} (h_r - h_{ff}) & h_{ff} &= C_{p_{bl}} T_w \\ \text{or} \\ \dot{q}_c &= \frac{\dot{q}_c}{\Delta T} (T_r - T_w) \end{aligned}$$

where h_r is the recovery enthalpy and T_r is the recovery temperature.

If the convective film coefficient is in terms of temperature rather than enthalpy, the specific heat ($C_{p_{bl}}$) of the boundary layer gases must be set equal to 1.0 for all values of gas temperature. The convective film coefficient is an input to the program and is considered to be a function of time.

The fourth term in the heat balance equation is the rate of energy loss from the front face due to thermal radiation. It is expressed by:

$$\dot{q}_{rr} = \epsilon \sigma T_w^4$$

where σ is the Stefan-Boltzmann constant which equals 0.476×10^{-12} BTU/sec Ft² and ϵ is the product of the surface emissivity and the configuration factor (F_a) between the point radiating and the cold (relative to the hot wall) external environment.

The fifth term is the decrease in the convective heat flux due to the injection of ablation gases into the boundary layer. This is commonly referred to as the "blocking action effect." The expressions describing the blocking action were derived from the correlation

of experimental data (References 14 to 34). The expressions for the blockage of the convective energy are:

Laminar:

$$\dot{q}_b = \dot{q}_c \left[.69 \left(\frac{M_2}{M_1} \right)^{1/3} \frac{\varphi_o}{P_r^{1/3}} \right]$$

Turbulent:

$$\dot{q}_b = \dot{q}_c \left[1 - e^{-.38 C_T \varphi} \right]$$

$$\varphi = \frac{\dot{M}_w}{\dot{q}_c / \Delta h}$$

where:

M_1 is the molecular weight of the injection gases

M_2 is the molecular weight of the boundary gases

C_T is the ratio of the specific heat of the injection gases to the specific heat of the boundary layer gases. $\left(\frac{C_{p1}}{C_{p2}} \right)$

P_r is the Prandtl number of the boundary layer gases.

\dot{M}_w is the mass injection rate at the front face. $\sim \text{lb/sec ft}^2$

The quantities (M_2/M_1) , C_T and P_r are input constants while $(\dot{q}_c/\Delta h)$ is the value of the convective film coefficient. If the blocking action is expected to be significant (however, for most materials exposed to a rocket engine environment, the blockage effects amount to only a few per-cent of the convective heat flux) it is necessary to use the film coefficient defined in terms of the enthalpy difference since that is how the above blocking action equations are correlated. Included for completeness is the laminar blocking action equation although for most rocket nozzle applications, the boundary layer is assumed to be turbulent.

The last term in the front face heat balance equation is the rate of thermal energy which is transferred by conduction into the material.

The heat transfer from the back face of the material is controlled by specifying the back face temperature (T_{BF}) or heat transfer rate (\dot{q}_{BF}) as a function of time. If radiation from the back face is desired, included is a routine to allow for an air-gap or a non-solid layer in the nozzle wall. Therefore, to account for radiation from the back face of a nozzle, the third layer from the last in the program is the actual nozzle backside, the second from last is the air-gap and the final layer is the nozzle surroundings for which the back face temperature is specified. Using the air-gap routine not only can radiation from the back face be accounted for but also natural convection and forced convection by the proper adjustment of constants. For the details of the mathematical equations, see Appendix B and E.

Front Face Recession

The front face recession is presently controlled by five methods: no melting, or recession, specified char length, graphite oxidation and sublimation, refrasil option and fixed melting temperature. The first method is normally used for the purpose of evaluating the temperature distribution within material which is known not to have a dimensional change. The options most commonly used are the specified char length, graphite sublimation and the fixed melting temperature. The fourth option which is referred to as the refrasil option is based on the work done by Munson and Spindler (Reference 12). For this option, the heat balance equation at the front face is:

$$-K \frac{dT}{dX} = \dot{q}_c + \dot{q}_{hgr} - \dot{q}_{rr} - \dot{q}_b - (\rho L) \dot{S}$$

Where the surface recession rate is given by:

$$\dot{S} = \beta_1 T_w^{\beta_2} e^{-\beta_3/T_w}$$

The constants β_1 , β_2 and β_3 are determined from experimental data. In their paper, Munson and Spindler listed the values of β_1 , β_2 and β_3 for silica phenolic as 0.00917 ft/sec^{0R²}, 2.0 and 1×10^5 °R.

The quantity $(\rho_c L)$, the surface or final char density and the latent heat of fusion or vaporization depending upon whether the material melts or is vaporized. Empirical and analytical (Reference 35) work done on the analysis of glassy materials within rocket nozzles has shown that the major portion of the surface loss to be by melting and not by vaporization. Therefore, the value of L for a phenolic refrasil material should be the heat of fusion for the char material which is primarily refrasil. The refrasil option has the disadvantage of being relatively slow (requires several times as much computation time as the fixed melting temperature option) since it must iterate on the rate of melt for each time step.

The fixed melting temperature option usually satisfies the rate of melt criterion after the first iteration. The net heat balance for the fixed melting temperature option is the same as for the refrasil option. However, the rate of melt (\dot{S}_m) is given by:

$$\dot{S}_m = \frac{K \frac{dT}{dX} + \dot{q}_{net}}{\Gamma \rho_c L}$$

where ρ_c is the density of the char and L is the latent heat of vaporization or melting depending on whether the material vaporizes or melts. The gasification factor Γ is the ratio of the char material which is either vaporized or melted to the total char that is lost. Some of the char may be lost by char popoff or some other mechanical means. The value of Γ must be determined experimentally. The front face is not allowed to recede until the front face temperature reaches the specified melting temperature.

The specified char thickness option is as the name implies, the char layer is allowed to grow until it reaches the specified value. Then the outer boundary moves at the same rate as the reaction zone. The maximum allowable char thickness is determined by the material and the environment to which it is exposed. The thickness values are determined from experimental data.

The graphite sublimation option for the control of front face recession also accounts for the oxidation of most graphite materials including pyrolytic graphite and carbonaceous chars. The rate of mass loss from the surface of graphitic materials depend on an oxidation process, which is rate-controlled at low (< 1500°R) surface temperatures, but rapidly become diffusion-controlled as the surface temperature rises (see Figures A2 and A3). For the range of surface temperatures, approximately between 2500°R and 5000°R, the rate of the overall mass loss is dominated by the slowest step, which is the counterdiffusion process in the multicomponent boundary layer. When the surface temperature is in this range, the oxidation rate levels off and becomes insensitive to the magnitude of surface temperature, simply because the mass loss is controlled by the diffusion of oxygen-bearing species to the surface rather than the specific reactivity of graphite. At even higher surface temperature ($T_w > 5000^\circ\text{R}$) the mass loss due to vaporization exceeds the diffusion controlled oxidation mass loss rate. This region is normally referred to as the sublimation regime. The results shown in Figure A3 were correlated (References 36 and 37) and the resulting equations were:

$$\dot{M}_t = \dot{M}_o \left[r + 2.64 \times 10^9 P_e^{-.67} e^{-\frac{11.05 \times 10^{-4}}{T_w}} \right]$$

where the \dot{M}_o is the mass loss within the diffusion controlled regime

$$\dot{M}_o = \frac{\dot{q}_c}{Q^*} = \frac{\dot{q}_c}{K_1 + K_2 (h_r - C_{pbl} T_w)} - (C_{pA} \cdot T_{REC} - C_{pA} T_{MELT})$$

The quantities K_1 and K_2 are input constants and for turbulent flow, their values are 4240 and 5.77 respectively. The rate of front face recession is given by:

$$\dot{S}_m = \frac{\dot{M}_t}{\rho_{\text{surface}}}$$

The heat balance at the front face is given by:

$$-K \frac{dT}{dX} = \dot{q}_c' + \dot{q}_{hgr} - \dot{q}_{rr} - \dot{q}_b$$

where:

$$\dot{q}_c' = \dot{q}_c \left[1 - S^* (3.96 \times 10^8) P_e^{-.67} e^{-\frac{11.05 \times 10^{-4}}{T_w}} \right]$$

The local edge pressure P_e is an input quantity which is a function of time and S^* is a table lookup which is a function of the recovery enthalpy.

NOMENCLATURE

A	surface area	ft^2
C_v	specific heat at constant volume	$\text{BTU/lbm } ^\circ\text{R}$
C_p	specific heat at constant pressure	$\text{BTU/lbm } ^\circ\text{R}$
\overline{C}_{p_g}	$\sum_i K_i C_{pi}$ = average specific heat	$\text{BTU/lbm } ^\circ\text{R}$
$C_{p_{bl}}$	specific heat of the boundary layer gases	BTU/lb
C_t	ratio of the specific heat of the injection gases to the specific heat of the boundary layer gases	-----
$D_{i,j}$	multicomponent diffusion coefficient	ft^2/sec
D_{12}	binary diffusion coefficient	ft^2/sec
e	specific internal energy	BTU/lbm
e_F	energy of formation	BTU/lbm
\vec{e}	unit base vector	-----
f_c	fraction of unreacted material that forms char	-----
h_r	recovery enthalpy	BTU/lb
h_{ff}	boundary layer gas enthalpy at wall temperature	BTU/lb
k	permeability	ft^2
K	thermal conductivity	$\text{BTU/ft-sec } ^\circ\text{R}$
K_i	$\frac{\rho_i}{\rho}$ = mass concentration	-----
$K_{i,j}$	conductivity tensor	$\text{BTU/ft-sec } ^\circ\text{R}$
K_1 & K_2	constants in mass loss equation	-----
M	molecular weight	lbm/mole

\bar{M}_g	$\frac{1}{\sum \frac{K_i}{M_i}}$ = average molecular weight	lbm/mole
M_1	molecular weight of the injection gases	-----
M_2	molecular weight of the boundary layer gases	lb/lb mole
\dot{M}_w	mass injection rate at the front face	lb/sec-ft ²
n	total number of moles per unit volume	moles/ft ³
p	pressure	lbf/ft ²
\vec{P}	surface force per unit area	lbf/ft ²
P_e	boundary layer edge pressure	lb/ft ²
Pr	Prandtl number of the boundary layer gases	-----
ϵ	porosity	-----
$\tilde{\rho}_c$	final density of the char based on the volume of the char	lbf/ft ³
$\tilde{\rho}_{vp}$ or ρ_{vp}	initial density of the virgin plastic	lbf/ft ³
\dot{q}_c	convective heat flux	BTU/ft ² -sec
\dot{q}_{hgr}	heat flux due to hot gas radiation	BTU/ft ² -sec
\dot{q}_{rr}	reradiative heat flux	BTU/ft ² -sec
\dot{q}_b	convective heat flux blocked due to mass injection	BTU/ft ² -sec
\dot{q}_{bf}	heat flux to the backface	BTU/ft ² -sec
\vec{q}_c or \vec{q}_c	conduction heat flux vector	BTU/ft ² -sec
\vec{q}_R or \vec{q}_R	radiant heat flux vector	BTU/ft ² -sec
R	universal gas constant	lbf ft/lbm mole °R
T	temperature	°R

T_r	recovery temperature	$^{\circ}\text{R}$
T_w	wall temperature	$^{\circ}\text{R}$
T_{bf}	temperature of backface	$^{\circ}\text{R}$
\underline{T}	stress tensor	lbf/ft^2
V	volume	ft^3
\vec{V}_i	absolute velocity of ith species	ft/sec
\vec{V}_{d_i}	diffusion velocity of ith species	ft/sec
\vec{V}	mass averaged velocity	ft/sec
\dot{W}_i or ω_i	net rate of production of the ith gaseous species due to all chemical reactions	lbm/ft^3
\dot{W}_i' or $\dot{\omega}_i'$	net rate of production of ith species due to gas phase reactions	lbm/ft^3
\dot{W}_g'' or $\dot{\omega}_g''$	rate of production of gas due to gas-solid phase reactions	lbm/ft^3
X	mole fraction	-----
\vec{n}	outward unit normal	-----
ρ	density	lbm/ft^3
σ_{ij}	component of the stress tensor	lbf/ft^2
$\underline{\tau}$	viscous stress tensor	lbf/ft^2
μ	gas viscosity	lbf-sec/ft^2
σ	Stefan-Boltzmann constant ($0.476 \times 10^{-12} \text{ Btu/sec-ft}^2$)	-----
Γ	gasification ratio	-----

APPENDIX A

REFERENCES

1. Von Karman, T., "Fundamental Equations in Aerothermochemistry" Proc. 2nd AGARD Combustion Collog., Liege, Belgium, Dec. 1955.
2. Scala, S.M., "The Equations of Motion in a Multicomponent Chemically Reacting Gas," General Electric Co. Missile and Ordnance Systems Dept., Doc. No. R58SD205, Dec. 1957.
3. Hirschfelder, J. D., Curtiss, C.F. and Bird, R.B., Molecular Theory of Gases and Liquids, John Wiley and Sons, 1954.
4. Bird, R.B., Stewart, W.E., and Lightfoot, E.N., Transport Phenomena, John Wiley and Sons, 1960.
5. Hayday, A.A., "Governing Equations of Multicomponent Fluid Continua with Chemical Reactions", University of Illinois, Technical Report No. ILL-6-P (Project SQUID), April 1962.
6. Sokolinikoff, I.S. and Redheffer, R.M., Mathematics of Physics and Modern Engineering, McGraw Hill, 1958.
7. Carslaw, H.S. and Jaeger, J.C., Conduction of Heat in Solids, Oxford Press 1959.
8. Aris, R.A., Vectors, Tensors and The Basic Equations of Fluid Mechanics Prentice Hall, 1962.
9. Muskat, M., The Flow of Homogeneous Fluids Through Porous Media, J.W. Edwards Inc., 1946.
10. Kratsch, K.M., Hearne, L.F. and McChesney, H.R., "Thermal Performance of Heat Shield Composites During Planetary Entry", paper presented at the AIAA-NASA National Meeting, Palo Alto, Calif., Oct. 1963.
11. Lafazan, S., and Welsh, W.E., Jr., "The Charring Ablator Concept: Application to Lifting Orbital and Superorbital Entry", paper presented at the Symposium on Dynamics of Manned, Lifting Planetary Entry, Philadelphia, Pa., 1963.
12. Munson, T.R. and Spindler, R.J., "Transient Thermal Behavior of Decomposing Materials, Part I: General Theory and Application to Convective Heating", paper presented at IAS 30th Annual Meeting, New York, N.Y. Jan. 1962.
13. Wells, P.B., "A Method for Predicting the Thermal Response of Charring Ablation Materials", The Boeing Co., Aero Space Div., Doc. No. D2-23256, June, 1964.
14. Pappas, C.C. and Okuno, A.F., "Measurements of Skin Friction of the Compressible Turbulent Boundary Layer on a Cone with Foreign Gas Injection," Journal of the Aerospace Sciences, May 1960.

15. Tewfik, O.E., Jurewicz, L.S., and Eckert, E.R.G., "Measurements of Heat Transfer from a Cylinder with Air Injection into a Turbulent Boundary Layer," ASME Paper No. 63-HT-45, August 1963.
16. Bartle, E.R. and Leadon, B.M., "The Effectiveness as a Universal Measure of Mass Transfer Cooling for a Turbulent Boundary Layer," Proceedings of the 1962 Heat Transfer and Fluid Mechanics Institute, Stanford Univ. Press, June, 1962.
17. Leadon, B.M. and Scott, C.J., "Measurement of Recovery Factors and Heat Transfer Coefficients with Transpiration Cooling in a Turbulent Boundary Layer at $M = 3$ Using Air and Helium as Coolants," Rosemount Aero. Lab. Research Report Number 126, February 1956.
18. Gross, Hartnett, Masson, & Gazley: "A Review of Binary Laminar Boundary Layer Characteristics" - International Journal of Heat and Mass Transfer, 3, 3, pages 198 to 221, October 1961.
19. Baron: "The Binary Boundary Layer Associated with Mass Transfer Cooling at High Speed" - MIT Naval Supersonic Lab Report 160 (1956).
20. Eckert, Schenider, Hayday and Larson: "Mass Transfer Cooling of a Laminar Boundary Layer by Injection of a Light Weight Gas" - Rand Symposium on Mass Transfer Cooling for Hypersonic Flight.
21. Sziklas and Banas: "Mass Transfer Cooling in Compressible Laminar Flow" - Rand Symposium on Mass Transfer Cooling for Hypersonic Flight.
22. Hartnett and Eckert: "Mass Transfer Cooling in a Laminar Boundary Layer with Constant Fluid Properties: - Trans. ASME, 79, 247 (1957).
23. Eckert: "Engineering Relations for Heat Transfer and Skin Friction in High Velocity Laminar and Turbulent Boundary Layer Flow over Surfaces with Constant Pressure and Temperature" - Trans. ASME 78, 1273 (1956).
24. Gross: "The Laminar Binary Boundary Layer" - RM-1915 - The Rand Corporation, September 1956.
25. Spalding: "Mass Transfer through Laminar Boundary Layers - 1. The Velocity Boundary Layer" Int. J. Ht. Mass Transfer, 3, Nos. 1 and 2, Pg. 15, March 1961.
26. Faulders: "Heat Transfer in the Laminar Boundary Layer with Ablation of Vapor of Arbitrary Molecular Weight" - J. Aero. Sci 29, 1, 76, Jan. 1962.
27. Eckert, Hayday and Minkowycz: "Heat Transfer, Temperature Recovery, and Skin Friction on a Flat Plate with Hydrogen Release into a Laminar Boundary Layer" - Int. J. Ht. Mass Trans. 4, Page 17, Dec. 1961.
28. Emmons and Leigh: "Tabulation of the Blasius Function with Blowing and Suction" - Harvard Report: Combustion Aero Lab Int. Tech. Rpt. #9 (1953).

29. Lew and Fanucci: "The Laminar Compressible Boundary Layers Over a Flat Plate with Suction or Injection" - J. Aeron. Sci. 22, 9, pg. 589-597, September 1955.
30. Brown: "Tables of Exact Laminar Boundary Layer Solutions when the Wall is Porous and Fluid Properties are Variable" - NACA TN 2479 - September 1951.
31. Eschenroeder: "The Compressible Laminar Boundary Layer with Constant Injected Mass Flux at the Surface" - Jour. Aero- Space Sciences, 26, 11, Pg. 762 (1959).
32. Mickley, Ross, Squyers, & Stewart: "Heat, Mass and Momentum Transfer for Flow Over a Flat Plate with Blowing and Suction" - NACA TN 3208 (1954).
33. Stewart: "Transpiration Cooling: An Engineering Approach" - General Electric Missile & Space Vehicle Department Report R59SD338 - May 1, 1959.
34. Schlichting: "Boundary Layer Theory," Pergamon Press (1955).
35. Nestler, D.E., "The Effects of Liquid Layers on Ablation Performance" - General Electric Co., RSD, Thermodynamics Fund. Memo No. 022, TFM-8151-022, December, 1963.
36. Scala, S. M., "The Ablation of Graphite in Dissociated Air, Part I - Theory", IAS Paper No. 62-154, Thirtieth National Summer Meeting, June 1962; also G.E. Co., MSD, TIS R62SD72, September 1962.
37. Scala, S. M., and Gilbert, L. M., "Aerothermochemical Behavior of Graphite at Elevated Temperatures", G.E. Co., MSD, TIS R63SD89, November, 1963.

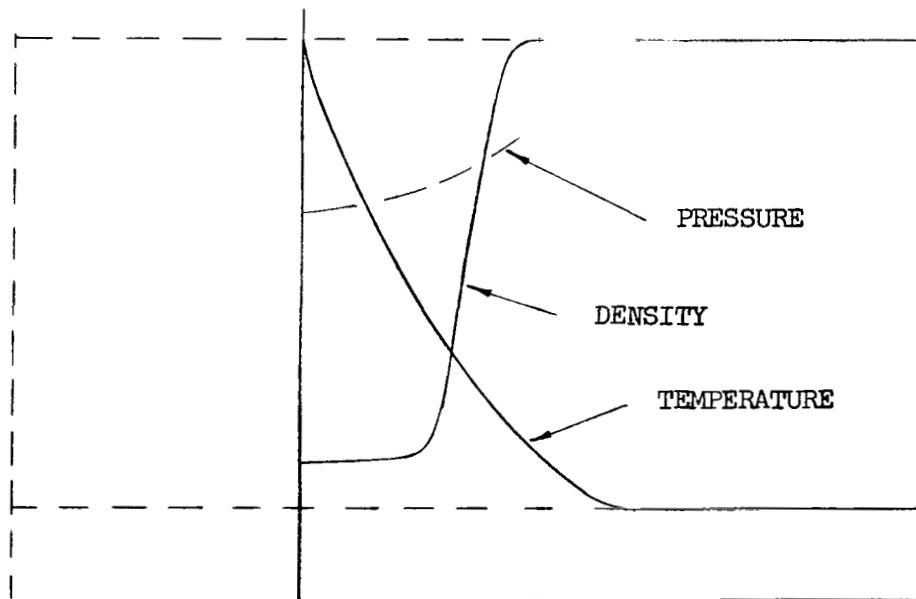
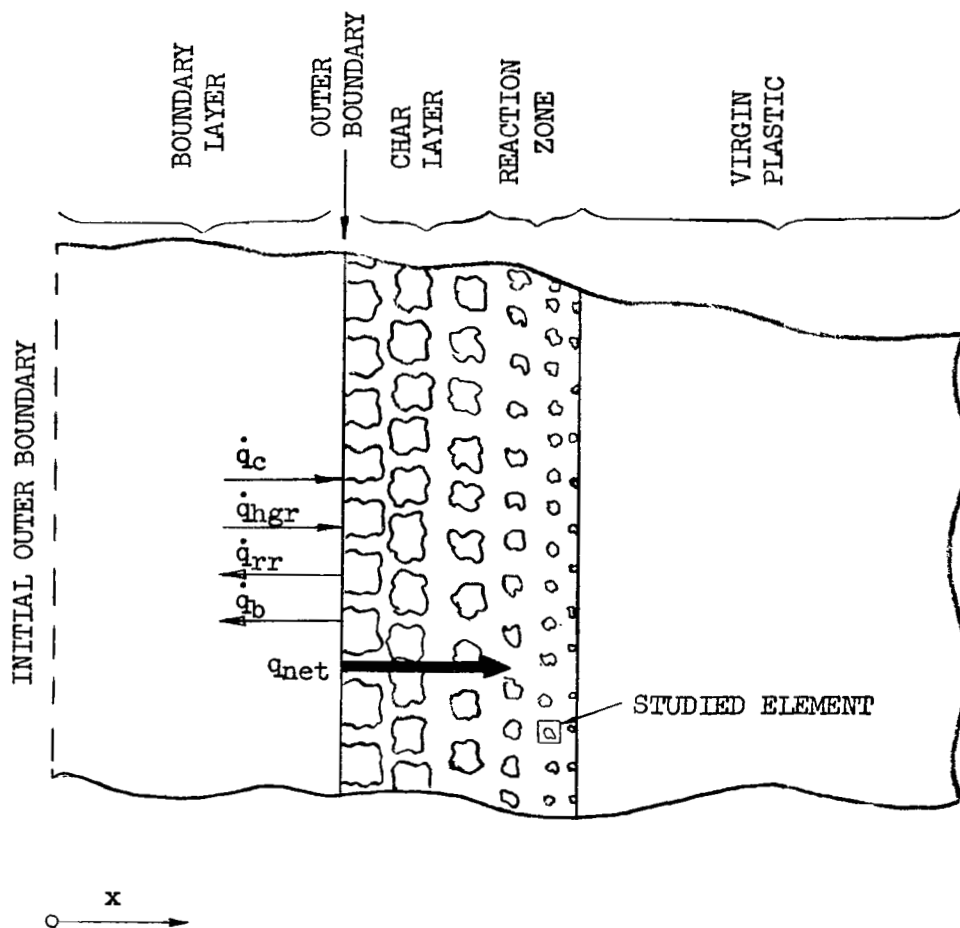


Figure A1. Schematic of a Degrading Plastic and Corresponding Profiles

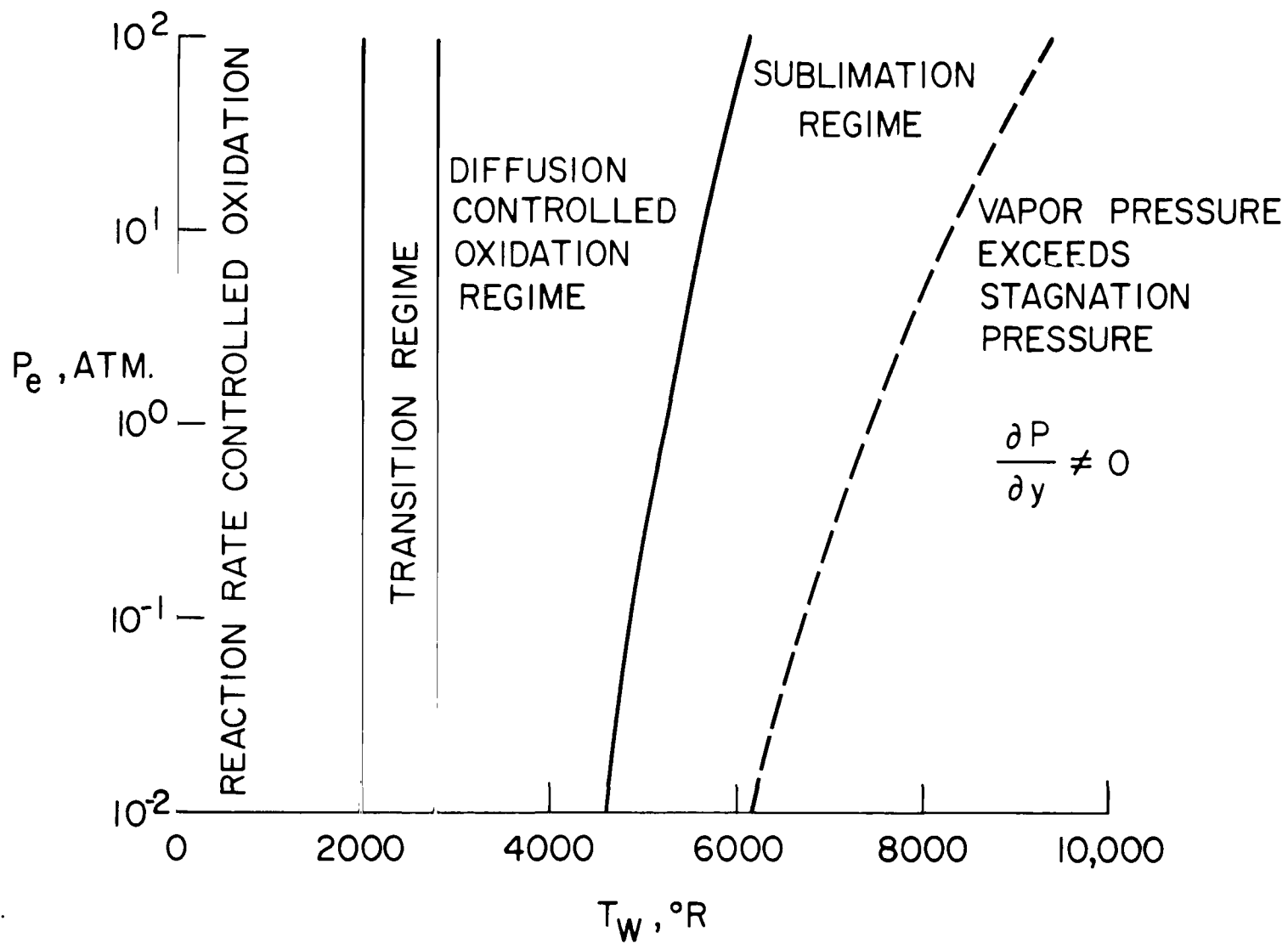


Figure A2. Mass Transfer Regimes for Ablating Graphite

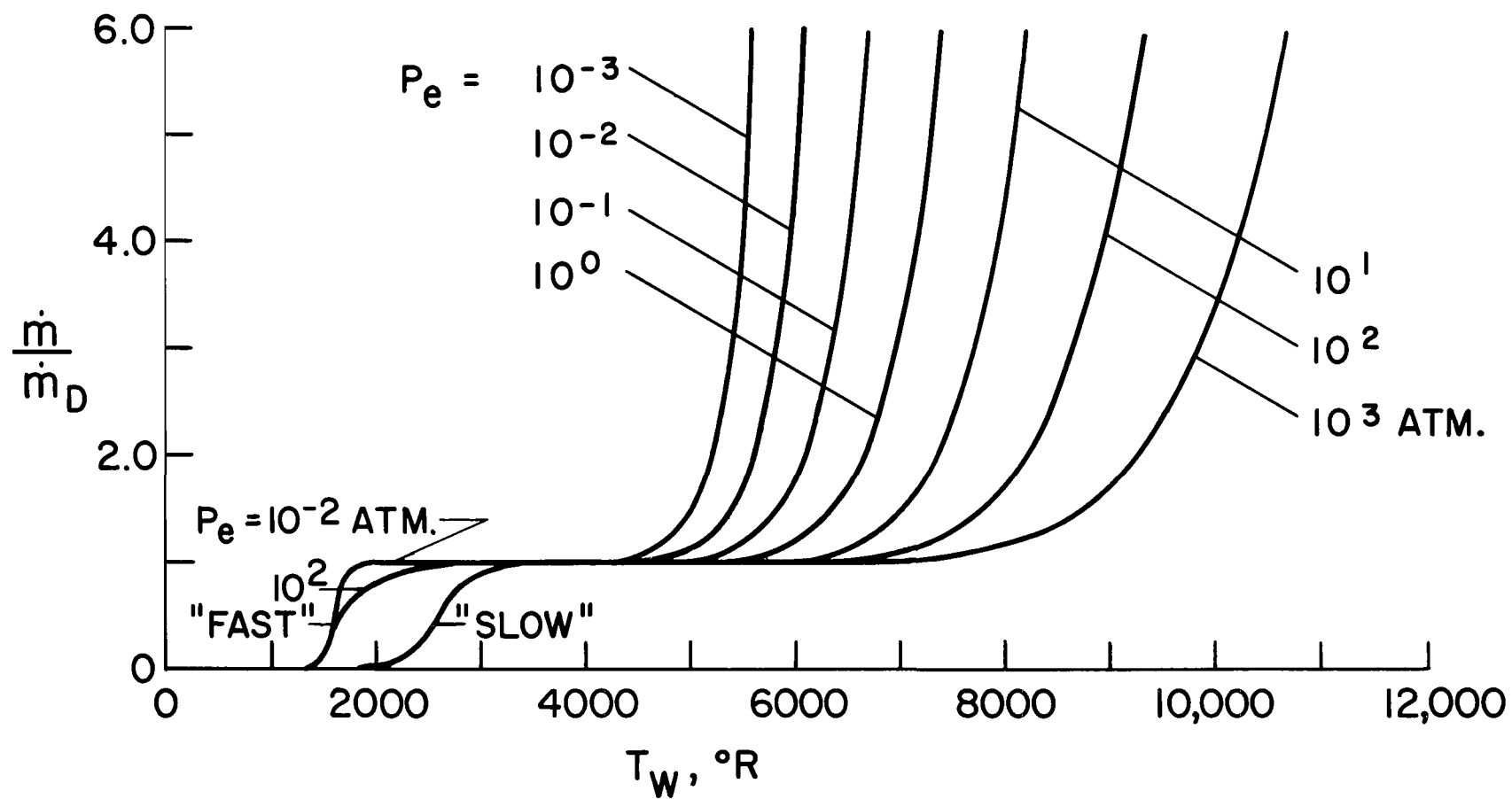


Figure A3. Normalized Ablation Rate of Graphite Over the Entire Range of Surface Temperature

APPENDIX B
NUMERICAL ANALYSIS

SECTION I

INTRODUCTION

The purpose of the Appendix is to describe the philosophy, methods, and capabilities of the REKAP computer program. The basic objective was to develop a computer program which meets these requirements:

1. Solve the basic mathematical problems which appear in the variety of one-dimensional heat conduction problems encountered.
2. Allow variations of the problem to be solved with a minimum of added difficulty.

A discussion of these two points follows.

Past experience has shown the following to be important aspects of a good mathematical solution:

1. A shrinking coordinate system. This allows melting to proceed without dropping mesh points. We employ Landau's transformation (reference 1). In this report, see Appendix B1.
2. Variable spacing. Many problems produce a very large temperature gradient at the frontface. Thus, it is desirable to solve for more points near the frontface than the back. This is accomplished with another space transformation (Appendix B2).
3. An explicit system of difference equations. There are those who might question the validity of treating this item as a fundamental objective of a one-dimensional heat conduction program. Nevertheless, we believe it to be quite important. Very often the solution for temperatures at one or more points requires an iteration. For example, in this program the boundary condition at the frontface produces an implicit relationship involving temperature. The same is true for the air gap equations. An implicit scheme requires that all temperatures be obtained at each stage of the iteration. Also, it might prove formidable even to write an iteration scheme to solve two such relationships in the same problem. Another advantage of the explicit scheme is better approximations for the coefficients of the partial differential equation. One can avoid the time lag that often occurs in implicit difference equations when evaluating these coefficients. The major argument against the explicit equation is, of course, the problem of stability. In the original program two explicit difference equations were employed:
 - a. The first is a modification of the "usual" explicit difference equation, and at times requires an unreasonably small time step (reference 2, p. 107).
 - b. The second is the Dufort-Frankel scheme. It is always stable but has a poor truncation error term (see reference 3 and reference 2, p. 107).

For the most part good results were obtained with these equations. However, two major problems appeared - both in the Dufort-Frankel scheme:

1. In some cases, particularly those involving a small temperature drop, the poor truncation error term became dominant and large errors resulted.
2. In some cases, involving a sensitive frontface boundary condition, there was difficulty in maintaining stability of the difference equation in conjunction with the frontface equation.

We were not able to satisfactorily resolve these problems, and so in the new program the two difference equations have been replaced with a third explicit difference equation (see Section III). The truncation error term is now similar to that which appears in the usual explicit scheme and so far we have experienced no insurmountable stability problems.

We come now to the second of our objectives - program flexibility. This concept, unfortunately, is a subtle thing which appears to be neither well-recognized nor well-defined. In prescribing objectives for the program, the following things must be kept in mind:

1. The mathematical techniques are such that a portion of the program that has worked successfully for many cases may not work for a new case. When everything is working, it really makes little difference how we write or organize the program. However, when there is difficulty, a poorly written program can make it extremely difficult to find the problem, let alone correct it.
2. Various mathematical models, which from a physical point of view appear to be entirely different, often turn out to be almost identical in terms of programming complexities.
3. The problem is of a long-range nature. There is an almost constant need for such programs. Thus, maintenance becomes a formidable task.

Some program objectives, then, would be these:

1. Isolate, through program techniques, those portions of the program in which mathematical problems may arise.
2. Isolate those portions of the program which appear to be subject to change as we vary the physical models.
3. Constant maintenance of the program.

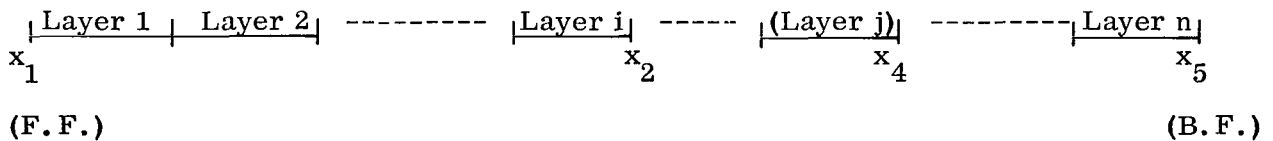
In writing, we attempted to meet the first two objectives through the use of sub-routines and through careful organization of the program.

SECTION II

The Physical Problem

We discuss first the portions of the problem that are general to all options now in the program (Part A). We then discuss special options which are presently available (Part B, Part C, Part D). (A fairly complete list of definitions of terms is contained in Appendix B6 of this report.)

A. We discuss the general mathematical model which the program is set up to solve.



1. We have one-dimensional heat flow, with up to ten layers. It should be noted that reduction of the problem to one dimension assumes something about the isotherms. Most of the problems here are in cartesian or cylindrical coordinates. This means the isotherms are assumed to be planes or cylindrical shells perpendicular to the line along which values are being computed.
2. Any of the layers, except the first, can be an air gap.
3. The thermal properties of each layer (specific heat and conductivity) are to be a function of temperature.
4. At the interior points of each layer some form of energy equation is assumed to be valid. It is put in this form:

$$\frac{\partial T}{\partial t} = b_1 \left(\frac{\partial^2 T}{\partial x^2} \right) + b_2 \left(\frac{\partial T^2}{\partial x} \right) + b_3 \left(\frac{\partial T}{\partial x} \right) + b_4$$

where the $b_i = b_i(x, t, T)$.

5. At each interior interface point (x_2 in diagram) we have this equation:

$$\left(-k \frac{\partial T}{\partial x} \right)_- - C_i \left(\frac{\partial T}{\partial t} \right) = \left(-k \frac{\partial T}{\partial x} \right)_+$$

$C_i = C_i(T)$ is intended to represent a $\rho c_p L$ term. It is inserted to account for small layers of material in which the gradients are so small as to make accurate computations difficult.

The term with subscript "-" is evaluated with properties of layer (i). The term with subscript "+" is evaluated with properties of layer (i+1).

6. At the back face (x_5 in diagram) there are two boundary conditions in the program.
(it is expected that for each particular case only one will be chosen!)

- Either the temperature of the backface is given as a function of time, or
- The heat flux at the backface is given as a function of time

$$\left(-k \frac{\partial T}{\partial x} \right) - C_i \left(\frac{\partial T}{\partial t} \right) = \dot{q}(t)$$

7. In the air gap we obtain temperatures at only the boundary points (x_3 and x_4 in diagram) no interior points are involved. We have these equations:

$$a. \left(-k \frac{\partial T}{\partial x} \right)_{-} - C_j \left(\frac{\partial T}{\partial t} \right)_{-} = (\dot{q}_r + \dot{q}_{cv} + \dot{q}_{cond})_o$$

$$b. (\dot{q})_o = \left(-k \frac{\partial T}{\partial x} \right)_{+} - C_{j+1} \left(\frac{\partial T}{\partial t} \right)_{+}$$

The C_i are as described in item 5 above. Terms with subscripts "-" are evaluated at x_3 with properties of layer (j-1).

Terms with subscript "+" are evaluated at x_4 with properties of layer (j+1).

Terms with subscript "o" are evaluated at midpoint of air gap with the properties of the air gap.

$$\dot{q}_r = \sigma F_e F_A \left[\left(T_{x_3} \right)^4 - \left(T_{x_4} \right)^4 \right]$$

$$\dot{q}_{cond} = -\bar{k}_c \left(\frac{\partial T}{\partial x} \right)$$

$$\dot{q}_{cv} = -h_c \left(k \frac{\partial T}{\partial x} \right)$$

$$h_c = c \left(\frac{A}{\bar{L}} \right)^m \left[G_r \frac{c_p \mu}{k} \right]^n$$

$$G_r = \left| \frac{(A)^4 (\rho)^2 (\bar{g}) \frac{\partial T}{\partial x}}{T(\mu)^2} \right|$$

$$\bar{g} = a_o + a_1 t + a_2 t^2 : a_i \text{ are computed from input constants.}$$

$$\left. \begin{array}{l} c = c_1 \\ n = n_1 \end{array} \right\} \text{ if } G_R \leq G_{R_1}$$

$$\left. \begin{array}{l} c = c_2 \\ n = n_2 \end{array} \right\} \text{ if } G_R > G_{R_1}$$

$$\dot{q} = \dot{q}_r + \dot{q}_{\text{cond}} + \dot{q}_{\text{cv}} - \rho c_p A \frac{\partial T}{\partial t}$$

(See Appendix B6 of analysis section for definition of other terms.)

8. At the frontface (x_1 in diagram) we again have a choice of two boundary conditions.
 - a. Either the temperature of the frontface is read in as a function of time, or
 - b. $\left(-k \frac{\partial T}{\partial x} \right) = f(t, T_{x_1})$
9. Melting can occur at the frontface. The various possibilities now in the program will be discussed below.
10. If the length of the layer is extremely small, a special calculation can be made - the thin skin option. For this case there is no melting or charring (or any other internal phenomena other than the "usual" heat conduction equation), and there can be only one layer of material. The entire layer is assumed to have the same temperature, which is calculated from this equation:

$$T^{n+1} = T^n + \frac{\Delta t}{\rho c_p} \dot{q}_{\text{net}}$$

(\dot{q}_{net} is as specified in II. C.1). See Appendix B5 of analysis section for a further discussion of this equation.

Any of these equations can be modified, if necessary. At present the items most commonly changed are the coefficients of the energy equation, the function $f(t, T_{x_1})$ in the frontface boundary condition, and the melting option. We now describe some of the cases permanently in the program. We will specify only items 4, 8, and 9. It is assumed that an appropriate choice will be made for each of the others.

B. We list the options, presently in the program, for computing the coefficients of the energy equation - item 4.

1. The simplest case is "normal" heat conduction:

$$b_1 = \frac{k}{\rho c_p}$$

$$b_2 = \frac{k'}{\rho c_p}$$

$$b_3 = b_4 = 0.$$

$$k' = \frac{d k}{d T}$$

k , k' , c_p are functions of temperature.
 ρ is constant.

2. The charring problem. (See Appendix A for definition of physical problem; in the analysis portion of this report see Appendix B1 for further discussion.) It is assumed that charring occurs only in the first layer. Past the first layer we use the definitions above. In the first layer:

$$b_1 = \frac{k}{\rho c_p}$$

$$b_2 = \left(\frac{k}{\rho c_p} \right) \left(\frac{k'_1}{k_1} \right)$$

$$b_3 = \left(\frac{k}{\rho c_p} \right) \left[\frac{k'_a}{k_a} \left(\frac{\partial \rho}{\partial x} \right) + \frac{c_g \dot{m}_g}{k} \right]$$

$$b_4 = - \left(\frac{g}{\rho c_p} \right)$$

$$k = k_1 + k_a$$

$$k_1 = k_1(T) - \text{table lookup}$$

$$k_a = k_a(\rho) = (1 - c_1) + c_1 \left(\frac{\rho - \rho_c}{\rho_{vp} - \rho_c} \right)^{N_1}$$

ρ_c is density of char

ρ_{vp} is density of virgin plastic

c_1 and N_1 are input constants.

$$c_p = c_{p_1} \cdot c_{p_a}$$

$$c_{p_1} = c_{p_1}(T) \text{ - table lookup}$$

$$c_{p_a} = c_{p_a}(\rho) = (1 - c_2) + c_2 \left(\frac{\rho - \rho_c}{\rho_{vp} - \rho_c} \right)^{N_2}$$

$$k'_a = \frac{dk_a}{d\rho} = \left(\frac{N_1}{\rho - \rho_c} \right) \left[k_a - (1 - c_1) \right]$$

$$c_g = c_{p_g} + H_{c_g}$$

$$c_{p_g} = c_{p_g}(T) \text{ - table lookup}$$

$$H_{c_g} = H_{c_g}(T) \text{ - table lookup}$$

$$\frac{\partial \rho}{\partial t} = -\rho_{vp} \left(\frac{\rho - \rho_c}{\rho_{vp}} \right)^{\eta_1} (z) e^{-E/RT}$$

$z = z(\rho)$ - table lookup

$E = E(\rho)$ - table lookup

R = universal gas constant

η_1 = input constant

(Note that a density distribution is calculated through the first layer by using the above equation at each point.)

$$\dot{m}_g(x, t) = - \int_x^{A_1} \left(\frac{\partial \rho}{\partial t} \right) dx$$

$$g = -H_{gf} \left(\frac{\partial \rho}{\partial t} \right)$$

$$H_{gf} = H_{gf}(T) \text{ - table lookup}$$

(See Appendix B1 of analysis portion of this report for further discussion of this equation.)

C. The following equations are presently in the program at the frontface. Since quite often \dot{q}_{net} and s'_m are specified together, they are given together.

$$1. \quad \dot{q}_{\text{net}} = \dot{q}_c + \dot{q}_{\text{hgr}} - \dot{q}_r - \dot{q}_{\text{block}}$$

$$\dot{q}_c:$$

a. Table lookup

$$b. \quad \dot{q}_c = F \left(h_r - h_{\text{ff}} \right)$$

F = film coefficient = $F(t)$ - table lookup

$$h_r = h_r(t) - \text{table lookup}$$

$$h_{\text{ff}} = c_{p_{\text{bl}}} \cdot T_w$$

$$c_{p_{\text{bl}}} = c_{p_{\text{bl}}}(T_w) - \text{table lookup}$$

$$\dot{q}_{\text{hgr}} = \dot{q}_{\text{hgr}}(t) - \text{table lookup}$$

$$\dot{q}_r = \epsilon \sigma T_w^4$$

$$\epsilon = \epsilon(T_w) - \text{table lookup}$$

$$\sigma = \text{Stephan-Boltzmann constant } (.476 \times 10^{-12})$$

$$\dot{q}_{\text{block}} = \begin{cases} \dot{q}_c \left[1 - e^{-.38 C_T \varphi_o} \right] : \text{turbulent} \\ \dot{q}_c \left[.69 \left(\frac{M_2}{M_1} \right)^{1/3} \frac{\varphi_o}{p_r^{1/3}} \right] : \text{laminar} \end{cases}$$

where C_{T_1} , $\frac{M_2}{M_1}$, p_r are input constants

$$\varphi_o = \dot{m}_w \left(\frac{h_r - h_w}{\dot{q}_c} \right)$$

$$\dot{m}_w = \dot{m} \text{ at frontface}$$

For this \dot{q}_{net} the following two options can be used to calculate \dot{s}_m :

$$\text{a. } \left(-k T_x \right) = \dot{q}_{\text{net}} \Gamma (\rho L) \dot{s}_m$$

\dot{s}_m : rate of melt

$\rho L = \rho L(t)$: table lookup

$\Gamma = \Gamma(t)$ table lookup

after the frontface temperature reaches the melting temperature, \dot{s}_m is obtained from the above equation.

$$\text{b. } \left(-k T_x \right) = \dot{q}_{\text{net}}$$

The maximum char length, s_{c_m} , is given as a function of time

$$\dot{s}_c(t) = \frac{\dot{m}_g^{\text{F.F.}}}{(\rho_{vp} - \rho_c)}$$

$$\dot{s}_m(t) = \begin{cases} 0: s_c - s_m \leq s_{c_m} \\ \dot{s}_c(t) - \dot{s}_{c_m}(t): s_c - s_m > s_{c_m} \end{cases}$$

$$s_c = \bar{s}_c + \sigma (s_c^* - \bar{s}_c)$$

s_c^* : coordinate of first point whose density equals $\epsilon \cdot \rho_{vp}$
(ϵ and σ are input)

2. Graphite Sublimation:

$$-k T_x = \dot{q}'_c + \dot{q}_{\text{hgr}} - \dot{q}_r - \dot{q}_{\text{bl}}$$

$$\dot{q}'_c = \dot{q}_c \left[1 - S * \left(3.96 \times 10^{+8} \right) \left(P_e^{-0.67} \right) e^{-\frac{11.05 \times 10^4}{T_w}} \right]$$

\dot{q}'_c , \dot{q}_{hgr} , \dot{q}_r , \dot{q}_{bl} are as defined in option 1.

$S = S(h_r)$: table lookup

$P_e = P_e(t)$: table lookup

$$\dot{s}_m = \frac{\dot{m}_t}{\rho_{\text{surface}}}$$

$$\dot{m}_t = \dot{m}_D \left[1 + 2.64 \times 10^9 P_e (-.67) e^{-\frac{11.05 \times 10^4}{T_w}} \right]$$

$$\dot{m}_D = \frac{\dot{q}_c}{K_1 + K_2 (h_r - c_{pbl} T_w)}$$

$$K_1 = K_1(t) - \text{table lookup}$$

$$K_2 = K_2(t) - \text{table lookup}$$

3. Refrasil

$$(-k T_x) = \dot{q}_{net} + (\rho L) \dot{s}_m$$

\dot{q}_{net} is as in option 1

$$\rho L = \rho L(t) - \text{table lookup}$$

$$\dot{s}_m = \beta_1 T_w^{\beta_2} e^{-\beta_3/T_w}$$

β_i are input constants

D. By data reduction we mean calculation of new quantities, from already known values, which have no effect on these known values. These can generally be added quite easily to the program, since by definition they add no mathematical problems to the rest of the program. Some examples are the following:

1. Printout of equally spaced temperatures: The points at which temperatures are obtained are not equidistant in real space; also, they move if melting occurs. This tends to make plotting difficult.
2. Heat balance calculation. This is intended to give an indication of accuracy of results. (See section IX of analysis portion of this report.)

3. Stress computations (Appendix C). The following calculations are performed at each time step at which output is required. Find first value of x , starting at backface, for which $T(x) \geq T_{AB}$: let this be x^* . Evaluate these integrals (trapezoidal rule):

$$I_1 = \int_{x^*}^{B.F.} dx$$

$$I_2 = \int_{x^*}^{B.F.} E dx$$

$$I_3 = \int_{x^*}^{B.F.} E x dx$$

$$I_4 = \int_{x^*}^{B.F.} E x^2 dx$$

$$I_5 = \int_{x^*}^{B.F.} E \left[\alpha T - (\alpha T)_{ref} \right] dx$$

$$I_6 = \int_{x^*}^{B.F.} E \left[\alpha T - (\alpha T)_{ref} \right] x dx$$

(Several other calculations are also made.)

$E = E(T)$ - table lookup (for each layer)

$\alpha T = \alpha T(T)$ - table lookup (for each layer)

$(\alpha T)_{ref} = \alpha T(T_{ref})$

T_{AB} and T_{ref} are input values.

SECTION III

ANOTHER DIFFERENCE EQUATION FOR THE HEAT CONDUCTION EQUATION

A. We are concerned with attempts to obtain solutions to differential equations through the application of difference equations. Actually one assumes that the particular difference equation being used is a member of a sequence of such equations. To validate this procedure only two questions need be answered:

1. Does the sequence converge to a solution of the differential equation?
2. What is the rate of convergence?

The first question assumes that appropriate spaces have been specified for the solution to the differential equation, and also for the solution to the difference equation operator. As is well-known, this is not a trivial matter (some examples are listed later). Since we want to apply any results obtained to actual computation (presumably by a computer), it is very important that the space to be chosen conform reasonably well to the spaces which we can reasonably approximate on the computer. The Banach spaces chosen by Richtmyer (reference 4) seem to be well-suited for this purpose. As pointed out there (p. 30), Banach spaces are certainly adequate for representing solutions to linear initial value problems. Also, one can think of Banach spaces as a "computer" function: one expects a perturbation of an interior point of a Banach space (such as truncation) to leave the point still in the Banach space. We will assume, therefore, that the solution of the differential equation and the solution of the difference operator both lie in suitable Banach spaces.

Because of the great wealth of literature on the topic, it is impossible (perhaps unfortunately) to discuss difference equations without bringing in the question of stability. The point of view to be taken here is that stability is to be studied only if it will bring some light to the basic questions raised before. Here again, the results of Richtmyer (reference 4) are consistent with this idea: Lax's equivalence theorem (p. 44) states that under the conditions given stability and convergence are equivalent. Forsythe and Wasow (reference 5) do not wish to restrict so strongly their function spaces, and so they carry along separate proofs of stability and convergence. It is difficult to see the significance of a difference operator which would be stable but not convergent, or perhaps convergent but not stable.

Some examples to illustrate these ideas might be the following:

1. Dahlquist (reference 6) proves convergence under more lenient conditions than could be obtained by using the methods of either Richtmyer or Forsythe and Wasow. But he has assumed his function to be analytic. As pointed out by Forsythe and Wasow (p. 27), analytic functions are not "computer" functions.
2. Henrici (reference 7) in discussing ordinary differential equations defines stability for linear difference equations. He later establishes the equivalence of

stability and convergence (p. 218). This seems to be a reasonable result. In defining the Runge-Kutta method, he can no longer apply his definition of stability. However, he does prove convergence even in the presence of the perturbation term (p. 73). From our point of view this again is a fine result, for it brings the domain of application to "computer" functions.

3. Birkhof and Rota (reference 8) in their discussion of difference equations for ordinary differential equations define stability in the same sense as Henrici (p. 195). They then find that the Milne method is not stable (p. 204), although it is convergent for any function in C^2 (problem 9, p. 207). Note that C^2 is not a space of "computer" functions.

B. The purpose of this note is to present another difference equation for the heat conduction problem. For constant coefficients it assumes the form:

$$\frac{\partial u}{\partial t} = \beta_1 \frac{\partial^2 u}{\partial x^2} \quad (\text{III. 1})$$

We will reduce our equation to one resembling the Dufort-Frankel scheme, from which we will infer the stability of our equation. Richtmyer shows that the Dufort-Frankel equation is stable (p. 85). He also shows that this is equivalent to boundedness (p. 44). However, an explicit equation showing that the Dufort-Frankel scheme is a bounded operator which achieves its maximum essentially on the boundary does not seem available. Such an equation is quite important for numerical work, as it brings out quite a bit of insight concerning the behavior of the equation. This property is easily established for the usual implicit and explicit methods (the latter, of course, under appropriate conditions), see Richtmyer (p. 47 and p. 13). We now establish a result of this kind for the Dufort-Frankel scheme.

We will use this notation:

$$u_j^n = u(n \Delta t, j \Delta x).$$

$$u_A^n \text{ in particular always refers to } x = A$$

We assume values given on the boundary:

$$u = f_1(t): x = 0$$

$$u = f_2(t): x = A$$

$$u = f_3(x): t = 0$$

The Dufort-Frankel scheme is obtained in this fashion:

$$\frac{\partial u}{\partial t} = \frac{u_j^{n+1} - u_j^n}{\Delta t}$$

$$\frac{\partial^2 u}{\partial x^2} = \frac{u_{j+1}^n - 2u_j^n + u_{j-1}^n}{(\Delta x)^2}$$

then let

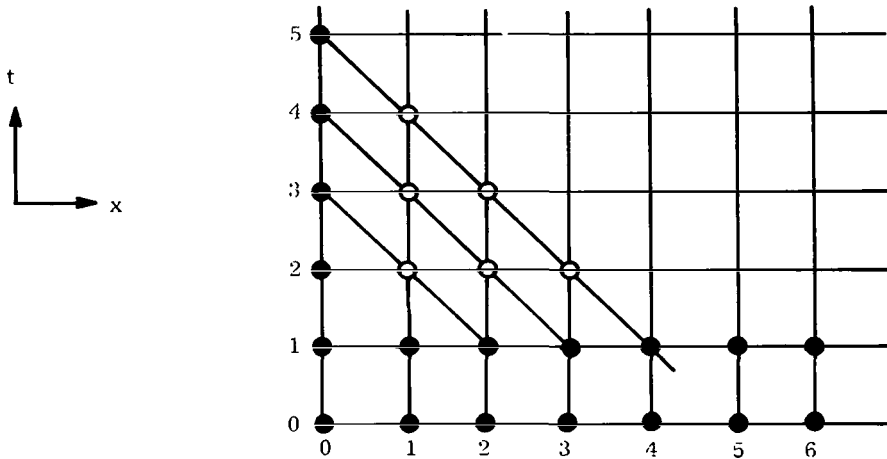
$$u_j^n = \frac{u_j^{n+1} + u_j^{n-1}}{2}$$

Letting $p = (2\beta_1) \frac{\Delta t}{(\Delta x)^2}$ and substituting into (III. 1), we obtain:

$$(1+p) u_j^{n+1} = (1-p) u_j^{n-1} + p (u_{j+1}^n + u_{j-1}^n) \quad (\text{III. 2})$$

as written this represents an explicit scheme, for all values at $n+1$ can be obtained independently of other values at $n+1$ by using values at n and $n-1$.

If we change the order of computation, it is also possible to consider (III. 2) as an implicit equation. Instead of obtaining at each step all values at next t , obtain all values on next diagonal:



We assume values given at $t = 0$, $t = \Delta t$, $x = 0$, $x = A$. Rewriting (III. 2)

$$(1+p) u_j^{n+1} - p u_{j+1}^n = (1-p) u_j^{n-1} + p u_{j-1}^n$$

We indicate how to proceed by solving diagonally:

a. Obtain u_1^2 :

$$(1+p) u_1^2 - p u_2^1 = (1-p) u_1^0 + p u_0^1$$

u_2^1, u_0^1, u_1^0 are known.

b. Obtain u_2^2 and u_1^3

$$(1+p) u_2^2 - p u_3^1 = (1-p) u_2^0 + p u_1^1$$

$$(1+p) u_1^3 - p u_2^2 = (1-p) u_1^1 + p u_0^2$$

$$u_3^1, u_2^0, u_1^1 \text{ are given - this gives } u_2^2$$

$$u_1^1, u_0^2 \text{ are given - this gives } u_1^3$$

c. At n^{th} step we have this system to solve:

$$\left. \begin{aligned} (1+p) u_1^{n+1} - p u_2^n &= (1-p) u_1^{n-1} + p u_0^n \\ (1+p) u_2^n - p u_3^{n-1} &= (1-p) u_2^{n-2} + p u_1^{n-1} \\ &\vdots \\ (1+p) u_{i+2}^{n-i} - p u_{i+3}^{n-i-1} &= (1-p) u_{i+2}^{n-i-2} + p u_{i+1}^{n-i-1} \\ &\vdots \\ (1+p) u_{n-1}^3 - p u_n^2 &= (1-p) u_{n-1}^1 + p u_{n-2}^2 \\ (1+p) u_n^2 - p u_{n+1}^1 &= (1-p) u_n^0 + p u_{n-1}^1 \end{aligned} \right\} \quad (\text{III. 3})$$

Remark: If the diagonal encounters the line $x = A$ before $t = 0$ the system would simply be cut off sooner. The same is true for the line $t = t_1$.

Let

$$L_j^m = (1-p) u_j^m + p u_{j-1}^{m+1} \quad (\text{III. 4})$$

Triangularizing equations (III. 3) - from bottom up -

$$\left. \begin{aligned} (1+p) u_n^2 &= p u_{n+1}^1 + L_n^0 \\ (1+p) u_{n-1}^3 &= \left(\frac{p}{1+p}\right) (p) u_{n+1}^1 + \left(\frac{p}{1+p}\right) L_n^0 + L_{n-1}^1 \\ (1+p) u_{n-2}^4 &= \left(\frac{p}{1+p}\right)^2 (p) u_{n+1}^1 + \left(\frac{p}{1+p}\right)^2 L_n^0 + \left(\frac{p}{1+p}\right) L_{n-1}^1 + L_{n-2}^2 \\ &\vdots \\ (1+p) u_{n-i+2}^i &= \left(\frac{p}{1+p}\right)^{i-2} (p) u_{n+1}^1 + \sum_{\nu=0}^{i-2} \left(\frac{p}{1+p}\right)^{(i-2-\nu)} L_{n-\nu}^\nu \\ &\vdots \\ (1+p) u_1^{n+1} &= \left(\frac{p}{1+p}\right)^{n-1} (p) u_{n+1}^1 + \sum_{\nu=0}^{n-1} \left(\frac{p}{1+p}\right)^{n-1-\nu} L_{n-\nu}^\nu \end{aligned} \right\} \quad (\text{III. 5})$$

$$\text{Let } \bar{L}_n = \max \left\{ \left| u_{n+1}^1 \right|, \left| L_{n-\nu}^\nu \right| \right\} \quad (\text{III. 6})$$

Note that the weights in equations (III. 5) are all positive. This need not be so in equation (III. 2).

Then, equations (III. 5) become:

$$\begin{aligned} (1+p) \left| u_{n-i+2}^i \right| &\leq \bar{L}_n \left\{ (p) \left(\frac{p}{1+p} \right)^{i-2} + \sum_{\nu=0}^{i-2} \left(\frac{p}{1+p} \right)^{i-2-\nu} \right\} \\ &= \bar{L}_n \cdot f(p, i) \text{ for } i \geq 2 \end{aligned}$$

We verify that $f(p, i) = 1+p$:

$$\sum_{\nu=0}^{i-2} \left(\frac{p}{1+p} \right)^{i-2-\nu} = \sum_{\nu=0}^{i-2} \left(\frac{p}{1+p} \right)^\nu = \frac{1 - \left(\frac{p}{1+p} \right)^{i-1}}{1 - \frac{p}{1+p}} = (1+p) - p \left(\frac{p}{1+p} \right)^{i-2}$$

$$f(p, i) = (p) \left(\frac{p}{1+p} \right)^{i-2} + (1+p) - p \left(\frac{p}{1+p} \right)^{i-2} = 1+p$$

or

$$\left| u_{n-i+2}^i \right| \leq \bar{L}_n \quad (\text{III. 7})$$

We now show that the $\{\bar{L}_n\}$ are a decreasing sequence.

$$L_{n-i}^i = (1-p) u_{n-i}^i + p u_{n-i-1}^{i+1}$$

Substituting equation (III. 5):

$$\begin{aligned} L_{n-i}^i &= \frac{(1-p)}{(1+p)} \left\{ \left(\frac{p}{1+p} \right)^{i-2} (p) u_{n-1}^1 + \sum_{\nu=0}^{i-2} \left(\frac{p}{1+p} \right)^{i-2-\nu} L_{n-2-\nu}^\nu \right\} \\ &\quad + \left(\frac{p}{1+p} \right) \left\{ \left(\frac{p}{1+p} \right)^{i-1} (p) u_{n-1}^1 + \sum_{\nu=0}^{i-1} \left(\frac{p}{1+p} \right)^{i-1-\nu} L_{n-2-\nu}^\nu \right\} \\ &= \left\{ \left(\frac{1-p}{1+p} \right) (p) \left(\frac{p}{1+p} \right)^{i-2} + \left(\frac{p}{1+p} \right) (p) \left(\frac{p}{1+p} \right)^{i-1} \right\} u_{n-1}^1 \\ &\quad + \sum_{\nu=0}^{i-2} \left[\left(\frac{1-p}{1+p} \right) \left(\frac{p}{1+p} \right)^{i-2-\nu} + \left(\frac{p}{1+p} \right)^{i-\nu} \right] L_{n-2-\nu}^\nu + \left(\frac{p}{1+p} \right) L_{n-1-i}^{i-1} \end{aligned}$$

$$L_{n-1}^i = f_1(p, i) u_{n-1}^1 + \sum_{\nu=0}^{i-2} f_2(p, i, \nu) \cdot L_{n-2-\nu}^\nu + \left(\frac{p}{1+p}\right) L_{n-1-i}^{i-1}$$

$$f_1(p, i) = \left(\frac{p}{1+p}\right)^{i-1} \left[(1-p) + \frac{p^2}{1+p}\right] = \left(\frac{p}{1+p}\right)^{i-1} \left[\frac{1-p^2+p^2}{1+p}\right] = \left(\frac{1}{p}\right) \left(\frac{p}{1+p}\right)^i$$

$$\begin{aligned} f_2(p, i, \nu) &= \left(\frac{p}{1+p}\right)^{i-1-\nu} \left[\left(\frac{1-p}{p}\right) + \frac{p}{1+p}\right] = \left(\frac{p}{1+p}\right)^{i-1-\nu} \frac{1}{p(1+p)} = \\ &= \left(\frac{1}{p^2}\right) \left(\frac{p}{1+p}\right)^{i-\nu} \end{aligned}$$

$$L_{n-i}^i = \left(\frac{1}{p}\right) \left(\frac{p}{1+p}\right)^i u_{n-1}^1 + \left(\frac{1}{p^2}\right) \left(\frac{p}{1+p}\right)^i \sum_{\nu=0}^{i-2} \left(\frac{1+p}{p}\right)^\nu L_{n-2-\nu}^\nu + \left(\frac{p}{1+p}\right) L_{n-1-i}^{i-1}$$

We note again that the weights are all positive:

$$\begin{aligned} \left|L_{n-i}^i\right| &\leq \left(\frac{1}{p}\right) \left(\frac{p}{1+p}\right)^i = \left|u_{n-1}^1\right| + \left(\frac{1}{p^2}\right) \left(\frac{p}{1+p}\right)^i \sum_{\nu=0}^{i-2} \left(\frac{1+p}{p}\right)^\nu \cdot \left|L_{n-2-\nu}^\nu\right| \\ &\quad + \left(\frac{p}{1+p}\right) \cdot \left|L_{n-2-i+1}^{i-1}\right| \end{aligned}$$

From (III. 6)

$$\left|L_{n-i}^i\right| \leq \bar{L}_{n-2} \left\{ \left(\frac{1}{p}\right) \left(\frac{p}{1+p}\right)^i + \left(\frac{1}{p^2}\right) \left(\frac{p}{1+p}\right)^i \sum_{\nu=0}^{i-2} \left(\frac{1+p}{p}\right)^\nu + \left(\frac{p}{1+p}\right) \right\} = \bar{L}_{n-2} \cdot f(p, i)$$

We verify that $f(p, i) = 1$:

$$\sum_{\nu=0}^{i-2} \left(\frac{1+p}{p}\right)^\nu = \frac{1 - \left(\frac{1+p}{p}\right)^{i-1}}{1 - \frac{1+p}{p}} = -p + p \left(\frac{1+p}{p}\right)^{i-1}$$

$$f(p, i) = \left(\frac{1}{p}\right) \left(\frac{p}{1+p}\right)^i - \left(\frac{1}{p}\right) \left(\frac{p}{1+p}\right)^i + \left(\frac{1}{p}\right) \left(\frac{p}{1+p}\right) + \frac{p}{1+p} = \frac{1}{1+p} + \frac{p}{1+p} = \frac{1+p}{1+p} = 1.$$

Thus, $\left|L_{n-i}^i\right| \leq \bar{L}_{n-2}$ for $i \geq 2$

or,

$$\bar{L}_n \leq \max \left[\bar{L}_{n-2}, \left|L_n^0\right|, \left|L_{n-1}^1\right|, \left|u_{n+1}^1\right| \right]$$

Suppose we let:

$$\left| u_i^0 \right| < M_1$$

$$\left| u_i^1 \right| < M_1$$

$$\left| u_0^n \right| < M_1$$

$$\left| L_n^0 \right| < M_2$$

$$\left| L_{n-1}^1 \right| < M_2$$

$$\text{Then, } \left| u_j^n \right| < \max \left[M_1, M_2 \right] \quad (\text{III. 8})$$

We will show that $M_2 \leq M_1 + \epsilon (\Delta t)$

or

$$\left| u_j^n \right| \leq M_1 + \epsilon (\Delta t), \quad \epsilon (\Delta t) \rightarrow 0 \text{ as } \Delta t \rightarrow 0 \quad (\text{III. 9})$$

$$L_n^0 = u_n^0 + p (u_{n-1}^1 - u_n^0)$$

$$u_{n-1}^1 = u_n^1 + \Delta x \left(\frac{du}{dx} \right)_n^1 + O(\Delta x^2)$$

$$u_n^1 = u_n^0 + \Delta t \left(\frac{du}{dt} \right)_n^0 + O(\Delta t^2)$$

$$u_{n-1}^1 - u_n^0 = \Delta x \left(\frac{du}{dx} \right)_n^1 + \Delta t \left(\frac{du}{dt} \right)_n^0 + O(\Delta x^2) + O(\Delta t^2)$$

$$p (u_{n-1}^1 - u_n^0) = C \left(\frac{\Delta t}{\Delta x^2} \right) (u_{n-1}^1 - u_n^0) =$$

$$C_1 \left(\frac{\Delta t}{\Delta x} \right) + C_2 \left(\frac{\Delta t}{\Delta x} \right)^2 + O(\Delta t) + O\left(\frac{\Delta t^3}{\Delta x^2} \right)$$

The consistency condition for the Dufort-Frankel scheme requires $\left(\frac{\Delta t}{\Delta x} \right) \rightarrow 0$

or

$$L_n^0 = u_n^0 + \epsilon (\Delta t)$$

The same is true for L_{n-1}^1 .

This completes the proof for the boundedness of the Dufort-Frankel method. Note that if the diagonal studied in the proof encounters the line $x = A$, the system of equations (i. e., equations (III. 5)) are simply cut off sooner. The result is the same. Clearly the same situation holds for the line $t = t_1$. We might also remark that if $\left(\frac{\Delta t}{\Delta x}\right) \rightarrow C$, the difference equations are still bounded, but the values are not so closely restricted by the boundary values. If $\left(\frac{\Delta t}{\Delta x}\right) \rightarrow +\infty$, our results do not give boundedness, although the usual theorem still gives stability. It might be that our results are too crude in this case; but it is interesting that even in this case all interior values are tied to the boundary - it is on the boundary that we do not have convergence.

C. We now define another simple operator. We then relate convergence of the new operator to that of the old.

Let

$$\Delta_j^n = u_j^n - u_j^{n-1}$$

We consider first linear difference equations with constant coefficients, and with "symmetric definition": the last condition is meant to imply that the equation about each point is defined as every other point. The general multi-level equation of this type is given by:

$$\sum_{p=0}^{\alpha_0} \left\{ \sum_{q=-r_p}^{s_p} a_{pq} u_{j+q}^{(n+\alpha_1)-p} \right\} = 0.$$

Such an equation is written about every point (n, j) for which we have enough neighboring points.

$$\sum_{p=0}^{\alpha_0} \left\{ \sum_{q=-r_p}^{s_p} a_{pq} \Delta_{j+q}^{(n+\alpha_1)-p} \right\} =$$

$$\sum_{p=0}^{\alpha_0} \left\{ \sum_{q=-r_p}^{s_p} a_{pq} u_{j+q}^{n+\alpha_1-p} \right\} + \sum_{p=0}^{\alpha_0} \left\{ \sum_{q=-r_p}^{s_p} a_{pq} u_{j+q}^{n-1+\alpha_1-p} \right\} = 0 + 0 = 0.$$

Thus, Δ_j^n satisfies the same difference equation, and so Δ_j^n converges or diverges as u_j^n .

Suppose we now have this situation:

a sequence of difference equations is given for u_j^n
for each of these equations a difference equation involving Δ_j^n can be uniquely defined.

Suppose that $\frac{\Delta_j^n}{\Delta t}$ (considered as a difference equation for u_t , which also satisfies III. 1) converges uniformly to u_t in the range. (Assume the boundary conditions appropriately modified.)

Then the difference equation for u_j^n converges uniformly to a solution of III. 1.

Proof:

$$\begin{aligned}
 1. \quad & \text{By definition, } u_j^n - u_0^n = \sum_{\nu=1}^n \Delta_j^\nu \\
 2. \quad & \int_0^{n\Delta t} (u_t) dt = \sum_{\nu=1}^n u_t \Delta t + O(\Delta t) \\
 & = \sum_{\nu=1}^n \left[\Delta_j^\nu + O(\Delta t) + O(\Delta x) \right] + O(\Delta t) \\
 & = \sum_{\nu=1}^n \Delta_j^\nu + O(\Delta t) + O(\Delta x)
 \end{aligned}$$

Comparing 1 and 2, the result is obtained.

D. We now define a difference equation for the heat conduction equation:

$$\frac{\partial u}{\partial t} = \beta_1 \frac{\partial^2 u}{\partial x^2} \quad (\text{III. 10. 1})$$

It will combine the usual implicit and explicit schemes, the result being explicit.

We assume the function given on the boundary:

$$u = f_1(t): x = 0, 0 \leq t \leq t_1 \quad (\text{III. 10. 2})$$

$$u = f_2(t): x = A, 0 \leq t \leq t_1 \quad (\text{III. 10. 3})$$

$$u = f_3(x): 0 \leq x \leq A; t = 0 \quad (\text{III. 10. 4})$$

During the first time step, evaluate every other point with the explicit scheme. (Suppose we begin with the first point.) The others are then evaluated with the implicit. However, since the explicit points were obtained first, each implicit equation contains only one unknown temperature. During the second time step, every other point, beginning with the second, is evaluated with an explicit equation, and the others with an implicit. These two cycles are repeated.

We will, as before, use this notation:

$$u_j^n = u \text{ at time } = n (\Delta t), \text{ and } x = j (\Delta x) \quad (\text{III. 10. 5})$$

$$u_A^n = u \text{ at time } = n (\Delta t), \text{ and } x = A \quad (\text{III. 10. 6})$$

$$u_j^{t_1} = u \text{ at time } t_1, \text{ and } x = j (\Delta x) \quad (\text{III. 10. 7})$$

$$(\delta^2)_j^n = u_{j+1}^n - 2 u_j^n + u_{j-1}^n \quad (\text{III. 10. 8})$$

For the explicit scheme we use:

$$u_j^{n+1} = p u_{j-1}^n + (1-2p) u_j^n + p u_{j+1}^n \quad (\text{III. 11. 1})$$

For the implicit:

$$u_j^{n+1} = p u_{j-1}^{n+1} - 2 p u_j^{n+1} + p u_{j+1}^{n+1} + u_j^n \quad (\text{III. 11. 2})$$

where

$$p = \frac{\Delta t}{(\Delta x)^2} \beta_1 \quad (\text{III. 11. 3})$$

The new difference equation then assumes this form:

$$u_{2j-1}^{2n-1} = p u_{2j-2}^{2n-2} + (1-2p) u_{2j-1}^{2n-2} + p u_{2j}^{2n-2} \quad (\text{III. 12. 1})$$

$$u_{2j}^{2n-1} = p u_{2j-1}^{2n-1} - 2 p u_{2j}^{2n-1} + p u_{2j+1}^{2n-1} + u_{2j}^{2n-2} \quad (\text{III. 12. 2})$$

and

$$u_{2j}^{2n} = p u_{2j-1}^{2n-1} + (1-2p) u_{2j}^{2n-1} + p u_{2j+1}^{2n-1} \quad (\text{III. 12. 3})$$

$$u_{2j-1}^{2n} = p u_{2j-2}^{2n} - 2 p u_{2j-1}^{2n} + p u_{2j}^{2n} + u_{2j-1}^{2n-1} \quad (\text{III. 12. 4})$$

With boundary conditions 10. 2 - 10. 4 this is well-defined.

It will be convenient to have the precise explicit formulation for III. 12. 1 through III. 12. 4.

We do this now:

From III. 12. 1,

$$u_{2j-1}^{2n-1} = u_{2j-1}^{2n-2} + p (\delta^2)_{2j-1}^{2n-2}$$

From III. 12. 3,

$$u_{2j}^{2n} = u_{2j}^{2n-1} + p (\delta^2)_{2j}^{2n-1}$$

From III. 12. 2,

$$\begin{aligned} (1+2p) u_{2j}^{2n-1} &= u_{2j}^{2n-2} + p \left[u_{2j-1}^{2n-1} + u_{2j+1}^{2n-1} \right] = \\ &= u_{2j}^{2n-2} + p \left\{ u_{2j-1}^{2n-2} + p (\delta^2)_{2j-1}^{2n-2} + u_{2j+1}^{2n-2} + p (\delta^2)_{2j+1}^{2n-2} \right\} \end{aligned}$$

This is valid for $(2j+1) (\Delta x) \neq A$

$$\begin{aligned} (1+2p) \left(u_{2j}^{2n-1} - u_{2j}^{2n-2} \right) &= p \left\{ p (\delta^2)_{2j-1}^{2n-2} + p (\delta^2)_{2j+1}^{2n-2} + (\delta^2)_{2j}^{2n-2} \right\} \\ u_{2j}^{2n-1} &= u_{2j}^{2n-2} + \left(\frac{p}{1+2p} \right) \left\{ p (\delta^2)_{2j-1}^{2n-2} + p (\delta^2)_{2j+1}^{2n-2} + (\delta^2)_{2j}^{2n-2} \right\} \end{aligned}$$

For $(2j+1) (\Delta x) = A$,

$$\begin{aligned} (1+2p) u_{A-1}^{2n-1} &= u_{A-1}^{2n-2} + p \left\{ u_{A-2}^{2n-2} + p (\delta^2)_{A-2}^{2n-2} + u_A^{2n-1} \right\} \\ (1+2p) \left(u_{A-1}^{2n-1} - u_{A-1}^{2n-2} \right) &= p \left\{ p (\delta^2)_{A-2}^{2n-2} + (\delta^2)_{A-1}^{2n-2} + u_A^{2n-1} - u_A^{2n-2} \right\} \\ u_{A-1}^{2n-1} &= u_{A-1}^{2n-2} + \left(\frac{p}{1+2p} \right) \left\{ p (\delta^2)_{A-2}^{2n-2} + (\delta^2)_{A-1}^{2n-2} + \left(u_A^{2n-1} - u_A^{2n-2} \right) \right\} \end{aligned}$$

From III. 12. 4, we obtain in like fashion:

$$u_{2j-1}^{2n} = u_{2j-1}^{2n-1} + \left(\frac{p}{1+2p} \right) \left\{ p (\delta^2)_{2j-2}^{2n-1} + p (\delta^2)_{2j}^{2n-1} + (\delta^2)_{2j-1}^{2n-1} \right\}$$

For $j=1$, this becomes:

$$u_{\Delta x}^{2n} = u_{\Delta x}^{2n-1} + \left(\frac{p}{1+2p} \right) \left\{ \left(u_0^{2n} - u_0^{2n-1} \right) + p (\delta^2)_{2\Delta x}^{2n-1} + (\delta^2)_{\Delta x}^{2n-1} \right\}$$

Thus, we have these equations:

$$u_{2j-1}^{2n-1} = u_{2j-1}^{2n-2} + p (\delta^2)_{2j-1}^{2n-2} \quad (\text{III. 13. 1})$$

$$u_{2j}^{2n-1} = u_{2j}^{2n-2} + \left(\frac{p}{1+2p} \right) \left\{ p (\delta^2)_{2j-1}^{2n-2} + p (\delta^2)_{2j+1}^{2n-2} + (\delta^2)_{2j}^{2n-2} \right\}$$

- for $(2j+1) (\Delta x) \neq A$ (III. 13. 2)

$$u_{A-1}^{2n-1} = u_{A-1}^{2n-2} + \left(\frac{p}{1+2p} \right) \left\{ p (\delta^2)_{A-2}^{2n-2} + (\delta^2)_{A-1}^{2n-2} + \left(u_A^{2n-1} - u_A^{2n-2} \right) \right\} \quad \text{(III. 13. 3)}$$

and

$$u_{2j}^{2n} = u_{2j}^{2n-1} + p (\delta^2)_{2j}^{2n-1} \quad \text{(III. 13. 4)}$$

$$u_{2j-1}^{2n} = u_{2j-1}^{2n-1} + \left(\frac{p}{1+2p} \right) \left\{ p (\delta^2)_{2j-2}^{2n-1} + p (\delta^2)_{2j}^{2n-1} + (\delta^2)_{2j-1}^{2n-1} \right\}$$

- for $j \neq 1$ (III. 13. 5)

$$u_{\Delta x}^{2n} = u_{\Delta x}^{2n-1} + \left(\frac{p}{1+2p} \right) \left\{ \left(u_0^{2n} - u_0^{2n-1} \right) + p (\delta^2)_{2\Delta x}^{2n-1} + (\delta^2)_{\Delta x}^{2n-1} \right\} \quad \text{(III. 13. 6)}$$

For $n > 1$ we can further simplify equations III. 12. 1 through III. 12. 4. For $n > 1$, III. 12. 4 gives:

$$p u_{2j-2}^{2n-2} + (1-2p) u_{2j-1}^{2n-2} + p u_{2j}^{2n-2} = 2 u_{2j-1}^{2n-2} - u_{2j-1}^{2n-3},$$

or III. 12. 1 becomes:

$$u_{2j-1}^{2n-1} = 2 u_{2j-1}^{2n-2} - u_{2j-1}^{2n-3}$$

Likewise, using III. 12. 2 in III. 12. 3:

$$u_{2j}^{2n} = 2 u_{2j}^{2n-1} - u_{2j}^{2n-2}$$

Thus, we have this system:

$$\left. \begin{aligned} u_{2j-1}^{2n-1} &= 2 u_{2j-1}^{2n-2} - u_{2j-1}^{2n-3} \\ u_{2j}^{2n-1} &= p (\delta^2)_{2j}^{2n-1} + u_{2j}^{2n-2} \end{aligned} \right\} \quad n > 1 \quad \text{(III. 14. 1)}$$

$$\left. \begin{aligned} u_{2j-1}^{2n-1} &= 2 u_{2j-1}^{2n-2} - u_{2j-1}^{2n-3} \\ u_{2j}^{2n-1} &= p (\delta^2)_{2j}^{2n-1} + u_{2j}^{2n-2} \end{aligned} \right\} \quad \text{(III. 14. 2)}$$

and

$$\left. \begin{aligned} u_{2j}^{2n} &= 2 u_{2j}^{2n-1} - u_{2j}^{2n-2} \\ u_{2j-1}^{2n} &= p (\delta^2)_{2j-1}^{2n} + u_{2j-1}^{2n-1} \end{aligned} \right\} \quad n > 1 \quad \text{(III. 14. 3)}$$

$$\left. \begin{aligned} u_{2j}^{2n} &= 2 u_{2j}^{2n-1} - u_{2j}^{2n-2} \\ u_{2j-1}^{2n} &= p (\delta^2)_{2j-1}^{2n} + u_{2j-1}^{2n-1} \end{aligned} \right\} \quad \text{(III. 14. 4)}$$

Finally, we rewrite our equations in terms of the Δ_j^n operator:

$$\Delta_j^n = u_j^n - u_j^{n-1} \quad (\text{III. 15. 1})$$

Equation III. 14. 1 becomes:

$$\Delta_{2j-1}^{2n-1} = \Delta_{2j-1}^{2n-2} \quad \text{for } n > 1 \quad (\text{III. 15. 2})$$

Equation III. 14. 3 becomes:

$$\Delta_{2j}^{2n} = \Delta_{2j}^{2n-1} : n \geq 1 \quad (\text{III. 15. 3})$$

Equation III. 14. 2 becomes:

$$\begin{aligned} (1+2p) u_{2j}^{2n-1} &= p \left[u_{2j-1}^{2n-1} + u_{2j+1}^{2n-1} \right] + u_{2j}^{2n-2} = \\ &= p \left[\Delta_{2j-1}^{2n-1} + \Delta_{2j+1}^{2n-1} \right] + p \left[u_{2j-1}^{2n-2} + u_{2j+1}^{2n-2} \right] + u_{2j}^{2n-2} = \\ &= p \left[\Delta_{2j-1}^{2n-1} + \Delta_{2j+1}^{2n-1} \right] + p \left[\Delta_{2j-1}^{2n-2} + \Delta_{2j+1}^{2n-2} \right] + \\ &\quad + u_{2j}^{2n-2} + p \left[u_{2j-1}^{2n-3} + u_{2j+1}^{2n-3} \right] \\ &= p \left[\Delta_{2j-1}^{2n-1} + \Delta_{2j+1}^{2n-1} + \Delta_{2j-1}^{2n-2} + \Delta_{2j+1}^{2n-2} \right] + p (\delta^2)_{2j}^{2n-3} \\ &\quad + u_{2j}^{2n-2} + 2 p u_{2j}^{2n-3} \end{aligned}$$

Substituting III. 13. 4 for $p (\delta^2)_{2j}^{2n-3}$:

$$\begin{aligned} (1+2p) u_{2j}^{2n-1} &= p \left[\Delta_{2j-1}^{2n-1} + \Delta_{2j+1}^{2n-1} + \Delta_{2j-1}^{2n-2} + \Delta_{2j+1}^{2n-2} \right] + \Delta_{2j}^{2n-2} \\ &\quad + (1+2p) u_{2j}^{2n-2} - 2 p \left[u_{2j}^{2n-2} - u_{2j}^{2n-3} \right] \\ (1+2p) \Delta_{2j}^{2n-1} &= p \left[\Delta_{2j-1}^{2n-1} + \Delta_{2j+1}^{2n-1} + \Delta_{2j-1}^{2n-2} + \Delta_{2j+1}^{2n-2} \right] + (1-2p) \Delta_{2j}^{2n-2} \end{aligned}$$

$$\begin{aligned}
(1+2p) \Delta_{2j}^{2n-1} &= 2p \left[\Delta_{2j-1}^{2n-2} + \Delta_{2j+1}^{2n-2} \right] + (1-2p) \Delta_{2j}^{2n-2} \\
&+ p \left[\Delta_{2j-1}^{2n-1} - \Delta_{2j-1}^{2n-2} \right] + p \left[\Delta_{2j+1}^{2n-1} - \Delta_{2j+1}^{2n-2} \right]
\end{aligned}$$

From III. 15. 2 we see that the last two terms are zero except for the case where $(2j+1)(\Delta x) = A$.
Also, $\Delta_{2j}^{2n-2} = \Delta_{2j}^{2n-3}$:

$$(1+2p) \Delta_{2j}^{2n-1} = 2p \left[\Delta_{2j-1}^{2n-2} + \Delta_{2j+1}^{2n-2} \right] + (1-2p) \Delta_{2j}^{2n-3}$$

$$\text{for } n > 1, (2j+1)(\Delta x) \neq A \quad (\text{III. 15. 4. 1})$$

$$(1+2p) \Delta_{A-1}^{2n-1} = 2p \left[\Delta_{A-2}^{2n-2} + \Delta_A^{2n-2} \right] + (1-2p) \Delta_{A-1}^{2n-3} + p \left[\Delta_A^{2n-1} - \Delta_A^{2n-2} \right] \text{ for } n > 1$$

(III. 15. 4. 2)

Equation III. 14. 4 becomes:

$$\begin{aligned}
(1+2p) \Delta_{2j-1}^{2n} &= -2p u_{2j-1}^{2n-1} + p \left[u_{2j-2}^{2n} + u_{2j}^{2n} \right] = \\
&= -2p u_{2j-1}^{2n-1} + p \left[\Delta_{2j-2}^{2n} + \Delta_{2j}^{2n} \right] + p \left[u_{2j-2}^{2n-1} + u_{2j}^{2n-1} \right] \\
&= p \left[\Delta_{2j-2}^{2n} + \Delta_{2j}^{2n} + \Delta_{2j-2}^{2n-1} + \Delta_{2j}^{2n-1} \right] - 2p \Delta_{2j-1}^{2n-1} + p (\delta^2)_{2j-1}^{2n-2}
\end{aligned}$$

Substituting III. 13. 1:

$$\begin{aligned}
(1+2p) \Delta_{2j-1}^{2n} &= p \left[\Delta_{2j-2}^{2n} + \Delta_{2j}^{2n} + \Delta_{2j-2}^{2n-1} + \Delta_{2j}^{2n-1} \right] + (1-2p) \Delta_{2j-1}^{2n-1} \\
(1+2p) \Delta_{2j-1}^{2n} &= 2p \left[\Delta_{2j-2}^{2n-1} + \Delta_{2j}^{2n-1} \right] + (1-2p) \Delta_{2j-1}^{2n-1} \\
&+ p \left[\Delta_{2j-2}^{2n} - \Delta_{2j-2}^{2n-1} \right] + p \left[\Delta_{2j}^{2n} - \Delta_{2j}^{2n-1} \right]
\end{aligned}$$

Suppose we now assume that:

$$\Delta_j^0 = \Delta_j^1 \quad (\text{III. 15. 5})$$

From III. 15. 3, the last two terms of above equation are zero for $j > 1$. Using III. 15. 2 also:

$$(1+2p) \Delta_{2j-1}^{2n} = 2p \left[\Delta_{2j-2}^{2n-1} + \Delta_{2j}^{2n-1} \right] + (1-2p) \Delta_{2j-1}^{2n-2} \text{ for } j > 1, n \geq 1 \quad (\text{III. 15. 6. 1})$$

$$\begin{aligned}
(1+2p) \Delta_{\Delta x}^{2n} &= 2p \left[\Delta_0^{2n-1} + \Delta_{2\Delta x}^{2n-1} \right] + (1-2p) \Delta_{\Delta x}^{2n-1} + \\
&+ p \left[\Delta_0^{2n} - \Delta_0^{2n-1} \right] \text{ for } n \geq 1
\end{aligned} \tag{III. 15. 6. 2}$$

To complete the definition of the Δ_j^n operator we need to specify Δ_j^1 so as to be consistent with the u_j^n :

From III. 13. 1, III. 13. 2, III. 13. 3:

$$\Delta_{2j-1}^1 = p (\delta^2)_{2j-1}^0 \tag{III. 15. 7. 1}$$

$$\Delta_{2j}^1 = \left(\frac{p}{1+2p} \right) \left\{ p (\delta^2)_{2j-1}^0 + p (\delta^2)_{2j+1}^0 + (\delta^2)_{2j}^0 \right\} \text{ for } (2j+1) (\Delta x) \neq A \tag{III. 15. 7. 2}$$

$$\Delta_{A-1}^1 = \left(\frac{p}{1+2p} \right) \left\{ p (\delta^2)_{A-2}^0 + (\delta^2)_{A-1}^0 + \Delta_A^1 \right\} \tag{III. 15. 7. 3}$$

We now summarize the definition of Δ_j^n :

$$1. \quad \Delta_0^n = u_0^n - u_0^{n-1} : \text{ known from III. 10. 2} \tag{III. 16. 1}$$

$$2. \quad \Delta_A^n = u_A^n - u_A^{n-1} : \text{ known from III. 10. 3} \tag{III. 16. 2}$$

$$3. \quad \Delta_j^0 = \Delta_j^1 \tag{III. 16. 3}$$

$$4. \quad \Delta_{2j-1}^1 = p (\delta^2)_{2j-1}^0 : \text{ known from III. 10. 4} \tag{III. 16. 4}$$

$$\begin{aligned}
\Delta_{2j}^1 &= \left(\frac{p}{1+2p} \right) \left\{ p (\delta^2)_{2j-1}^0 + p (\delta^2)_{2j+1}^0 + (\delta^2)_{2j}^0 \right\} \text{ for } (2j+1) (\Delta x) \neq A: \\
&\text{known from III. 10. 4}
\end{aligned} \tag{III. 16. 5}$$

$$\Delta_{A-1}^1 = \left(\frac{p}{1+2p} \right) \left\{ p (\delta^2)_{A-2}^0 + (\delta^2)_{A-1}^0 + \Delta_A^1 \right\} : \text{ known from III. 10. 4} \tag{III. 16. 6}$$

$$5. \quad \Delta_{2j-1}^{2n-1} = \Delta_{2j-1}^{2n-2} : n \geq 1 \tag{III. 16. 7}$$

$$6. \quad \Delta_{2j}^{2n} = \Delta_{2j}^{2n-1} : n \geq 1 \tag{III. 16. 8}$$

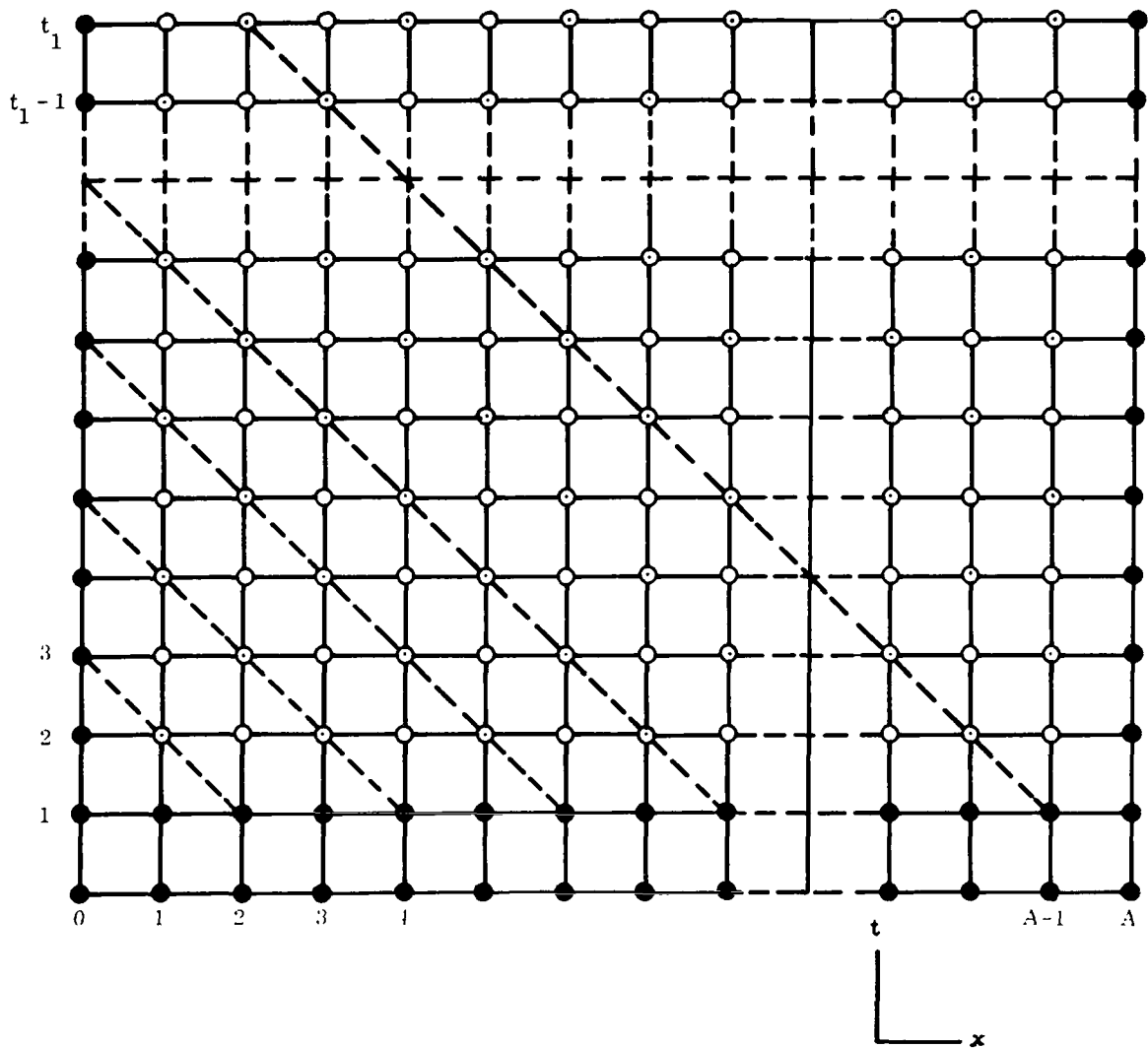
$$\begin{aligned}
7. \quad (1+2p) \Delta_{2j}^{2n-1} &= 2p \left[\Delta_{2j-1}^{2n-2} + \Delta_{2j+1}^{2n-2} \right] + (1-2p) \Delta_{2j}^{2n-3} \\
&\text{for } n > 1, (2j+1) (\Delta x) \neq A
\end{aligned} \tag{III. 16. 9}$$

$$\begin{aligned}
8. \quad (1+2p) \Delta_{A-1}^{2n-1} &= 2p \left[\Delta_{A-2}^{2n-2} + \Delta_A^{2n-2} \right] + (1-2p) \Delta_{A-1}^{2n-3} \\
&+ p \left[\Delta_A^{2n-1} - \Delta_A^{2n-2} \right] \text{ for } n > 1 \quad (\text{III. 16. 10})
\end{aligned}$$

$$9. \quad (1+2p) \Delta_{2j-1}^{2n} = 2p \left[\Delta_{2j-2}^{2n-1} + \Delta_{2j}^{2n-1} \right] + (1-2p) \Delta_{2j-1}^{2n-2} \text{ for } j > 1, n \geq 1 \quad (\text{III. 16. 11})$$

$$\begin{aligned}
10. \quad (1+2p) \Delta_{\Delta x}^{2n} &= 2p \left[\Delta_0^{2n-1} + \Delta_{2\Delta x}^{2n-1} \right] + (1-2p) \Delta_{\Delta x}^{2n-2} + \\
&+ p \left[\Delta_0^{2n} - \Delta_0^{2n-1} \right] \text{ for } n \geq 1 \quad (\text{III. 16. 12})
\end{aligned}$$

DIAGRAM I



Δ_j^n for black points are assumed known III. 16. 1, III. 16. 2, III. 16. 3, III. 16. 4
 III. 16. 5, III. 16. 6

Δ_j^n for "O" points are obtained from III. 16. 7, III. 16. 8 (near $x = A$ and $t = t$, "O" and "O" could be reversed)

Δ_j^n for "O" points are obtained from III. 16. 9, III. 16. 10, III. 16. 11, III. 16. 12.

E. We now investigate truncation error and convergence of the difference equation.

For truncation error we look at III. 13. 1 through III. 13. 4.

We assume known:

$$\frac{(\delta^2)_j^n}{(\Delta x)^2} = (u_{xx})_j^n + O(\Delta x^2)$$

$$\frac{u_j^{n+1} - u_j^n}{\Delta t} = (u_t)_j^n + O(\Delta t)$$

Equation III. 13. 1 becomes:

$$\frac{u_{2j-1}^{2n-1} - u_{2j-1}^{2n-2}}{\Delta t} = \beta_1 \frac{(\delta^2)_{2j-1}^{2n-2}}{(\Delta x)^2}$$

$$(u_t)_{2j-1}^{2n-2} + O(\Delta t) = \beta_1 (u_{xx})_{2j-1}^{2n-2} + O(\Delta x^2)$$

If we have exact values at time $2n-2$, $(u_t)_{2j-1}^{2n-2} = \beta_1 (u_{xx})_{2j-1}^{2n-2}$, or the truncation error is $O(\Delta t) + O(\Delta x^2)$.

Equation III. 13. 4 is similar.

Equation III. 13. 2 is slightly more complicated:

$$(u_{xx})_{2j+1}^{2n-2} = (u_{xx})_{2j}^{2n-2} + (\Delta x) (u_{xxx})_{2j}^{2n-2} + O(\Delta x^2)$$

$$(u_{xx})_{2j-1}^{2n-2} = (u_{xx})_{2j}^{2n-2} - (\Delta x) (u_{xxx})_{2j}^{2n-2} + O(\Delta x^2)$$

$$\frac{p (u_{xx})_{2j+1}^{2n-2} + p (u_{xx})_{2j-1}^{2n-2} + (u_{xx})_{2j}^{2n-2}}{(1+2p)} = (u_{xx})_{2j}^{2n-2} + \left(\frac{p}{1+2p} \right) O(\Delta x^2)$$

Note that $\left(\frac{p}{1+2p} \right)$ is bounded for $p > 0$.

$$(u_t)_{2j}^{2n-2} = \frac{p (u_{xx})_{2j+1}^{2n-2} + p (u_{xx})_{2j-1}^{2n-2} + (u_{xx})_{2j}^{2n-2}}{(1+2p)} \beta_1 + O(\Delta x^2)$$

$$\frac{u_{2j}^{2n-1} - u_{2j}^{2n-2}}{\Delta t} = \left(\frac{1}{1+2p} \right) \left[p (\delta^2)_{2j+1}^{2n-2} + p (\delta^2)_{2j-1}^{2n-2} + (\delta^2)_{2j}^{2n-2} \right] \frac{\beta_1}{(\Delta x)^2} + O(\Delta t) + O(\Delta x^2)$$

since $p = \frac{\Delta t \beta_1}{(\Delta x)^2}$, we obtain truncation error $O(\Delta t) + O(\Delta x^2)$.

Equation III. 13. 5 is similar.

Equation III. 13. 3 becomes:

$$\begin{aligned} \frac{u_{A-1}^{2n-1} - u_{A-1}^{2n-2}}{\Delta t} &= \left(\frac{\beta_1}{1+2p} \right) \left[p \frac{(\delta^2)_{A-2}^{2n-2}}{(\Delta x)^2} + \frac{(\delta^2)_{A-1}^{2n-2}}{(\Delta x)^2} + p (u_{xx})_A^{2n-2} \right] \\ &\quad + O(\Delta t) + O(\Delta x^2) \\ p_1 (u_{xx})_A^{2n-2} &= (u_t)_A^{2n-2} = \frac{u_A^{2n-1} - u_A^{2n-2}}{\Delta t} + O(\Delta t) \\ \frac{u_{A-1}^{2n-1} - u_{A-1}^{2n-2}}{\Delta t} &= \left(\frac{\beta_1}{1+2p} \right) \frac{\left[p (\delta^2)_{A-2}^{2n-2} + (\delta^2)_{A-1}^{2n-2} + (u_A^{2n-1} - u_A^{2n-2}) \right]}{(\Delta x)^2} \\ &\quad + O(\Delta t) + O(\Delta x^2) \end{aligned}$$

Thus, we again have truncation error $O(\Delta t) + O(\Delta x^2)$, and equation III. 13. 6 is similar.

Summarizing the truncation error:

Equations III. 13. 1 through III. 13. 6 give truncation error

$$O(\Delta t) + O(\Delta x^2).$$

We conclude that the consistency condition of Richtmyer is satisfied (p. 55-58).

We now investigate the stability of our system. Because of the non-symmetric definition, equations III. 13. 1 through III. 13. 6 do not seem appropriate for the Fourier Series approach of Richtmyer. Thus, we attempt to use the other criterion. Accordingly, we study the Δ_j^n system defined by equations III. 16. 1 through III. 16. 12. We first note that the "O" points (diagram 1) form a system independent of the "O" points. The equations for these points involve other "O" points and boundary points. Note also that III. 16. 9 and III. 16. 11 are the same except for subscripts, and they are the equations of Dufort-Frankel except

we have replaced p with $2p$ (see equation III. 2). Thus, $\frac{\Delta_j^n}{\Delta t}$ converges to a solution of III. 1 at alternate points if $\frac{\Delta t}{\Delta x} \rightarrow 0$. The remaining terms can have an additional error of at most $O(\Delta t)$. Thus, $\Delta_j^n/\Delta t$ converges to a solution of III. 1 at all points. Now, by the criterion of Part C, the difference equation III. 12. 1 through III. 12. 4 converges uniformly to a solution of III. 1 if $\frac{\Delta t}{\Delta x} \rightarrow 0$.

At the beginning of this paper we mentioned two questions: one was convergence, which we have already discussed; the other was "rate of convergence." A major criticism by Forsythe and Wasow of the methods used here is that no effective technique is available to study this problem, and this criticism is probably valid. A natural approach might be to study Δ_j^n . The problem would be to specify $\epsilon > 0$, and then find $\overline{\Delta t} \rightarrow \Delta t < \overline{\Delta t} \Rightarrow |\Delta_j^n| < \epsilon$. For our difference equation, since $\max |\Delta_j^n| = O(\Delta t)$, we can state that all interior points will converge as fast as the boundary points; it would seem unreasonable to expect anything more than this. As mentioned earlier, the usual explicit and implicit schemes can also be written in terms of Δ_j^n . The result would be the same. If convergent, the interior points converge as fast as the boundary points. In light of the previous boundedness proof for the Dufort-Frankel scheme, a similar statement is true here also: from equation III. 9, we would have $|\Delta_j^n| \leq M_1 + \epsilon(\Delta t) = O(\Delta t) + \epsilon(\Delta t) - \epsilon(\Delta x) \rightarrow 0$, so convergence probably would not be as fast. (Clearly, a rigorous result would require tying the rate of convergence of Δ_j^n to u_j^n ; this I was unable to do.)

Summarizing, the difference equation we have presented (equations III. 12. 1 through III. 12. 4) has been shown to be convergent if $\frac{\Delta t}{\Delta x} \rightarrow 0$. We feel it has certain advantages over the equations now in use:

1. The usual explicit equation has a much more stringent convergence criterion.
2. The usual implicit equation is hard to extend to non-linear cases. (The equation presented here is explicit in the usual sense as in the Dufort-Frankel scheme; however, point by point iterations are necessary in non-linear cases.)
3. The Dufort-Frankel scheme has a worse truncation error term, and does not appear to converge as rapidly. Actual use has revealed the convergence problem quite strongly.

SECTION IV

NUMERICAL SOLUTION OF ENERGY EQUATION AND BOUNDARY CONDITIONS

In Part A of this section we discuss the numerical approximations to the parabolic partial differential equation (the energy equation). In Part B, Part C, and Part D we discuss the boundary conditions: these include the frontface, backface, interfaces, and the air gap. In Part E we discuss convergence problems arising from the simultaneous solution of the differential equation and the boundary condition.

A. The equation to be solved in A15 (Appendix B1), which is obtained from II. 4 through the space transformation (see Appendix B2):

$$T_t = \beta_1 T_{\eta\eta} + \beta_2 (T_\eta)^2 + \beta_3 T_\eta + \beta_4 \quad (\text{IV. 1})$$

The β_i are assumed to be functions of t , η , T . Note that density, ρ , appears in these coefficients. Its calculation can involve another partial differential equation. The problem of solving these simultaneously is discussed in Section V.

The difference equation used is described in Section III for the case where $\beta_2 = \beta_3 = \beta_4 = 0$ and β_1 is constant. Briefly, we alternate the "usual" explicit and implicit difference equations. The extension to non-constant β_i is straightforward: it simply means they must be evaluated at the proper time level. However, there still appears to be much freedom in the choice of an approximation to T_η . The terms $\beta_2 (T_\eta)^2$ and $\beta_3 T_\eta$ will now be discussed. The $\beta_3 T_\eta$ term has produced difficulties. Suppose now $\beta_2 = \beta_4 = 0$. The implicit scheme for IV. 1 would give:

$$T_j^{n+1} = T_j^n + \frac{\Delta t \beta_1}{(\Delta \eta)^2} \left[T_{j+1}^{n+1} - 2 T_j^{n+1} + T_{j-1}^{n+1} \right] + \Delta t \beta_3 T_\eta$$

The "best" approximation to T_η would be this one:

$$T_\eta = \frac{T_{j+1}^{n+1} - T_{j-1}^{n+1}}{2 \Delta \eta} .$$

Then, with $p_1 = \frac{\Delta t \beta_1}{\Delta \eta^2}$ and $p_2 = \frac{\Delta t \beta_3}{\Delta \eta}$, we obtain:

$$T_j^{n+1} = T_j^n + p_1 (T_{j+1}^{n+1} - 2 T_j^{n+1} + T_{j-1}^{n+1}) + p_2 \Delta \eta (T_{j+1}^{n+1} - T_{j-1}^{n+1})$$

or

$$(1+2p_1) T_j^{n+1} = T_j^n + (p_1 + p_2 \Delta \eta) T_{j+1}^{n+1} + (p_1 - p_2 \Delta \eta) T_{j-1}^{n+1}$$

In this form it is not necessary to satisfy a boundedness condition. It would seem that the $p_2 \Delta \eta$ term should not affect the stability of the system: Richtmyer (reference 4, p. 98) shows that for constant β_1 this term can be ignored in so far as stability is concerned. Since stability concerns only the behavior as Δt and $\Delta \eta$ approach zero, this is not unreasonable: if $\Delta \eta$ is small enough, $p_1 - p_2 \Delta \eta > 0$ and a boundedness condition is satisfied. However, we have encountered cases where this term caused oscillations which stopped the run. It is possible to maintain boundedness for all values of $\Delta \eta$ by changing the approximation to T_η :

$$\text{Let } T_\eta = \alpha_1 \left(\frac{T_{j+1}^{n+1} - T_j^{n+1}}{\Delta \eta} \right) + \alpha_2 \left(\frac{T_j^{n+1} - T_{j-1}^{n+1}}{\Delta \eta} \right) \quad (\text{IV. 2})$$

We then obtain:

$$\begin{aligned} T_j^{n+1} &= T_j^n + p_1 (T_{j+1}^{n+1} - 2 T_j^{n+1} + T_{j-1}^{n+1}) + p_2 \Delta \eta \left[\alpha_1 T_{j+1}^{n+1} + \right. \\ &\quad \left. + (\alpha_2 - \alpha_1) T_j^{n+1} - \alpha_2 T_{j-1}^{n+1} \right] \\ \left[1 + 2p_1 + (\alpha_1 - \alpha_2) p_2 \Delta \eta \right] T_j^{n+1} &= T_j^n + (p_1 + \alpha_1 p_2 \Delta \eta) T_{j+1}^{n+1} + (p_1 - \alpha_2 p_2 \Delta \eta) T_{j-1}^{n+1} \end{aligned}$$

We want to choose α_1 and α_2 so as to have all coefficients positive:

a. Suppose $p_2 > 0$:

$$\text{Let } \alpha_2 = \min \left[\frac{1}{2}, \frac{p_1}{p_2 \Delta \eta} \right]$$

$$\alpha_1 = 1 - \alpha_2$$

$$\text{Then, } \alpha_2 \leq \frac{1}{2} \text{ and } \alpha_1 - \alpha_2 > 0$$

Thus, all coefficients are positive.

b. Suppose $p_2 < 0$:

$$\text{Let } \alpha_1 = \min \left[\frac{1}{2}, \frac{p_1}{|p_2| \Delta \eta} \right]$$

$$\alpha_2 = 1 - \alpha_1$$

Then, $\alpha_1 - \alpha_2 < 0$, and again all coefficients are positive.

Summarizing, we approximate T_η by IV.2 where α_1 and α_2 are defined as follows:

$$\alpha = \min \left[\frac{1}{2} ; \frac{p_1}{|p_2| \Delta \eta} \right]$$

$$\left. \begin{array}{l} \alpha_2 = \alpha \\ \alpha_1 = 1 - \alpha \end{array} \right\} p_2 > 0$$

$$\left. \begin{array}{l} \alpha_1 = \alpha \\ \alpha_2 = 1 - \alpha_1 \end{array} \right\} p_2 < 0$$

The $\beta_2 (T_\eta)^2$ has also produced difficulties. The problem here has been somewhat different: It appears that this term can produce a multiple-valued solution to the difference equation. One of these solutions is clearly "incorrect," so the problem is to cause the iteration procedure to converge to the correct value. Consider now equation IV.1 with $\beta_4 = 0$.

$$\text{Let } \bar{\beta}_2 = \frac{T_{j+1}^{n+1} - T_{j-1}^{n+1}}{2 \Delta \eta}$$

(We are considering only the implicit case.) Then IV.1 takes this form:

$$T_t = \beta_1 T_{\eta\eta} + \beta_2 \bar{\beta}_2 T_\eta + \beta_3 T_\eta$$

or

$$T_t = \beta_1 T_{\eta\eta} + (\beta_2 \bar{\beta}_2 + \beta_3) T_\eta$$

If we now let $\beta_2 \bar{\beta}_2 + \beta_3$ replace β_3 in our previous discussion, we can apply the previous results so as to be sure T_j^{n+1} remains in the range of its neighboring values. This should prevent convergence to a spurious solution.

We now substitute all approximations into IV.1. Let

$$\delta = \begin{cases} 0: & \text{explicit scheme} \\ 1: & \text{implicit scheme} \end{cases} \quad (\text{IV. 3})$$

$$r_0 = \frac{\Delta t}{(\Delta \eta)^2} \quad (\text{IV. 4})$$

$$r_1 = \frac{T_{j+1}^{n+\delta} - T_{j-1}^{n+\delta}}{2 \Delta \eta} \quad (\text{IV. 5})$$

$$r_2 = T_{j+1}^{n+\delta} + T_{j-1}^{n+\delta} \quad (\text{IV. 6})$$

$$\left. \begin{aligned} \bar{\beta}_3 &= \beta_3 + \beta_2 r_1 \\ \alpha &= \min \left[\frac{1}{2} ; \frac{\beta_1}{|\bar{\beta}_3| \Delta \eta} \right] \\ \alpha_2 &= \alpha \\ \alpha_1 &= 1 - \alpha_2 \end{aligned} \right\} \bar{\beta}_3 > 0$$

$$\left. \begin{aligned} \alpha_1 &= \alpha \\ \alpha_2 &= 1 - \alpha_1 \end{aligned} \right\} \bar{\beta}_3 < 0 \quad (\text{IV. 7})$$

$$T_j^{n+1} = T_j^n + \Delta t \left\{ \frac{\beta_1}{(\Delta \eta)^2} \left[r_2^{-2} T_j^{n+\delta} \right] + \right.$$

$$\left. + \frac{\bar{\beta}_3}{\Delta \eta} \left[\alpha_1 T_{j+1}^{n+\delta} - \alpha_2 T_{j-1}^{n+\delta} + (\alpha_2 - \alpha_1) T_j^{n+\delta} \right] + \beta_4 \right\}$$

$$T_j^{n+1} = T_j^n + r_o \left\{ (\beta_1 + \alpha_1 \Delta \eta \bar{\beta}_3) T_{j+1}^{n+\delta} + (\beta_1 - \alpha_2 \Delta \eta \bar{\beta}_3) T_{j-1}^{n+\delta} \right.$$

$$\left. + \left[(\alpha_2 - \alpha_1) \bar{\beta}_3 \Delta \eta - 2 \beta_1 \right] T_j^{n+\delta} + \Delta t \beta_4 \right\}$$

Let

$$r_3 = T_j^n + r_o (\beta_1 + \alpha_1 \Delta \eta \bar{\beta}_3) T_{j+1}^{n+\delta} + r_o (\beta_1 - \alpha_2 \Delta \eta \bar{\beta}_3) T_{j-1}^{n+\delta} + \Delta \eta \beta_4 \quad (\text{IV. 8})$$

Thus,

$$T_j^{n+1} = \left\{ \begin{aligned} &r_o \left[(\alpha_2 - \alpha_1) \Delta \eta \bar{\beta}_3 - 2 \beta_1 \right] T_j^n + r_3: \text{ explicit} \\ &\frac{r_3}{1 + r_o \left[2 \beta_1 + (\alpha_1 - \alpha_2) \Delta \eta \bar{\beta}_3 \right]} : \text{ implicit} \end{aligned} \right\} \quad (\text{IV. 9})$$

Note that the explicit equation requires that the β_i be evaluated at (n, j) . Since everything is known at time n , this is not a problem. The implicit calculation requires that the β_i be evaluated at $(n+1, j)$. Since this involves the unknown, T_j^{n+1} , an iteration is required here. Another problem arising here is the rate of melt, which appears in the β_i . Since we need it at time $n+1$, and since it is a function of the values at $n+1$, an over-all iteration for all points calculated by the implicit scheme would be required: the variable being iterated on would be the rate of melt. We have encountered cases where

this has been necessary. All iteration problems are handled by the method described in Appendix B3.

Since the explicit and implicit calculations are alternated, a simplification of the explicit equations is possible. Note that $\frac{r_3 - T_j^n}{\Delta t}$ used for an implicit calculation for T_j^{n+1} remains unchanged for the explicit calculation for T_j^{n+2} . Let

$$\Delta t_o = t_{n+2} - t_{n+1}$$

$$\Delta t_{-1} = t_{n+1} - t_n$$

From IV. 9,

$$T_j^{n+1} = \frac{\overline{r_3}}{1 + \overline{r_o} \left[2 \beta_1 + (\alpha_1 - \alpha_2) \Delta \eta \overline{\beta_3} \right]}$$

$$T_j^{n+2} = r_3 + r_o \left[(\alpha_2 - \alpha_1) \Delta \eta \overline{\beta_3} - 2 \beta_1 \right] T_j^{n+1}$$

as noted above,

$$1. \quad \overline{r_3} - T_j^n = \frac{\Delta t_{-1}}{\Delta t_o} (r_3 - T_j^{n+1})$$

$$2. \quad \overline{r_o} = \frac{\Delta t_{-1}}{\Delta t_o} r_o$$

Then,

$$T_j^{n+2} = \frac{\Delta t_o}{\Delta t_{-1}} (\overline{r_3} - T_j^n) + T_j^{n+1} - r_o \left[(\alpha_1 - \alpha_2) \Delta \eta \overline{\beta_3} + 2 \beta_1 \right] T_j^{n+1}$$

and

$$- \overline{r_o} \left[(\alpha_1 - \alpha_2) \Delta \eta \overline{\beta_3} + 2 \beta_1 \right] = T_j^{n+1} = T_j^{n+1} - \overline{r_3}$$

$$\begin{aligned} T_j^{n+2} &= T_j^{n+1} + \frac{\Delta t_o}{\Delta t_{-1}} (\overline{r_3} - T_j^n) + \frac{\Delta t_o}{\Delta t_{-1}} (T_j^{n+1} - \overline{r_3}) \\ &= \left(1 + \frac{\Delta t_o}{\Delta t_{-1}} \right) T_j^{n+1} - \left(\frac{\Delta t_o}{\Delta t_{-1}} \right) T_j^n \end{aligned}$$

Thus, after the first time step we have:

$$T_j^{n+1} = \begin{cases} \left(1 + \frac{\Delta t_o}{\Delta t_{-1}} \right) T_j^n - \left(\frac{\Delta t_o}{\Delta t_{-1}} \right) T_j^{n-1} : \text{explicit} \\ \frac{r_3}{1 + r_o \left[2 \beta_1 + (\alpha_1 - \alpha_2) \Delta \eta \overline{\beta_3} \right]} : \text{implicit} \end{cases} \quad (\text{IV. 10})$$

B. We consider now the boundary condition at the frontface. The two possibilities are given in II. A. 2. The first, reading in the frontface temperature as a function of time, presents no problem. The second is of this form:

$$\left(-k \frac{\partial T}{\partial x} \right) = f(t, T_o^{n+1})$$

after transformations, using B1.2 and B2.7, we obtain:

$$-k \eta_x T_\eta = f(t, T_o^{n+1})$$

We use this approximation for T_η at $\eta = 0$:

$$T_\eta = \alpha_3 \left[\frac{-3 T_o^{n+1} + 4 T_1^{n+1} - T_2^{n+1}}{2 \Delta \eta_1} \right] + (1-\alpha_3) \left[\frac{T_2^{n+1} - T_o^{n+1}}{2 \Delta \eta_1} \right]$$

$\alpha_3 = 1$ gives equation B4.3

$$\alpha_3 = \frac{1}{2} \text{ gives } T_\eta = \frac{T_1^{n+1} - T_o^{n+1}}{\Delta \eta_1}$$

Normally $\alpha_3 = 1$. The occasional necessity for other values of α_3 is discussed in Part E of this section.

Substituting,

$$\begin{aligned} -\frac{k \eta_x}{2 \Delta \eta_1} \left[-(1+2\alpha_3) T_o^{n+1} + 4 \alpha_3 T_1^{n+1} + (1-2\alpha_3) T_2^{n+1} \right] &= f \\ T_o^{n+1} &= \frac{2 \Delta \eta_1 f}{k \eta_x (1+2\alpha_3)} + \frac{1}{1+2\alpha_3} \left[4 \alpha_3 T_1^{n+1} + (1-2\alpha_3) T_2^{n+1} \right] \end{aligned} \quad (\text{IV. 11})$$

This is now of the form:

$$T_o^{n+1} = g(T_o^{n+1})$$

and so it is solved by the method described in Appendix B3. Note that if T_1^{n+1} is to be obtained from the implicit equation, then IV. 10 and IV. 11 must be solved simultaneously for T_1^{n+1} and T_o^{n+1} . This problem is again solved by the method of Appendix B3. For each guess at T_o^{n+1} which is obtained in converging to a solution of IV. 11, T_1^{n+1} is obtained from IV. 10.

It should also be noted that if pressures are being computed, p_1^{n+1} would need to be obtained for each guess at T_o^{n+1} and T_1^{n+1} . In addition, if charring is occurring, for each

guess at T_0^{n+1} and T_1^{n+1} , ρ_0^{n+1} and ρ_1^{n+1} must be obtained from V.11 and V.12. Finally, an outer iteration, for the rate of melt, may be occurring over the whole system.

The function, f , which appears in IV.11 is usually \dot{q}_{net} (see II.C). However, for the case where we melt at a fixed temperature, f involves the rate of melt also. In this case, IV.11 is used to obtain the rate of melt (after reaching melting temperature).

C. Consider now the interface boundary conditions. From paragraph II.A.5 we have this equation:

$$(-k T_x)_- - C_i T_t = (-k T_x)_+$$

Let T be temperature of interface

Let T_{-1} be temperature at node before interface

Let T_{-2} be temperature at second node before interface.

etc.

After transformations, using A.2, A.4, B.7, and B.8,

$$(-k \eta_x T_\eta)_- - C_i (\eta_t T_\eta + T_t) = (-k \eta_x T_\eta)_+$$

Note that η_t at $\eta=1$ in first layer is zero. Also, since no transformation, except the normalizing one, is made in layers past the first, $\eta_t = 0$ in all interface equations. Note also that $(\eta_x)_-$ is not the same as $(\eta_x)_+$, even though they are evaluated at the same point. At any rate the equation to be solved is:

$$(-k \eta_x T_\eta)_- - C_i T_t = (-k \eta_x T_\eta)_+ \quad (\text{IV.12})$$

We approximate $(T_\eta)_-$ with this equation:

$$(T_\eta)_- = \frac{T_{-2}^{n+1} - 4 T_{-1}^{n+1} + 3 T^{n+1}}{2 \Delta \eta_-}$$

(This is equation B4.7 in Appendix B4.)

$\Delta \eta_-$ is $\Delta \eta$ for layer in front of the interface.

We approximate $(T_\eta)_+$ with this equation:

$$(T_\eta)_+ = - \frac{-3 T^{n+1} + 4 T_1^{n+1} - T_2^{n+1}}{2 \Delta \eta_+}$$

(This is equation B4.3 in Appendix B4.)

$\Delta \eta_+$ is $\Delta \eta$ for layer past the interface.

We approximate T_t with this equation:

$$T_t = \gamma_4 T^{n-1} + \gamma_5 T^n + \gamma_6 T^{n+1} \quad (\text{IV. 13})$$

where

$$\gamma_4 = \frac{\Delta t_o}{\Delta t_{-1} (\Delta t_{-1} + \Delta t_o)}$$

$$\gamma_5 = - \frac{\Delta t_o + \Delta t_{-1}}{\Delta t_o \Delta t_{-1}}$$

$$\gamma_6 = \frac{\Delta t_{-1} + 2 \Delta t_o}{\Delta t_o (\Delta t_o + \Delta t_{-1})}$$

$$\Delta t_o = t_{n+1} - t_n$$

$$\Delta t_{-1} = t_n - t_{n-1}$$

(This is equation B4.6 in Appendix B4.)

If we are at the first time step,

$$\gamma_4 = 0$$

$$\gamma_5 = - \frac{1}{\Delta t_o}$$

$$\gamma_6 = \frac{1}{\Delta t_o}$$

(This is equation B4.8 in Appendix B4.)

Substituting into IV. 12,

$$\begin{aligned} & \left(\frac{-k \eta_x}{2 \Delta \eta} \right)_- \left[T_{-2}^{n+1} - 4 T_{-1}^{n+1} + 3 T^{n+1} \right] \\ & - C_i \left[\gamma_4 T^{n-1} + \gamma_5 T^n + \gamma_6 T^{n+1} \right] \\ & = \left(\frac{-k \eta_x}{2 \Delta \eta} \right)_+ \left[-3 T^{n+1} + 4 T_1^{n+1} - T_2^{n+1} \right] \end{aligned}$$

Let

$$B_1 = \left(\frac{-k \eta_x}{2 \Delta \eta} \right)_-$$

$$B_2 = \left(\frac{-k \eta_x}{2 \Delta \eta} \right)_+$$

Then,

$$\begin{aligned} \left[3 B_1 - C_i \gamma_6 + 3 B_2 \right] T^{n+1} = & B_1 \left(4 T_{-1}^{n+1} - T_{-2}^{n+1} \right) + C_i (\gamma_4 T^{n-1} + \gamma_5 T^n) + \\ & + B_2 (4 T_1^{n+1} - T_2^{n+1}) \end{aligned}$$

or,

$$T^{n+1} = \frac{B_1 (4 T_{-1}^{n+1} - T_{-2}^{n+1}) + C_i (\gamma_4 T^{n-1} + \gamma_5 T^n) + B_2 (4 T_1^{n+1} - T_2^{n+1})}{3 B_1 - C_i \gamma_6 + 3 B_2} \quad (\text{IV. 14})$$

Equation IV.14 represents an implicit equation in T^{n+1} : B_1 , B_2 , and C_i are functions of T^{n+1} . However, at present we do not solve this iteration problem. Thus far we have encountered no cases with enough sensitivity at the interfaces to necessitate a more exact solution. The program evaluates B_1 , B_2 , and C_i with a guess at T^{n+1} .

As in the frontface equation, we may need to solve simultaneously for T^{n+1} , T_{-1}^{n+1} , and T_{+1}^{n+1} .

At the backface we have two boundary conditions. The first, reading in the temperature as a function of time, is straightforward. The second is the following (see paragraph II. A. 6 in Section II):

$$(-k T_x) - C_i T_t = \dot{q}(t)$$

as before, after transformations,

$$-k \eta_x T_\eta - C_i T_t = \dot{q}(t) \quad (\text{IV. 15})$$

We see that IV.15 is the same as IV.12, except that $\dot{q}(t)$ replaces $(-k \eta_x T_\eta)_+$. Proceeding with the same approximations as before, and letting:

$$B_1 = \frac{-k \eta_x}{2 \Delta \eta}$$

we obtain:

$$T^{n+1} = \frac{B_1 (4 T_{-1}^{n+1} - T_{-2}^{n+1}) + C_i (\gamma_4 T^{n-1} + \gamma_5 T^n) + \dot{q}(t)}{3 B_1 - C_i \gamma_6} \quad (\text{IV. 16})$$

as in equation IV.14, the iteration problem is not solved: B_1 and C_1 are evaluated with a guess for T^{n+1} .

D. We now discuss the air gap equations. From paragraph II.A.7 the equations are:

$$(-k T_x)_- - (C_{j-1} T_t)_- = (\dot{q}_r + \dot{q}_{cv} + \dot{q}_{cond})_0$$

$$(\dot{q})_0 = (-k T_x)_+ + (C_j T_t)_+$$

It is assumed here that the air gap is layer j . Terms with subscript "-" are evaluated at left point of air gap (point x_3 in diagram at beginning of Section II.A) with properties of layer $j-1$. Terms with subscript "+" are evaluated at right point of air gap (point x_4) with properties of layer $j+1$. Terms with subscript "0" are evaluated at midpoint of air gap.

After transformations, and using:

$$(\dot{q})_0 = (\dot{q}_r + \dot{q}_{cv} + \dot{q}_{cond})_0 - (\rho c_p A T_t)_0$$

we obtain:

$$(-k \eta_x T_\eta)_- - (C_{j-1} T_t)_- = (\dot{q}_r + \dot{q}_{cv} + \dot{q}_{cond})_0 \quad (IV.17)$$

$$(-k \eta_x T_\eta)_- - (C_{j-1} T_t)_- = (-k \eta_x T_\eta)_+ + (C_j T_t)_+ + (\rho c_p A T_t)_0 \quad (IV.18)$$

We let T_{x3} represent temperature at left point of the air gap, and T_{x4} the temperature at the right point. T_{-1} and T_{+1} represent, as before, temperatures at first interior points on either side of air gap. Let

$$(T_t)_0 = \frac{1}{2} \left\{ (T_t)_- + (T_t)_+ \right\}$$

Then the air gap equations become:

$$(-k \eta_x T_\eta)_- - (C_{j-1} T_t)_- = (\dot{q}_r + \dot{q}_{cv} + \dot{q}_{cond})_0 \quad (IV.19)$$

$$\begin{aligned} (-k \eta_x T_\eta)_- - (-k \eta_x T_\eta)_+ = \\ \left[(C_{j-1})_- + \frac{(\rho c_p A)_0}{2} \right] (T_t)_- + \left[(C_j)_+ + \frac{(\rho c_p A)_0}{2} \right] (T_t)_+ \end{aligned} \quad (IV.20)$$

We use the same approximations as before:

$$(T_{\eta})_{-} = \frac{T_{-2}^{n+1} - 4 T_{-1}^{n+1} + 3 T_{x_3}^{n+1}}{2 \Delta \eta_{j-1}}$$

$$(T_{\eta})_{+} = \frac{-3 T_{x_4}^{n+1} + 4 T_1^{n+1} - T_2^{n+1}}{2 \Delta \eta_{j+1}}$$

$$(T_t)_{-} = \gamma_4 T_{x_3}^{n-1} + \gamma_5 T_{x_3}^n + \gamma_6 T_{x_3}^{n+1}$$

$$(T_t)_{+} = \gamma_4 T_{x_4}^{n-1} + \gamma_5 T_{x_4}^n + \gamma_6 T_{x_4}^{n+1}$$

(The γ_i are defined in equation IV. 13.)

Equation IV. 19 becomes:

$$\left(\frac{-k \eta_x}{2 \Delta \eta} \right)_{-} \left[T_{-2}^{n+1} - 4 T_{-1}^{n+1} + 3 T_{x_3}^{n+1} \right] - (C_{j-1})_{-} (\gamma_4 T_{x_3}^{n-1} + \gamma_5 T_{x_3}^n + \gamma_6 T_{x_3}^{n+1}) = (\dot{q}_r + \dot{q}_{cv} + \dot{q}_{cond})_0$$

Equation IV. 20 becomes:

$$\begin{aligned} & \left(\frac{-k \eta_x}{2 \Delta \eta} \right)_{-} \left[T_{-2}^{n+1} - 4 T_{-1}^{n+1} + 3 T_{x_3}^{n+1} \right] - \left(\frac{-k \eta_x}{2 \Delta \eta} \right)_{+} \left[-3 T_{x_4}^{n+1} + 4 T_1^{n+1} - T_2^{n+1} \right] \\ &= \left[(C_{j-1})_{-} + \frac{(\rho c_p A)}{2} 0 \right] (\gamma_4 T_{x_3}^{n-1} + \gamma_5 T_{x_3}^n + \gamma_6 T_{x_3}^{n+1}) \\ &+ \left[(C_j)_{+} + \frac{(\rho c_p A)}{2} 0 \right] (\gamma_4 T_{x_4}^{n-1} + \gamma_5 T_{x_4}^n + \gamma_6 T_{x_4}^{n+1}) \end{aligned}$$

Let

$$B_1 = \left(\frac{-k \eta_x}{2 \Delta \eta} \right)_{-}$$

$$B_2 = \left(\frac{-k \eta_x}{2 \Delta \eta} \right)_{+}$$

$$\bar{C}_1 = 3 B_2 - \gamma_6 \left[(C_j)_{+} + \frac{(\rho c_p A)}{2} 0 \right]$$

$$\begin{aligned}
\overline{C}_2 &= 3 B_1 - \gamma_6 \left[(C_{j-1})_- + \frac{(\rho c_p A)_0}{2} \right] \\
\overline{C}_3 &= B_1 (4 T_{-1}^{n+1} - T_{-2}^{n+1}) + B_2 (4 T_1^{n+1} - T_2^{n+1}) \\
&\quad + \left[(C_{j-1})_- + \frac{(\rho c_p A)_0}{2} \right] (\gamma_4 T_{x_3}^{n-1} + \gamma_5 T_{x_3}^n) \\
&\quad + \left[(C_{j-1})_+ + \frac{(\rho c_p A)_0}{2} \right] (\gamma_4 T_{x_4}^{n-1} + \gamma_5 T_{x_4}^n) \\
\overline{C}_4 &= B_1 (4 T_{-1}^{n+1} - T_{-2}^{n+1}) + (C_{j-1})_- (\gamma_4 T_{x_3}^{n-1} + \gamma_5 T_{x_3}^n) \\
\overline{C}_5 &= \frac{1}{3 B_1 - (C_{j-1})_- \gamma_6} \\
\overline{C}_6 &= (\dot{q}_r + \dot{q}_{cv} + \dot{q}_{cond})_0
\end{aligned}$$

Then we obtain these equations:

$$T_{x_3}^{n+1} = \overline{C}_5 (\overline{C}_4 + \overline{C}_6) \quad (\text{IV. 21})$$

$$\overline{C}_1 T_{x_4}^{n+1} + \overline{C}_2 T_{x_3}^{n+1} = \overline{C}_3 \quad (\text{IV. 22})$$

Note that the \overline{C}_i are functions of $T_{x_3}^{n+1}$ and $T_{x_4}^{n+1}$. (Quantities with subscript "0" are evaluated with the average of $T_{x_3}^{n+1}$ and $T_{x_4}^{n+1}$.) If we consider $T_{x_4}^{n+1}$ as given from IV. 21 in terms of $T_{x_3}^{n+1}$, then we can consider IV. 20 as being in the form:

$$T_{x_3}^{n+1} = f(T_{x_3}^{n+1}). \quad (\text{IV. 23})$$

This iteration problem is then solved by the method of Appendix B3. (Actually, for each guess at a solution of IV. 23, IV. 22 is solved by the same method for $T_{x_4}^{n+1}$.) Thus far we have found that a solution as precise as the one indicated is not necessary; accordingly, all the B_i and \overline{C}_i are held constant for the iteration with the exception of \overline{C}_6 .

If the air gap is the last layer, then IV. 18 is modified. $(-k \eta_x T_\eta)$ is replaced by $\dot{q}(t)$. The same change occurs in IV. 20. If $\dot{q}(t)$ is added to \overline{C}_3 and B_2^+ set = 0, then equations IV. 21 and IV. 22 remain valid for this case.

Also note that the \bar{g} , gravity, which is used for G_R , is computed as a quadratic polynomial in t . Let t_1 be the final time for the run. Three values of \bar{g} are given:

$$g_0 = \bar{g}(0)$$

$$g_1 = \bar{g}\left(\frac{t_1}{2}\right)$$

$$g_2 = \bar{g}(t_1)$$

Then,

$$\bar{g} = a_1 t^2 + a_2 t + a_3$$

$$a_1 = \frac{2}{(t_1)^2} \left[g_0 - 2g_1 + g_2 \right]$$

$$a_2 = \frac{-3g_0 + 4g_1 - g_2}{t_1}$$

$$a_3 = g_0$$

As in the boundary condition equations, it may be necessary to solve simultaneously for the interior temperatures T_{-1}^{n+1} and T_{+1}^{n+1} .

E. Convergence of the difference equations has been shown under the assumptions of linear differential equations and known values on the boundary. When the coefficients are non-linear and when the boundary conditions change, we extend the difference equations in an almost obvious fashion and hope for the best. However, strange situations can arise. The following is an example of a difficulty that has occurred in the coupling of the front-face equation and the first interior point.

Suppose $\beta_2 = \beta_4 = 0$. Then the equations to be solved are these:

$$T_t = \beta_1 T_{\eta\eta} + \beta_3 T_{\eta}$$

$$\dot{q}_{\text{net}} = (-k \eta_x T_{\eta})_0.$$

From IV.11 we have for the frontface equation:

$$T_0^{n+1} = \left(\frac{2 \Delta \eta}{3k \eta_x} \right) \dot{q}_{\text{net}} + \frac{1}{3} (4 T_1^{n+1} - T_2^{n+1}).$$

(This assumes $\alpha_3 = 1$, which was the case originally.)

The dependence of \dot{q}_{net} and k on T_0^{n+1} is not significant for this discussion. Assuming them to be constant, we obtain:

$$T_0^{n+1} = C_1 + \frac{1}{3} (4 T_1^{n+1} - T_2^{n+1}). \quad (\text{IV. 24})$$

For the first interior point we have from IV. 9 (with $\alpha_1 = \alpha_2 = \frac{1}{2}$):

$$\begin{aligned} (1 + 2 r_o \beta_1) T_1^{n+1} &= r_3 = T_1^n + r_o r_2 \beta_1 + r_o r_1 \Delta \eta \beta_3 \\ &= T_1^n + r_o \beta_1 (T_2^{n+1} + T_0^{n+1}) + r_o \Delta \eta \beta_3 \frac{(T_2^{n+1} - T_0^{n+1})}{2} \\ (1 + 2 r_o \beta_1) T_1^{n+1} &= T_1^n + (r_o \beta_1 - \frac{r_o \Delta \eta \beta_3}{2}) T_0^{n+1} \\ &\quad + (r_o \beta_1 + \frac{r_o \Delta \eta \beta_3}{2}) T_2^{n+1} \end{aligned} \quad (\text{IV. 25})$$

(T_2^{n+1} is assumed known for this calculation.) Equations IV. 24 and IV. 25 are to be solved simultaneously. Suppose we substitute IV. 24 into IV. 25.

$$\begin{aligned} (1 + 2 r_o \beta_1) T_1^{n+1} &= T_1^n + (r_o \beta_1 - \frac{r_o \Delta \eta \beta_3}{2}) (C_1 + \frac{4}{3} T_1^{n+1} - \frac{1}{3} T_2^{n+1}) \\ &\quad + (r_o \beta_1 + \frac{r_o \Delta \eta \beta_3}{2}) T_2^{n+1} + \\ (1 + \frac{2}{3} r_o \beta_1 + \frac{2 r_o \Delta \eta \beta_3}{3}) T_1^{n+1} &= T_2^n + C_1 \left(r_o \beta_1 - \frac{r_o \Delta \eta \beta_3}{2} \right) \\ &\quad + \left(\frac{2}{3} r_o \beta_1 + \frac{2 r_o \Delta \eta \beta_3}{3} \right) T_2^{n+1} \end{aligned}$$

or,

$$\begin{aligned} \left[1 + \frac{2}{3} r_o (\beta_1 + \Delta \eta \beta_3) \right] T_1^{n+1} &= T_1^n + C_1 r_o (\beta_1 - \frac{\Delta \eta \beta_3}{2}) \\ &\quad + \frac{2}{3} r_o (\beta_1 + \Delta \eta \beta_3) T_2^{n+1} \end{aligned} \quad (\text{IV. 26})$$

The difficulty occurred when β_3 became a large negative number. This allowed the coefficient of T_1^{n+1} to go to zero, causing incalculable consternation. Note that this is not a true convergence problem, since for $\Delta \eta$ sufficiently small, $\beta_1 + \Delta \eta \beta_3 > 0$ and there

is no problem. Also, the numerical approximation is no worse than it ever was. The problem is that the temperature we want to obtain has dropped out of the approximation.

Once a computer run has started, we are free to adjust Δt , but not $\Delta \eta$. In the actual case β_3 was large only for a short period of time. This means that many points must be carried for the whole run, while they are really needed for only part of the run.

The first attempt to solve the problem was to cut Δt . Since $r_o = \frac{\Delta t}{\Delta \eta}$, we could make the term $1 + \frac{2}{3} r_o (\beta_1 + \Delta \eta \beta_3)$ as close to 1 as desired, but it had to be less than 1.

This resulted in Δt becoming unreasonably small, and eventually trouble still developed. The fact that the coefficient of T_2^{n+1} remains negative most probably contributes to the difficulty.

We then used the approximation to T_η given by IV. 2. This results in equation IV. 10.

$$\left\{ 1 + r_o \left[2 \beta_1 + (\alpha_1 - \alpha_2) \Delta \eta \beta_3 \right] \right\} T_1^{n+1} = T_j^n + r_o (\beta_1 + \alpha_1 \Delta \eta \beta_3) T_2^{n+1} + r_o (\beta_1 - \alpha_2 \Delta \eta \beta_3) T_0^{n+1} \quad (\text{IV. 27})$$

Substituting IV. 24 into IV. 27:

$$\begin{aligned} \left\{ 1 + r_o \left[2 \beta_1 + (\alpha_1 - \alpha_2) \Delta \eta \beta_3 \right] \right\} T_1^{n+1} &= T_j^n + r_o (\beta_1 + \alpha_1 \Delta \eta \beta_3) T_2^{n+1} + r_o (\beta_1 - \alpha_2 \Delta \eta \beta_3) C_1 \\ &+ r_o (\beta_1 - \alpha_2 \Delta \eta \beta_3) \left(\frac{4}{3} T_1^{n+1} - \frac{1}{3} T_2^{n+1} \right) \\ 1 + r_o \left[\frac{2}{3} \beta_1 + (\alpha_1 - \alpha_2 + \frac{4}{3} \alpha_2) \Delta \eta \beta_3 \right] T_1^{n+1} &= T_j^n + r_o C_1 (\beta_1 - \alpha_2 \Delta \eta \beta_3) + \\ &+ r_o \left[\frac{2}{3} \beta_1 + (\alpha_1 + \frac{1}{3} \alpha_2) \Delta \eta \beta_3 \right] T_2^{n+1} \end{aligned}$$

We want to insure that:

$$X = 2 \beta_1 + 3 \Delta \eta \beta_3 (\alpha_1 + \frac{1}{3} \alpha_2) > 0$$

$$\alpha_1 + \alpha_2 = 1 \Rightarrow \alpha_1 + \frac{1}{3} \alpha_2 = \alpha_1 + \frac{1}{3} - \frac{1}{3} \alpha_1 = \frac{2}{3} \alpha_1 + \frac{1}{3} = \frac{1}{3} (2 \alpha_1 + 1)$$

$$X = 2 \beta_1 + (2 \alpha_1 + 1) \Delta \eta \beta_3 > 0$$

If $\beta_3 > 0$, there is no problem. Suppose $\beta_3 < 0$

$$X = \beta_1 - \left| \Delta \eta \beta_3 \right| \left(\alpha_1 + \frac{1}{2} \right)$$

The "best" case would be $\alpha_1 = 0$:

$$X^* = \beta_1 - \left| \frac{\Delta \eta \beta_3}{2} \right|$$

Thus, it is not possible to insure $X > 0$. Note also that if $X^* > 0$, $\alpha_1 = \alpha_2 = \frac{1}{2}$ and:

$$X = \beta_1 - \left| \Delta \eta \beta_3 \right|$$

This means that the definition of α_1 and α_2 will not insure boundedness when solved simultaneously with the frontface equation.

Finally, we changed the frontface approximation:

$$\dot{q}_{\text{net}} = -k \eta_x \frac{(T_1^{n+1} - T_0^{n+1})}{\Delta \eta}$$

$$T_0^{n+1} = \frac{2}{3} C_1 + T_1^{n+1} \quad (\text{IV. 28})$$

(C_1 is as defined in IV. 24.) Substituting IV. 28 into IV. 27:

$$\begin{aligned} \left\{ 1 + r_o \left[2 \beta_1 + (\alpha_1 - \alpha_2) \Delta \eta \beta_3 \right] \right\} T_1^{n+1} &= T_j^n \\ &+ r_o (\beta_1 + \alpha_1 \Delta \eta \beta_3) T_2^{n+1} + r_o (\beta_1 - \alpha_2 \Delta \eta \beta_3) \left(\frac{2}{3} C_1 + T_1^{n+1} \right) \\ \left\{ 1 + r_o \left[\beta_1 + \alpha_1 \Delta \eta \beta_3 \right] \right\} T_1^{n+1} &= T_j^n + \\ &+ r_o (\beta_1 + \alpha_1 \Delta \eta \beta_3) T_2^{n+1} + r_o (\beta_1 - \alpha_2 \Delta \eta \beta_3) \left(\frac{2}{3} C_1 \right) \end{aligned}$$

and we have already chosen α_1 such that $\beta_1 + \alpha_1 \Delta \eta \beta_3 > 0$. Thus, this equation is quite satisfactory. However, the approximation at the frontface is not nearly as good. So far we have encountered only one case in which this difficulty at the frontface occurred. Therefore, IV. 28 is used only for this special case. Otherwise IV. 24 is used.

It is possible to approximate T_η at the frontface so as to go smoothly from one case to the other:

$$\begin{aligned}
 T_\eta &= \alpha_3 \left[\frac{-3 T_0^{n+1} + 4 T_1^{n+1} - T_2^{n+1}}{2 \Delta \eta} \right] + (1 - \alpha_3) \left(\frac{T_2^{n+1} - T_0^{n+1}}{2 \Delta \eta} \right) \\
 &= \frac{1}{2 \Delta \eta} \left[- (3 \alpha_3 + 1 - \alpha_3) T_0^{n+1} + 4 \alpha_3 T_1^{n+1} + (1 - 2 \alpha_3) T_2^{n+1} \right] \\
 T_\eta &= \frac{1}{2 \Delta \eta} \left[- (1 + 2 \alpha_3) T_0^{n+1} + 4 \alpha_3 T_1^{n+1} + (1 - 2 \alpha_3) T_2^{n+1} \right]
 \end{aligned}$$

where

$$\frac{1}{2} \leq \alpha_3 \leq 1$$

If $\alpha_3 = 1$,

$$T_\eta = \frac{1}{2 \Delta \eta} \left[-3 T_0^{n+1} + 4 T_1^{n+1} - T_2^{n+1} \right]$$

If $\alpha_3 = \frac{1}{2}$,

$$T_\eta = \frac{1}{2 \Delta \eta} \left[-2 T_0^{n+1} + 2 T_1^{n+1} \right] = \frac{T_1^{n+1} - T_0^{n+1}}{\Delta \eta}$$

Substituting into the frontface equation:

$$\begin{aligned}
 \frac{2 \Delta \eta}{k \eta_x} \dot{q}_{\text{net}} &= - \left[- (1 + 2 \alpha_3) T_0^{n+1} + 4 \alpha_3 T_1^{n+1} + (1 - 2 \alpha_3) T_2^{n+1} \right] \\
 T_0^{n+1} &= \frac{2 \Delta \eta \dot{q}_{\text{net}}}{k \eta_x (1 + 2 \alpha_3)} + \left(\frac{1}{1 + 2 \alpha_3} \right) \left[4 \alpha_3 T_1^{n+1} + (1 - 2 \alpha_3) T_2^{n+1} \right] \\
 T_0^{n+1} &= \left(\frac{3}{1 + 2 \alpha_3} \right) C_1 + \left(\frac{1}{1 + 2 \alpha_3} \right) \left[4 \alpha_3 T_1^{n+1} + (1 - 2 \alpha_3) T_2^{n+1} \right] \quad (\text{IV. 29})
 \end{aligned}$$

where C_1 is as defined in IV. 24.

Let

$$s_1 = \beta_1 + \alpha_1 \Delta \eta \beta_3$$

$$s_2 = \beta_1 + \alpha_2 \Delta \eta \beta_3$$

$$s_3 = s_1 + s_2$$

Then IV. 27 becomes:

$$(1 + r_o s_3) T_1^{n+1} = T_1^n + r_o s_1 T_2^{n+1} + r_o s_2 T_0^{n+1}$$

Substituting IV. 29:

$$\begin{aligned} (1 + r_o s_3) T_1^{n+1} &= T_1^n + r_o s_1 T_2^{n+1} \\ &\quad + r_o s_2 \left[\frac{3 C_1}{1+2\alpha_3} + \frac{4 \alpha_3}{1+2\alpha_3} T_1^{n+1} + \frac{1-2\alpha_3}{1+2\alpha_3} T_2^{n+1} \right] \\ \left[1 + r_o \left(s_3 - \frac{4 \alpha_3}{1+2\alpha_3} s_2 \right) \right] T_1^{n+1} &= T_1^n + \frac{3 C_1 r_o s_2}{1+2\alpha_3} \\ &\quad + r_o \left[s_1 + s_2 \left(\frac{1-2\alpha_3}{1+2\alpha_3} \right) \right] T_2^{n+1} \end{aligned}$$

Let

$$s_4 = s_3 - \frac{4 \alpha_3}{1+2\alpha_3} s_2 = \frac{(1+2\alpha_3) s_1 + (1+2\alpha_3 - 4\alpha_3) s_2}{1+2\alpha_3} = s_1 + \left(\frac{1-2\alpha_3}{1+2\alpha_3} \right) s_2$$

Thus,

$$(1 + r_o s_4) T_1^{n+1} = T_1^n + \frac{3 C_1 r_o s_2}{1+2\alpha_3} + r_o s_4 T_2^{n+1}$$

We want to choose α_3 such that $s_4 \geq 0$:

$$\begin{aligned} s_4 &= \beta_1 + \alpha_1 \Delta \eta \beta_3 + \left(\frac{1-2\alpha_3}{1+2\alpha_3} \right) (\beta_1 - \alpha_2 \Delta \eta \beta_3) \\ (1+2\alpha_3) s_4 &= 2 \beta_1 + \Delta \eta \beta_3 \left[\alpha_1 (1+2\alpha_3) - \alpha_2 (1-2\alpha_3) \right] \end{aligned}$$

From IV. 7, $\alpha_1 + \alpha_2 = 1$.

$$\begin{aligned} (1+2\alpha_3) s_4 &= 2 \beta_1 + \Delta \eta \beta_3 \left[\alpha_1 (1+2\alpha_3) - (1-\alpha_1) (1-2\alpha_3) \right] \\ &= 2 \beta_1 + \Delta \eta \beta_3 \left[2 \alpha_1 - (1-2\alpha_3) \right] \\ \left(\frac{1+2\alpha_3}{2} \right) s_4 &= \beta_1 + \alpha_1 \Delta \eta \beta_3 - \Delta \eta \beta_3 (1-2\alpha_3) \end{aligned}$$

$$s_4 \geq 0 \Rightarrow \Delta \eta \beta_3 (1-2\alpha_3) \leq \beta_1 + \alpha_1 \Delta \eta \beta_3$$

Suppose $\beta_3 \geq 0$:

$$1-2\alpha_3 \leq \frac{\beta_1 + \alpha_1 \Delta \eta \beta_3}{\Delta \eta \beta_3}$$

Thus we can choose α_3 at its maximum: $\alpha_3 = 1$.

Suppose $\beta_3 < 0$:

$$1-2\alpha_3 \geq \frac{\beta_1 + \alpha_1 \Delta \eta \beta_3}{\Delta \eta \beta_3}$$

$$2\alpha_3-1 \leq \frac{\beta_1 + \alpha_1 \Delta \eta \beta_3}{|\Delta \eta \beta_3|}$$

From IV.7, if $\alpha_1 < \frac{1}{2}$, $\beta_1 + \alpha_1 \Delta \eta \beta_3 = 0$. Then we must choose α_3 at its minimum:
 $\alpha_3 = \frac{1}{2}$ of $\beta_1 + \Delta \eta \beta_3/2 > 0$:

$$\alpha_3 = \min \left[1; \frac{\beta_1 + \frac{\Delta \eta \beta_3}{2}}{|\Delta \eta \beta_3|} + \frac{1}{2} \right]$$

Summarizing:

a. $\beta_3 \geq 0$: $\alpha_3 = 1$

b. $\beta_3 < 0$:

$$\alpha_3 = \begin{cases} \frac{1}{2} : \beta_1 + \frac{\Delta \eta \beta_3}{2} < 0 \\ \min \left[1; \frac{1}{2} + \frac{\beta_1 + \Delta \eta \beta_3/2}{|\Delta \eta \beta_3|} \right] : \beta_1 + \frac{\Delta \eta \beta_3}{2} > 0 \end{cases}$$

Remark: This still does not take into consideration a non-zero β_2 term.

SECTION V

CALCULATION OF DENSITY

The equation for the rate of change of density is generally given in this form:

$$\frac{\partial \rho}{\partial t} = \dot{W}_p = \dot{W}_p(\rho, T)$$

or

$$\rho_t = \dot{W}_p \quad (V.1)$$

The form of \dot{W}_p now used is given in Section II .A.2.

The space transformation gives us new coordinates: $(x, t) \rightarrow (\eta, \tau)$. Then,

$$\rho_t = \rho_\eta \eta_\tau + \rho_\tau \tau_t$$

η_t is given by equation B2.6 in Appendix B2.

$\tau_t = 1$: we actually do not change the time variable.

We then obtain:

$$\eta_\tau \rho_\eta + \rho_t = \dot{W}_p$$

replacing τ by t :

$$\rho_t + (\eta_t) \rho_\eta = \dot{W}_p \quad (V.2)$$

This equation can now be considered as a hyperbolic first order partial differential equation in ρ . The question now arises as to the boundary conditions. Note first that V.1 presented no problems, since it really is an ordinary differential equation (if we consider T given somehow). From B2.6.1 we see:

$$\eta_t = \eta_r r_t + \eta_\xi \xi_{\bar{x}} \bar{x}_t = \eta_r r_t + \eta_x \left(\frac{\bar{x}_t}{\bar{x}_x} \right)$$

From B2.6.2 $\eta_r = 0$ at $\eta = 0$ and $\eta = 1$.

From B2.5.1, $\eta_x \neq 0$.

$$\text{at } \eta = 0, \frac{\bar{x}_t}{\bar{x}_x} = -s'_m$$

$$\text{at } \eta = 1, \frac{\bar{x}_t}{\bar{x}_x} = 0.$$

This means that at $\eta = 1$, $\eta_t = 0$ and V.2 becomes: $\rho_t = \dot{W}_p$. As noted above, we can consider this an ordinary differential equation. At $\eta = 0$, however, $\eta_t = -s'_m \eta_x$, and we find ourselves in the position of evaluating a partial differential equation at a boundary point. Apparently this is alright as long as we can convince ourselves that the partial differential equation does hold at the boundary point. In our case this seems clear. The coefficient, η_t , is accounting for the fact that the point at $\eta = 0$ is actually moving with time.

We now want to choose a difference equation for V.2. First note that for purposes of studying the convergence of the difference equation, \dot{W}_p will contribute a term $= O(\Delta t)$. Thus, we can ignore it. Let us also ignore the complications on the boundary discussed above. This, then, is the equation to be studied:

$$\left. \begin{aligned} \rho_t + \eta_t \rho_\eta &= 0 \\ \rho &= f_1(t) \text{ on } \eta = 0 \\ \rho &= f_2(t) \text{ on } \eta = 1 \\ \rho &= f_3(\eta) \text{ on } t = 0 \end{aligned} \right\} \quad (V.3)$$

It is well-known that one cannot hope to obtain a solution along a so-called characteristic path in the (t, η) - plane. (See, for example, reference 5, p. 44-49, or reference 9, p. 36-37.) The second reference, Sommerfeld, gives an argument for linear second order partial differential equations. For a first order equation his derivation would be as follows:

Let ρ be given on a curve γ in the (t, η) - plane.

Let $p = \rho_t$, $q = \rho_\eta$

From V.2,

$$p + (\eta_t) q = \dot{W}_p \quad (V.4.1)$$

and, in general, along γ :

$$(\Delta t) p + (\Delta \eta) q = d\rho \quad (V.4.2)$$

These two equations, V. 4. 1 and V. 4. 2, can be solved for p and q as long as the determinant of the coefficients is not zero:

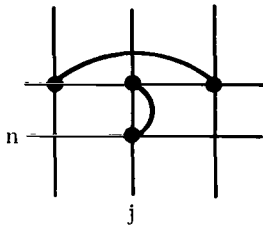
$$\begin{vmatrix} 1 & \eta_t \\ \Delta t & \Delta \eta \end{vmatrix} \neq 0.$$

or, we cannot have $\frac{\Delta t}{\Delta \eta} = \frac{1}{\eta_t}$. Since $\eta_t = 0$ when the coordinate system is stationary, we must expect always to have this restriction on Δt :

$$\Delta t \leq (\Delta \eta) \left| \frac{1}{\eta_t} \right| \quad (V. 5)$$

We now return to the problem of choosing a difference equation for V. 3. Let us first look at the usual implicit equation: $\left[\rho_j^n = \rho(n \Delta t, j \Delta \eta) \right]$:

A.



$$\frac{\partial \rho}{\partial t} = \frac{\rho_j^{n+1} - \rho_j^n}{2 \Delta t}$$

$$\frac{\partial \rho}{\partial \eta} = \frac{\rho_{j+1}^{n+1} - \rho_{j-1}^{n+1}}{2 \Delta \eta}$$

The stability of this system can be studied by the Fourier Series approach of Richtmyer if we assume that η_t is constant; (see reference 19):

$$\rho_j^n = \sum_{m=0}^{\infty} A_{(m)} \xi_{(m)}^n B_{(m)}^j$$

The typical term to be substituted is:

$$\rho_j^n = \xi^n B^j : B = e^{i(k \Delta \eta)}$$

$$B = \cos(k \Delta \eta) + i \sin(k \Delta \eta)$$

$$B^{-1} = \cos(k \Delta \eta) - i \sin(k \Delta \eta)$$

and

$$B + B^{-1} = 2 \cos(k \Delta \eta)$$

$$B - B^{-1} = 2 i \sin(k \Delta \eta)$$

Let $\alpha = \left(\frac{\Delta t}{\Delta \eta} \right) \eta_t$

Substituting differences into V. 3:

$$\rho_j^{n+1} - \rho_j^n + \frac{\alpha}{2} \left(\rho_{j+1}^{n+1} - \rho_{j-1}^{n+1} \right) = 0$$

Substituting $\rho_j^n = \xi^n B^j$,

$$\xi^{n+1} B^j - \xi^n B^j + \frac{\alpha}{2} \left(\xi^{n+1} B^{j+1} - \xi^{n+1} B^{j-1} \right) = 0$$

$$\xi - 1 + \left(\frac{\alpha}{2} \right) (\xi) (B - B^{-1}) = 0$$

$$\xi - 1 + \alpha \xi \left[i \sin(k \Delta \eta) \right] = 0$$

$$\xi = \frac{1}{1 + i \alpha \sin(k \Delta \eta)}$$

or

$$|\xi|^2 = \frac{1}{1 + \alpha^2 \sin^2(k \Delta \eta)} \leq 1$$

Thus, the "growth" factors are ≤ 1 , and so according to Richtmyer's theory the difference equation is convergent.

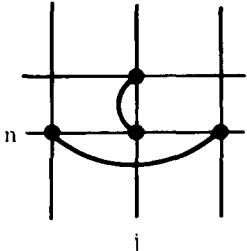
The disadvantages of the implicit scheme are, of course, the same as those encountered in using an implicit scheme in the energy equation:

1. A simultaneous system of linear equations would need to be solved.
2. The term \dot{W}_p in equation V. 2 would need to be evaluated at the previous time step.

As in the case of the energy equation, these factors appear to be too great. Consequently, we search for an explicit scheme.

The "usual" explicit scheme would be as follows:

B.



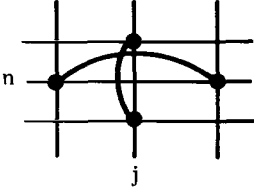
$$\frac{\partial \rho}{\partial t} = \frac{\rho_j^{n+1} - \rho_j^n}{\Delta t}$$

$$\frac{\partial \rho}{\partial \eta} = \frac{\rho_{j+1}^n - \rho_{j-1}^n}{2 \Delta \eta}$$

Using the Fourier Series as above, it is easy to see that this equation is unconditionally unstable.

Another explicit difference equation is the following:

C.



$$\frac{\partial \rho}{\partial t} = \frac{\rho_j^{n+1} - \rho_j^{n-1}}{2 \Delta t}$$

$$\frac{\partial \rho}{\partial \eta} = \frac{\rho_{j+1}^n - \rho_{j-1}^n}{2 \Delta \eta}$$

Substituting into V. 3:

$$\rho_j^{n+1} - \rho_j^{n-1} + \left(\frac{\Delta t}{\Delta \eta} \right) (\eta_t) \left(\rho_{j+1}^n - \rho_{j-1}^n \right) = 0.$$

Letting $\alpha = \left(\frac{\Delta t}{\Delta \eta} \right) (\eta_t)$ and $\rho_j^n = \xi^n B^j$,

$$\xi^2 - 1 + (\alpha \xi) (2i) \sin(k \Delta \eta) = 0.$$

Let $\bar{\alpha} = 2 \alpha \sin(k \Delta \eta)$:

$$\xi^2 + i \bar{\alpha} \xi - 1 = 0$$

$$\xi = \frac{-i \bar{\alpha} \pm \sqrt{-(\bar{\alpha})^2 + 4}}{2}$$

Now note that from V. 5, $|\alpha| \leq 1$. Thus, $|\bar{\alpha}|^2 = \bar{\alpha}^2 \leq 4$. Then $4 - \bar{\alpha}^2 \geq 0$, and:

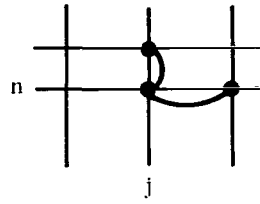
$$|\xi|^2 = \frac{4 - \bar{\alpha}^2 + \bar{\alpha}^2}{4} = 1.$$

This is somewhat unusual in that the growth factors are all identically equal to one. Nevertheless, this is enough to insure convergence. In actual practice, however, this difference equation become unstable. But at that time we had not imposed condition V. 5. Had we done so, it is very probable that this would have behaved well. Before putting V. 5 into the program, we decided to look for a difference equation which might give better behavior of the growth factors.

We then looked at the "alternating" difference equation. This would be defined in the same way as the alternating difference equation for the energy equation. (See Section III of the analysis portion of this report, or Section IV.) This turned out to be similar to equation (C) and so it was not used.

The difference equation finally chosen is a modified version of the following (see reference 4, pp. 142-143, or reference 5, pp. 49-53):

$$\eta_t \leq 0 \text{ at } (n, j) \quad (V. 6)$$

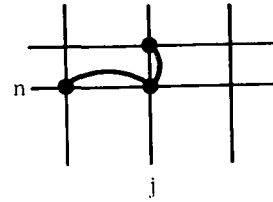


$$\frac{\partial \rho}{\partial t} = \frac{\rho_j^{n+1} - \rho_j^n}{\Delta t}$$

$$\frac{\partial \rho}{\partial \eta} = \frac{\rho_{j+1}^n - \rho_j^n}{\Delta \eta}$$

$\eta_t \geq 0$ at (n, j)

(V.7)



$$\frac{\partial \rho}{\partial t} = \frac{\rho_j^{n+1} - \rho_j^n}{\Delta t}$$

$$\frac{\partial \rho}{\partial \eta} = \frac{\rho_j^n - \rho_{j-1}^n}{\Delta \eta}$$

Consider first V.7

$$\rho_j^{n+1} - \rho_j^n + \left(\frac{\Delta t}{\Delta \eta} \right) (\eta_t) (\rho_j^n - \rho_{j-1}^n) = 0.$$

From V.5, $\left(\frac{\Delta t}{\Delta \eta} \right) |\eta_t| \leq 1$. Since we assume $\eta_t > 0$, we can say $0 \leq \alpha \leq 1$, where $\alpha = \left(\frac{\Delta t}{\Delta \eta} \right) (\eta_t)$.

$$\rho_j^{n+1} = (1-\alpha) \rho_j^n + \alpha \rho_{j-1}^n$$

$$\left| \rho_j^{n+1} \right| \leq (1-\alpha+\alpha) \left| \rho_j^n \right| = \left| \rho_j^n \right|$$

Here we assume $\left| \rho^n \right| = \max_j \left[\left| \rho_j^n \right| \right]$. This, then, establishes convergence according to Richtmyer's boundedness condition. (See Appendix B3 of the analysis section of this report for a further discussion of this point.)

Consider now V.6:

$$\rho_j^{n+1} - \rho_j^n + \left(\frac{\Delta t}{\Delta \eta} \right) (\eta_t) (\rho_{j+1}^n - \rho_j^n) = 0.$$

$$\rho_j^{n+1} - \rho_j^n - \alpha (\rho_{j+1}^n - \rho_j^n) = 0.$$

Here we let $\alpha = - \left(\frac{\Delta t}{\Delta \eta} \right) \eta_t$. Since $\eta_t \leq 0$, and imposing V.5, we see that $0 \leq \alpha \leq 1$.

$$\rho_j^{n+1} = \alpha \rho_{j+1}^n + (1-\alpha) \rho_j^n$$

or

$$\left| \rho_j^{n+1} \right| \leq \left| \rho_j^n \right|$$

This difference equation, V.6 and V.7, was programmed and worked quite well. On extreme cases, however, we still encountered instability. Up to this point we have ignored the fact that this partial differential equation was being solved simultaneously with the energy equation. In working with systems of partial differential equations, we have assumed the following approach:

The equations are ordered according to some ill-defined criterion of dominance. Each equation is written in terms of only one of the variables: the other variables are considered to appear only in the coefficients of this equation. Needless to say, we assume that no two equations are written in terms of the same variable. A difference equation is then chosen for the first equation. For the second equation any difference scheme can be chosen, as long as it is consistent with the peculiarities of the first equation. A difference approximation can now be made for the third equation, as long as it is consistent with the peculiarities of the first two, etc.

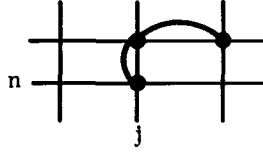
In our case we have two equations. Temperature is the variable in the energy equation, and density is the variable in equation V.2. We assume the energy equation to be the dominant one. In Section III and Section IV, we have discussed the difference equation we have used. We note here only the "pecularity" of the method:

Every other point is evaluated with the explicit scheme. This means that if T_j^{n+1} is the new value, the coefficients must be evaluated at (n, j) . The other points are evaluated with the implicit scheme. This means that T_j^{n+1} must be evaluated by computing the coefficients at $(n+1, j)$.

Difference equations V.6 and V.7 are consistent with the explicit portion of the above "pecularity": the partial differential equation is evaluated at (n, j) . However, they are not consistent with the implicit portion.

Suppose we now assume that every other point is evaluated by V.6 and V.7. We will evaluate the intermediate points by these equations:

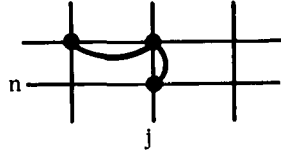
$$\eta_t \leq 0 \text{ at } (n+1, j) \tag{V.8}$$



$$\frac{\partial \rho}{\partial t} = \frac{\rho_j^{n+1} - \rho_j^n}{\Delta t}$$

$$\frac{\partial \rho}{\partial \eta} = \frac{\rho_{j+1}^{n+1} - \rho_j^{n+1}}{\Delta \eta}$$

$$\eta_t \geq 0 \text{ at } (n+1, j)$$



$$\frac{\partial \rho}{\partial t} = \frac{\rho_j^{n+1} - \rho_j^n}{\Delta t}$$

$$\frac{\partial \rho}{\partial \eta} = \frac{\rho_j^{n+1} - \rho_{j-1}^{n+1}}{\Delta \eta}$$

Consider first V. 9:

Letting $\alpha = \left(\frac{\Delta t}{\Delta \eta} \right) (\eta_t)$ and imposing V. 5, we can say $0 \leq \alpha \leq 1$. Substituting into V. 3,

$$\rho_j^{n+1} - \rho_j^n + \alpha \left(\rho_j^{n+1} - \rho_{j-1}^{n+1} \right) = 0.$$

$$(1+\alpha) \rho_j^{n+1} = \rho_j^n + \alpha \rho_{j-1}^{n+1}$$

From V. 7,

$$\rho_{j-1}^{n+1} = (1-\alpha) \rho_{j-1}^n + \alpha \rho_{j-2}^n$$

or

$$\rho_j^{n+1} = \frac{\rho_j^n + \alpha (1-\alpha) \rho_{j-1}^n + \alpha^2 \rho_{j-2}^n}{1+\alpha}$$

$$\left| \rho_j^{n+1} \right| \leq \left| \rho_j^n \right| \left(\frac{1 + \alpha - \alpha^2 + \alpha^2}{1 + \alpha} \right) = \left| \rho_j^n \right|.$$

Thus, we satisfy the boundedness condition. Consider V. 8:

Letting $\alpha = - \left(\frac{\Delta t}{\Delta \eta} \right) \eta_t$ and imposing V. 5, we can say $0 \leq \alpha \leq 1$. Substituting into V. 3,

$$\rho_j^{n+1} - \rho_j^n - \alpha \left(\rho_{j+1}^{n+1} - \rho_j^{n+1} \right) = 0$$

$$(1+\alpha) \rho_j^{n+1} = \rho_j^n + \alpha \rho_{j+1}^{n+1}$$

From V. 6,

$$\rho_{j+1}^{n+1} = \alpha \rho_{j+2}^n + (1-\alpha) \rho_{j+1}^n$$

or

$$\rho_j^{n+1} = \frac{\rho_j^n + \alpha^2 \rho_{j+2}^n + \alpha (1-\alpha) \rho_{j+1}^n}{1+\alpha}$$

$$\left| \rho_j^{n+1} \right| \leq \left| \rho_j^n \right| \left(\frac{1 + \alpha^2 + \alpha - \alpha^2}{1 + \alpha} \right) = \left| \rho_j^n \right|.$$

We now substitute equations V. 6 through V. 9 into equation V. 2, which is the one we want to solve. For the explicit equations:

$$\rho_j^{n+1} = \rho_j^n + (\Delta t) (\dot{W}_p) - \left(\frac{\Delta t}{\Delta \eta} \right) (\eta_t) (\Delta \rho), \quad (V. 10)$$

where η_t and \dot{W}_p are evaluated at (n, j) , and

$$\Delta \rho = \begin{cases} \rho_{j+1}^n - \rho_j^n : \eta_t \leq 0 \\ \rho_j^n - \rho_{j-1}^n : \eta_t \geq 0 \end{cases}$$

For the implicit equations:

$$\text{Let } \alpha = \left| \left(\frac{\Delta t}{\Delta \eta} \right) \eta_t \right|$$

$$\rho_j^{n+1} = \frac{\rho_j^n + (\Delta t) (\dot{W}_p) + \alpha \bar{\rho}}{1+\alpha} \quad (V. 11)$$

where η_t and \dot{W}_p are evaluated at $(n+1, j)$ and

$$\bar{\rho} = \begin{cases} \rho_{j-1}^{n+1} : \eta_t \geq 0 \\ \rho_{j+1}^{n+1} : \eta_t \leq 0 \end{cases}$$

at the backface, $\eta_t = 0$:

$$\rho_A^{n+1} = \rho_A^n + (\Delta t) (\dot{W}_p) \quad (V. 12)$$

At the frontface we use an implicit calculation:

$$\rho_t = \frac{\rho_0^{n+1} - \rho_0^n}{\Delta t}$$

$$\rho_\eta = \frac{\rho_{\Delta\eta}^{n+1} - \rho_0^{n+1}}{\Delta\eta}$$

Substituting into V. 2, and letting $\alpha = - \left(\frac{\Delta t}{\Delta\eta} \right) (\eta_t)$

$$\rho_0^{n+1} = \rho_0^n + (\Delta t) (\dot{W}_p) + \alpha \left(\rho_{\Delta\eta}^{n+1} - \rho_0^{n+1} \right)$$

$$\rho_0^{n+1} = \frac{\rho_0^n + (\Delta t) (\dot{W}_p) + \alpha \rho_{\Delta\eta}^{n+1}}{1+\alpha} \quad (V. 13)$$

We have seen that at $\eta = 0$, $\eta_t \leq 0$: thus, $0 < \alpha < 1$. We now show that V. 13 satisfies a boundedness condition (as before, we set $\dot{W}_p = 0$ for this calculation):

Suppose $\rho_{\Delta\eta}^{n+1}$ is evaluated with an explicit method:

$$\rho_{\Delta\eta}^{n+1} = \rho_{\Delta\eta}^n + \alpha \left(\rho_{2\Delta\eta}^n - \rho_{\Delta\eta}^n \right) = (1-\alpha) \rho_{\Delta\eta}^n + \alpha \rho_{2\Delta\eta}^n$$

$$\rho_0^{n+1} = \frac{\rho_0^n + \alpha (1-\alpha) \rho_{\Delta\eta}^n + \alpha^2 \rho_{2\Delta\eta}^n}{1+\alpha}$$

or

$$\left| \rho_0^{n+1} \right| \leq \left| \rho_0^n \right|$$

Suppose $\rho_{\Delta\eta}^n$ is evaluated with an implicit method:

$$\rho_{\Delta\eta}^{n+1} = \frac{\rho_{\Delta\eta}^n + \alpha \rho_{2\Delta\eta}^{n+1}}{1+\alpha} = \frac{\rho_{\Delta\eta}^n + \alpha \left[(1-\alpha) \rho_{2\Delta\eta}^n + \alpha \rho_{3\Delta\eta}^n \right]}{1+\alpha}$$

and again,

$$\left| \rho_{\Delta\eta}^{n+1} \right| \leq \left| \rho_{\Delta\eta}^n \right|$$

Summarizing, we expect equations V. 10, V. 11, V. 12, and V. 13 to be a convergent set of difference equations as long as condition V. 5 is obeyed, even if used in conjunction with the difference equation for the energy equation. Thus far we have had no difficulty.

As in the temperature equation, the explicit equations reduce after the first time step:

a. Let $\eta_t \leq 0$:

Let

$$\rho_j^{n+1} = \rho_j^n + \Delta t_1 (\dot{W}_p) + \left| \frac{\Delta t_1 \eta_t}{\Delta \eta} \right| (\rho_{j+1}^{n+1} - \rho_j^{n+1})$$

or,

$$\frac{\rho_j^{n+1} - \rho_j^n}{\Delta t_1} = \dot{W}_p + \left| \frac{\eta_t}{\Delta \eta} \right| (\rho_{j+1}^{n+1} - \rho_j^{n+1})$$

Then,

$$\frac{\rho_j^{n+2} - \rho_j^{n+1}}{\Delta t_2} = \dot{W}_p + \left| \frac{\eta_t}{\Delta \eta} \right| (\rho_{j+1}^{n+1} - \rho_j^{n+1})$$

or,

$$\rho_j^{n+2} - \rho_j^{n+1} = \frac{\Delta t_2}{\Delta t_1} (\rho_j^{n+1} - \rho_j^n)$$

or,

$$\rho_j^{n+2} = \left(1 + \frac{\Delta t_2}{\Delta t_1} \right) \rho_j^{n+1} - \left(\frac{\Delta t_2}{\Delta t_1} \right) \rho_j^n$$

b. Let $\eta_\eta \geq 0$:

$$\frac{\rho_j^{n+1} - \rho_j^n}{\Delta t_1} = \dot{W}_p + \left| \frac{\eta_t}{\Delta \eta} \right| (\rho_{j-1}^{n+1} - \rho_j^{n+1})$$

$$\frac{\rho_j^{n+2} - \rho_j^{n+1}}{\Delta t_2} = \dot{W}_p + \left| \frac{\eta_t}{\Delta \eta} \right| (\rho_{j-1}^{n+1} - \rho_j^{n+1})$$

and

$$\rho_j^{n+2} = \left(1 + \frac{\Delta t_2}{\Delta t_1} \right) \rho_j^{n+1} - \left(\frac{\Delta t_2}{\Delta t_1} \right) \rho_j^n$$

Concerning the calculation, one final comment can be made. If V. 11 is evaluated at $j=1$ (at the first interior point), and if $\eta_t > 0$, then V. 11 and V. 13 should be solved simultaneously: ρ_0^{n+1} enters both equations. However, we expect $\eta_t \leq 0$ at this point; only if points were shifting rapidly toward the frontface (due to a change in the squeezing parameter) could $\eta_t > 0$. Thus, this iteration is not in the program.

SECTION VI INITIAL TEMPERATURE DISTRIBUTION

The program contains an option for employing an analytical solution to give a temperature distribution at a specified time. Actually two analytical solutions are available. The first is valid under the following conditions:

1. Infinite slab
2. Constant initial temperature
3. Constant thermal properties
4. Constant heat flux at frontface.

The second is valid under these conditions:

1. Infinite slab
2. Constant initial temperature
3. Constant thermal properties
4. Linear heat flux at frontface.

Aside from the better accuracy that is obtained using these analytical solutions, they also can save computer time in cases where the above conditions are well-approximated over a long period of time. Rather than use a step-by-step numerical procedure, we can calculate the temperature distribution at the end of that period, and then begin numerical integration. Note that because of the assumption of an infinite slab, these solutions should not be used past the time that the backface of the first layer begins to experience a significant temperature rise.

In deriving the formulas the following equations and definitions will be used:

$$\operatorname{erf} c(z) = 1 - \operatorname{erf}(z) = \frac{2}{\sqrt{\pi}} \int_z^{\infty} e^{-\xi^2} d\xi = i^0 \operatorname{erf} c(z) \quad (\text{VI. 1})$$

$$i^n \operatorname{erf} c(z) = \int_z^{\infty} i^{n-1} \operatorname{erf} c(\xi) d\xi \quad (\text{VI. 2})$$

$$2(n+1) i^{n+1} \operatorname{erf} c(z) = i^{n-1} \operatorname{erf} c(z) - 2z i^n \operatorname{erf} c(z) \quad (\text{VI. 3})$$

For $n = 0$, the last formula is valid

$$\text{if } i^{(-1)} \operatorname{erf} c(z) = \frac{2}{\sqrt{\pi}} e^{-z^2}$$

We also let

$$\alpha = \frac{\rho c_p}{k}$$

The solution for the first case, where \dot{q} is the constant heat flux, can be written in this form: (reference 10, p. 11, equation 1):

$$\Delta T(x, t) = \frac{2 \dot{q}}{k \sqrt{\alpha}} \left[t^{1/2} i \operatorname{erfc} \left(\frac{x}{2} \sqrt{\frac{\alpha}{t}} \right) \right]$$

From the previously stated error function formulas:

$$2 i \operatorname{erfc}(z) = i^{(-1)} \operatorname{erfc}(z) - 2 z \operatorname{erfc}(z) = \frac{2}{\sqrt{\pi}} e^{-z^2} - 2 z \left[1 - \operatorname{erfc}(z) \right]$$

or

$$\Delta T(x, t) = \frac{2 \dot{q}}{k} \sqrt{\frac{t}{\alpha}} \left\{ \frac{e^{-z^2}}{\sqrt{\pi}} - z \left[1 - \operatorname{erfc}(z) \right] \right\} \quad (\text{VI. 4})$$

where

$$z = \left(\frac{x}{2} \right) \sqrt{\frac{\alpha}{t}}$$

The solution for the second case, where $\dot{q} = m t$, can be written in this form: (reference 10, p. 16, equation 4; let $\theta = \beta \bar{\theta} = t_0$):

$$\Delta T = \frac{8 m t_0}{k \sqrt{\alpha}} \left\{ \left(\frac{t_0^{3/2}}{t_0} \right) i^3 \operatorname{erfc} \left(\frac{x}{2} \sqrt{\frac{\alpha}{t_0}} \right) \right\}$$

From the error function formulas:

$$\begin{aligned} 6 i^3 \operatorname{erfc}(z) &= i \operatorname{erfc}(z) - 2 z i^2 \operatorname{erfc}(z) \\ &= i \operatorname{erfc}(z) - \frac{z}{2} \left[i^0 \operatorname{erfc}(z) - 2 z i \operatorname{erfc}(z) \right] \\ &= -\frac{z}{2} \cdot \operatorname{erfc}(z) + i \operatorname{erfc}(z) \cdot \left[1 + z^2 \right] \\ &= -\frac{z}{2} \operatorname{erfc}(z) + \left(\frac{1+z^2}{2} \right) \left[i^{(-1)} \operatorname{erfc}(z) - 2 z \operatorname{erfc}(z) \right] \\ &= -\frac{z}{2} \operatorname{erfc}(z) + \left(\frac{1+z^2}{2} \right) \left[\frac{2}{\sqrt{\pi}} e^{-z^2} - 2 z \operatorname{erfc}(z) \right] \end{aligned}$$

$$\begin{aligned}
&= -\operatorname{erfc}(z) \cdot \left[\frac{z}{2} + z(1+z^2) \right] + \frac{1+z^2}{\sqrt{\pi}} e^{-z^2} \\
&= -\operatorname{erfc}(z) \cdot \left[\left(\frac{z}{2} \right) (1+2+2z^2) \right] + \frac{1+z^2}{\sqrt{\pi}} e^{-z^2}
\end{aligned}$$

or

$$i^3 \operatorname{erfc}(z) = \frac{1+z^2}{6\sqrt{\pi}} e^{-z^2} - \left(\frac{z}{12} \right) (3+2z^2) [1 - \operatorname{erfc}(z)]$$

and

$$\Delta T = \frac{8 m t_o^{3/2}}{k\sqrt{\alpha}} \left\{ \frac{1+z^2}{6\sqrt{\pi}} e^{-z^2} - \left(\frac{z}{12} \right) (3+2z^2) [1 - \operatorname{erfc}(z)] \right\}$$

where

$$z = \frac{x}{2} \sqrt{\frac{\alpha}{t_o}} \quad \text{(VI. 5)}$$

The program uses a polynomial approximation for $\operatorname{erfc}(z)$ - reference 11.

Let T_o be the initial constant temperature.

Let t_o be time at which we are to compute a temperature distribution.

At $x = 0$, for the case of constant heat flux, equation VI. 4 becomes:

$$\Delta T(0, t_o) = \frac{2 \dot{q}}{k} \sqrt{\frac{t_o}{\alpha \pi}}$$

At $x = 0$, for the case of linear heat flux, equation VI. 5 becomes:

$$\Delta T(0, t_o) = \frac{8 \dot{q}}{k} \sqrt{\frac{t_o}{\alpha \pi}} \left(\frac{1}{6} \right) = \frac{4 \dot{q}}{3k} \sqrt{\frac{t_o}{\alpha \pi}}$$

If we let

$$r_1 = \begin{cases} 1: & \text{linear heat flux} \\ \frac{3}{2}: & \text{constant heat flux} \end{cases}$$

$$\Delta T(0, t_o) = \frac{r_1 4 \dot{q}}{3k} \sqrt{\frac{t_o}{\alpha \pi}}$$

Let $T^* = T_o + \Delta T(0, t_o)$

Then we need to find T^* such that

$$T^* = T_o + \frac{r_1}{3k} \frac{4\dot{q}}{3} \sqrt{\frac{t_o}{\alpha\pi}} \quad (\text{VI. 6})$$

In order to use the analytic solution correctly, the right side of equation VI. 6 should be independent of T^* . In most instances this is not the case. We feel it is safer to solve equation VI. 6 as though the right side were a function of T^* . It is up to the user to see that t_o is small enough to use the analytic solutions correctly. Equation VI. 6 then takes the form:

$$T^* = f(T^*)$$

The iteration problem is the same as that encountered in the solution of the frontface boundary condition, and it is solved in precisely the same fashion.

In order to evaluate equations VI. 4 and VI. 5 we also need the transformation that relates the real space variable x to the transformed variable η . This problem is discussed in Section VII. C.

For programming simplicity we can combine equation VI. 4 and equation VI. 5:

Let

$$r_1 = \begin{cases} 1 & \text{: linear heat flux} \\ 3/2 & \text{: constant heat flux} \end{cases}$$

Then,

$$\Delta T(x, t) = r_1 \left(\frac{4}{3} \right) \left(\frac{\dot{q}}{k t_o} \right) \frac{t_o^{3/2}}{\sqrt{\alpha}} \left\{ (1+z^2)^{(3-2r_1)} \frac{e^{-z^2}}{\sqrt{\pi}} - z \left[1 - \text{erf}(z) \right] \left(\frac{3+2z^2}{2} \right)^{(3-2r_1)} \right\} \quad (\text{VI. 7})$$

SECTION VII

THE SPACING PARAMETER

In order to allow unequal spacing of points, the following space transformation is made:

$$\eta = \frac{1 - e^{-r} \xi}{1 - e^{-r}}$$

$$\xi = \bar{x} e^c (\bar{x}^2 - \bar{x})$$

where \bar{x} is the normalized space variable. (See Appendix B2 for a more thorough discussion of some properties of the transformation.) The parameter r is a function of time, while c is a constant. This transformation has the effect of keeping equal spacing in the η coordinate, while points in real space are unequally spaced. Rather than specify r , it seems more sensible to give the degree of squeezing at the frontface: $\frac{d\eta}{d\bar{x}}(0)$.

In the remainder of this section, these three problems are discussed:

1. Given $\frac{d\eta}{d\bar{x}}(0)$, solve for r .
2. Specify $\frac{d\eta}{d\bar{x}}(0)$ as a function of time.
3. Given r , solve for \bar{x} .

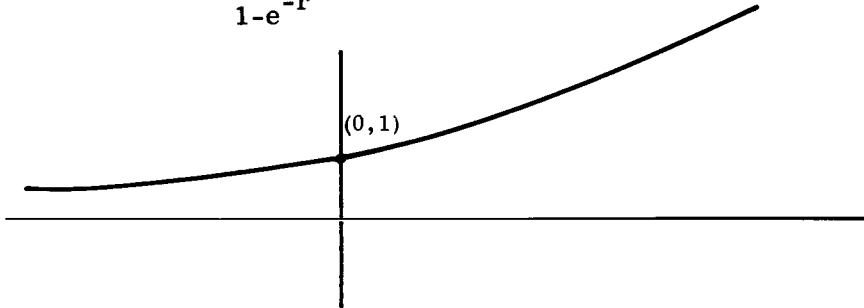
A. Let $\frac{d\eta}{d\xi}(0) = \bar{\eta}$.

The problem is to solve this equation for r :

$$\frac{r}{1 - e^{-r}} = \bar{\eta} > 0$$

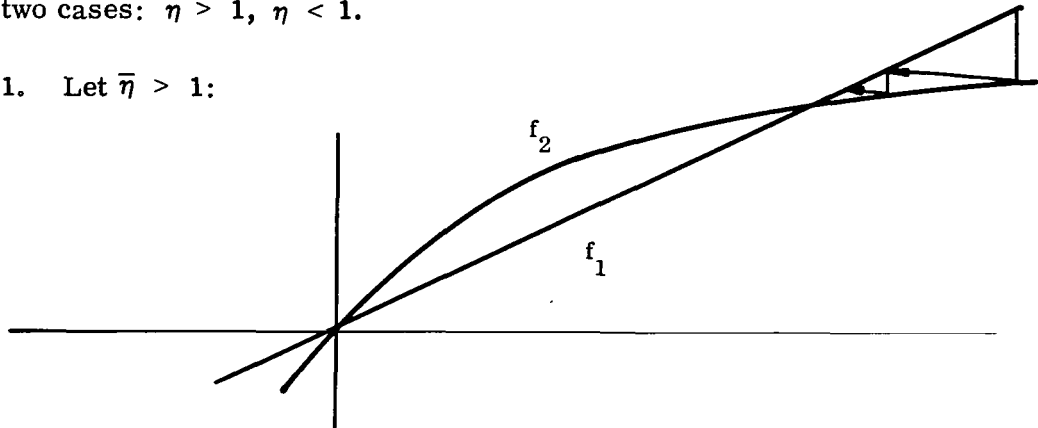
It cannot be claimed that this is a terribly difficult problem, but nevertheless a procedure must be specified.

We see in Appendix B2 that $\frac{r}{1 - e^{-r}}$ looks like:



Let $f_1(r) = \frac{r}{\bar{\eta}}$. Let $f_2(r) = 1 - e^{-r}$. We need to find r such that $f_1(r) = f_2(r)$. We consider two cases: $\bar{\eta} > 1$, $\bar{\eta} < 1$.

1. Let $\bar{\eta} > 1$:



If we can obtain a first guess for r which is too large, we can proceed as indicated in the diagram. Note that for $\bar{\eta} > 0$, $\frac{\bar{\eta}}{1 - e^{-\bar{\eta}}} > \bar{\eta}$. Thus, for a first guess we can let $r_1 = \bar{\eta}$. The next guess is the intersection of these lines:

- The line parallel to the x-axis and going through $f_2(r_1)$
- The line $f_1(r)$.

or,

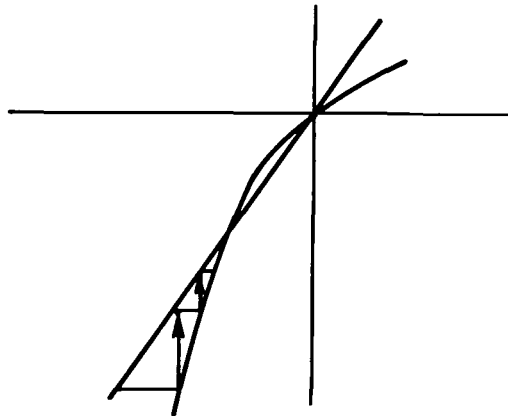
$$1 - e^{-r_1} = \frac{r_2}{\bar{\eta}}$$

and in general,

$$r_{i+1} = \bar{\eta} (1 - e^{-r_i})$$

We continue until convergence is as close as desired.

2. Let $\bar{\eta} < 1$



If we can obtain a first value of r which is too small, we can then proceed as indicated in the diagram. We claim that $f_2(r_1) < f_1(r_1)$ for:

$$r_1 = \begin{cases} -\bar{\eta} \left[1 + \frac{2(2 - e^{\bar{\eta}})}{(e^{\bar{\eta}} - 1)^2} \right] : e^{\bar{\eta}} < 2 \\ -2\bar{\eta} : e^{\bar{\eta}} > 2 \end{cases}$$

Proof:

We need $1 - e^{-r_1} < \frac{r_1}{\bar{\eta}} : r_1 < 0$

Let $r_1 = -n\bar{\eta}$ where n is a positive integer

Let $A = e^{\bar{\eta}}$:

since $0 < \bar{\eta} < 1$, $1 < A < e$

Let $A = 1 + \epsilon$, $\epsilon \geq 0$

We need $1 - A^n < -n$

or, $A^n - (1+n) > 0$

$$A^n = 1 + n\epsilon + \frac{n(n-1)}{2}\epsilon^2 + \sum_{\nu=3}^n \binom{n}{\nu} \epsilon^\nu$$

∴,

$$A^n - (1+n) = n(\epsilon-1) + \frac{n(n-1)}{2}\epsilon^2 + \sum_{\nu=3}^n \binom{n}{\nu} \epsilon^\nu$$

Now, if $\epsilon > 0$ we can choose n as any positive integer.

If $\epsilon < 1$, we are alright if

$$\frac{n(n-1)}{2}\epsilon^2 + n(\epsilon-1) > 0$$

$$(n-1)\epsilon^2 + 2(\epsilon-1) > 0$$

$$(n-1) > \frac{2(1-\epsilon)}{\epsilon^2}$$

$$n > 1 + \frac{2(1-\epsilon)}{\epsilon^2} = 1 + \frac{2(2-A)}{(A-1)^2} = 1 + \frac{2(2 - e^{\bar{\eta}})}{(e^{\bar{\eta}} - 1)^2}$$

and

$$r_1 < -\bar{\eta} \left[1 + \frac{2(2 - e^{\bar{\eta}})}{(e^{\bar{\eta}} - 1)^2} \right]$$

For the next guess we need the intersection of these two curves:

- The line parallel to the x-axis and going through $f_1(r_1)$
- The curve $f_2(r)$

or,

$$\frac{r_1}{\bar{\eta}} = 1 - e^{-r}$$

$$r_2 = -\ln \left(1 - \frac{r_1}{\bar{\eta}}\right)$$

and

$$r_{i+1} = -\ln \left(1 - \frac{r_i}{\bar{\eta}}\right)$$

B. We now discuss specification of $\frac{d\bar{\eta}}{d\xi}(0) = \bar{\eta}$ as a function of time. Since the derivative of this function enters the equations, it was decided that a well-behaved analytic function should be used. The restrictions on the function would be as follows:

1. $\bar{\eta}(t_0)$ would be given = t_0 is initial time.
2. $\bar{\eta}(t_\ell)$ would be given: t_ℓ is final time.
3. $\bar{\eta}(t_1)$ would be given: $t_0 < t_1 < t_\ell$.
4. $\frac{d\bar{\eta}}{dt} = 0$ at $t = 0$.
5. $\max \bar{\eta} = \max \left[\bar{\eta}(t_0), \bar{\eta}(t_1), \bar{\eta}(t_\ell) \right]$.
 $\min \bar{\eta} = \min \left[\bar{\eta}(t_0), \bar{\eta}(t_1), \bar{\eta}(t_\ell) \right]$.

The last restriction is to insure that the squeezing does not exceed the given bounds.

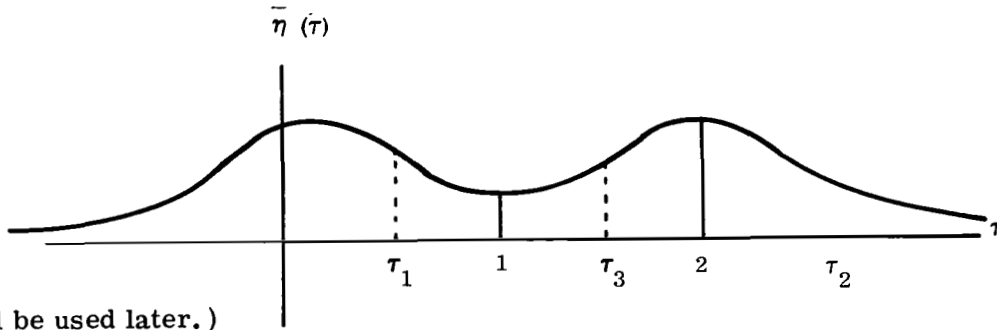
We eventually decided on this function:

$$\bar{\eta} = A e^{-B \tau^2 \left(1 - \frac{\tau}{2}\right)^2}$$

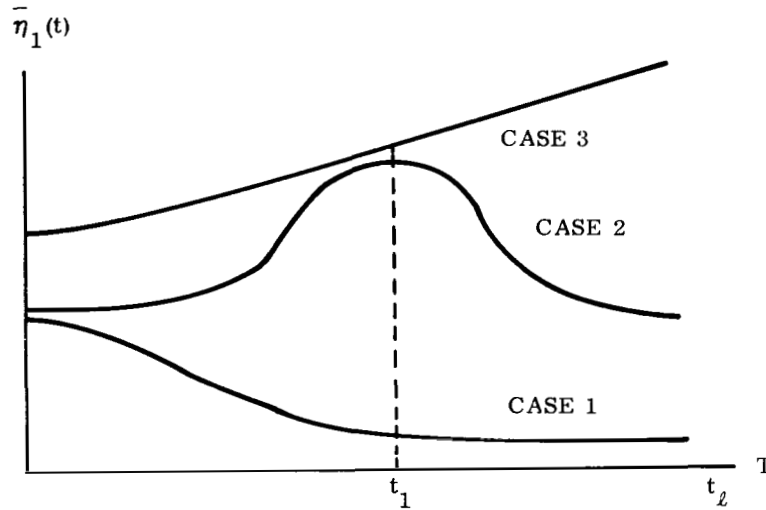
where A and B are constants, and $\tau = \tau(t)$ is still to be specified.

$$\begin{aligned} \frac{d\bar{\eta}}{d\tau} &= -B \bar{\eta} \left[2\tau \left(1 - \frac{\tau}{2}\right)^2 + 2\tau^2 \left(1 - \frac{\tau}{2}\right) \left(-\frac{1}{2}\right) \right] \\ &= -B \bar{\eta} (2\tau) \left(1 - \frac{\tau}{2}\right) \left[1 - \frac{\tau}{2} - \frac{\tau}{2} \right] \\ &= -2B \bar{\eta} (\tau) \left(1 - \frac{\tau}{2}\right) (1 - \tau) \\ &= -B \bar{\eta} \tau (1 - \tau) (2 - \tau) \end{aligned}$$

Thus, if A and $B > 0$,



To simplify things a bit more it was decided to allow only these three types of configurations for $\bar{\eta}(t)$:



For each case we will choose a certain portion of the $\bar{\eta}(\tau)$ curve:

Case I: $0 \leq \tau \leq 1$: monotonically decreasing

Case II: $1 \leq \tau \leq \tau_2$: maximum at t_1

Case III: $1 \leq \tau \leq 2$: monotonically increasing

In Case I A , B , and τ_1 are to be obtained from $\bar{\eta}(t_0)$, $\bar{\eta}(t_\ell)$, $\bar{\eta}(t_1)$. In Case II A , B , and τ_2 are to be obtained. In Case III A , B , and τ_3 are to be obtained. In the following discussion let $\eta_1 = \bar{\eta}(t_0)$, $\eta_2 = \bar{\eta}(t_1)$, $\eta_3 = \bar{\eta}(t_\ell)$.

Case I: $\eta_1 > \eta_2 > \eta_3$ on the $\bar{\eta}(\tau)$ curve, $\bar{\eta}(0) = \eta_1$, $\bar{\eta}(\tau_1) = \eta_2$, and $\bar{\eta}(1) = \eta_3$.

Then, $\eta_1 = A$, $\eta_3 = \eta_1 e^{-B/4}$ or, $B = 4 \ln(\eta_1/\eta_3) = 4 k_1 > 0$.

To determine τ_1 : $-B(\tau_1)^2 \left(1 - \frac{\tau_1}{2}\right)^2$
 $\eta_2 = \eta_1 e$

$$B(\tau_1)^2 \left(1 - \frac{\tau_1}{2}\right)^2 = \ln \frac{\eta_1}{\eta_2} = k_2 > 0$$

$$\frac{B}{4} (\tau_1)^2 (2 - \tau_1)^2 = k_2$$

$$(\tau_1)^2 (2 - \tau_1)^2 = \frac{k_2}{k_1}$$

$$\tau_1 (2 - \tau_1) = \pm k_3$$

Note that $k_3 = +\sqrt{k_2/k_1} < 1$

$$\tau_1^2 - 2\tau_1 \pm k_3 = 0$$

$$\tau_1 = \frac{2 \pm \sqrt{4 \pm 4k_3}}{2} = 1 \pm \sqrt{1 \pm k_3}$$

Since we want $\tau_1 < 1$, we must take

$$\tau_1 = 1 - \sqrt{1 \pm k_3}$$

Since we want $\tau_1 > 0$, we must take:

$$\tau_1 = 1 - \sqrt{1 - k_3}$$

To complete the definition we need a transformation $t \rightarrow \tau$ such that:

$$0 \rightarrow 0, t_1 \rightarrow \tau_1, t_\ell \rightarrow 1$$

or

$$\frac{t}{t-t_1} = k_4 \frac{\tau}{\tau-\tau_1}$$

$$\frac{t_\ell}{t_\ell-t_1} = k_4 \left(\frac{1}{1-\tau_1} \right)$$

or

$$k_4 = (1-\tau_1) \left(\frac{t_\ell}{t_\ell-t_1} \right): \text{ this gives } k_4 \text{ and } \tau t - \tau_1 t = k_4 \tau t - k_4 \tau t_1$$

$$\tau(t - k_4 t + k_4 \tau_1) = \tau_1 t$$

$$\tau = \frac{\tau_1 t}{(1-k_4)t + k_4 \tau_1}$$

We need not be concerned about a pole in the range $0 \leq t \leq t_j$. In this range $0 \leq \tau \leq 1$ and it is easily seen from a graph that the pole cannot occur here.

Case II: $\eta_1 < \eta_2$, $\eta_3 < \eta_2$ on the $\bar{\eta}(\tau)$ curve, $\bar{\eta}(1) = \eta_1$
 $\bar{\eta}(2) = \eta_2$
 $\bar{\eta}(\tau_2) = \eta_3$

$$\eta_2 = A$$

$$\eta_1 = \eta_2 e^{-B/4}$$

$$B/4 = \ln\left(\frac{\eta_2}{\eta_1}\right), \text{ or } B = 4 k_1$$

$$k_1 = \ln\left(\frac{\eta_2}{\eta_1}\right) > 0.$$

$$\eta_3 = \eta_2 e^{-B(\tau_2)^2 \left(1 - \frac{\tau_2}{2}\right)^2}$$

$$\left(\frac{B}{4}\right)(\tau_2)^2 (2-\tau_2)^2 = k_2: k_2 = \ln\left(\frac{\eta_3}{\eta_2}\right) > 0$$

$$\tau_2 (2-\tau_2) = \pm \sqrt{\frac{k_2}{k_1}} = \pm k_3:$$

$$k_3 = \sqrt{\frac{k_2}{k_1}} > 0$$

$$(\tau_2)^2 - 2\tau_2 \pm k_3 = 0$$

$$\tau_2 = \frac{2 \pm \sqrt{4 \mp 4k_3}}{2} = 1 \pm \sqrt{1 \mp k_3}$$

Since we want $\tau_2 > 2$,

$$\tau_2 = 1 + \sqrt{1 + k_3}$$

For the transformation $t \rightarrow \tau$ we need:

$$0 \rightarrow 1, t_1 \rightarrow 2, t_\ell \rightarrow \tau_2$$

$$\frac{t}{t-t_1} = k_4 \left(\frac{\tau-1}{\tau-2} \right)$$

$$k_4 = \left(\frac{\tau_2-2}{\tau_2-1} \right) \left(\frac{t_\ell}{t_\ell-t_1} \right)$$

This defines k_4 .

$$\tau t - 2t = k_4 \left[\tau (t-t_1) - (t-t_1) \right]$$

$$\tau \left[t - k_4 t + k_4 t_1 \right] = 2t - (t-t_1) k_4$$

$$\tau = \frac{(2-k_4)t + t_1 k_4}{(1-k_4)t + t_1 k_4}$$

Case III: $\eta_1 < \eta_2 < \eta_3$ on the $\bar{\eta}(\tau)$ curve, $\eta_1 = \bar{\eta}(1)$
 $\eta_2 = \bar{\eta}(\tau_3)$
 $\eta_3 = \bar{\eta}(2)$

$$\eta_3 = A$$

$$\eta_1 = \eta_3 e^{-B/4}$$

$$B = 4k_1 : k_1 = \ln \left(\frac{\eta_3}{\eta_2} \right) > 0$$

$$\eta_2 = \eta_3 e^{-B(\tau_3)^2 \left(1 - \frac{\tau_3}{2}\right)^2}$$

$$B(\tau_3)^2 \left(\frac{2-\tau_3}{2} \right)^2 = k_2 : k_2 = \ln \left(\frac{\eta_3}{\eta_2} \right) > 0$$

$$(\tau_3)^2 (2-\tau_3)^2 = \frac{k_2}{k_1}$$

$$\tau_3 (2-\tau_3) = \pm k_3$$

$$k_3 = \sqrt{\frac{k_2}{k_1}} \quad (\text{note that } k_3 < 1)$$

$$\tau_3^2 - 2\tau_3 \pm k_3 = 0$$

$$\tau_3 = \frac{2 \pm \sqrt{4 \mp 4k_3}}{2} = 1 \pm \sqrt{1 \mp k_3}$$

$$\text{since } \tau_3 > 1, \tau_3 = 1 + \sqrt{1 \mp k_3}$$

$$\text{since } \tau_3 < 2, \tau_3 = 1 + \sqrt{1 - k_3}$$

For the $t \rightarrow \tau$ transformation:

$$0 \rightarrow 1, t_1 \rightarrow \tau_3, t_\ell \rightarrow 2$$

$$\frac{t}{t-t_1} = k_4 \left(\frac{\tau-1}{2-\tau_3} \right)$$

and

$$k_4 = (2-\tau_3) \left(\frac{t_\ell}{t_\ell-t_1} \right)$$

$$\tau t - \tau_3 t = k_4 \left[\tau (t-t_1) - (t-t_1) \right]$$

$$\tau \left[t - k_4 (t-t_1) \right] = \tau_3 t - k_4 (t-t_1)$$

$$\tau = \frac{(\tau_3 - k_4) t + k_4 t_1}{(1 - k_4) t + k_4 t_1}$$

These three cases can be summarized as follows:

$$\text{Let } \eta_i = \max \left[\eta_1, \eta_2, \eta_3 \right]$$

$$j_1 = 7 - 8i + 2i^2$$

$$j_2 = 5 - 5i + i^2$$

$$j_3 = 22 - 27i + 7i^2$$

$$j_4 = 2 + j_2$$

$$j_5 = 4 - j_2 - i$$

$$k_1 = \ln \left(\frac{\eta_i}{\eta_{j_4}} \right) \quad k_2 = \ln \left(\frac{\eta_i}{\eta_{j_5}} \right) \quad k_3 = \sqrt{\frac{k_2}{k_1}}$$

$$A = \eta_i$$

$$B = 4 k_1$$

$$\bar{\tau} = 1 - j_2 \sqrt{1 - j_1 k_3}$$

$$k_4 = \left[\frac{-j_1 \bar{\tau} + \frac{j_3}{2}}{(j_5 - 2) \bar{\tau} + j_1} \right] \left(\frac{t_\ell}{t_\ell - t_1} \right)$$

$$f' = \left(\frac{1+j_1}{2} \right) \bar{\tau} + \left(\frac{j_2-1}{2} \right) k_4 + (1-j_1)$$

$$f = f' t + \left(\frac{1-j_2}{2} \right) k_4 t_1$$

$$\tau = \frac{f}{(1-k_4)t + k_4 t_1}$$

$$\bar{\eta} = A e^{-B \tau^2 \left(1 - \frac{\tau}{2}\right)^2}$$

$$\frac{d \bar{\eta}}{d t} = \left(\frac{d \bar{\eta}}{d \tau} \right) \left(\frac{d \tau}{d t} \right) = \left(\frac{d \bar{\eta}}{d \tau} \right) \tau'$$

$$= \bar{\eta} (-B) \left[2 \tau \left(1 - \frac{\tau}{2}\right)^2 + \tau^2 (2) \left(1 - \frac{\tau}{2}\right) \left(-\frac{1}{2}\right) \right] \tau'$$

$$= -B \bar{\eta} \left[\frac{\tau}{2} (2-\tau)^2 - \frac{\tau^2}{2} (2-\tau) \right] \tau'$$

$$= -B \bar{\eta} \tau (2-\tau) \left[\left(\frac{2-\tau}{2} \right) - \frac{\tau}{2} \right] \tau'$$

$$= -B \bar{\eta} \tau (2-\tau) [1-\tau] \tau'$$

$$= -B \bar{\eta} \tau (1-\tau) (2-\tau) \tau'$$

$$\tau' = \frac{f'}{(1-k_4)t + k_4 t_1} - \frac{f(1-k_4)}{\left[(1-k_4)t + k_4 t_1 \right]^2}$$

$$= \frac{f'}{f} \tau - \frac{(1-k_4)}{f} \tau^2$$

$$= \frac{f' \tau - \tau^2 (1-k_4)}{f}$$

We now check these formulas for the three cases:

Case I:

$$i = 1$$

$$j_1 = 1 \quad j_2 = 1 \quad j_3 = 2 \quad j_4 = 3 \quad j_5 = 2$$

$$k_1 = \ln \left(\frac{\eta_1}{\eta_3} \right) \quad k_2 = \ln \left(\frac{\eta_1}{\eta_2} \right) \quad k_3 = \sqrt{\frac{k_2}{k_1}}$$

$$A = \eta_1 \quad B = 4 k_1 \quad \bar{\tau} = 1 - \sqrt{1-k_3}$$

$$f' = \bar{\tau} \quad f = \bar{\tau} t$$

$$k_4 = (1-\bar{\tau}) \left(\frac{t_\ell}{t_\ell - t_1} \right)$$

$$\tau = \frac{\bar{\tau} t}{(1-k_4) t + k_4 t_1}$$

Case II:

$$i = 2 \quad k_1 = \ln \left(\frac{\eta_2}{\eta_1} \right)$$

$$j_1 = -1$$

$$j_2 = -1 \quad k_2 = \ln \left(\frac{\eta_2}{\eta_3} \right)$$

$$j_3 = -4$$

$$j_4 = 1 \quad k_3 = \sqrt{\frac{k_2}{k_1}}$$

$$j_5 = 3$$

$$A = \eta_2 \quad B = 4 k_1 \quad \bar{\tau} = 1 + \sqrt{1+k_3}$$

$$k_4 = \left(\frac{\bar{\tau} - 2}{\bar{\tau} - 1} \right) \left(\frac{t_\ell}{t_\ell - t_1} \right)$$

$$f' = 2 - k_4 \quad f = k_4 t_1 + (2-k_4) t$$

$$\tau = \frac{(2-k_4) t + k_4 t_1}{(1-k_4) t + k_4 t_1}$$

Case III:

$$\begin{aligned} i &= 3 & k_1 &= \ln \left(\frac{\eta_3}{\eta_1} \right) \\ j_1 &= 1 \\ j_2 &= -1 & k_2 &= \ln \left(\frac{\eta_3}{\eta_2} \right) \\ j_3 &= 4 \\ j_4 &= 1 & k_3 &= \sqrt{\frac{k_2}{k_1}} \\ j_5 &= 2 \end{aligned}$$

$$A = \eta_3 \quad B = 4 k_1 \quad \bar{\tau} = 1 + \sqrt{1-k_3}$$

$$k_4 = (2-\bar{\tau}) \left(\frac{t_\ell}{t_\ell - t_1} \right)$$

$$f' = \bar{\tau} - k_4 \quad f = f' t + k_4 t_1$$

$$\tau = \frac{(\bar{\tau} - k_4) t + k_4 t_1}{(1-k_4) t + k_4 t_1}$$

C. We need to be able to transform from η back to the \bar{x} variable.

$$\xi = \begin{cases} \eta : r = 0 \\ \frac{\ln \left[(1-\eta) + \eta e^{-r} \right]}{-r} : r \neq 0 \end{cases}$$

The remaining problem is to solve this for \bar{x} :

$$\xi = \bar{x} e^{c(\bar{x}^2 - \bar{x})}$$

or

$$\bar{x} = \xi e^{c(\bar{x} - \bar{x}^2)} = f(\bar{x})$$

$$f'(\bar{x}) = c \cdot f(\bar{x}) \cdot (1-2\bar{x})$$

$$f'\left(\frac{1}{2}\right) = 0$$

$$x = \frac{1}{2} \Rightarrow \xi = \frac{1}{2} e^{-\frac{c}{4}} = \xi^*$$

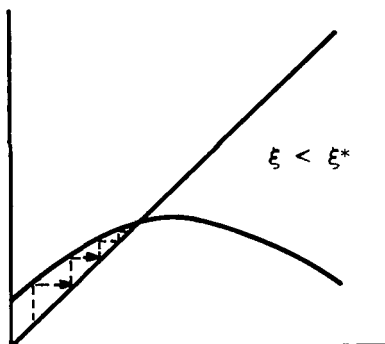
Thus,

$$\xi < \xi^* \Rightarrow x < \frac{1}{2}$$

$$\xi > \xi^* \Rightarrow x > \frac{1}{2}$$

We have, then, these two cases:

a.

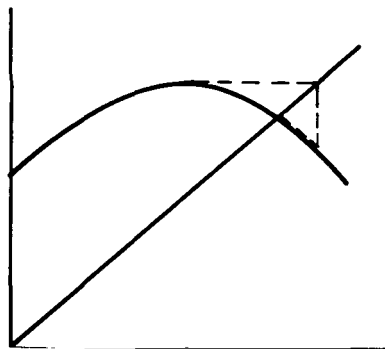


If the first guess is too small, successive approximations should converge (as indicated):

$$\bar{x}_{i+1} = f(\bar{x}_i)$$

Note that $\bar{x} - \xi = \left[e^c (\bar{x} - \bar{x}_1^2) - 1 \right] \xi > 0$ since $\bar{x} \leq 1$. Thus, if the first guess is ξ , this should work.

b.



The following iteration procedure should work: \bar{x}_{i+1} is intersection of these lines:

$$1) \quad y = \bar{x}$$

$$2) \quad y = f(\bar{x}_i) + (\bar{x} - \bar{x}_i) \cdot f'(\bar{x}_i)$$

or,

$$\bar{x}_{i+1} = \frac{f(\bar{x}_i) - \bar{x}_i \cdot f'(\bar{x}_i)}{1 - f'(\bar{x}_i)}$$

If $\bar{x}_1 > \frac{1}{2}$, $f'(\bar{x}_1) < 0$ and this should converge.

If first guess is $\bar{x}_1 = \frac{1}{2}$, $f'(\frac{1}{2}) = 0$,

$$f(\frac{1}{2}) = \bar{x}_2 = \xi e^{c/4}.$$

Thus, let $\bar{x}_1 = \xi e^{c/4}$.

SECTION VIII

PROCEDURE FOR OBTAINING SOLUTION

Initially all variables are assumed to be constant, with the possible exception of temperature. If desired, an initial temperature distribution can be computed, at some input time t_0 , according to an analytic solution (Section VI). In this case T at the frontface at time t_0 is obtained by iteration so as to satisfy equation VI. 6. The remaining values are obtained from equation VI. 4 or VI. 5, after the spacing parameters have been computed.

At the initial time, t_0 , it is assumed that quantities such as $\frac{\partial \rho}{\partial t}$, $\frac{d s_m}{dt}$, \dot{m}_g are effectively zero. If this were not the case, the analytical solution would make no sense, nor would a constant temperature distribution.

An approximate program procedure follows. Suppose everything is known at time t_1 .

1. Compute Δt . Compute $t_2 = t_1 + \Delta t$. The program attempts to use the value of Δt given as input. This may be reduced because of these factors:
 - a. The stability criterion for the density equation (V. 5).
 - b. To avoid melting too much per time step.
 - c. To prevent Δt from increasing too rapidly.

2. Compute the explicit values of the variables (equations IV. 10 and V. 10).

3. Compute $s_m(t_2)$ and $s_c(t_2)$:

$$s_m(t_2) = s_m(t_1) + \Delta t \dot{s}_m(t_1)$$

$$s_c(t_2) = s_c(t_1) + \Delta t s'_c(t_1).$$

Remark: This integration method (Euler's) is probably the most inaccurate one available. However, for our cases it seems sufficient. If one wanted to insert a more accurate method, the iteration procedure for the rate of melt would need to be somewhat modified: steps 3 and 4 would be repeated for each guess at $\dot{s}_m(t_2)$.

4. Compute the spacing parameters for time t_2 (Section VII. A and Section VII. B). Compute the real space coordinates of the points (Section VII. C). Compute these terms which arise from the space transformation: η_x (equation B2.5), η_{xx} (equation B2.7).
5. Compute first guess at $\dot{s}_m(t_2)$.
6. Compute spacing parameter, η_t (equation B2.6).
7. The "short" iteration on the rate of melt proceeds as follows:
 - a. If appropriate, compute second interior point by implicit equations (IV. 10, V. 11).

- b. Compute frontface values (IV.11, V.13). If necessary, also compute first interior point. The iteration here centers around the frontface: for each guess at the frontface, obtain interior point values.
 - c. Compute $\dot{s}_m(t_2)$.
 - d. If iterating, obtain next guess and go back to a.
8. Obtain implicit values (IV.11, V.11), except for points next to boundary points.
9. Compute interface values (IV.14). If adjacent points are implicit, calculate them also. The iteration centers around the interface; for each guess at the interface obtain the interior values.
10. If appropriate, obtain air gap values (IV.21, IV.22). If adjacent points are implicit, calculate them also. Again, the iteration centers around the air gap values.
11. Compute frontface values (IV.11, V.13). If necessary, obtain first interior points. As before, the iteration centers around the frontface.
12. Compute $\dot{s}_m(t_2)$.
13. If performing long iteration on the rate of melt, obtain next guess and go back to 6.
14. Compute the heat balance values.

SECTION IX

ACCURACY OF PROGRAM

In discussing accuracy of the numerical results, one must first distinguish problems arising at boundary points from those arising at interior points. In Section III the second problem was discussed. Convergence was established under various conditions, one of which was the assumption that all temperatures are known on the boundary. In Section IV problems arising from non-linearity were pointed out.

When more general boundary conditions are given, the theory is not well-developed, and consequently not very helpful. Some of the problems were mentioned in Section I. In particular it was noted there that in a previous program we had difficulty maintaining stability of its difference equation in conjunction with a severe frontface boundary condition. Experience has indicated certain steps that should be taken. Accordingly, the following features are in the program:

1. Solution of boundary conditions with implicit equations. This prevents a "temperature lag" which at times can cause serious oscillations (particularly at the frontface and in the air gap).
2. Space transformations (see Appendix B2): the first transformation (Landau's) allows melting to proceed without dropping nodes; the second allows unequal spacing of points (this is particularly useful in cases with large temperature gradients at the frontface).
3. Second order approximations: whenever possible all numerical approximations at boundary points have second order accuracy (three-point approximation). (See Appendix B4)
4. Analytical solution for first time step: see Section VI. In cases which begin with a constant temperature distribution spacial truncation error can be excessive for the first few time steps. The analytical solution enables the numerical procedure to begin with a distribution which is quite consistent with the front-face boundary condition.

The previous remarks have actually been concerned with the problem of maintaining accuracy of the numerical solution. In the remainder of this section we concern ourselves with the following, more decisive, question: given a computer run, how accurate is it?

For a particular problem we feel the following two checks should be made:

1. Make several runs with decreasing time and space increments. When they agree to desired accuracy (that is, convergence is indicated), we assume the program is solving some differential equation correctly.
2. Perform a heat balance. If this is satisfactory, we are willing to suppose that it is indeed the heat conduction equation that is being solved.

The first check is probably not as bad as it sounds. Generally, a set of runs are made at one time. If for one of these, Δt and $\Delta \eta$ were properly determined, the remaining runs could probably be handled quickly.

It should be noted that a heat balance alone does not assure good results. Many different temperature distributions could conceivably result in the same amount of heat being stored in the body. In difference equations which are derived by maintaining a heat balance from node to node, it is clear that such a balance is not too significant for, by definition, the numerical check must be good. However, in this program the question of heat balance played no part in the derivation of the difference equations. Thus, we feel that a good check here indicates that things are not going too badly. If accuracy is lost in the temperatures, it will also be displayed in the numerical calculation of a heat balance.

It appears, therefore, that a satisfactory heat balance would actually perform both of the previous checks. They have been stated separately only to indicate that in cases where a good balance is not achieved, the first check may need to be made separately. Because of its importance it was decided to include a heat balance check in the program. We now discuss the calculation.

It is assumed for the purpose of this calculation that the original equation:

$$T_t = b_1 T_{xx} + b_2 (T_x)^2 + b_3 T_x + b_4$$

was originally of this form:

$$\rho c_p T_t = (k T_x)_x - s_2 T_x - s_3 \quad (\text{IX. 1})$$

It is assumed that:

$$\begin{aligned} k &= k_1 k_a : \\ k_1 &= k_1(T) \\ k_a &= k_a(\rho) \end{aligned}$$

The algebra is carried out in Appendix B1. From equation B1.8 we obtain:

$$b_1 = \frac{k}{\rho c_p}$$

$$\left. \begin{aligned} b_2 &= \left(\frac{k'_1}{k_1} \right) \left(\frac{k}{\rho c_p} \right) \\ b_3 &= - \left(\frac{s_2}{\rho c_p} \right) + \left(\frac{k}{\rho c_p} \right) \left(\frac{k'_a}{k_a} \right) \rho_x \\ b_4 &= - \frac{s_3}{\rho c_p} \end{aligned} \right\} \quad (\text{IX. 2})$$

From IX. 1,

$$(-k T_x)_x = -\rho c_p T_t - s_2 T_x - s_3$$

Thus, in each layer,

$$\int_0^{A_i} (-k T_x)_x dx = \dot{q}_{B.F.} - \dot{q}_{F.F.} = - \int_0^{A_i} [\rho c_p T_t + s_2 T_x + s_3] dx$$

$$\text{Letting } Q_i = - \int_0^t \left(\dot{q}_{B.F.} - \dot{q}_{F.F.} \right)_i dt \quad (\text{IX. 3})$$

$$(Q_i)_t = + \int_{s_m}^{A_i} [\rho c_p T_t + s_2 T_x + s_3] dx$$

Using B1.2 and B1.4,

$$\begin{aligned} (Q_i)_t &= + \int_0^1 [\rho c_p (T_t + \eta_t T_\eta) + s_2 \eta_x T_\eta + s_3] \left(\frac{1}{\eta_x} \right) d\eta \\ &= + \int_0^1 [\rho c_p T_t + (\rho c_p \eta_t + s_2 \eta_x) T_\eta + s_3] \left(\frac{1}{\eta_x} \right) d\eta \\ &= + \int_0^1 \left(\frac{\rho c_p}{\eta_x} \right) \left[T_t + \left(\eta_t + \frac{s_2 \eta_x}{\rho c_p} \right) T_\eta + \left(\frac{s_3}{\rho c_p} \right) \right] d\eta \end{aligned}$$

From IX. 2,

$$\rho c_p = \frac{k}{b_1}$$

$$\frac{s_2}{\rho c_p} = + b_1 \left(\frac{k'_a}{k_a} \right) \rho_x - b_3 = b_1 \eta_x \left(\frac{k'_a}{k_a} \right) \rho_\eta - b_3 = s_4 - b_3$$

$$\frac{s_3}{\rho c_p} = - b_4$$

$$\left(Q_i \right)_t = \int_0^1 \left(\frac{k}{b_1 \eta_x} \right) \left[T_t + (\eta_t + s_4 \eta_x - b_3 \eta_x) T_\eta - b_4 \right] d\eta$$

From Bl.5,

$$b_1 \eta_x = \frac{\beta_1}{\eta_x}$$

$$\eta_t - b_3 \eta_x = b_1 \eta_{xx} - \beta_3 = \beta_1 \frac{\eta_{xx}}{(\eta_x)^2} - \beta_3$$

$$b_4 = \beta_4$$

$$\left(Q_i \right)_t = \int_0^1 \left(\frac{k \eta_x}{\beta_1} \right) \left[T_t + \left(\frac{\beta_1 \eta_{xx}}{\eta_x^2} - \beta_3 + s_4 \eta_x \right) T_\eta - \beta_4 \right] d\eta \quad \left. \begin{array}{l} \eta_x s_4 = \beta_1 \left(\frac{k'_a}{k_a} \right) \rho_\eta \end{array} \right\} \quad (\text{IX. 4})$$

The indicated integration is performed by the trapezoidal rule.

From the equation given in Section II, paragraph A.5 we have for each layer i:

$$\left(\dot{q}_{B.F.} \right)_i = C_i T_t + \left(\dot{q}_{F.F.} \right)_{i+1} : i + 1 \leq n$$

Thus,

$$\begin{aligned} \sum_{i=1}^n \left(Q_i \right)_t &= \sum_{i=1}^n \left(\dot{q}_{F.F.} \right)_i - \sum_{i=1}^n \left(\dot{q}_{B.F.} \right)_i \\ &= \sum_{i=1}^n \left(\dot{q}_{F.F.} \right)_i - \sum_{i=1}^{n-1} C_i T_t - \sum_{i=1}^{n-1} \left(\dot{q}_{F.F.} \right)_{i+1} - \left(\dot{q}_{B.F.} \right)_n \end{aligned}$$

or,

$$\sum_{i=1}^n (Q_i)_t = (\dot{q}_{F.F.})_1 - (\dot{q}_{B.F.})_n - \sum_{i=1}^{n-1} C_i T_t$$

$$= \dot{q}_{net} - \dot{q}_{B.V.} - \sum_{i=1}^{n-1} C_i T_t$$

Let

$$Q_{total} = \sum_{i=1}^n Q_i + \int_0^{t_1} \dot{q}_{B.F.} dt + \int_0^{t_1} \left(\sum_{i=1}^{n-1} C_i T_t \right) dt \quad (IX. 5)$$

Then the heat balance check consists in comparing these two numbers: Q_{total} and $\int_0^{t_1} \dot{q}_{net} dt$.

All indicated integrations are performed by the trapezoidal rule. Note that $\dot{q}_{B.F.}$ is calculated from the temperature distribution: this accounts for the apparent disappearance of $C_n T_t$. If, however, the air gap is the last layer, it is not possible to calculate $\dot{q}_{B.F.}$ from the temperatures. Then $\dot{q}_{B.F.}$ is set equal to the input $\dot{q}_{B.F.}$ (which should be zero) and $C_n T_n$ is included in the heat balance.

In the air gap, since there are no interior points, equation IX. 4 can be simplified:

$$(Q_i)_t = A_i (\rho c_p)_i T_t \quad (IX. 6)$$

where T_t is to be averaged over the air gap.

Finally, if an analytical solution is used to time t_0 , we assume the check is satisfactory to that time. Thus, if the analytical solution was used incorrectly, the heat balance check would not reveal this.

SECTION X: PRESSURE OPTION

This section describes the procedure used to solve the combined temperature and pressure equations. Part A contains the governing equations. Part B describes the difference equation used for the gas density equation (density is obtained instead of pressure). Part C describes the difference equations used for the temperature equation. Part D discusses some stability considerations. Part E describes various computations that need to be made.

Although treated separately, all equations finally obtained are solved simultaneously.

(A) The governing equations are as follows:

Continuity Equation:

$$\left(\rho_g\right)_t + \nabla \cdot \left(\rho_g \mathbf{V}_g\right) = \dot{W}_g \quad (\text{X.1.1})$$

$$\dot{W}_g = -\dot{W}_s = \beta e^{-\frac{E}{RT}} \rho_{vp} \left(\frac{\rho_s - \rho_{cf}}{\rho_{vp}}\right)^n \quad (\text{X.1.2})$$

$$\left. \begin{aligned} p_g &= \rho_g \bar{R}T \\ \rho_g &= \epsilon \rho'_g \\ p_g &= \epsilon p'_g \\ \dot{W}_g &= \epsilon \dot{W}'_g \end{aligned} \right\} \quad (\text{X.1.3})$$

Energy Equation (gas):

$$\left. \begin{aligned} \rho_g \bar{C}_{p_g} \left(T_g\right)_t &= -\rho_g \bar{C}_p \mathbf{V}_g \cdot \nabla T_g + \left(p_g\right)_t + \nabla \cdot \left(\epsilon \mathbf{K}_g \cdot \nabla T_g\right) \\ &+ Q_{\text{transferred from gas}} + h_g \dot{W}_g \\ &+ \nabla \cdot \left(\epsilon \tau'_{ij} \cdot \mathbf{V}_g\right) - \left[\rho_g \mathbf{V}_g \left(\mathbf{V}_g\right)_t + \rho_g \mathbf{V}_g \cdot \left(\mathbf{V}_g \cdot \nabla \mathbf{V}_g\right) \right. \\ &\left. + \left(\mathbf{V}_g\right)^2 \dot{W}_g / 2 \right] \end{aligned} \right\} \quad (\text{X.1.4})$$

Energy Equation (solid):

$$(1 - \epsilon) \left(\rho'_p C_{vp} + \rho'_c C_{vc} \right) \left(T_s \right)_t = \nabla \cdot \left[(1 - \epsilon) (K_s \nabla T_s) - \left(e_c \dot{W}_c + e_{vp} \dot{W}_{vp} \right) \right] - Q_{\text{transferred from gas}} \quad (\text{X.1.5})$$

Where:

$$\dot{W}_s = \dot{W}_c + \dot{W}_p$$

Defining a gasification ratio Γ as

$$\left. \begin{aligned} \Gamma &= \frac{\dot{W}_s}{\dot{W}_p} = \text{constant} = 1 - \frac{\rho_{cf}}{\rho_{vp}} \\ \rho_p &= (1 - \epsilon) \rho'_{vp} \\ \rho_c &= (1 - \epsilon) \rho'_c \\ \rho_p &= \frac{1}{\Gamma} \left(\rho_s - \rho_{cf} \right) \\ \rho_c &= \rho_s - \rho_{vp} \end{aligned} \right\} \quad (\text{X.1.6})$$

$$\frac{k}{\epsilon} = k_f \epsilon^{(m)-1} : 1 < m < 3 \quad (\text{X.1.7})$$

Momentum Equation:

$$V_g = \nabla \cdot \left[\frac{g \bar{RT}}{\mu} \cdot \left(\frac{k}{\epsilon} \rho_g \right) \right] \quad (\text{X.1.8})$$

$$\epsilon = 1 - \rho_c \left(\frac{1}{\tilde{\rho}_c} - \frac{1}{\tilde{\rho}_{vp}} \right) - \frac{\rho_s}{\tilde{\rho}_p} \quad (\text{X.1.9})$$

$$(1 - \epsilon) K_s = \frac{1}{\rho_s} \left(\rho_p K_p + \rho_c K_c \right)$$

$\tilde{\rho}_c$ and $\tilde{\rho}_p$ are input constants

Properties of the gas are assumed to be independent of the composition of the gas. Thus an average value which is dependent on temperature is used.

$$\begin{aligned}
 \bar{C}_p &= f(T) \\
 C_v &= f(T) \\
 C_v^p &= f(T) \\
 e_c &= f(T) \\
 e_p &= f(T) \\
 \bar{m} &= \text{constant} \\
 R &= f(T) = \frac{R}{\bar{m}} \\
 h_g &= f(T) \\
 \mu &= \mu_o T^{(2/3)} \\
 K_p &= f(T) \\
 K_c &= f(T) \\
 K_g &= f(T)
 \end{aligned} \tag{X.1.10}$$

As a boundary condition we assume given at the front-face $P_g(t)$. Then,

$$\rho_g(o, t) = \epsilon P_g(t) / \bar{R} T$$

At the backface we assume $\frac{\partial \rho_g}{\partial x} = 0$.

(B) We discuss a difference equation for the continuity equation, X.1.1. For purposes of stability this will be considered an equation in ρ_g . For ease in notation let $\rho_g = \rho$.

Let

$$d_1 = \left(\frac{g \bar{R} T}{\mu} \right) \left(\frac{k}{\epsilon} \right) = d_1(T, \rho_s) \tag{X.2.1}$$

Then,

$$\rho_t = \nabla \cdot (\rho \nabla d_1 \rho) + \dot{W}_g$$

In one dimension,

$$\rho_t = \left[\rho (d_1 \rho)_x \right]_x + \dot{W}_g$$

$$\rho_t = \rho (d, \rho)_{xx} + \rho_x (d, \rho)_x + \dot{W}_g$$

$$\rho_t = \rho \left[d, \rho_{xx} + 2 \rho_x d_{1x} + \rho d_{1xx} \right] + \rho_x \left(d_{1x} \rho + \rho_x d_1 \right) + \dot{W}_g$$

$$\rho_t = \rho d_1 \rho_{xx} + 3 \rho d_{1x} \rho_x + d_1 (\rho_x)^2 + \rho^2 d_{1xx} + \dot{W}_g$$

Let,

$$d_2 = 3 d_{1x} \quad (X.2.2)$$

$$d_3 = d_{1xx} \quad (X.2.3)$$

$$d_4 = -\dot{W}_s = \dot{W}_g \quad (X.2.4)$$

Then,

$$\rho_t = d_1 \rho \rho_{xx} + d_2 \rho \rho_x + d_1 (\rho_x)^2 + d_3 \rho^2 + \dot{W}_g$$

Performing the space transformations (Equations A.2, A.3, A.4)

$$\begin{aligned} \rho_t + \eta_t \rho_\eta &= d_1 \rho \left(\eta_x^2 \rho_{\eta\eta} + \eta_{xx} \rho_\eta \right) + d_2 \rho \left(\eta_x \rho_\eta \right) \\ &\quad + d_1 \eta_x^2 (\rho_\eta)^2 + d_3 \rho^2 + \dot{W}_g \\ \rho_t &= \left(d_1 \rho \eta_x^2 \right) \rho_{\eta\eta} + \left(\rho d_1 \eta_{xx} + \rho d_2 \eta_x - \eta_t \right) \rho_\eta \\ &\quad + d_1 \eta_x^2 (\rho_\eta)^2 + d_3 \rho^2 + \dot{W}_g \end{aligned} \quad (X.3.1)$$

$$d_1 = \left(\frac{g R T^{1/3}}{\mu_o} \right) \left(\frac{k}{\epsilon} \right) \quad (X.3.2)$$

$$d_2 = 3 \eta_x d_{1\eta} \quad (X.3.3)$$

$$d_3 = (\eta_x)^2 d_{1\eta\eta} + \eta_{xx} d_{1\eta} \quad (X.3.4)$$

$$d_4 = -\dot{W}_s \quad (X.3.5)$$

Let

$$\beta_1 = d_1 \eta_x^2 \quad (\text{X.3.6})$$

$$\beta_2 = d_1 \eta_{xx} + d_2 \eta_x \quad (\text{X.3.7})$$

$$\beta_3 = \beta_1 \left(\frac{\rho_{j+1} - \rho_{j-1}}{2\Delta\eta} \right) \quad (\text{X.3.8})$$

$$\beta_4 = \beta_3 - \eta_t \quad (\text{X.3.9})$$

Note that the difference in β_3 has not specified the time step. We will attempt the same difference equation as for the temperature (Sections III and IV). Thus, when using an explicit equation, β_3 will be evaluated at time step "n"; when using an implicit equation, "n+1" will be used.

Then,

$$\rho_t = \beta_1 \rho_{\eta\eta} + \beta_2 \rho_{\eta} + \beta_4 \rho_{\eta} + d_3 \rho^2 + d_4 \quad (\text{X.4})$$

The "normal" explicit-implicit difference equation can be applied to X.4. The only question is the approximation for $\beta_2 \rho_{\eta}$ and $\beta_4 \rho_{\eta}$. Assuming $d_3 = d_4 = 0$, we want the numerical scheme to be such that for the implicit equation, a boundedness condition is satisfied. Specifically, we want

$$\rho_{\min} \leq \rho_j^{n+1} \leq \rho_{\max} \quad \text{where}$$

$$\rho_{\min} = \min \left[\rho_{j+1}^{n+1}, \rho_{j-1}^{n+1}, \rho_j^n \right]$$

$$\rho_{\max} = \max \left[\rho_{j+1}^{n+1}, \rho_{j-1}^{n+1}, \rho_j^n \right]$$

Consider first the case

$$\beta_2 = \beta_4 = d_3 = d_4 = 0$$

Then,

$$\rho_j^{n+1} - \rho_j^n = \left(\frac{\Delta t \beta_1}{\Delta \eta^2} \right) \left(\rho_j^{n+1} \right) \left(\rho_{j+1}^{n+1} + \rho_{j-1}^{n+1} - 2 \rho_j^{n+1} \right)$$

Suppose $\rho_j^n, \rho_{j+1}^{n+1}, \rho_{j-1}^{n+1}$ are all positive. This equation is to be solved for ρ_j^{n+1} . Since we have a quadratic, there are two solutions. This will be discussed later, but for now assume $\rho_j^{n+1} > 0$. To show that the boundedness condition is satisfied, we proceed as follows:

$$a) \quad \rho_j^{n+1} > \rho_j^n \Rightarrow \rho_j^{n+1} \leq \text{MAX} \left[\rho_{j+1}^{n+1}, \rho_{j-1}^{n+1} \right]$$

$$b) \quad \rho_j^{n+1} < \rho_j^n \Rightarrow \rho_j^{n+1} \geq \text{MIN} \left[\rho_{j+1}^{n+1}, \rho_{j-1}^{n+1} \right]$$

Suppose now $\beta_4 = d_3 = d_4 = 0$. Suppose $\beta_2 > 0$.

Let

$$p_1 = \frac{\Delta t \beta_1}{\Delta \eta^2}, \quad p_2 = \frac{\Delta t \beta_2}{\Delta \eta}$$

$$\begin{aligned} \rho_j^{n+1} - \rho_j^n &= \rho_j^{n+1} \left[p_1 \left(\rho_{j+1}^{n+1} + \rho_{j-1}^{n+1} - 2\rho_j^n \right) + p_2 \left(\rho_{j+1}^{n+1} - \rho_j^{n+1} \right) \right] \\ &= \rho_j^{n+1} \left[\left(p_1 + p_2 \right) \rho_{j+1}^{n+1} + p_1 \rho_{j-1}^{n+1} - \left(2p_1 + p_2 \right) \rho_j^{n+1} \right] \\ &= \rho_j^{n+1} \left[a_1 \rho_{j+1}^{n+1} + a_2 \rho_{j-1}^{n+1} - \left(a_1 + a_2 \right) \rho_j^{n+1} \right] \end{aligned}$$

where a_1 and $a_2 > 0$.

As before,

$$a) \quad \rho_j^{n+1} > \rho_j^n \Rightarrow \rho_j^{n+1} \leq \text{MAX} \left[\rho_{j+1}^{n+1}, \rho_{j-1}^{n+1} \right]$$

$$b) \quad \rho_j^{n+1} < \rho_j^n \Rightarrow \rho_j^{n+1} \geq \text{MIN} \left[\rho_{j+1}^{n+1}, \rho_{j-1}^{n+1} \right]$$

If $\beta_2 < 0$, use $\rho_j^{n+1} - \rho_{j-1}^{n+1}$ for ρ_η and the same result follows.

Suppose now that $d_3 = d_4 = 0$. Suppose $\beta_2 > 0, \beta_4 > 0$. Let

$$p_3 = \beta_4 \frac{\Delta t}{\Delta \eta}$$

$$\begin{aligned}
\rho_j^{n+1} - \rho_j^n &= \rho_j^{n+1} \left[(p_1 + p_2) \rho_{j+1}^{n+1} + p_1 \rho_{j-1}^{n+1} - (2p_1 + p_2) \rho_j^{n+1} \right] \\
&\quad + p_3 \left(\rho_{j+1}^{n+1} - \rho_j^{n+1} \right) \\
&= \rho_{j+1}^{n+1} \left[(p_1 + p_2) \rho_j^{n+1} + p_3 \right] + \rho_{j-1}^{n+1} \left[p_1 \rho_j^{n+1} \right] \\
&\quad - \rho_j^{n+1} \left[\rho_j^{n+1} (2p_1 + p_2) + p_3 \right] \\
&= a_1 \rho_{j+1}^{n+1} + a_2 \rho_{j-1}^{n+1} - (a_1 + a_2)
\end{aligned}$$

Although the a_i depend on ρ_j^{n+1} , suppose the solution to the quadratic equation is such that $a_i > 0$. Then we can apply the same arguments as before. If $\beta_4 < 0$, use $\rho_j^{n+1} - \rho_{j-1}^{n+1}$ to obtain the same result. Summarizing,

$$\beta_2 \rho_\eta = \frac{\beta_2}{\Delta\eta} \left[\alpha_1 \rho_{j+1} + (\alpha_1 - 1) \rho_{j-1} + (1 - 2\alpha_1) \rho_j \right]$$

where

$$\alpha_1 = \begin{cases} 1 : \beta_2 \geq 0 \\ 0 : \beta_2 < 0 \end{cases} \quad (\text{X.5.1})$$

Let

$$\rho_{\eta\eta} = \frac{\rho_{j+1} + \rho_{j-1} - 2\rho_j}{\Delta\eta^2} \quad (\text{X.5.2})$$

Then,

$$\beta_2 \rho_\eta = \left(\beta_2 \right) \left(\Delta\eta \alpha_1 \right) \rho_{\eta\eta} + \left(\frac{\rho_j - \rho_{j-1}}{\Delta\eta} \right) \beta_2 \quad (\text{X.5.3})$$

Also,

$$\beta_4 \rho_\eta = \left(\Delta\eta \right) \left(\beta_4 \alpha_2 \right) \rho_{\eta\eta} + \left(\frac{\rho_j - \rho_{j-1}}{\Delta\eta} \right) \beta_4 \quad (\text{X.5.4})$$

where

$$\alpha_2 = \begin{cases} 1 : \beta_4 \geq 0 \\ 0 : \beta_4 < 0 \end{cases}$$

Substituting into X.4,

$$\begin{aligned} \frac{\rho_j^{n+1} - \rho_j^n}{\Delta t} = & \left(\beta_1 \rho_j + \beta_2 \rho_j \Delta \eta \alpha_1 + \beta_4 \Delta \eta \alpha_2 \right) \rho_{\eta\eta} \\ & + \left(\beta_2 \rho_j + \beta_4 \right) \left(\rho_j - \rho_{j-1} \right) \left(\frac{1}{\Delta \eta} \right) + d_3 \left(\rho_j \right)^2 + d_4 \end{aligned}$$

Let

$$r_0 = \frac{\Delta t}{\Delta \eta^2} \quad (\text{X.5.5})$$

$$r_1 = \frac{\Delta t}{\Delta \eta} \quad (\text{X.5.6})$$

Then,

$$\begin{aligned} \rho_j^{n+1} - \rho_j^n = & r_0 \left[\left(\beta_1 + \beta_2 \Delta \eta \alpha_1 \right) \rho_j + \beta_4 \Delta \eta \alpha_2 \right] \left[\rho_{j+1} + \rho_{j-1} - 2\rho_j \right] \\ & + r_1 \left(\beta_2 \rho_j + \beta_4 \right) \left(\rho_j - \rho_{j-1} \right) + d_3 \Delta t \left(\rho_j \right)^2 + d_4 \Delta t \end{aligned}$$

Let

$$\gamma_1 = \left(\beta_1 + \beta_2 \Delta \eta \alpha_1 \right) r_0 \quad (\text{X.5.7})$$

$$\gamma_2 = \gamma_1 - \Delta \eta \beta_2 r_0 = \gamma_1 - \beta_2 r_1 \quad (\text{X.5.8})$$

$$\gamma_3 = r_1 \beta_4 \alpha_2 \quad (\text{X.5.9})$$

$$\gamma_4 = \gamma_3 - r_1 \beta_4 \quad (\text{X.5.10})$$

$$\begin{aligned}
\rho_j^{n+1} - \rho_j^n &= \left(\gamma_1 \rho_j + \gamma_3 \right) \left(\rho_{j+1} + \rho_{j-1} - 2\rho_j \right) + r_1 \left(\beta_2 \rho_j + \beta_4 \right) \left(\rho_j - \rho_{j-1} \right) \\
&\quad + d_3 \Delta t \left(\rho_j \right)^2 + d_4 \Delta t \\
&= \left(\rho_j \right)^2 \left[-2\gamma_1 - r_1 \beta_2 + d_3 \Delta t \right] \\
&\quad + \rho_j \left[\gamma_1 \left(\rho_{j+1} + \rho_{j-1} \right) - 2\gamma_3 + \beta_4 r_1 - \beta_2 r_1 \rho_{j-1} \right] \\
&\quad + \left[\gamma_3 \left(\rho_{j+1} + \rho_{j-1} \right) - r_1 \beta_4 \rho_{j-1} + d_4 \Delta t \right] \\
&= - \left(\gamma_1 + \gamma_2 - d_3 \Delta t \right) \left(\rho_j \right)^2 + \left(\gamma_1 \rho_{j+1} + \gamma_2 \rho_{j-1} - \gamma_3 - \gamma_4 \right) \rho_j \\
&\quad + \left(\gamma_3 \rho_{j+1} + \gamma_4 \rho_{j-1} + d_4 \Delta t \right)
\end{aligned}$$

Let

$$A = \gamma_1 + \gamma_2 - d_3 \Delta t \quad (\text{X.6.1})$$

$$\bar{B} = \gamma_3 + \gamma_4 - \gamma_1 \rho_{j+1} - \gamma_2 \rho_{j-1} \quad (\text{X.6.2})$$

$$B = 1 + \bar{B} \quad (\text{X.6.3})$$

$$\bar{C} = \gamma_3 \rho_{j+1} + \gamma_4 \rho_{j-1} + d_4 \Delta t \quad (\text{X.6.4})$$

$$C = \bar{C} + \rho_j^n \quad (\text{X.6.5})$$

Then,

Explicit scheme:

$$\rho_j^{n+1} = \left(1 - \bar{B} \right) \rho_j^n - A \left(\rho_j^n \right)^2 + \bar{C} \quad (\text{X.6.6})$$

where A , \bar{B} , \bar{C} are evaluated at (n, j)

Implicit scheme:

$$A \left(\rho_j^{n+1} \right)^2 + B \left(\rho_j^{n+1} \right) - C = 0$$

The coefficients are evaluated at $(n+1, j)$. Note that $\gamma_i \geq 0$. Thus, we assume $A > 0$ and $C > 0$. (If not, this can be achieved by cutting Δt). To determine the choice of ρ_j^{n+1} proceed as follows:

$$\left(\frac{A}{B}\right) \rho_j^{n+1}{}^2 + \rho_j^{n+1} - \frac{C}{B} = 0$$

$$\rho_j^{n+1} = \left[-1 \pm \sqrt{1 + \frac{4AC}{B^2}} \right] \left(\frac{B}{2A}\right)$$

as

$$\Delta t \rightarrow 0, B \rightarrow 1, C \rightarrow \rho_j^n$$

$$\rho_j^{n+1} \rightarrow \frac{1}{2A} \left[-1 \pm (1 + 2AC) \right] = \frac{-2 \pm 2AC}{2A}, +C$$

Clearly, then we need the "plus" root.

$$\rho_j^{n+1} = \frac{B}{2A} \left[-1 + \sqrt{1 + D} \right]$$

$$D = \frac{4AC}{B^2} \tag{X.6.7}$$

If $A > 0$, $C > 0$, the roots are of opposite sign. Thus, the correct one cannot be mistaken. If A or C is negative, it becomes confused.

For $|D|$ small, the program uses a series expansion in place of the radical:

IF $|D| < .02$,

$$-1 + \sqrt{1+D} = \frac{D}{2} \left[1 - \frac{D}{4} + \frac{D^2}{8} - \frac{5}{64} D^3 \right]$$

The error should be less than 10^{-8} .

There is still another aspect to be considered. Let us look at equation X.4 again and suppose that $\beta_1 = 0 = d_3 = d_4$. Then the equation is hyperbolic, and of the form:

$$\rho_t = \left(\beta_2 \rho + \beta_4 \right) \rho_\eta = \beta_5 \rho_\eta$$

This equation would have a stability criterion imposed by the characteristic: $\frac{dt}{d\eta} = \frac{1}{\beta_5}$

(See discussion of density equation - Section V). In cases where $\beta_1 \neq 0$ (which is always the situation in a problem), this characteristic does not exist. However, when β_5 becomes large, the equation appears to behave as though it were hyperbolic. We have found it necessary to apply the criteria:

$$\frac{dt}{d\eta} \leq \frac{1}{|\beta_5|}$$

Also, since β_4 already has a difference in it, we have considered the terms separately. This, then, is the restriction on Δt imposed by the gas density equation:

Let

$$\beta = \max \left[|\beta_2 \rho|, |\beta_4| \right] \quad (\text{X.6.9})$$

Then,

$$\frac{\Delta t}{\Delta \eta} \leq \frac{\epsilon}{\beta} \quad (\text{X.6.10})$$

(we presently have chosen $\epsilon = 3/4$).

(C) Now considering the energy equation. First assume $T_s = T_g = T$, and add X.1.4 to X.1.5

$$\begin{aligned} & \left[\rho_g \bar{C}_p + (1-\epsilon) \left(\rho'_p C_{vp} + \rho'_c C_{vc} \right) \right] T_t = \nabla \cdot \left[\left[\epsilon K_g + (1-\epsilon) K_s \right] \nabla T \right] \\ & + \left(P_g \right)_t + h_g \dot{W}_g - \left(e_c \dot{W}_c + e_p \dot{W}_p \right) - \rho_g \bar{C}_p V_g \nabla T \\ & + \nabla \left(\epsilon \tau_{ij} V_g \right) - \left[\rho_g V_g \left(V_g \right)_t + \rho_g V_g \left(V_g \nabla V_g \right) + \frac{\left(V_g \right)^2 \dot{W}_g}{2} \right] \end{aligned}$$

Let

$$\begin{aligned} (\rho C_p)^* &= \rho_g \bar{C}_p + (1-\epsilon) \left(\rho'_p C_{vp} + \rho'_c C_{vc} \right) \\ &= \rho_g \bar{C}_p + \rho_p C_{vp} + \rho_c C_{vc} \\ &= \rho_g \bar{C}_p + \frac{C_{vp}}{\Gamma} (\rho_s - \rho_{cf}) + C_{vc} (\rho_s - \rho_p) \\ &= \rho_g \bar{C}_p + \frac{C_{vp}}{\Gamma} (\rho_s - \rho_{cf}) + \frac{C_{vc}}{\Gamma} \left[\Gamma \rho_s - \rho_s + \rho_{cf} \right] \\ &= \rho_g \bar{C}_p + \rho_s \left[C_{vc} + \frac{C_{vp} - C_{vc}}{\Gamma} \right] + \rho_{cf} \left[\frac{C_{vc} - C_{vp}}{\Gamma} \right] \end{aligned}$$

Let

$$C_v = \frac{C_{vp} - C_{vc}}{\Gamma} \quad (\text{X.7.1})$$

$$\left(\rho C_p\right)^* = \rho_g \bar{C}_p + \left(C_{vc} + C_v\right) \rho_s - C_v \rho_{cf} \quad (\text{X.7.2})$$

Let

$$\begin{aligned} K_{\text{eff}} &= \epsilon K_g + (1-\epsilon) K_s \\ &= \epsilon K_g + \left(\frac{\rho_p}{\rho_s}\right) K_p + \left(\frac{\rho_c}{\rho_s}\right) K_c \quad : \text{from X.1.9} \\ &= \epsilon K_g + \frac{1}{\rho_s} \left[\rho_p K_p + \left(\rho_s - \rho_p\right) K_c \right] \\ &= \epsilon K_g + \frac{\rho_p}{\rho_s} \left(K_p - K_c \right) + K_c \\ &= \epsilon K_g + \left(\frac{K_p - K_c}{\Gamma} \right) \left(1 - \frac{\rho_{cf}}{\rho_s} \right) + K_c \end{aligned}$$

Let

$$\epsilon K'_g = K_g \quad (\text{X.7.3})$$

$$\frac{K_p - K_c}{\Gamma} = K \quad (\text{X.7.4})$$

Then

$$\begin{aligned} K_{\text{eff}} &= K_g + \left(1 - \frac{\rho_{cf}}{\rho_s} \right) K + K_c \quad (\text{X.7.5}) \\ e_c \dot{W}_c + e_p \dot{W}_p &= e_c \dot{W}_s \left(1 - \frac{1}{\Gamma} \right) + e_p \left(\frac{\dot{W}_s}{\Gamma} \right) \\ &= \dot{W}_s \left[\frac{e_c (\Gamma - 1) + e_p}{\Gamma} \right] \end{aligned}$$

Let

$$\bar{e} = \frac{e_p - e_c}{\Gamma} + e_c \quad (\text{X.7.6})$$

$$e_c \dot{W}_c + e_p \dot{W}_p = \bar{e} \dot{W}_s \quad (\text{X.7.7})$$

Assume now that there is only one space dimension to be considered, that FPS units are to be used; and that $\tau_{ij} \equiv 0$. This equation is obtained:

$$\begin{aligned} \left(\rho C_p\right)^* T_t &= \left(K_{\text{eff}} T_x\right)_x + \frac{\left(P_g\right)_t}{J} + \dot{W}_s \left(-\bar{e} - h_g\right) - \rho_g \bar{C}_p V_g T_* \\ &- \frac{1}{gJ} \left[P_g V_g \left(V_g\right)_t + \rho_g V_g^2 \left(V_g\right)_x + \left(V_g\right)^2 \frac{\dot{W}_s}{2} \right] \end{aligned} \quad (\text{X.7.8})$$

where $g = 32.2$, $J = 778$.

$$\begin{aligned} \left(\rho C_p\right)^* T_t &= K_{\text{eff}} T_{xx} + \left(K_{\text{eff}}\right)_T \left(T_x\right)^2 + \left(K_{\text{eff}}\right)_{\rho_s} \left(\rho_s\right)_x T_x - \dot{W}_s \left(\bar{e} + h_g\right) \\ &+ \left(\frac{P_g}{J}\right)_t - C_p \rho_g V_g T_x - \frac{P_g V_g \left(V_g\right)_t}{gJ} - \frac{\left(\rho_g\right) \left(V_g\right)^2 \left(V_g\right)_x}{gJ} - \frac{\left(V_g\right)^2 \dot{W}_s}{2gJ} \end{aligned} \quad (\text{X.7.9})$$

For purposes of difference equations, this is to be considered an equation in T . Thus, most of the terms need to be expanded.

$$\begin{aligned} \left(P_g\right)_t &= \left(\rho_g \bar{R} T\right)_t = \bar{R} T \left(\rho_g\right)_t + \rho_g \left(\bar{R}_T T + \bar{R}\right) T_t \\ &- V_g = \left[\left(\frac{g \bar{R} T}{\mu}\right) \left(\frac{k}{\epsilon}\right) \rho_g \right]_x = \left[\frac{g \bar{R} T^{1/3}}{\mu_o} \left(\frac{k}{\epsilon} \rho'_g\right) \right]_x \\ &= \frac{g}{\mu_o} \left[\left(\bar{R}_T T^{1/3} + \frac{\bar{R} T^{-2/3}}{3}\right) \left(T_x\right) \left(\frac{k}{\epsilon} \rho'_g\right) + \bar{R} T^{1/3} \left(\frac{k}{\epsilon} \rho'_g\right)_x \right] \\ &= \frac{g \bar{R} T^{1/3}}{\mu_o} \left[\left(\frac{k}{\epsilon} \rho'_g\right)_x + \left(\frac{1}{3T} + \frac{\bar{R} T}{\bar{R}}\right) \left(\frac{k}{\epsilon} \rho'_g\right) T_x \right] \\ \frac{\bar{R} T}{k} &= \left(\ln R\right)_T = \left[\ln R - \ln \bar{m}\right]_T = - \frac{\bar{m}_T}{\bar{m}} \end{aligned} \quad (\text{X.8.1})$$

Let

$$f_1 = \frac{1}{3T} - \frac{\bar{m}_T}{\bar{m}} \quad (\text{X.8.2})$$

$$V_g = - \left(a_1 T_x + a_2 \right) \quad (X.8.3)$$

$$a_1 = \left(\frac{g \bar{R} T^{1/3}}{\mu_o} \right) \left(f_1 \right) \left(\frac{\bar{k}}{\epsilon} \rho'_g \right) \quad (X.8.4)$$

$$a_2 = + \left(\frac{g \bar{R} T^{1/3}}{\mu_o} \right) \left(\frac{k}{\epsilon} \rho'_g \right)_x \quad (X.8.5)$$

$$\begin{aligned} (V_g)^2 &= (a_1^2) (T_x)^2 + 2 a_1 a_2 T_x + (a_2^2) \\ (V_g)_t &= - \left(a_1 T_{xt} + a_{1t} T_x + a_{2T} \right) \end{aligned} \quad (X.8.6)$$

$$\begin{aligned} a_{1t} &= \left(\frac{g \bar{R} T^{1/3} f_1}{\mu_o} \right) \left(\frac{k}{\epsilon} \rho_g \right)_t + \left(\frac{g \bar{R} T^{1/3}}{\mu_o} \right) \left(\frac{k}{\epsilon} \rho'_g \right) \left(f_1 \right)_t \\ &\quad + f_1 \left(\frac{k}{\epsilon} \rho_g \right) \left(\frac{g}{\mu} \right) \left(\bar{R}_T T^{1/3} + \frac{\bar{R} T^{1/3}}{3T} \right) T_t \end{aligned} \quad (X.8.7)$$

Let

$$\begin{aligned} a_3 &= \left(\frac{g \bar{R} T^{1/3} f_1}{\mu_o} \right) \left(\frac{k}{\epsilon} \rho_g \right)_t \\ (a_1)_t &= a_3 + a_1 \frac{(f_1)_t}{f_1} + a_1 (f_1)_{Tt} \end{aligned} \quad (X.8.8)$$

$$\begin{aligned} (a_1)_t &= a_3 + \left(\frac{a_1}{f_1} \right) \left[f_{1T} + (f_1)^2 \right] T_t \\ a_{2t} &= \left(\frac{g \bar{R} T^{1/3}}{\mu_o} \right) \left(\frac{k}{\epsilon} \rho_g \right)_{xt} + a_2 f_1 T_t \end{aligned}$$

Let

$$a_4 = \left(\frac{g \bar{R} T^{1/3}}{\mu_o} \right) \left(\frac{k}{\epsilon} \rho_g \right)_{xt} \quad (X.8.9)$$

$$a_{2_t} = a_4 + a_2 f_1 T_t \quad (X.8.10)$$

$$\begin{aligned} (V_g)_t &= - \left[a_1 T_{xt} + (a_3) T_x + \frac{a_1}{f_1} \left(f_{1_T} + f_1^2 \right) T_t T_x \right] - a_4 - a_2 f_1 T_t \\ (V_g)_x &= - \left(a_1 T_{xx} + a_{1_x} T_x + a_{2_x} \right) \end{aligned} \quad (X.8.11)$$

$$a_{1_x} = a_2 f_1 + \frac{a_1}{f_1} \left(f_{1_T} + f_1^2 \right) T_x \quad (X.8.12)$$

$$a_{2_x} = a_5 + a_2 f_1 T_x \quad (X.8.13)$$

$$a_5 = \left(\frac{g \bar{R} T^{1/3}}{\mu_o} \right) \left(\frac{k}{\epsilon} \rho'_g \right)_{xx} \quad (X.8.14)$$

$$\begin{aligned} (V_g)_x &= - \left[a_1 T_{xx} + a_2 f_1 T_x + \frac{a_1}{f_1} \left(f_{1_T} + f_1^2 \right) \left(T_x \right)^2 + a_5 + a_2 f_1 T_x \right] \\ &= - a_1 T_{xx} - 2 a_2 f_1 T_x - \frac{a_1}{f_1} \left(f_{1_T} + f_1^2 \right) \left(T_x \right)^2 - a_5 \end{aligned} \quad (X.8.15)$$

Substituting the various terms into X.7.9:

$$\begin{aligned}
(\rho C_p)^* T_t = & K_{\text{eff}} T_{xx} + \left(K_{\text{eff}} \right)_T (T_x)^2 + \left(K_{\text{eff}} \right)_{\rho_s} T_x \left(\rho_s \right)_x - \dot{W}_s \left(\bar{e} + h_g \right) \\
& + \frac{\bar{R} T}{J} \left(\rho'_g \right)_t + \frac{\rho'_g \bar{R}}{J} \left(1 + \frac{T \bar{R}_T}{\bar{R}} \right) T_t + \bar{C}_p \rho'_g \left(a_1 T_x + a_2 \right) T_x \\
& - \frac{\rho'_g}{gJ} \left(a_1 T_x + a_2 \right) \left(a_1 T_{xt} + a_3 T_x + \frac{a_1}{f_1} \left(f_{1T} + f_1^2 \right) T_x T_t + a_4 + a_2 f_1 T_t \right) \\
& + \frac{\rho'_g}{gJ} \left(a_1^2 T_x^2 + 2 a_1 a_2 T_x + a_2^2 \right) \left[a_1 T_{xx} + 2 a_2 f_1 T_x + a_5 \right. \\
& \left. + \frac{a_1}{f_1} \left(f_{1T} + f_1^2 \right) (T_x)^2 \right] \\
& - \frac{\dot{W}_s}{2gJ} \left(a_1^2 T_x^2 + 2 a_1 a_2 T_x + a_2^2 \right) \\
(\rho C_p)^* T_t = & K_{\text{eff}} T_{xx} + \left(K_{\text{eff}} \right)_T (T_x)^2 + \left(K_{\text{eff}} \right)_{\rho'_s} \left(\rho_s \right)_x T_x - \dot{W}_s \left(\bar{e} + h_g \right) \\
& + \frac{\bar{R} T}{J} \left(\rho'_g \right)_t + \frac{\rho'_g \bar{R}}{J} \left(1 + \frac{T \bar{R}_T}{\bar{R}} \right) T_t + \bar{C}_p \rho'_g \left(a_1 T_x + a_2 \right) T_x \\
& - \frac{\rho_g}{gJ} \left\{ a_1^2 T_x T_{xt} + a_1 a_3 T_x^2 + \frac{a_1^2}{f_1} \left(f_{1T} + f_1^2 \right) T_x^2 T_t \right. \\
& + a_1 a_4 T_x + a_1 a_2 f_1 T_x T_t + a_2 a_1 T_{xt} + a_2 a_3 T_x \\
& \left. + \frac{a_2 a_1}{f_1} \left(f_{1T} + f_1^2 \right) T_x T_t + a_4 a_2 + a_2^2 f_1 T_t \right\} \\
& + \frac{\rho_g}{gJ} \left\{ a_1 a_2^2 T_{xx} + 2 a_2^3 f_1 T_x + a_2^2 a_5 + \frac{a_1 a_2^2}{f_1} \left(f_{1T} + f_1^2 \right) (T_x)^2 \right. \\
& + a_1 T_x \left(a_1 T_x + 2 a_2 \right) \left[a_1 T_{xx} + 2 a_2 f_1 T_x + a_5 + \frac{a_1}{f_1} \left(f_{1T} + f_1^2 \right) (T_x)^2 \right] \left. \right\} \\
& - \frac{\dot{W}_s}{2gJ} \left[a_1 T_x \left(a_1 T_x + 2 a_2 \right) + a_2^2 \right]
\end{aligned}$$

Let

$$\left(\rho C_p\right)_{\text{eff}} = \left(\rho C_p\right)^* - \frac{\rho_g \bar{R}}{J} \left(1 + \frac{T \bar{R}_T}{R}\right) + \frac{\rho_g a_2^2 f_1}{gJ}$$

$$b_{41} = -\dot{W}_s \left(\bar{e} + h_g + a_2^2 / 2gJ\right) - \frac{\rho_g a_2^2}{gJ} \left(a_4 - a_2 a_5\right) + \frac{\bar{R} T}{J} \left(\rho_g\right)_t$$

$$b_{42} = \bar{C}_p \rho_g \left(a_1 T_x + a_2\right) T_x$$

$$b_{43} = -\frac{\dot{W}_s a_1}{2gJ} \left(a_1 T_x + 2a_2\right) T_x$$

$$b_{44} = \frac{\rho_g a_1 a_5}{gJ} \left(a_1 T_x + 2a_2\right) T_x$$

$$b_{45} = \frac{\rho_g a_2^2}{gJ} \left[2a_2 f_1 + \frac{a_1}{f_1} \left(f_{1T} + f_1^2\right) T_x + 4a_1 T_x f_1\right] T_x$$

$$b_{46} = \frac{\rho_g a_1^2}{gJ} T_x T_{xx} \left(2a_2 + a_1 T_x\right)$$

$$b_{47} = -\frac{\rho_g a_3}{gJ} \left(a_1 T_x + a_2\right) T_x$$

$$b_{48} = -\frac{\rho_g a_1 a_4}{gJ} T_x$$

$$b_{49} = \frac{\rho_g a_1^2 (T_x)^2}{f_1 gJ} \left[a_1 \left(f_{1T} + f_1^2\right) T_x + 2a_2 f_1^2 + 2a_2 \left(f_{1T} + f_1^2\right)\right] T_x$$

$$b_{410} = -\frac{\rho_g}{gJ} \left[a_1^2 T_x T_{xt} + a_1 a_2 T_{xt} + \frac{a_1^2}{f_1} \left(f_1^2 + f_{1T}\right) T_x^2 T_t\right. \\ \left. + \frac{a_1 a_2}{f_1} \left(2f_1^2 + f_{1T}\right) T_x T_t\right]$$

Then,

$$\begin{aligned} \left(\rho C_p\right)_{\text{eff}} T_t = & \left[K_{\text{eff}} + \frac{\rho_g a_1 a_2^2}{gJ} \right] T_{xx} + \left(K_{\text{eff}}\right)_T \left(T_x\right)^2 + \left(K_{\text{eff}}\right)_{\rho'_s} \left(\rho_s\right)_x T_x \\ & + b_{41} + b_{42} + b_{43} + b_{44} + b_{45} + b_{46} + b_{47} + b_{48} + b_{49} + b_{410} \end{aligned}$$

Let

$$b_1 = \left(K_{\text{eff}} + \frac{\rho_g a_1 a_2^2}{gJ} \right) \frac{1}{\left(\rho C_p\right)_{\text{eff}}} \quad (\text{X.9.1})$$

$$b_2 = \left(K_{\text{eff}}\right)_T / \left(\rho C_p\right)_{\text{eff}} \quad (\text{X.9.2})$$

$$b_3 = \left(K_{\text{eff}}\right)_{\rho'_s} \left(\rho_s\right)_x / \left(\rho C_p\right)_{\text{eff}} \quad (\text{X.9.3})$$

$$b_4 = \left[b_{41} + b_{42} + b_{43} + b_{44} + b_{45} + b_{46} + b_{47} + b_{48} + b_{49} + b_{410} \right] / \left(\rho C_p\right)_{\text{eff}} \quad (\text{X.9.4})$$

Then,

$$T_t = b_1 T_{xx} + b_2 \left(T_x\right)^2 + b_3 T_x + b_4 \quad (\text{X.9.5})$$

Note that this has been the form of the "general" equation - see II.4. However, b_4 involves derivatives and so will require special treatment.

Performing the space transformation (equations A.2, A.3, A.4) on X.9.5, this is obtained:

$$T_t = \beta_1 T_{\eta\eta} + \beta_2 \left(T_{\eta}\right)^2 + \beta_3 T_{\eta} + \beta_4 \quad (\text{X.10.1})$$

$$\beta_1 = b_1 \eta_x^2$$

$$\beta_2 = b_2 \eta_x^2$$

$$\beta_3 = b_3 \eta_x + b_1 \eta_{xx} - \eta_t$$

$$\beta_4 = b_4$$

$$\begin{aligned}
b_{41} &= \dot{W}_s \left(\bar{e} + h_g + a_2^2 / 2gJ \right) - \frac{\rho_g a_2}{gJ} \left(a_4 - a_2 a_5 \right) + \frac{\bar{R} T}{J} \left[(\rho_g)_t + \eta_t (\rho_g)_\eta \right] \\
b_{42} &= \bar{C}_p \rho_g \eta_x \left(a_1 \eta_x T_\eta + a_2 \right) T_\eta \\
b_{43} &= - \frac{\dot{W}_s a_1 \eta_x}{2gJ} \left(a_1 \eta_x T_\eta + 2a_2 \right) T_\eta \\
b_{44} &= \frac{\rho_g a_1 a_5 \eta_x}{gJ} \left(a_1 \eta_x T_\eta + 2a_2 \right) T_\eta \\
b_{45} &= \frac{\rho_g a_2^2 \eta_x}{gJ} \left[2a_2 f_1 + \frac{a_1}{f_1} \left(f_{1T} + 5f_1^2 \right) \eta_x T_\eta \right] T_\eta \\
b_{46} &= \frac{\rho_g a_1^2}{gJ} \left(\eta_x T_\eta \right) \left(\eta_x^2 T_{\eta\eta} + \eta_{xx} T_\eta \right) \left(2a_2 + a_1 \eta_x T_\eta \right) \\
b_{47} &= - \frac{\rho_g a_3}{gJ} \left(a_1 \eta_x T_\eta + a_2 \right) \eta_x T_\eta \\
b_{48} &= - \left(\frac{\rho_g a_1 a_4 \eta_x}{gJ} \right) T_\eta \\
b_{49} &= \frac{\rho_g a_1^2 \eta_x^3 T_\eta^2}{f_1 gJ} \left[a_1 \left(f_{1T} + f_1^2 \right) \eta_x T_\eta + 2a_2 \left(f_{1T} + 2f_1^2 \right) \right] T_\eta
\end{aligned}$$

$$\begin{aligned}
b_{410} &= -\frac{\rho_g}{gJ} \left[a_1^2 \eta_x T_\eta (\eta_x T_\eta)_t + a_1 a_2 (\eta_x T_\eta)_t + \frac{a_1^2}{f_1} (f_1^2 + f_{1T}) (\eta_x^2 T_\eta^2) (T_t + \eta_t T_\eta) \right. \\
&\quad \left. + \frac{a_1 a_2}{f_1} (2f_1^2 + f_{1T}) (\eta_x T_\eta) (T_\tau + \eta_t T_\eta) \right] \\
&= -\frac{\rho_g}{gJ} \left\{ a_1^2 \eta_x T_\eta \left[\eta_x (T_\eta)_t + T_\eta (\eta_x)_t \right] + a_1 a_2 \left[\eta_x (T_\eta)_t + T_\eta (\eta_x)_t \right] \right. \\
&\quad \left. + \frac{a_1^2}{f_1} (f_1^2 + f_{1T}) (\eta_x^2 T_\eta^2) (T_\tau + \eta_t T_\eta) + \frac{a_1 a_2}{f_1} (2f_1^2 + f_{1T}) (\eta_x T_\eta) (T_\tau + \eta_t T_\eta) \right\} \\
&= -\frac{\rho_g}{gJ} \left\{ a_1 (a_2 + a_1 \eta_x T_\eta) \left[\eta_x (T_\eta \tau + \eta_t T_\eta \eta) + T_\eta (\eta_t)_\eta \eta_x \right] \right. \\
&\quad \left. + \frac{a_1^2}{f_1} (f_1^2 + f_{1T}) (\eta_x^2 T_\eta^2) (T_\tau + \eta_t T_\eta) \right. \\
&\quad \left. + \frac{a_1 a_2}{f_1} (2f_1^2 + f_{1T}) (\eta_x T_\eta) (T_\tau + \eta_t T_\eta) \right\}
\end{aligned}$$

The a_i must also be transformed. The only one requiring any unusual care is a_4 . From X.8.9,

$$\begin{aligned}
a_4 &= \left(\frac{g \bar{R} T^{1/3}}{\mu_o} \right) \left[\left(\frac{k}{\epsilon} \rho_g \right)_\tau + \eta_t \left(\frac{k}{\epsilon} \rho_g \right)_\eta \right]_x = \left(\frac{g \bar{R} T^{1/3}}{\mu_o} \right) \left[\left(\frac{k}{\epsilon} \rho_g \right)_{\eta \tau} \right. \\
&\quad \left. + \left(\eta_t \right)_\eta \left(\frac{k}{\epsilon} \rho_g \right)_\eta + \eta_t \left(\frac{k}{\epsilon} \rho_g \right)_{\eta \eta} \right] \eta_x
\end{aligned}$$

Now summarizing all the equations and rearrange β_4 .

$$T_t = \beta_1 T_{\eta \eta} + \beta_2 (T_\eta)^2 + \beta_3 T_\eta + \beta_4 \quad (X.11.1)$$

$$\begin{aligned}
\beta_1 &= b_1 \eta_x^2 \\
\beta_2 &= b_2 \eta_x^2 \\
\beta_3 &= b_3 \eta_x + b_1 \eta_{xx} - \eta_t
\end{aligned}
\tag{X.11.2}$$

$$\begin{aligned}
\beta_4 &= \sum_{i=1}^{13} \beta_{4i} \\
b_1 &= \frac{1}{\rho C_{p \text{ eff}}} \left\{ K_{\text{eff}} + \frac{\rho_g a_1 a_2^2}{gJ} \right\} \\
b_2 &= \frac{1}{\rho C_{p \text{ eff}}} \left\{ (K_{\text{eff}})_T \right\}
\end{aligned}
\tag{X.11.3}$$

$$\begin{aligned}
b_3 &= \frac{1}{\rho C_{p \text{ eff}}} (K_{\text{eff}})_{\rho_s} \eta_x (\rho_s)_\eta \\
(\rho C_p)_{\text{eff}} &= (\rho C_p)^* - \frac{\rho_g \bar{R} T}{J} \left(\frac{1}{T} - \frac{\bar{m}_T}{\bar{m}} \right) + \frac{\rho_g a_2^2 f_1}{gJ} \\
f_1 &= \frac{1}{3T} - \frac{\bar{m}_T}{\bar{m}} \\
f_2 &= \frac{g \bar{R} T^{1/3}}{\mu_o}
\end{aligned}
\tag{X.11.4}$$

$$\begin{aligned}
a_1 &= f_1 f_2 \left(\frac{k}{\epsilon} \rho_g \right) \\
a_2 &= f_2 \left(\frac{k}{\epsilon} \rho_g \right)_\eta \eta_x \\
a_3 &= f_1 f_2 \left\{ \left(\frac{k}{\epsilon} \rho_g \right)_t + \eta_t \left(\frac{k}{\epsilon} \rho_g \right)_\eta \right\} \\
a_4 &= f_2 \left\{ \left(\frac{k}{\epsilon} \rho_g \right)_\eta + \left(\eta_t \right)_\eta \left(\frac{k}{\epsilon} \rho_g \right)_\eta + \eta_t \left(\frac{k}{\epsilon} \rho_g \right)_{\eta\eta} \right\} \eta_x \\
a_5 &= f_2 \left\{ \eta_x^2 \left(\frac{k}{\epsilon} \rho_g \right)_{\eta\eta} + \eta_{xx} \left(\frac{k}{\epsilon} \rho_g \right)_\eta \right\}
\end{aligned}$$

$$\begin{aligned}
\beta_{41} &= -\dot{W}_s \left(\bar{e} + h_g + \frac{a_2^2}{2gJ} \right) - \frac{\rho_g a_2}{gJ} (a_4 - a_2 a_5) \\
&\quad + \frac{\bar{R}T}{J} \left\{ \left(\rho_g \right)_t + \eta_t \left(\rho_g \right)_\eta \right\} \\
\beta_{42} &= \bar{C}_p \rho_g \eta_x \left(a_1 \eta_x T_\eta + a_2 \right) T_\eta \\
\beta_{43} &= - \frac{\dot{W}_s a_1 \eta_x}{2gJ} \left(a_1 \eta_x T_\eta + a_2 \right) T_\eta \\
\beta_{44} &= \frac{\rho_g a_1 a_5 \eta_x}{gJ} \left(a_1 \eta_x T_\eta + 2a_2 \right) T_\eta \\
\beta_{45} &= \frac{\rho_g a_2^2 \eta_x}{gJ} \left\{ 2a_2 f_1 + \frac{a_1}{f_1} \left(f_{1T} + 5f_1^2 \right) \eta_x T_\eta \right\} T_\eta \\
\beta_{46} &= \frac{\rho_g a_1^2 \eta_x^3}{gJ} \left\{ \left(2a_2 + a_1 \eta_x T_\eta \right) - \frac{\eta_t}{\eta_x} \right\} \left(T_\eta T_\eta \right) \\
\beta_{47} &= \frac{\rho_g a_1^2 \eta_x T_\eta}{gJ} \left\{ \left(2a_2 + a_1 \eta_x T_\eta \right) \eta_{xx} - \eta_x \left(\eta_t \right)_\eta \right\} T_\eta \\
\beta_{48} &= - \frac{\rho_g a_3}{gJ} \left(a_1 \eta_x T_\eta + a_2 \right) \left(\eta_x \right) T_\eta \\
\beta_{49} &= - \frac{\rho_g a_1 a_4 \eta_x}{gJ} T_\eta \\
\beta_{410} &= \frac{\rho_g a_1^2 \eta_x^3 T_\eta^2}{f_1 gJ} \left\{ a_1 \left(f_{1T} + f_1^2 \right) \eta_x T_\eta + 2a_2 \left(f_{1T} + 2f_1^2 \right) \right\} T_\eta
\end{aligned}
\tag{X.11.5}$$

$$\begin{aligned}
\beta_{46} &= \frac{\rho_g a_1^2 \eta_x^3}{gJ} \left\{ \left(2a_2 + a_1 \eta_x T_\eta \right) - \frac{\eta_t}{\eta_x} \right\} \left(T_\eta T_\eta \right) \\
\beta_{47} &= \frac{\rho_g a_1^2 \eta_x T_\eta}{gJ} \left\{ \left(2a_2 + a_1 \eta_x T_\eta \right) \eta_{xx} - \eta_x \left(\eta_t \right)_\eta \right\} T_\eta \\
\beta_{48} &= - \frac{\rho_g a_3}{gJ} \left(a_1 \eta_x T_\eta + a_2 \right) \left(\eta_x \right) T_\eta \\
\beta_{49} &= - \frac{\rho_g a_1 a_4 \eta_x}{gJ} T_\eta \\
\beta_{410} &= \frac{\rho_g a_1^2 \eta_x^3 T_\eta^2}{f_1 gJ} \left\{ a_1 \left(f_{1T} + f_1^2 \right) \eta_x T_\eta + 2a_2 \left(f_{1T} + 2f_1^2 \right) \right\} T_\eta
\end{aligned}
\tag{X.11.6}$$

$$\begin{aligned}
\beta_{411} &= -\frac{\rho_g a_1}{gJ} \left\{ \frac{a^2}{f_1} \left(2f_1^2 + f_{1T} \right) \eta_x \eta_t T_\eta + \frac{a_1}{f_1} \left(f_1^2 + f_{1T} \right) \eta_x^2 \eta_t T_\eta^2 \right. \\
&\quad \left. + a_2 \eta_x \left(\eta_t \right)_\eta \right\} T_\eta \\
\beta_{412} &= - \left(\frac{\rho_g a_1 \eta_x \eta_t a_1}{gJ} \right) T_{\eta\eta} \\
\beta_{413} &= - \left(\frac{\rho_g a_1 a_2 \eta_x}{gJ} \right) T_{\eta\tau} - \left(\frac{\rho_g a_1^2 \eta_x^2}{gJ} \right) T_\eta T_{\eta\tau} \\
&\quad - \frac{\rho_g a_1^2 \eta_x^2 \left(f_1^2 + f_{1T} \right)}{gJ f_1} \left(T_\eta^2 T_\tau \right) - \frac{\rho_g a_1 a_2 \eta_x \left(2f_1^2 + f_{1T} \right)}{gJ f_1} T_\eta T_\tau
\end{aligned} \tag{X.11.7}$$

The arrangement of the β_4 term is somewhat arbitrary. Usual stability theory gives little information concerning the best manner of evaluating these terms. In the past, difficulty has been encountered with terms of this sort. The arrangement given is simply a guess; hopefully it will facilitate finding these difficulties when they occur.

It remains now to specify a difference equation for X.11.1. This equation is considered an equation in T . (At each point, however, the variables are solved for simultaneously: T , ρ_g , ρ_s are obtained simultaneously from X.11.1, X.3.1, and X.1.2).

1. The A_i , b_i , and all coefficients such as β_1 , β_2 , β_3 , and β_{4i} are evaluated with whatever guess is available for the variables.
2. β_1 , β_2 , β_3 terms are handled in the manner described in Section III.
3. β_{41} , no complication.
4. β_{42} , β_{43} , β_{44} , β_{45} , β_{47} , β_{48} , β_{49} , β_{410} , β_{411} are treated in this fashion.

Let the term be $A T_\eta$

$$\text{If } A \leq 0, T_\eta = \frac{T_i - T_{i-1}}{\Delta\eta}$$

$$\text{If } A > 0, T_\eta = \frac{T_{i+1} - T_i}{\Delta\eta}$$

(This is the same procedure as applied to β_3 - see IV.7 except $\alpha_1 = 0$ or 1).

5. β_{46} : Let $\beta_{46} = AT_{\eta}$. ($T_{\eta\eta}$ is included in A). The same procedure as just discussed is then applied.
6. β_{412} : Usual formula for $T_{\eta\eta}$ is used.
7. β_{413} : The terms having T_{η} are written AT_{η} .

T_{τ} is approximated in the usual manner

$$T_{\eta\tau} \text{ is given by } \frac{T_{i+1}^{n+1} - T_{i-1}^{n+1} - T_{i+1}^{n-1} + T_{i-1}^{n-1}}{4 \Delta t \Delta \eta}$$

One term remains which involves only $T_{\eta t}$. The approximation just given is used.

(D) Some stability considerations are discussed below. Consider first the term $(\rho C_p)_{\text{eff}}$. From X.11.4 and X.7.1,

$$\begin{aligned} (\rho C_p)_{\text{eff}} &= (C_{v_c} + C_v) \rho_s - C_v \rho_{cf} + \rho_g \bar{C}_p - \frac{\rho_g \bar{R}}{J} + \rho_g \frac{\bar{R} T}{J} \left(\frac{\bar{m}_T}{\bar{m}} \right) + \frac{\rho_g a_2^2 f_1}{gJ} \\ &= (C_{v_c} + C_v) \rho_s - C_v \rho_{cf} + \rho_g \left\{ \bar{C}_p - \frac{\bar{k}}{J} + \frac{a_2^2 f_1}{gJ} + \frac{\bar{R} T}{J} \left(\frac{\bar{m}_T}{\bar{m}} \right) \right\} \end{aligned}$$

We expect the effect of increasing ρ_g to be a decrease in T . Thus, the coefficient of ρ_g should be positive. So far, the cases run have had $C_p - \frac{\bar{R}}{J} < 0$.

The major problem concerning stability is the fact that a non-linear system is involved. We have specified difference equations as though they were uncoupled (although the final equations are solved simultaneously). To obtain some intuitive information, let us assume all coefficients are positive, let us ignore all terms in T equation involving T_{η} and all terms in ρ_g equations involving $(\rho_g)_{\eta}$.

This type of system remains

$$\rho_t = a_1 \rho_{\eta\eta} + a_i T_{\eta\eta} \quad (\text{X.12.1})$$

$$T_t = b_1 T_{\eta\eta} + b_2 \rho_t + b_3 T_{\eta t} \quad (\text{X.12.2})$$

where

$$a_i > 0, b_i > 0$$

(In X.4, d_3 and d_4 have been set to zero except for the $T_{\eta\eta}$ term; in X.11.1, β_{41} has been ignored except for the $(\rho_g)_t$ term; ρ_g has been written as ρ).

Consider X.11.2 with $b_2 = 0$.

$$T_t = b_1 T_{\eta\eta} + b_3 T_{\eta t} \quad (X.12.3)$$

according to Sommerfield (22, p. 36), the classification for this equation is determined by the expression:

$$AC - B^2 \text{ where } A = b_1, B = b_3, C = 0$$

Thus $AC - B^2 = (b_3)^2$ or this is a hyperbolic equation, instead of a parabolic equation. This can have a profound influence on the boundary conditions as well as the numerical approximations. This fact has been ignored so far. If any instability occurs, the term involving b_3 (or the d_3 term in X.4) should be looked at closely.

Suppose now $b_3 = 0$. We then have this system of equations:

$$\rho_t = a_1 \rho_{\eta\eta} + a_2 T_{\eta\eta} \quad (X.12.4)$$

$$T_t = b_1 T_{\eta\eta} + b_2 \rho_x \quad (X.12.5)$$

It is of interest to investigate the Dufort-Frankel scheme as applied to these equations. Since the equation we use (explicit-implicit) is so closely related to the Dufort-Frankel (See Section III), this should give us valuable information. Unfortunately, even for constant coefficients this becomes quite complex. However, some results for special cases can be obtained.

The Dufort-Frankel equations give the following:

$$\frac{\rho_j^{n+1} - \rho_j^{n-1}}{2 \Delta t} = \frac{a_1}{\Delta \eta^2} \left(\rho_{j+1}^n + \rho_{j-1}^n - \rho_j^{n+1} - \rho_j^{n-1} \right) + \frac{a_2}{\Delta \eta} \left(T_{j+1}^n + T_{j-1}^n - T_j^{n+1} - T_j^{n-1} \right)$$

$$\frac{T_j^{n+1} - T_j^{n-1}}{2 \Delta t} = \frac{b_1}{\Delta \eta^2} \left(T_{j+1}^n + T_{j-1}^n - T_j^{n+1} - T_j^{n-1} \right) + \frac{b_2}{2 \Delta t} \left(\rho_j^{n+1} - \rho_j^{n-1} \right)$$

Let

$$\alpha_1 = 2 a_1 \frac{\Delta t}{\Delta \eta^2} \quad \alpha_2 = 2 a_2 \frac{\Delta t}{\Delta \eta^2} \quad \beta_1 = 2 b_1 \frac{\Delta t}{\Delta \eta^2} \quad \beta_2 = b_2$$

$$\rho_j^{n+1} (1+\alpha_1) + \alpha_2 T_j^{n+1} = \alpha_1 \left(\rho_{j+1}^n + \rho_{j-1}^n \right) + \alpha_2 \left(T_{j+1}^n + T_{j-1}^n \right) + (1-\alpha_1) \rho_j^{n-1} - \alpha_2 T_j^{n-1}$$

$$T_j^{n+1} (1+\beta_1) - \beta_2 \rho_j^{n+1} = \beta_1 \left(T_{j+1}^n + T_{j-1}^n \right) + (1-\beta_1) T_j^{n-1} - \beta_2 \rho_j^{n-1}$$

To reduce this to a two-level equation, we follow Richtmyer (4, p. 45)

Let

$$U_j^{n+1} = \rho_j^n$$

$$V_j^{n+1} = T_j^n$$

Then,

$$(1 + \alpha_1) \rho_j^{n+1} + \alpha_2 T_j^{n+1} - \alpha_1 \left(\rho_{j+1}^n + \rho_{j-1}^n \right) - \alpha_2 \left(T_{j+1}^n + T_{j-1}^n \right) - (1 - \alpha_1) U_j^n + \alpha_2 V_j^n = 0$$

$$(1 + \beta_1) T_j^{n+1} - \beta_2 \rho_j^{n+1} - \beta_1 \left(T_{j+1}^n + T_{j-1}^n \right) - (1 - \beta_1) V_j^n + \beta_2 U_j^n = 0$$

Let

$$W_j^n = \begin{pmatrix} \rho_j^n \\ U_j^n \\ T_j^n \\ V_j^n \end{pmatrix}$$

Then,

$$A_1 W_j^{n+1} + A_2 W_j^n + A_3 \left(W_{j+1}^n + W_{j-1}^n \right) = 0$$

where

$$A_1 = \begin{pmatrix} (1+\alpha_1) & 0 & \alpha_2 & 0 \\ 0 & 1 & 0 & 0 \\ -\beta_2 & 0 & (1+\beta_1) & 0 \\ 0 & 0 & 0 & 1 \end{pmatrix}$$

$$A_2 = \begin{pmatrix} 0 & -(1-\alpha_1) & 0 & \alpha_2 \\ -1 & 0 & 0 & 0 \\ 0 & \beta_2 & 0 & -(1-\beta_1) \\ 0 & 0 & -1 & 0 \end{pmatrix}$$

$$A_3 = \begin{pmatrix} -\alpha_1 & 0 & -\alpha_2 & 0 \\ 0 & 0 & 0 & 0 \\ 0 & 0 & -\beta_1 & 0 \\ 0 & 0 & 0 & 0 \end{pmatrix}$$

Following Richtmyer again (4, p. 54), let

$$W_j^n = W_n e^{(ik\Delta x)_j} \quad : \quad \text{- typical term}$$

Then,

$$A_1 W_{n+1} - A_2 W_n + A_3 W_n \left(e^{i(k\Delta x)} + e^{-i(b\Delta x)} \right) = 0$$

$$e^{i\theta} + e^{-i\theta} = 2 \cos \theta = 2q$$

$$A_1 W_{n+1} + A_2 W_n + A_3 W_n 2q = 0$$

$$A_1 W_{n+1} + (A_2 + 2q A_3) W_n = 0$$

$$W_{n+1} = -A_1^{-1} (A_2 + 2q A_3) W_n$$

$$-(A_2 + 2qA_3) = \begin{pmatrix} +2q\alpha_1 & +(1-\alpha_1) & +2q\alpha_2 & -\alpha_2 \\ +1 & 0 & 0 & 0 \\ 0 & -\beta_2 & 2q\beta_1 & (1-\beta_1) \\ 0 & 0 & +1 & 0 \end{pmatrix} = A_4$$

Let

$$D = (1+\alpha_1)(1+\beta_1) + \beta_2\alpha_2$$

Then,

$$A_1^{-1} = 1/D \begin{pmatrix} (1+\beta_1) & 0 & -\alpha_2 & 0 \\ 0 & D & 0 & 0 \\ \beta_2 & 0 & (1+\alpha_1) & 0 \\ 0 & 0 & 0 & D \end{pmatrix}$$

Let

$$A_5 = A_1^{-1} A_4$$

$$A_5 = \begin{pmatrix} \frac{2q\alpha_1(1+\beta_1)}{D} & \frac{(1+\beta_1)(1-\alpha_1)+\alpha_2\beta_2}{D} & \frac{2q}{D} \left[\alpha_2(1+\beta_1) - \alpha_2\beta_1 \right] & \frac{-(1+\beta_1)\alpha_2 - \alpha_2(1-\beta_1)}{D} \\ 1 & 0 & 0 & 0 \\ \frac{2q\alpha_1\beta_2}{D} & \frac{\beta_2(1-\alpha_1) - \beta_2(1+\alpha_1)}{D} & \frac{2q}{D} \left| \beta_2\alpha_2 + \beta_1(1+\alpha_1) \right| & \frac{-\beta_2\alpha_2 + (1+\alpha_1)(1-\beta_1)}{D} \\ 0 & 0 & 1 & 0 \end{pmatrix}$$

$$A_5 = \begin{pmatrix} \frac{2q\alpha_1(1+\beta_1)}{D} & \frac{(1+\beta_1)(1-\alpha_1) - \alpha_2\beta_2}{D} & \frac{2q\alpha_2}{D} & \frac{-2q\alpha_2}{D} \\ 1 & 0 & 0 & 0 \\ \frac{2q\alpha_1\beta_2}{D} & \frac{-2\alpha_1\beta_2}{D} & \frac{2q}{D} \left[\beta_2\alpha_2 + \beta_1(1+\alpha_1) \right] & \frac{(1+\alpha_1)(1-\beta_1) - \beta_2\alpha_2}{D} \\ 0 & 0 & 1 & 0 \end{pmatrix}$$

According to Richtmyer again (19, p.63) we need to see that the eigenvalues of A_5 are in the unit circle. The result for the full matrix has not as yet been obtained. However, special cases can be studied.

(a) Let $\alpha_2 = 0$ (or $A_2 = 0$)

Then,

$$A_5 = \begin{pmatrix} \frac{2q\alpha_1}{1+\alpha_1} & \frac{1-\alpha_1}{1+\alpha_1} & 0 & 0 \\ 1 & 0 & 0 & 0 \\ \frac{2q\alpha_1\beta_2}{D} & \frac{-2\alpha_1\beta_2}{D} & \frac{2q\beta_1}{1+\beta_1} & \frac{1-\beta_1}{1+\beta_1} \\ 0 & 0 & 1 & 0 \end{pmatrix}$$

The eigenvalues are those of the subsystem:

$$A_6 = \begin{pmatrix} \frac{2q\alpha_1}{1+\alpha_1} & \frac{1-\alpha_1}{1+\alpha_1} \\ 1 & 0 \end{pmatrix}, \quad A_7 = \begin{pmatrix} \frac{2q\beta_1}{1+\beta_1} & \frac{1-\beta_1}{1+\beta_1} \\ 1 & 0 \end{pmatrix}$$

The eigenvalues of this matrix are shown to be in the unit circle (4, p.85).

(b) $\beta_2 = 0$: The matrices A_6 and A_7 are obtained as before.

(c) $\alpha_1 = 0$:

$$A_5 = \begin{pmatrix} 0 & 1 & \frac{2q\alpha_2}{D} & \frac{-2\alpha_2}{D} \\ 1 & 0 & 0 & 0 \\ 0 & 0 & \frac{2q}{D}(\beta_1 + \beta_2\alpha_2) & \frac{(1-\beta_1) - \beta_2\alpha_2}{D} \\ 0 & 0 & 1 & 0 \end{pmatrix}$$

The eigenvalues are ± 1 and the eigenvalue of A_6 :

$$A_6 = \begin{pmatrix} \frac{2q}{D}(\beta_1 + \beta_2\alpha_2) & \frac{(1-\beta_1) - \beta_2\alpha_2}{D} \\ 1 & 0 \end{pmatrix}$$

$$D = 1 + \beta_1 + \beta_2\alpha_2 > 1$$

$$\beta_1 + \beta_2\alpha_2 = D-1$$

$$1 - \beta_1 - \beta_2\alpha_2 = 2-D$$

$$A_6 = \begin{pmatrix} +2q \frac{(D-1)}{D} & \frac{2-D}{D} \\ 1 & 0 \end{pmatrix}$$

Let $D_1 = \frac{D-1}{D} \quad 0 \leq D_1 \leq 1$

$$\frac{2-D}{D} = \frac{1}{D} + \frac{1-D}{D} = 1-D_1 - D_1 = 1 - 2D_1$$

$$A_6 = \begin{pmatrix} 2qD_1 & 1-2D_1 \\ 1 & 0 \end{pmatrix}$$

Then the eigenvalues are given by:

$$\lambda^2 - (2qD_1) \lambda - (1 - 2D_1) = 0$$

$$\lambda = \frac{2qD_1 \pm \sqrt{4q^2 D_1^2 + 4(1-2D_1)}}{2} = qD_1 \pm \sqrt{(qD_1)^2 + (1-2D_1)}$$

The largest value of λ is obtained by allowing q to have its maximum: $q = 1$. Then

$$\lambda = D_1 \pm \sqrt{(1-D_1)^2} = D_1 \pm (1-D_1)$$

$$\lambda = 1, 2D_1 - 1$$

Since $0 \leq D_1 \leq 1$, $-1 \leq 2D_1 - 1 \leq$

Thus, all eigenvalues are in unit circle.

(E) In this section we consider some of the computations involved in the calculation of the coefficients.

$$(1) \text{ Let } f_1 = \frac{1}{3T} - \frac{\bar{m}_T}{\bar{m}} \quad (X.13.1)$$

$$f_{1T} = \left[-\frac{1}{3T^2} - \frac{\bar{m}_{TT}}{\bar{m}} + \frac{(\bar{m}_T)^2}{(\bar{m})^2} \right] \quad (X.13.2)$$

$$(2) \text{ Let } f_2 = \frac{\bar{R} g T^{1/3}}{\mu_o} \quad (X.13.3)$$

$$f_{2\eta} = \frac{g}{\mu_o} (\bar{R} T^{1/3})_{\eta} = \frac{g}{\mu_o} \left[\frac{\bar{R} T^{1/3}}{3T} + \bar{R}_T T^{1/3} \right] T_{\eta} \\ = f_2 f_1 T_{\eta} \quad (X.13.4)$$

$$f_{2\eta\eta} = (f_{2\eta} f_1 + f_2 f_{1T} T_{\eta}) T_{\eta} + f_2 f_1 T_{\eta\eta} \quad (X.13.5)$$

$$f_{2\tau} = f_2 f_1 T_{\tau} \quad (X.13.6)$$

$$f_{2\eta\tau} = (f_{2\eta} f_1 + f_2 f_{1\tau} T_{\eta}) T_{\tau} + f_2 f_1 T_{\eta\tau} \quad (X.13.7)$$

(T_{η} , $T_{\eta\eta}$, T_{τ} , $T_{\eta\tau}$ are obtained by differences)

$$\begin{aligned}
(3) \quad \epsilon &= 1 - \frac{\rho_s}{\tilde{\rho}_p} - \rho_c \left(\frac{1}{\tilde{\rho}_c} - \frac{1}{\tilde{\rho}_p} \right) \\
&= 1 - \frac{\rho_s}{\tilde{\rho}_p} - \left(\frac{1}{\tilde{\rho}_c} - \frac{1}{\tilde{\rho}_p} \right) \left(\rho_s - \frac{\rho_s}{\Gamma} + \frac{\rho_{cf}}{\Gamma} \right) \quad \text{see X.1.9} \\
&= 1 - \rho_s \left[\frac{1}{\tilde{\rho}_p \Gamma} + \frac{\Gamma - 1}{\Gamma} \left(\frac{1}{\tilde{\rho}_c} \right) \right] - \frac{\rho_{cf}}{\Gamma} \left(\frac{1}{\tilde{\rho}_c} - \frac{1}{\tilde{\rho}_p} \right) \quad (X.13.8)
\end{aligned}$$

$$\epsilon_\eta = - \left(\rho_s \right)_\eta \left[\frac{1}{\Gamma \tilde{\rho}_p} + \frac{\Gamma - 1}{\Gamma \tilde{\rho}_c} \right] \quad (X.13.9)$$

$$\epsilon_{\eta\eta} = - \left(\rho_s \right)_{\eta\eta} \left[\frac{1}{\Gamma \tilde{\rho}_p} + \frac{\Gamma - 1}{\Gamma \tilde{\rho}_c} \right] \quad (X.13.10)$$

$$\epsilon_t = - \left(\rho_s \right)_t \left[\frac{1}{\Gamma \tilde{\rho}_p} + \frac{\Gamma - 1}{\Gamma \tilde{\rho}_c} \right] \quad (X.13.11)$$

$$\epsilon_{\eta t} = - \left(\rho_s \right)_{\eta t} \left[\frac{1}{\Gamma \tilde{\rho}_p} + \frac{\Gamma - 1}{\Gamma \tilde{\rho}_c} \right] \quad (X.13.12)$$

Differences are used for $\left(\rho_s \right)_\eta$ etc.

$$(4) \quad \frac{k}{\epsilon} = k_f \epsilon^{m-1} \quad (X.14.1)$$

$$\left(\frac{k}{\epsilon} \right) = (m-1) \left(\frac{k}{\epsilon} \right) \left(\frac{\epsilon}{\epsilon} \right) \quad (X.14.2)$$

$$\left(\frac{k}{\epsilon} \right)_{\eta\eta} = (m-1) \left(\frac{k}{\epsilon} \right)_{\eta} \left(\frac{\epsilon}{\epsilon} \right) + (m-1) \left(\frac{k}{\epsilon} \right) \left(\frac{\epsilon \epsilon_{\eta\eta} - \epsilon_\eta^2}{\epsilon^2} \right) \quad (X.14.3)$$

$$\left(\frac{k}{\epsilon} \right)_t = (m-1) \left(\frac{k}{\epsilon} \right) \frac{\epsilon_t}{\epsilon} \quad (X.14.4)$$

$$\left(\frac{k}{\epsilon} \right)_{\eta t} = (m-1) \left(\frac{k}{\epsilon} \right)_\eta \left(\frac{\epsilon_t}{\epsilon} \right) + (m-1) \left(\frac{k}{\epsilon} \right) \left(\frac{\epsilon \epsilon_{\eta t} - \epsilon_t \epsilon_\eta}{\epsilon^2} \right) \quad (X.14.5)$$

$$(5) \quad d_1 = f_2 \left(\frac{k}{\epsilon} \right) \quad \text{see equation X.3.1} \quad (X.15.1)$$

$$d_{1\eta} = f_{2\eta} \left(\frac{k}{\epsilon} \right) + f_2 \left(\frac{k}{\epsilon} \right)_{\eta} \quad (X.15.2)$$

$$d_{1\eta\eta} = f_{2\eta\eta} + 2 f_{2\eta} \left(\frac{k}{\epsilon} \right)_{\eta} + f_2 \frac{k}{\epsilon}{}_{\eta\eta} \quad (X.15.3)$$

(6) The quantities α_i in X.11.4 are evaluated by performing the indicated differentiations, and then applying the above formulas.

APPENDIX B1

DERIVATION OF FINAL FORM OF PARTIAL DIFFERENTIAL EQUATION

In Part I of this section we consider the transformation of the general differential equation solved by the program. In Part II we looked at the energy equation solved by the program.

A. We consider the equation

$$\frac{\partial u}{\partial t} = b_1 \left(\frac{\partial^2 u}{\partial x^2} \right) + b_2 \left(\frac{\partial u}{\partial x} \right)^2 + b_3 \left(\frac{\partial u}{\partial x} \right) + b_4 \quad (B1.1)$$

The two space transformations (B2.1 and B2.4) can be written as one transformation:

$$\eta = \frac{1 - e^{-r\xi}}{1 - e^{-r}} \quad \text{with} \quad \xi = \bar{x} e^c (\bar{x}^2 - \bar{x})$$

$$\bar{x} = \frac{x - s_m}{A_i}$$

$$\tau = t$$

s_m is the amount of the layer melted, and A_i is the instantaneous length:

$$A_i = A_i(t) = A_i(0) - s_m(t)$$

If $u = u(\eta, \tau)$,

$$\frac{\partial u}{\partial x} = u_x = u_\eta \eta_x + u_\tau \tau_x = u_\eta \eta_x : \tau_x = 0 \quad (B1.2)$$

$$\frac{\partial^2 u}{\partial x^2} = u_{\eta\eta} (\eta_x)^2 + u_{\eta\eta\eta} \eta_{xx} \quad (B1.3)$$

$$u_t = u_\eta \eta_t + u_\tau \tau_t$$

or

$$u_t = (\eta_t) u_\eta + u_\tau \quad (B1.4)$$

With B1.2, B1.3, B1.4 equation B1.1 becomes:

$$\eta_t u_\eta + u_\tau = b_1 \left[(\eta_x)^2 u_{\eta\eta} + \eta_{xx} u_\eta \right] + b_2 (\eta_x)^2 (u_\eta)^2 + b_3 \eta_x u_\eta + b_4$$

Replacing τ with t :

$$\left. \begin{aligned} \frac{\partial u}{\partial t} &= \beta_1 \left(\frac{\partial^2 u}{\partial \eta^2} \right) + \beta_2 \left(\frac{\partial u}{\partial \eta} \right)^2 + \beta_3 \left(\frac{\partial u}{\partial \eta} \right) + \beta_4 \\ \beta_1 &= b_1 (\eta_x)^2 \\ \beta_2 &= b_2 (\eta_x)^2 \\ \beta_3 &= b_3 \eta_x + b_1 \eta_x - \eta_t \\ \beta_4 &= b_4 \end{aligned} \right\} \quad (B1.5)$$

where η_x , η_{xx} , and η_t are given by equations B2.5, B2.6 and B2.7.

Note that the b_i may also require transformation, depending on their particular form.

B. We look now at the particular form of the energy equation now in the program. The standard heat conduction equation is as follows:

$$\begin{aligned} \frac{\partial}{\partial x} \left(k \frac{\partial T}{\partial x} \right) &= \rho c_p \frac{\partial T}{\partial t} \\ k \frac{\partial^2 T}{\partial x^2} + k' \left(\frac{\partial T}{\partial x} \right)^2 &= \rho c_p \frac{\partial T}{\partial t} \\ \frac{\partial^2 T}{\partial x^2} + \left(\frac{k'}{k} \right) \left(\frac{\partial T}{\partial x} \right)^2 &= \alpha \frac{\partial T}{\partial t} \end{aligned} \quad (B1.6)$$

$$\alpha = \frac{\rho c_p}{k}, \quad k = k(T), \quad c_p = c_p(T), \quad k' = \frac{dk}{dT}$$

It is interesting to note that B1.6 is the same as the equation for constant k except for the term $\left(\frac{k'}{k} \right) \left(\frac{\partial T}{\partial x} \right)^2$. An attempt is sometimes made to treat variable k by allowing it to vary in the term α , while dropping the term involving k' . In our work it does not seem reasonable to assume that this term is insignificant, so we carry the equation as it is.

An interesting transformation is available here:

$$G(x, t) = \int_{T_0}^{T(x, t)} k(T) dT$$

$$\frac{\partial G}{\partial x} = k(T(x, t)) \left(\frac{\partial T}{\partial x} \right) = k \frac{\partial T}{\partial x}$$

$$\frac{\partial G}{\partial t} = k \frac{\partial T}{\partial t}$$

$$\frac{\partial^2 G}{\partial x^2} = k \frac{\partial^2 T}{\partial x^2} + k' \left(\frac{\partial T}{\partial x} \right)^2$$

Then B1.6 becomes:

$$\frac{\partial^2 G}{\partial x^2} = \alpha \frac{\partial G}{\partial t}$$

This is a much neater equation. However, it would seem that the time and effort needed to transform back to T makes this form too difficult to use. Also, we have k as a function of density as well as temperature. In this case the transformation does not remove all the problems. Thus, we work with B1.6.

Generally the equation has more terms. Suppose it looks like:

$$\frac{\partial}{\partial x} \left(k \frac{\partial T}{\partial x} \right) = s_1 \left(\frac{\partial T}{\partial t} \right) + s_2 \left(\frac{\partial T}{\partial x} \right) + s_3 \quad (B1.7)$$

where $k = k(T, \rho)$, $s_i = s_i(T, \rho, x, t)$

$$k \frac{\partial^2 T}{\partial x^2} + \frac{\partial T}{\partial x} \left[\left(\frac{\partial k}{\partial T} \right) \left(\frac{\partial T}{\partial x} \right) + \left(\frac{\partial k}{\partial \rho} \right) \left(\frac{\partial \rho}{\partial x} \right) \right] = s_1 \left(\frac{\partial T}{\partial t} \right) + s_2 \left(\frac{\partial T}{\partial x} \right) + s_3$$

or

$$\frac{\partial T}{\partial t} = \left(\frac{k}{s_1} \right) \left(\frac{\partial^2 T}{\partial x^2} \right) + \frac{\left(\frac{\partial k}{\partial T} \right) \left(\frac{\partial T}{\partial x} \right)^2}{s_1} + \frac{\left[\left(\frac{\partial k}{\partial \rho} \right) \left(\frac{\partial \rho}{\partial x} \right) - s_2 \right]}{s_1} \left(\frac{\partial T}{\partial x} \right) - \frac{s_3}{s_1}$$

If we let $k = k_1 k_a$,

$$k_1 = k_1(T), \quad k_a = k_a(\rho)$$

$$\frac{\partial k}{\partial T} = k'_1 k_a = \left(\frac{k'_1}{k_1} \right) k$$

$$\frac{\partial k}{\partial \rho} = k_1 k'_a = \left(\frac{k'_a}{k_a} \right) k$$

and,

$$\begin{aligned} \frac{\partial T}{\partial t} = & \left(\frac{k}{s_1} \right) \frac{\partial^2 T}{\partial x^2} + \left(\frac{k'_1}{k_1} \right) \left(\frac{k}{s_1} \right) \left(\frac{\partial T}{\partial x} \right)^2 \\ & + \frac{k}{s_1} \left[\left(\frac{k'_a}{k_a} \right) \left(\frac{\partial \rho}{\partial x} \right) - \frac{s_2}{k} \right] \left(\frac{\partial T}{\partial x} \right) - \frac{s_3}{s_1} \end{aligned} \quad (B1.8)$$

In the charring problem, Section II. B. 2,

$$s_1 = \rho c_p$$

$$s_2 = -c_g \dot{m}_g$$

$$s_3 = g$$

and this gives the energy equation as stated there.

APPENDIX B2

SPACE TRANSFORMATIONS USED IN THE PROGRAM

We employ two space transformations; the first allows a moving boundary, while the second allows for unequally spaced points. As originally formulated, the space variable x ranges from 0 to A_i in each layer: $0 \leq x \leq A_i$.

If we allow melting, $A_i = A_i(t)$. In particular $A_i(0)$ is the original length. Let $s_m(t)$ be the amount melted at time t .

The first transformation is that of Landau (reference 1):

$$\bar{x} = \frac{x - s_m(t)}{A_i(0) - s_m(t)} = \frac{x - s_m}{A_i} \quad (\text{B2.1})$$

Past the first layer $s_m \equiv 0$. Thus, in these layers the transformation serves only to standardize the space variable: in each layer $0 \leq \bar{x} \leq 1$. In the first layer B2.1 allows melting to proceed without dropping mesh points.

In transforming the differential equations, we need the following formulas:

$$\frac{\partial \bar{x}}{\partial x} = \frac{1}{A_i} \quad (\text{B2.2})$$

$$\frac{\partial \bar{x}}{\partial t} = \frac{-A_i \dot{s}_m + (x - s_m) \dot{s}_m}{(A_i)^2} = \frac{\dot{s}_m [x - s_m - A_i]}{(A_i)^2}$$

$$\frac{x - s_m - A_i}{A_i} = \bar{x} - 1$$

or

$$\frac{\partial \bar{x}}{\partial t} = - \frac{\dot{s}_m (1 - \bar{x})}{A_i} \quad (\text{B2.3})$$

The need for unequally spaced points arises from the fact that very often the major portion of the reaction occurs in a small portion of the material (for example, a very steep temperature gradient at the frontface). One solution is to solve for points which are unequally spaced in the body. This has the disadvantage of greatly complicating the difference equations. It would also be somewhat inflexible in that the initial spacing would

presumably be kept for the whole run. It would seem more desirable to make another space transformation; in this case in terms of the new space variable the transformed equations would be solved at equally spaced points.

We would like to vary this transformation with time so as to keep the most points in the most desirable place. However, this becomes quite complicated. In the case of char, it is conceivable that more points would be desired toward the middle of the region, rather than at the end points. For the sake of simplicity this possibility has been put aside until such time that its usefulness becomes more evident (and also until such time that a solution becomes more evident). Thus, we are content with a transformation that squeezes points either toward the frontface or the backface.

First note that the following more common transformations are not entirely suitable:
(Let η be the new variable)

$$\eta = (\bar{x})^n: \text{ for } n < 1, \left(\frac{d \eta}{d \bar{x}} \right)_0 = +\infty$$

$$\text{for } n > 1, \left(\frac{d \eta}{d \bar{x}} \right)_0 = 0$$

$$\eta = (1-\bar{x})^n \text{ has similar difficulties}$$

$$\eta = \sin \left[\left(\frac{\pi}{2} \bar{x} \right)^n \right] : \text{ same}$$

At any rate this transformation was eventually chosen:

$$\eta = \frac{1-e^{-r\bar{x}}}{1-e^{-r}}$$

It was then decided that this transformation was too extreme, since if r was chosen so as to squeeze points toward the frontface, there were not enough toward the back. To overcome this difficulty the transformation was generalized as follows:

$$\left. \begin{aligned} \eta &= \frac{1-e^{-r\xi}}{1-e^{-r}} \\ \xi &= \bar{x} e^c (\bar{x}^2 - \bar{x}) \\ r &= r(t) \end{aligned} \right\} \quad (B2,4)$$

This is now in the program.

$$\frac{\partial \eta}{\partial \bar{x}} = \left(\frac{\partial \eta}{\partial \xi} \right) \left(\frac{\partial \xi}{\partial \bar{x}} \right) + \frac{\partial \eta}{\partial r} \left(\frac{\partial r}{\partial \bar{x}} \right)$$

but $\frac{\partial r}{\partial \bar{x}} = 0$

or

$$\frac{\partial \eta}{\partial \bar{x}} = \left(\frac{\partial \eta}{\partial \xi} \right) \left(\frac{\partial \xi}{\partial \bar{x}} \right)$$

$$\frac{\partial \eta}{\partial \xi} = \frac{r e^{-r} \xi}{1 - e^{-r}}$$

Later in this section the function $\frac{r}{1 - e^{-r}}$ is graphed. It is always positive, or $\frac{\partial \eta}{\partial \xi} > 0$.

$$\frac{\partial \xi}{\partial \bar{x}} = e^c (\bar{x}^2 - \bar{x}) + \bar{x} e^c (\bar{x}^2 - \bar{x}) (c) (2\bar{x} - 1) = e^c (\bar{x}^2 - \bar{x}) \left[1 + c \bar{x} (2\bar{x} - 1) \right]$$

This is positive as long as $f(\bar{x}) = 1 + c (2\bar{x}^2 - \bar{x}) > 0$.

$$f'(\bar{x}) = c (4\bar{x} - 1)$$

$$f'(\bar{x}) = 0 \Rightarrow \bar{x} = \frac{1}{4}$$

\therefore ,

$f(\bar{x})$ has a minimum at $\bar{x} = \frac{1}{4}$:

$$f\left(\frac{1}{4}\right) = 1 + c \left(\frac{1}{4}\right) \left(\frac{1}{2} - 1\right) = 1 - \frac{c}{8} = \frac{8-c}{8}$$

\therefore ,

$$\frac{\partial \xi}{\partial \bar{x}} > 0 \text{ requires } c < 8$$

Thus, if $c < 8$, $\frac{\partial \eta}{\partial \bar{x}} > 0$ and this is a legitimate transformation. Also, since $\eta(1) = 1$, $\eta(0) = 0$, $0 < \eta \leq 1$.

Note that $\frac{r}{1 - e^{-r}} < 1$ for $r < 0$ and $\frac{r}{1 - e^{-r}} > 1$ for $r > 0$.

$$\left(\frac{\partial \eta}{\partial \bar{x}} \right)_0 = \frac{r}{1 - e^{-r}}$$

Thus, $r > 0$ squeezes toward the frontface and $r < 0$ squeezes away from the frontface.

$$\left(\frac{\partial \eta}{\partial \bar{x}}\right)_1 = \left(\frac{r e^{-r}}{1-e^{-r}}\right) (1+c)$$

If r and c are chosen so that $\left(\frac{\partial \eta}{\partial \bar{x}}\right)_1 > 1$ and $\left(\frac{\partial \eta}{\partial \bar{x}}\right)_0 > 1$ the transformation would squeeze both toward the back and the front. If r and c are chosen so that both are < 1 , the maximum squeezing would be inside. However, as can be seen from the graphs at the end of this section, this is not feasible for reasonable values of r and c .

To allow more flexibility r is treated as a function of time: $r = r(t)$. Care must be taken here, for if r is allowed to vary too rapidly or too far, the transformation may become extreme. The present method for computing r is discussed in Section VII.

At the present time it seems unnecessary to perform the transformation in any layer except the first. Thus, in layers past the first there is only the trivial transformation, $\eta = \bar{x}$.

In transforming the partial differential equations, we need the following formulas:

$$\frac{\partial \eta}{\partial \bar{x}} = \left(\frac{\partial \eta}{\partial \xi}\right) \left(\frac{\partial \xi}{\partial \bar{x}}\right) \left(\frac{\partial \bar{x}}{\partial x}\right) = (\eta_\xi) (\xi_{\bar{x}}) (\bar{x}_x) \quad (\text{B2.5.1})$$

$$\eta_\xi = \frac{r e^{-r} \xi}{1-e^{-r}} \quad (\text{B2.5.2})$$

$$\xi_{\bar{x}} = e^c (\bar{x}^2 - \bar{x}) \left[1 + c \bar{x} (2\bar{x} - 1)\right] \quad (\text{B2.5.3})$$

$$\bar{x}_x = \frac{1}{A_i} \quad (\text{B2.5.4})$$

$$\frac{\partial \eta}{\partial t} = \eta_r r_t + \eta_\xi \xi_{\bar{x}} \bar{x}_t \quad (\text{B2.6.1})$$

$$\eta_r = \frac{A_i}{r} \left[\frac{\eta_x \bar{x}}{1 + c \bar{x} (2\bar{x} - 1)} - \frac{\eta (\eta_x)_1}{1+c} \right] \quad (\text{B2.6.2})$$

$$\bar{x}_t = - \frac{\dot{s}_m (1-\bar{x})}{A_i} \quad (\text{B2.6.3})$$

$$\bar{\eta} = e^{-r \xi}$$

$$\frac{\partial^2 \eta}{\partial x^2} = \eta_{xx} = \left[(\eta_{\xi})_{\xi x} \xi_{\bar{x}} + \eta_{\xi} (\xi_{\bar{x}})_{\bar{x}} \right] \bar{x}_x$$

$$(\eta_{\xi})_{\xi x} = \eta_{\xi \xi} \xi_{\bar{x}} \bar{x}_x$$

$$(\xi_{\bar{x}})_{\bar{x}} = \xi_{\bar{x} \bar{x}} \bar{x}_x$$

$$\eta_{xx} = \left[\eta_{\xi \xi} (\xi_{\bar{x}})^2 \bar{x}_x + \eta_{\xi} \xi_{\bar{x} \bar{x}} \bar{x}_x \right] \bar{x}_x$$

$$\eta_{xx} = (\bar{x}_x)^2 \left[\eta_{\xi \xi} (\xi_{\bar{x}})^2 + \eta_{\xi} \xi_{\bar{x} \bar{x}} \right] \quad (\text{B2.7.1})$$

$$\eta_{\xi \xi} = -r \eta_{\xi} \quad (\text{B2.7.2})$$

$$\xi_{\bar{x} \bar{x}} = c (2\bar{x}-1) e^{c(\bar{x}^2 - \bar{x})} \left[1 + c \bar{x} (2\bar{x}-1) \right] + e^{c(\bar{x}^2 - \bar{x})} (c) (4\bar{x}-1)$$

$$\begin{aligned} \xi_{xx} &= c e^{c(\bar{x}^2 - \bar{x})} \left\{ (2\bar{x}-1) \left[1 + c \bar{x} (2\bar{x}-1) \right] + 4 \bar{x}-1 \right\} \\ &= c e^{c(\bar{x}^2 - \bar{x})} \left\{ (2\bar{x}-1) + c \bar{x} (2\bar{x}-1)^2 + 4 \bar{x}-1 \right\} \\ &= c e^{c(\bar{x}^2 - \bar{x})} \left\{ 2 (3\bar{x}-1) + c \bar{x} (2\bar{x}-1)^2 \right\} \end{aligned} \quad (\text{B2.7.3})$$

The remainder of this section is devoted to a derivation and discussion of equation B2.6.2.

$$\begin{aligned} \frac{\partial \eta}{\partial r} &= \frac{\xi e^{-r \xi}}{1-e^{-r}} + \frac{(1-e^{-r \xi}) (-e^{-r})}{(1-e^{-r})^2} \\ &= \frac{\xi e^{-r \xi}}{1-e^{-r}} - \left(\frac{e^{-r}}{1-e^{-r}} \right) (\eta) \\ &= \frac{\xi}{r} \frac{r e^{-r \xi}}{1-e^{-r}} - \frac{r e^{-r}}{r (1-e^{-r})} (\eta) \end{aligned}$$

$$\begin{aligned}
&= \left(\frac{\xi}{r} \right) (\eta_{\xi}) - (\eta_{\xi})_1 \left(\frac{\eta}{r} \right) \\
&= \left(\frac{\xi}{r} \right) \frac{\eta_x}{(\xi_x) (\bar{x}_x)} - \left(\frac{\eta}{r} \right) \frac{(\eta_x)_1}{(\xi_x)_1 \bar{x}_x} \\
&= \frac{A_i}{r} \left[\frac{\xi \eta_x}{\xi_x} - \frac{\eta (\eta_x)_1}{(1+c)} \right]
\end{aligned}$$

$$\frac{\xi}{\xi_x} = \frac{\bar{x} e^{c(\bar{x}^2 - \bar{x})}}{e^{c(\bar{x}^2 - \bar{x})} \left[1 + c \bar{x} (2\bar{x} - 1) \right]} = \frac{\bar{x}}{1 + c \bar{x} (2\bar{x} - 1)}$$

∴,

$$\eta_r = \frac{A_i}{r} \left[\frac{\eta_x \bar{x}}{1 + c \bar{x} (2\bar{x} - 1)} - \frac{\eta (\eta_x)_1}{1+c} \right]$$

It is also desirable to have some information concerning the behavior of $\frac{\partial \eta}{\partial r}$. For this another form is more convenient:

$$e^{-r} \xi = \bar{\eta} = 1 - \eta (1 - e^{-r})$$

$$\xi = \frac{\ln \bar{\eta}}{-r}$$

$$1 - e^{-r} \xi = \eta (1 - e^{-r})$$

For this discussion we let $c = 0$: $\xi = \bar{x}$

$$\begin{aligned}
\frac{\partial \eta}{\partial r} &= \left(\frac{\ln \bar{\eta}}{-r} \right) (\bar{\eta}) - \frac{\eta e^{-r}}{1 - e^{-r}} \\
&= - \left(\frac{e^{-r}}{1 - e^{-r}} \right) \left[\eta + \frac{\bar{\eta} \ln \bar{\eta}}{r e^{-r}} \right]
\end{aligned}$$

Let

$$h(\eta) = \frac{\partial \eta}{\partial r}$$

$$\frac{\partial h}{\partial \eta} = h'(\eta) = - \left(\frac{e^{-r}}{1 - e^{-r}} \right) \left[1 + \frac{\partial \bar{\eta}}{\partial \eta} \left(\frac{1 + \ln \bar{\eta}}{r e^{-r}} \right) \right] =$$

$$= - \left(\frac{e^{-r}}{1-e^{-r}} \right) \left[1 + \left(\frac{1 + \ln \bar{\eta}}{r e^{-r}} \right) (e^{-r} - 1) \right]$$

$$h'(\eta) = \frac{1 + \ln \bar{\eta}}{r} - \frac{e^{-r}}{1-e^{-r}}$$

$$h''(\eta) = \frac{e^{-r} - 1}{r \bar{\eta}} = - \frac{1}{\bar{\eta}} \left(\frac{1 - e^{-r}}{r} \right)$$

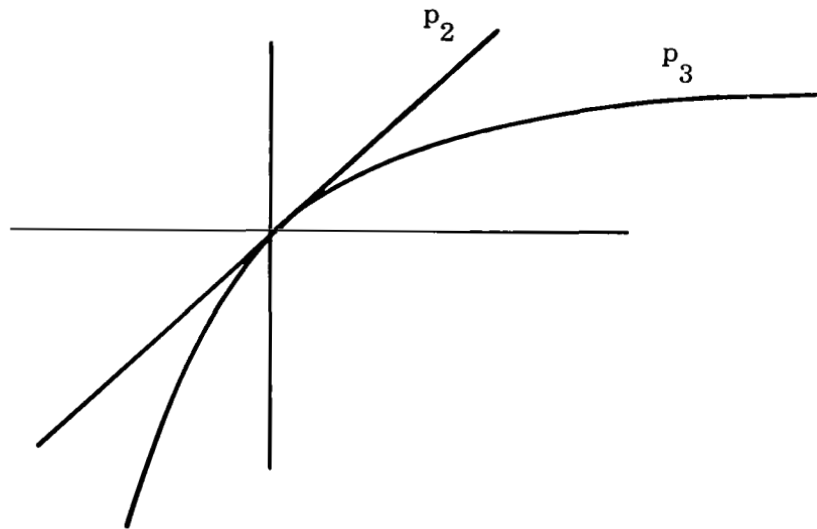
We now graph the following two functions:

$$p_1(r) = \frac{r}{1-e^{-r}} \quad q_1(r) = \frac{r}{e^r - 1}$$

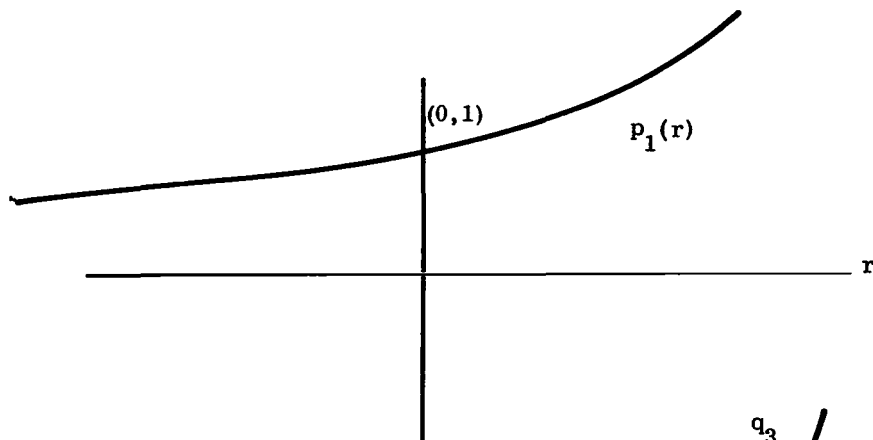
$$p_1(r) = \frac{p_2(r)}{p_3(r)} \quad p_2(r) = r$$

$$p_3(r) = 1 - e^{-r}$$

$$p_3^{S_1}(r) = e^{-r}$$

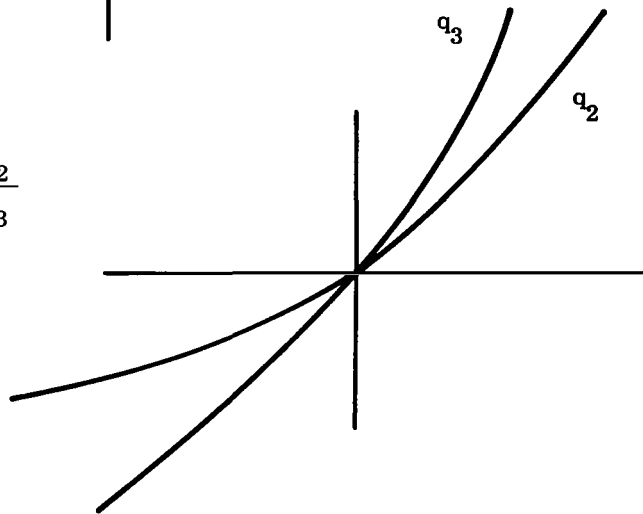


Thus,

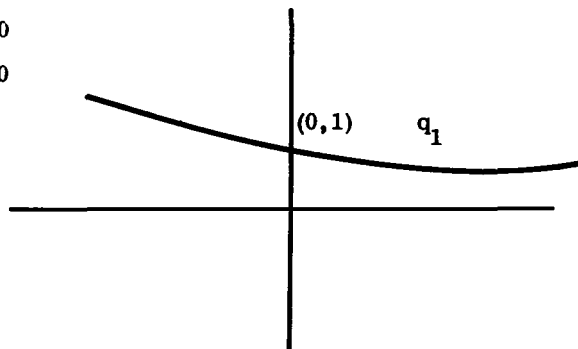
$$p_1(r) \text{ is } \begin{cases} > 1 \text{ for } r > 0 \\ < 1 \text{ for } r < 0 \end{cases}$$


Likewise,

$$q_1(r) = \frac{q_2}{q_3}$$



or q_1 is $\begin{cases} < 1 \text{ for } r > 0 \\ > 1 \text{ for } r < 0 \end{cases}$



Since $\frac{1-e^{-r}}{r} > 0$ and $\bar{\eta} > 0$ in $0 \leq \eta \leq 1$,

$h''(\eta) < 0$ for all r and all η in $[0, 1]$.

also,

$$h'(0) = \frac{1+0}{r} - \frac{e^{-r}}{1-e^{-r}} = \frac{1}{r} \left[1 - \frac{r e^{-r}}{1-e^{-r}} \right] = \frac{1}{r} \left[1 - \frac{r}{e^r - 1} \right]$$

From previous diagram,

$$1 - \frac{r}{e^r - 1} \text{ is } \begin{cases} > 0 \text{ for } r > 0 \\ < 0 \text{ for } r < 0 \end{cases}$$

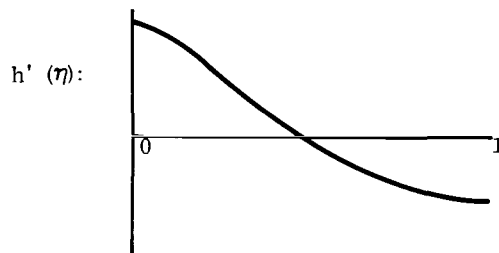
or, $h'(0) > 0$

$$\begin{aligned} h'(1) &= \frac{1-r}{r} - \frac{e^{-r}}{1-e^{-r}} = \frac{1}{r} \left[(1-r) - \frac{r}{e^r - 1} \right] \\ &= \frac{1}{r} \left[1 - r \left(1 + \frac{1}{e^r - 1} \right) \right] = \frac{1}{r} \left[1 - r \left(\frac{e^r}{e^r - 1} \right) \right] = \frac{1}{r} \left[1 - \frac{r}{1-e^{-r}} \right] \end{aligned}$$

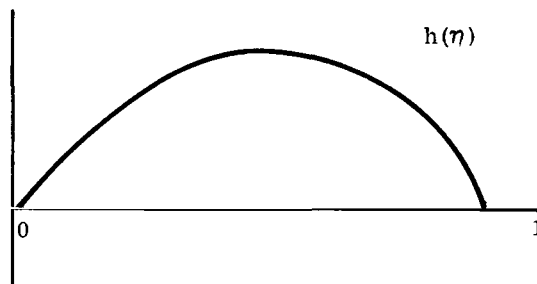
From previous diagram,

$$1 - \frac{r}{1-e^{-r}} \text{ is } \begin{cases} < 0 \text{ for } r > 0 \\ > 0 \text{ for } r < 0 \end{cases}$$

or, $h'(1) < 0$.



$h(0) = h(1) = 0$ and $b(\eta)$:



This work is not really rigorous for $r = 0$. We use L'Hospital's rule for $r = 0$:

$$\frac{\partial \eta}{\partial r} = \frac{\bar{\eta} \ln \bar{\eta} + r \eta e^{-r}}{-r(1-e^{-r})} = \frac{0}{0} \text{ at } r = 0$$

$$\begin{aligned} \lim_{r=0} \frac{\partial \eta}{\partial r} &= \frac{-\eta \left[e^{-r} - r e^{-r} \right] - (1 + \ln \bar{\eta}) (-\eta e^{-r})}{+ (1-e^{-r}) + r e^{-r}} = \\ &= \frac{-\eta e^{-r} \left[(1-r) - (1 + \ln \bar{\eta}) \right]}{r e^{-r} + (1-e^{-r})} = \\ &= \frac{+\eta e^{-r} \left[r + \ln \bar{\eta} \right]}{(r-1) e^{-r} + 1} = \frac{\eta (r + \ln \bar{\eta})}{(r-1) + e^{+r}} = \frac{0}{0} \end{aligned}$$

$$\lim_{r=0} h(\eta) = \frac{\eta \left[1 + \frac{1}{\bar{\eta}} (-\eta e^{-r}) \right]}{1+e^r}$$

$$\eta \text{ at } r = 0, \bar{\eta} = 1$$

$$\lim_{r=0} h(\eta) = \frac{\eta (1-\eta)}{2}$$

To obtain information concerning $\max h(\eta)$ we can proceed as follows:

$$h(\eta) \text{ has max at } \frac{dh}{d\eta} = 0: 1 + \ln \bar{\eta} = \frac{r e^{-r}}{1-e^{-r}}$$

$$r \ln \bar{\eta} = 1 - \left(\frac{\partial \eta}{\partial \xi} \right)_1 = 1 - (\eta_{\xi})_1$$

$$\begin{aligned} h(\eta) &= - \left(\frac{e^{-r}}{1-e^{-r}} \right) \left[\frac{1-e^{-r}\xi}{1-e^{-r}} + \frac{e\bar{\eta} \ln \bar{\eta}}{r e^{-r}} \right] \\ &= - \frac{e^{-r}}{(1-e^{-r})^2} \left\{ 1-e^{-r}\xi + \frac{1-e^{-r}}{r e^{-r}} \left[(\eta_{\xi})_1 - 1 \right] e^{\left[(\eta_{\xi})_1 - 1 \right]} \right\} \end{aligned}$$

$$\begin{aligned}
&= - \frac{e^{-r}}{(1-e^{-r})^2} \left\{ 1 - e^{-r\xi} + \left(1 - \frac{1}{(\eta_{\xi 1})}\right) e^{-r\xi} \right\} \\
&= \frac{e^{-r}}{(1-e^{-r})^2} \left\{ \frac{e^{-r\xi}}{(\eta_{\xi 1})} - 1 \right\} = \frac{e^{-r}}{(1-e^{-r})^2} \left\{ \frac{e^{\left[(\eta_{\xi 1}) - 1\right]}}{(\eta_{\xi 1})} - 1 \right\}
\end{aligned}$$

$$\text{let } f(\xi) = \frac{e^{\left[(\eta_{\xi 1}) - 1\right]}}{(\eta_{\xi 1})} \cdot \frac{(\eta_{\xi 0})}{\left[(\eta_{\xi 0}) - 1\right]} = e^{\left[(\eta_{\xi 1}) - (\eta_{\xi 0})\right]} \left[\frac{(\eta_{\xi 0})}{(\eta_{\xi 1})} \right]$$

$$(\eta_{\xi 1}) - (\eta_{\xi 0}) = \frac{r e^{-r}}{1-e^{-r}} - \frac{r}{1-e^{-r}} = -r$$

$$\frac{(\eta_{\xi 0})}{(\eta_{\xi 1})} = e^r$$

$$\text{or } f(\xi) = e^{-r} e^r = 1$$

$$\therefore, \quad \max h(\eta) = \frac{e^{-r}}{(1-e^{-r})^2} \left\{ \frac{e^{\left[(\eta_{\xi 0}) - 1\right]}}{(\eta_{\xi 0})} - 1 \right\} \quad (\text{B2.8})$$

as $r \rightarrow +\infty$,

$$\max h(\eta) \rightarrow e^{-r} \left\{ \frac{e^{(r-1)}}{r} - 1 \right\} = \frac{1}{r} - e^{-r} \rightarrow 0$$

as $r \rightarrow -\infty$,

$$\max h(\eta) \rightarrow \frac{e^r}{(e^r - 1)} \left\{ e^{-r} e^{+r} - 1 \right\} \rightarrow 0$$

It seems difficult to reduce B2.8 any further. Some computed values are as follows:

$$r = 2: \max h(\eta) \approx 1$$

$$r = 3: \max h(\eta) \approx .33$$

$$r = 4: \max h(\eta) \approx .25$$

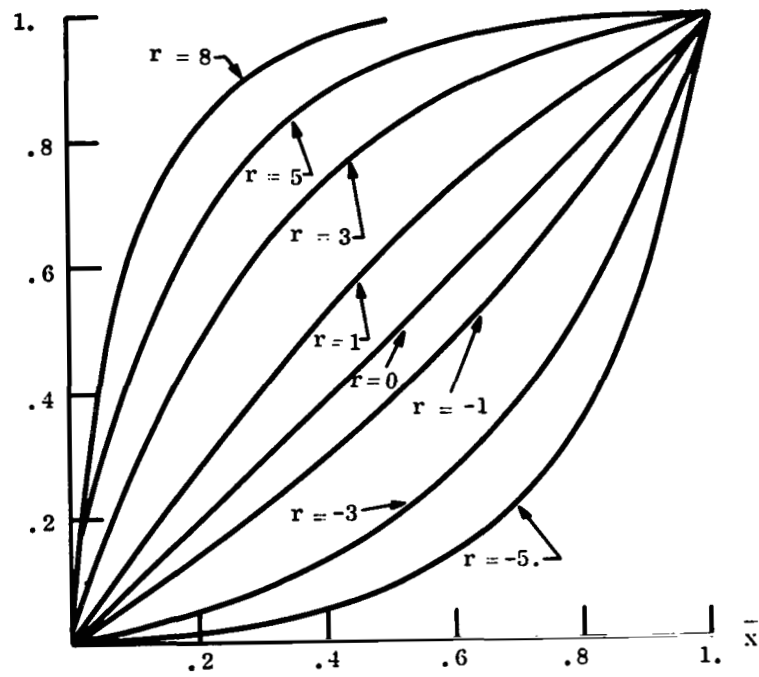


Figure B2.1. $\eta(\bar{x})$; $c = 0$ (See Equation B2.4)

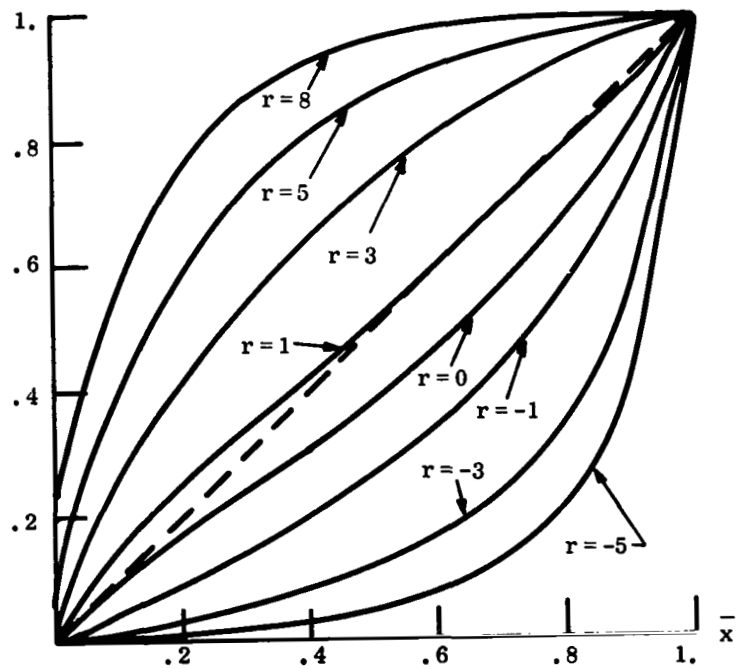


Figure B2.4. $\eta(\bar{x})$; $c = 1$ (See Equation B2.4)

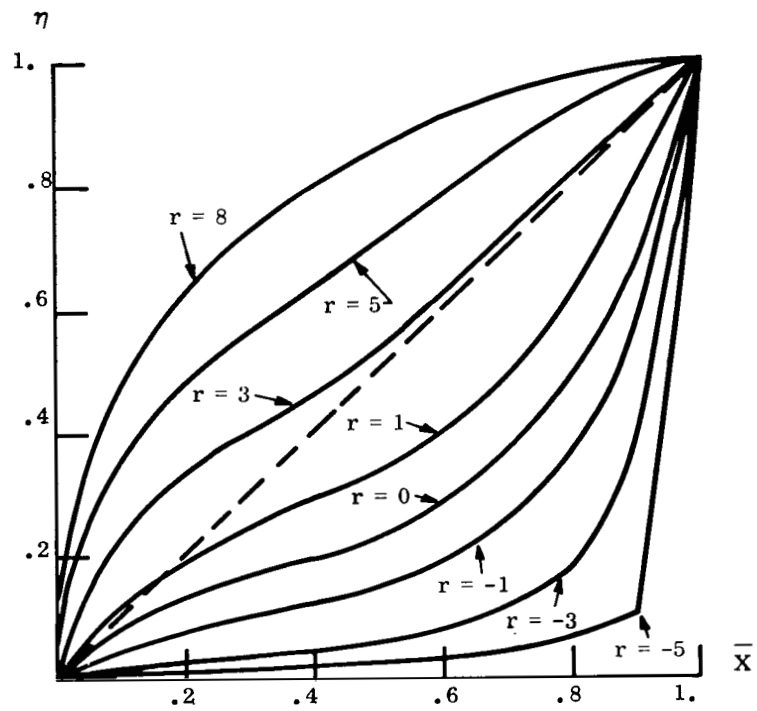


Figure B2.3. $\eta(\bar{\xi})$; $c = 3$ (See Equation B2.4)

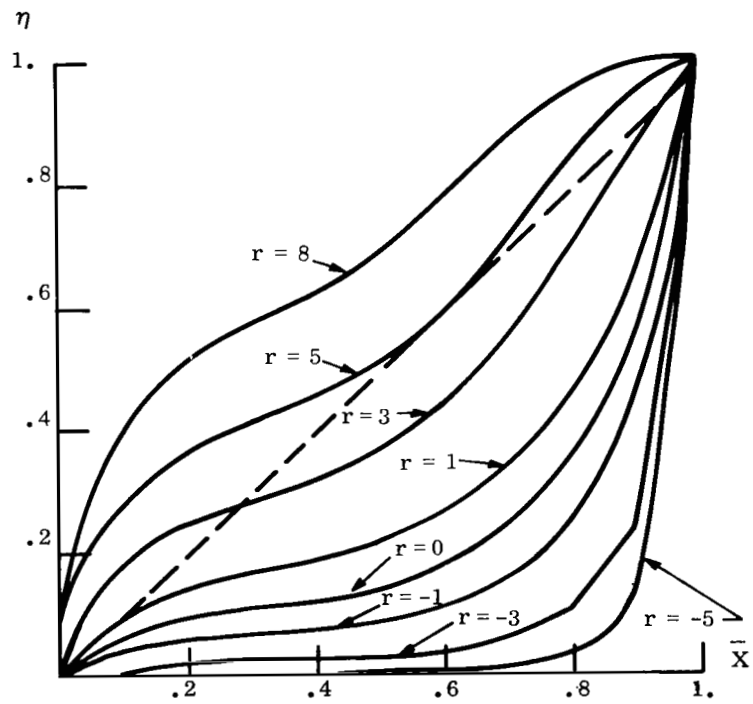


Figure B2.4. $\eta(\bar{\xi})$; $c = 5$ (See Equation B2.4)

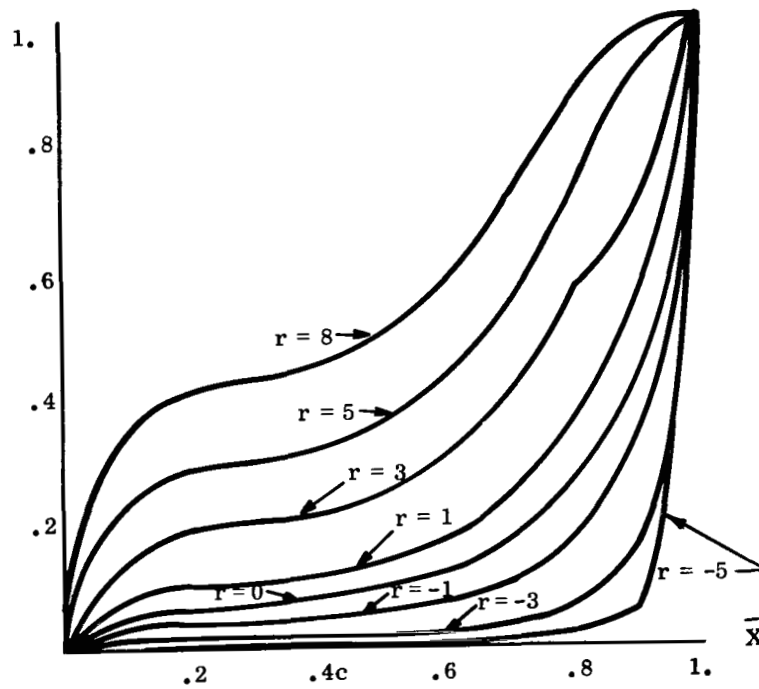


Figure B2.5. $\eta(\bar{x})$; $c = 7$ (See Equation B2.4)

APPENDIX B3

AN ITERATION PROCEDURE

Throughout the program many relationships are encountered which require iteration. Rather than have a separate procedure for each case, we found it advantageous to write one fairly general technique: it is then necessary to make each case conform to the specified format.

We assume that the equation can be intelligently written in the form:

$$x = f(x)$$

Note that any root problem can be put in this form:

Suppose we want a root of $g(x) = 0$. An equivalent problem is to solve:

$$x = f(x), \text{ where } f(x) = x + g(x)$$

A well-known method of iteration is that of successive approximations:

$$x_{n+1} = f(x_n)$$

The conditions for convergence are also well-known:

$$|f'(x)| < 1 \text{ in the vicinity of the solution (reference 12, p. 201)}$$

Another iteration procedure is as follows:

Let x_1 be the first guess.

Then x_{n+1} is the intersection of these lines:

$$y = x_{n+1}$$

$$y = \left[f'(x_n) \right] x + \left[f(x_n) - x_n f'(x_n) \right]$$

[The second line is the line through $(x_n, f(x_n))$ with slope $f'(x_n)$].

or,

$$x_{n+1} = x_{n+1} f'(x_n) + f(x_n) - x_n f'(x_n)$$

$$x_{n+1} = \frac{f(x_n) - x_n f'(x_n)}{1 - f'(x_n)}$$

This process will also converge under certain conditions. We will establish convergence under these conditions:

- a. $f'(x) < 0$
- b. $f'(x)$ monotone

Let \bar{x} be solution: $\bar{x} = f(\bar{x})$

$$x_{n+1} - \bar{x} = \frac{f(x_n) - \bar{x} - f'(x_n) [x_n - \bar{x}]}{1 - f'(x_n)}$$

$$\frac{x_{n+1} - \bar{x}}{x_n - \bar{x}} = \frac{\frac{f(x_n) - \bar{x}}{x_n - \bar{x}} - f'(x_n)}{1 - f'(x_n)}$$

$$\frac{x_{n+1} - \bar{x}}{x_n - \bar{x}} = \frac{f'(\xi) - f'(x_n)}{1 - f'(x_n)} : \xi \text{ is between } x_n \text{ and } \bar{x}$$

\therefore ,

$$\frac{x_{n+1} - \bar{x}}{x_n - \bar{x}} = \frac{a - t}{a + 1},$$

where $a = -f'(x_n) > 0$

$$t = -f'(\xi) > 0$$

Note that for $0 \leq t \leq a$,

$$0 \leq \frac{a-t}{a+1} < 1$$

Suppose now that $f'(x)$ is monotonically decreasing: $x_1 < x_2 \Rightarrow f'(x_1) > f'(x_2)$

We have two cases to consider:

- a. $x_n > \bar{x}$:

Then $\bar{x} < \xi < x_n$ and $f'(\xi) > f'(x_n)$

$$\text{or } -f'(x_n) - (-f'(\xi)) > 0$$

or

$$a - t > 0$$

\therefore ,

from above we obtain:

$$0 < \frac{x_{n+1} - \bar{x}}{x_n - \bar{x}} < 1$$

$$\left. \begin{array}{l} \text{or,} \\ x_{n+1} > \bar{x} \\ \text{and} \\ x_{n+1} < x_n \end{array} \right\} \bar{x} < x_{n+1} < x_n$$

Thus, x_{n+1} will indeed converge.

Suppose it does not converge to \bar{x} :

Suppose $x_n \rightarrow \tilde{x} > \bar{x}$:

$$\frac{x_{n+1} - \bar{x}}{x_n - \bar{x}} \rightarrow 1 \Rightarrow f'(\xi) \Rightarrow +1,$$

but $f'(\xi) < 0$

b. $x_n < \bar{x}$:

Then $x_n < \xi < \bar{x} \Rightarrow f'(x_n) > f'(\xi)$

\therefore ,

$$\frac{x_{n+1} - \bar{x}}{x_n - \bar{x}} < 0 \Rightarrow x_{n+1} > \bar{x}, \text{ or we are back in a.}$$

A similar proof is also possible for the case where $f'(x)$ is monotonically increasing.

We attempt to apply these two methods, and even assume, therefore, that the function satisfies one of these two conditions:

- a. $|f'(x)| < 1$ in vicinity of solution
- b. $f'(x) < 0$ and monotone in vicinity of solution.

Note that the phrase "vicinity of solution" is actually sufficient if the first guess gets you there. Normally our first guesses are quite good, since the program proceeds in a step-by-step fashion.

A precise application of these methods would require an evaluation of $f'(x)$. This is usually impractical, so the following procedure has been adopted. We hope it will take us to the appropriate method. So far we have had very little difficulty.

Let x_1 be first guess

Let $x_{n+1} = f(x_n)$

1. As long as the $\{x_i\}$ are monotone, we assume the process is converging and we continue.
2. As soon as $x_i < x_{i+1} > x_{i+2}$ or $x_i > x_{i+1} < x_{i+2}$, we have lost monotonicity. We then proceed by halving the interval:

a. Let $\bar{x}_1 = \min [x_i, x_{i+1}, x_{i+2}]$

b. $\bar{x}_2 = \max [x_i, x_{i+1}, x_{i+2}]$

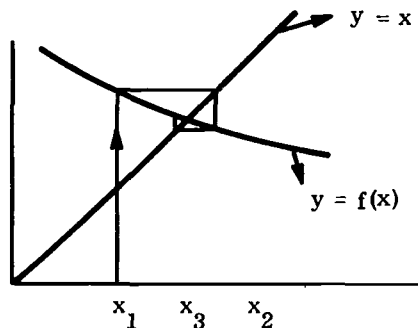
c. Let $x^* = \frac{\bar{x}_1 + \bar{x}_2}{2}$

d. $x^{**} = f(x^*)$

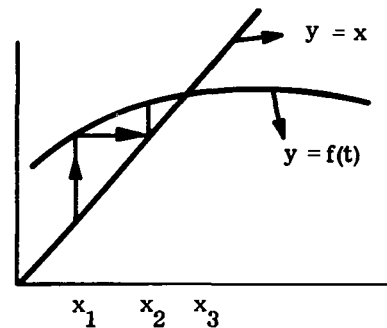
if $\begin{cases} x^* < x^{**} \\ x^* > x^{**} \end{cases}$ then $\begin{cases} \bar{x}_1 = x^* \\ \bar{x}_2 = x^* \end{cases}$ and go back to c

The first step is clearly related to the method of successive approximations. The second step is actually part B of the second procedure. In order to go back to part A we would need the derivative.

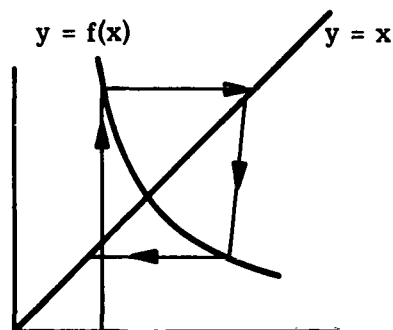
We look at a few examples of the above procedure:



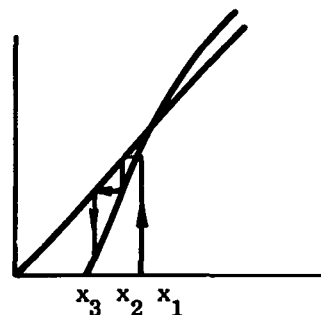
since x_1, x_2, x_3 are not monotone, we would halve the interval



we would proceed by successive approximations



successive approximations will not converge, but halving interval will.



divergence appears imminent!

Because of the possibility that this procedure might not converge under some conditions, the program will stop after a specified number of iterations.

We mention finally that the program is capable of handling simultaneous problems (ten is presently the maximum):

for example,

$$x = f(x, y, z)$$

$$y = g(x, y, z)$$

$$z = h(x, y, z)$$

actually, we could write:

$x = f(x, f_1(x), f_2(x)) = \ell(x)$, which is the correct form. The program proceeds as follows:

choose x_1 :

We need to solve:

$$y = g(x_1, y, z)$$

$$z = h(x_1, y, z)$$

choose y_1 :

solve $z = h(x_1, y_1, z)$. Let the solution be \bar{z} then obtain $y_2 = g(x_1, y_1, \bar{z})$, and solve $z = h(x_1, y_2, z)$. Proceed until we obtain

$$\bar{y} = g(x_1, \bar{y}, \bar{z})$$

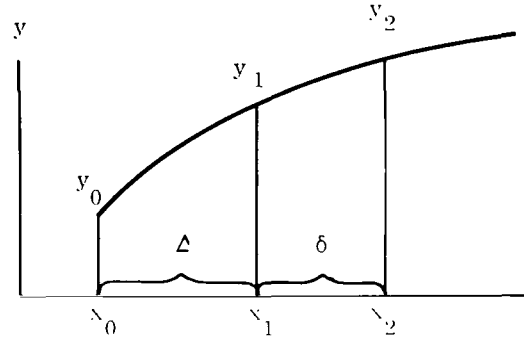
$$\bar{z} = h(x_1, \bar{y}, \bar{z})$$

Then obtain $x_2 = f(x_1, \bar{y}, \bar{z})$.

Repeat cycle with new guess for x until $x = f(x, \bar{y}, \bar{z})$ is obtained. (\bar{y} and \bar{z} are computed for each x_i .)

APPENDIX B4
FORMULAS USED IN NUMERICAL APPROXIMATIONS

Three point difference equations are used at various points in the program to approximate the first derivative of a function. One way to derive these formulas is to pass a quadratic through the three points involved, and then evaluate it at the appropriate point.



We assume:

$$y'_0 = A y_0 + B y_1 + C y_2 \quad (\text{B4.1})$$

where $y'_0 = \frac{dy}{dx}$ at $x = x_0$

We require that B4.1 be valid for $y = \text{constant}$, $y = x$, and $y = x^2$. We can assume $x_0 = 0$.

$$y = k : 0 = A k + B k + C k$$

or,

$$0 = A + B + C$$

$$y = x : 1 = 0 + B \Delta + C (\delta + \Delta)$$

$$y = x^2 : 0 = 0 + B \Delta^2 + C (\delta + \Delta)^2$$

These three equations are to be solved for A, B, C.

$$\Delta = B \Delta^2 + C (\delta + \Delta) \Delta$$

$$0 = B \Delta^2 + C (\delta + \Delta)^2$$

$$C [\Delta (\delta + \Delta) - (\delta + \Delta)^2] = \Delta$$

$$C = \frac{\Delta}{(\delta + \Delta) (\Delta - \delta - \Delta)} = -\frac{\Delta}{\delta (\delta + \Delta)}$$

$$B = \frac{1-C(\delta+\Delta)}{\Delta} = \frac{1+\frac{\Delta}{\delta}}{\Delta} = \frac{\delta+\Delta}{\Delta\delta}$$

$$\begin{aligned} A &= -\left(\frac{\delta+\Delta}{\Delta\delta}\right) + \frac{\Delta}{\delta(\delta+\Delta)} = \frac{\Delta^2 - (\delta+\Delta)^2}{\Delta\delta(\delta+\Delta)} \\ &= \frac{\Delta^2 - \delta^2 - 2\delta\Delta - \Delta^2}{\Delta\delta(\delta+\Delta)} = \frac{-\delta(\delta+2\Delta)}{\Delta\delta(\delta+\Delta)} \\ &= \frac{-(\delta+2\Delta)}{\Delta(\delta+\Delta)} \end{aligned}$$

We obtain, then, this formula:

$$\frac{dy}{dx} \text{ at } x = x_0 = y'_0 = A y_0 + B y_1 + C y_2 \quad \text{(B4.2)}$$

$$A = \frac{-(\delta+2\Delta)}{\Delta(\delta+\Delta)}$$

$$B = \frac{\delta+\Delta}{\Delta\delta}$$

$$C = \frac{\Delta}{-\delta(\delta+\Delta)}$$

$$\text{If } \Delta = \delta, A = \frac{-3\Delta}{2\Delta^2} = \frac{-3}{2\Delta}$$

$$B = \frac{2\Delta}{\Delta^2} = \frac{2}{\Delta}$$

$$C = \frac{\Delta}{-2\Delta^2} = \frac{-1}{2\Delta}$$

and

$$y'_0 = \frac{1}{2\Delta} \left[-3 y_0 + 4 y_1 - y_2 \right] \quad \text{(B4.3)}$$

$$\text{Likewise, } \frac{dy}{dx} \text{ at } x = \Delta = y'_1 = A y_0 + B y_1 + C y_2 \quad \text{(B4.4)}$$

$$A = \frac{-\delta}{\Delta(\Delta+\delta)}$$

$$B = \frac{\delta-\Delta}{\Delta\delta}$$

$$C = \frac{\Delta}{\delta (\Delta + \delta)}$$

$$\text{If } \Delta = \delta, A = \frac{-\Delta}{2\Delta^2} = \frac{-1}{2\Delta}$$

$$B = 0$$

$$C = \frac{\Delta}{2\Delta^2} = \frac{1}{2\Delta}$$

and

$$y'_1 = \frac{y_2 - y_0}{2\Delta} \quad (\text{B4.5})$$

In the same manner,

$$\frac{dy}{dx} \text{ at } x = \Delta + \delta = y'_2 = A y_0 + B y_1 + C y_2 \quad (\text{B4.6})$$

$$A = \frac{\delta}{\Delta (\Delta + \delta)}$$

$$B = - \left(\frac{\Delta + \delta}{\Delta \delta} \right)$$

$$C = \frac{\Delta + 2\delta}{\delta (\Delta + \delta)}$$

If $\Delta = \delta$,

$$A = \frac{1}{2\Delta}$$

$$B = -\frac{2}{\Delta}$$

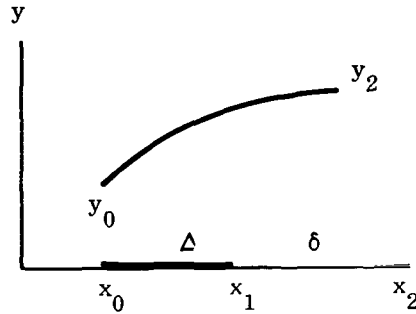
$$C = \frac{3}{2\Delta}$$

and

$$y'_2 = \frac{1}{2\Delta} \left[y_0 - 4 y_1 + 3 y_2 \right] \quad (\text{B4.7})$$

These formulas all have error of $O(\Delta x^2)$, since all that has been done here is to take the first three terms of the power series.

In the case that only two points are available:



Then, $y'_0 = y'_1 = y'_2 = \frac{y_2 - y_0}{\Delta + \delta}$ (B4.8)

This formula has error of $O(\Delta x)$.

In addition, we use an approximation for $\frac{d^2 y}{dx^2}$. This is needed only at x_1 for the case where $\Delta = \delta$. We obtain the usual formula:

$$y''_1 = \frac{1}{\Delta^2} \left[y_0 - 2y_1 + y_2 \right] \quad (\text{B4.9})$$

The program contains an option for differentiating given input tables. The formulas used are B4.2, B4.3 and B4.6. Also, the following tests are made:

1. If the first two elements in the table are equal, the first derivative table entry is zero.
2. If the last two elements in the table are equal, the last derivative table entry is zero.

APPENDIX B5
THIN SKIN OPTION

In the case that the layer of material is very thin or has a very small temperature gradient it is possible to simplify the problem considerably.

Suppose:

1. The internal equation is:

$$(k T_x)_x = \rho c_p T_t : 0 \leq x \leq A$$

2. $(-k T_x)_0 = \dot{q}_{\text{net}} : \text{given}$

3. $(-k T_x)_A = 0$

4. This approximation is "good enough":

$$\left[(k T_x)_x \right]_{A/2} = \frac{(k T_x)_A - (k T_x)_0}{A}$$

Then, if we let T represent the temperature of the entire layer:

$$A \rho c_p T_t = \dot{q}_{\text{net}} (T)$$

This is now an ordinary differential equation and is solved by a modified form of Picard's method of successive approximations (reference 12, p. 240):

$$T^{n+1} = T^n + \frac{\Delta t}{A \rho c_p} \dot{q}_{\text{net}}$$

$$\dot{q}_{\text{net}} = \dot{q}_{\text{net}} (t, T^{n+1})$$

$$c_p = c_p (T^{n+1})$$

This equation is solved at each step by iteration.

Note that if the expected temperature gradient will affect only the 3rd to 8th digits, then this option should be used. If these small changes are actually significant, then the values should be normalized so as to bring the changes in temperature to the first and second places.

APPENDIX B6
TERMINOLOGY AND DEFINITIONS

1. A_i : length of layer i
2. α : $\frac{\rho c_p}{k}$
3. C_g : $c_{p_g} + H_{c_g}$
4. C_i : $\rho c_p L$
5. c_{p_g} : specific heat (of gas)
6. $c_p = c_{p_1} c_{p_a}$: specific heat
 $c_{p_1} = c_{p_1}(T)$
 $c_{p_a} = c_{p_a}(\rho)$
7. Δt : time increment
 $\Delta x, \Delta \eta$: space increment
8. E: activation energy
9. \dot{W}_p : $\frac{\partial \rho}{\partial t}$
10. g: heat of depolmerization
11. H_{c_g} : heat of cracking
12. H_{gf} : heat of gas formation
13. $k = k_1 k_a$: conductivity
 $k_1 = k_1(T)$
 $k_a = k_a(\rho)$
14. \dot{m}_g : mass flux (of gas)
15. ρ : density of solid
 ρ_c : char density
 ρ_{vp} : density of virgin plastic
16. p: pressure
17. \dot{q} : heat flux

18. r : "squeezing" parameter in space transformation $r' = \frac{dr}{dt}$
19. R : universal gas constant
20. $s_c = s_c(t)$: amount charred at time t
 $s_m = s_m(t)$: amount "melted" at time t
 $s'_c = \frac{ds_c}{dt}$
 $s'_m = \frac{ds_m}{dt}$
 s_{c_m} : maximum allowable char length
21. σ : Stephan-Boltzmann constant
22. T : temperature
23. t : time variable
24. x, η : space variable
25. z : collision frequency
26. Quantities used at frontface:
 - 1) \dot{q}_{net} : heat flux entering body
 - 2) \dot{q}_c : convective heat flux
 - 3) \dot{q}_{hgr} : heat flux due to hot gas radiation
 - 4) \dot{q}_r : radiative heat flux
 - 5) \dot{q}_{block} : heat flux blocked by mass injection into boundary layer
 - 6) h_r : recovery enthalpy
 - 7) h_{ff} : frontface enthalpy
 - 8) \bar{A} : coefficient of blocking heat flux
 - 9) $c_{p_{Bl}}$: specific heat of boundary layer
 - 10) ϵ : emissivity
 - 11) \bar{M}_{ff} : average molecular weight of gas as it is injected into the boundary layer
 - 12) \dot{m}_{ff} : mass flux at frontface
27. Quantities used only in air gap:
 - 1) \dot{q}_r : radiative heat flux

- 2) \dot{q}_{cv} : convective heat flux
 - 3) \dot{q}_{cond} : conductive heat flux
 - 4) \bar{A} : effective area
 - 5) F_a : configuration factor
 - 6) F_e : emissivity factor
 - 7) \bar{g} : acceleration of gravity
 - 8) G_R : Grashof number
 - 9) k_c : conductivity of spacer rod
 - 10) \bar{L} : vertical height
 - 11) μ : viscosity
28. $O(\Delta)$: $w = O(\Delta) \Rightarrow \frac{w}{\Delta} < C$, for some constant C , as $\Delta t \rightarrow 0$.

APPENDIX B7

REFERENCES

1. Landau, H.G., "Heat Conduction in a Melting Solid," Ballistic Research Laboratories, Aberdeen Proving Grounds, (1948). The basic results of this paper pertain to an infinite slab. We do, however, make use of his suggested space transformation.
2. Gordon, P., "One-Dimensional Heat Conduction in a Decomposing Plastic," TIS No. 62SD145, MSVD, General Electric Company. This report contains the analysis for the original program.
3. Dufort, E.C. and Frankel, S.P., "Stability Condition in the Numerical Treatment of Parabolic Differential Equations," Mathematical Tables and Other aids to Computation, Vol. 7, p. 135 (1953). The difference equation presented here was used in the first program (ref. 2). An interesting intuitive approach to stability presented.
4. Richtmyer, R.D., "Difference Methods for Initial Value Problems," New York, Interscience Publishers Inc., 1957. We refer to this book in discussing our difference equation (Section III). The approach to stability and convergence is somewhat opposed to that of Forsythe and Wasow (see reference 6). Of the literature I have encountered, I consider Richtmyer's book to be the finest. The various concepts as defined in a very clear, intuitive, and rigorous fashion. Quite a bit of the discussion concerns the heat conduction equation and various difference equations are presented.
5. Forsythe, G.E. and Wasow, W.R., "Finite Difference Methods for Partial Differential Equations," New York, Wiley (1960). We refer to this book in discussing our difference equation (Section III). This book presents an approach to stability which is somewhat opposite to that of Richtmyer (ref. 19). They apparently feel that their approach is more general than that of Richtmyer, but I feel it is more restrictive. Regardless of personal preference, it is very well written. The book presents many interesting concepts and examples.
6. Dahlquist, G., "Convergence and Stability for a Hyperbolic Difference Equation with Analytic Initial Values," Math. Scand., Vol. 2, pp. 91-102 (1954). This paper is referred to in the discussion of the difference equation (Section III). It is quite interesting and points out very emphatically the relationship between the conditions for stability and the class of functions being considered.
7. Henrici, P., "Discrete Variable Methods in Ordinary Differential Equations," New York, Wiley, 1962. Reference is made to this book in discussing our difference equation (Section III). Stability is defined as in reference 1. From our point of view this is the finest book of its kind. It reads nicely, and develops meaningful concepts of convergence and stability.
8. Birkhoff, G. and Rota, Gian-Carlo, "Ordinary Differential Equations," Boston, Ginn, 1962. Although it appears that the concept of stability was first defined for partial differential equations, it is interesting to note that in defining the concept for ordinary differential equations, one is able to obtain further insight into its role in partial differential equations. In discussing our difference equation (Section III), we refer to Birkhoff and Rota's treatment of the Milne Method.

9. Sommerfeld, A., "Partial Differential Equations in Physics, " Academic Press Inc., Publishers, New York, N.Y. (1949). This book gives a reasonably simple introduction to partial differential equations. It is concerned essentially with second order equations. The theory of characteristics (and its significance) is presented concisely and in a readable fashion.
10. Nolan, E.J. and Young, J.P., "Graphical and Analytical Solutions to Certain Transient Aerodynamic Heat Conduction Problems" (TIS No. R60SD310, February, 1960). The abstract reads as follows:

"Analytical solutions are given for certain types of heat conduction problems occurring during aerodynamic heating. For ease in application certain solutions are also presented in graphical form. Extensive tables are presented of the repeated integrals of the error function, up to the fourth repeated integral."

In particular, the program uses two analytical solutions for the first time step - if desired. (Section VI of the analysis memo.).
11. Hasting, C., "Approximations for Digital Computers," Princeton, New Jersey, Princeton University Press, 1955. The program uses the approximation to the Error Function given on page 187.
12. Scarborough, J.B., Numerical Mathematical Analysis, third edition, Baltimore, Johns Hopkins Press, 1955. We had occasion to refer to only two chapters of this fine book: Chapter IX (The Solution of Numerical Algebraic and Transcendental Equations) and Chapter XI (The Numerical Solution of Ordinary Differential Equations).

APPENDIX C

DERIVATION OF STRESS

EQUATIONS

INTRODUCTION

The purpose of this Appendix is to present a method for the calculation of the stresses within a charring ablator.

Charring ablators are characterized by a pyrolysis zone (figure C1) in which the virgin material decomposes to form gases and a solid residue. This solid residue, a porous carbonaceous (or other refractory) material, forms a beneficial layer of char. The refractory nature of the char allows higher surface temperatures, leading to increased heat dissipation by surface re-radiation and by reduction of the driving temperature gradient from the boundary layer to the solid.

Thickness of the char layer is limited by several mechanisms which tend to remove material (ref. 1). These char removal or erosion mechanisms may be classified as either chemical erosion or mechanical erosion. Chemical erosion including sublimation and surface reactions, has been treated extensively in references 2 to 6.

Mechanical erosion may be further classified according to whether a true surface erosion mechanism is involved or whether a process in depth is involved. The spallation or pop-off phenomena falls into the second of these classes. Figure C2 shows the various factors contributing to each type of mechanical erosion.

Surface erosion is caused by particle abrasion or the action of surface shears. The abrasive particles may come from the upstream products of ablation, or (in the case of nozzles for solid propellant rocket motors), from unburned constituents of the grain. These particles impinge on the surface, causing additional char material to be removed. Erosion through the action of surface shears is due to the viscous boundary layer acting upon the rough surface of char, tending to "scrub" off surface material. It should be noted that chemical erosion of the surface may be aggravated by increasing stress levels (the strain energy stored) in the material. Stress corrosion may also be important for some of the materials which are considered for ablation purposes.

Spallation, the mechanism through which material is removed in depth, is the primary concern of this Appendix. The factors contributing to material spallation in an ablation environment are manyfold and are listed here in two categories; those producing stresses and those affecting the failure criteria. Phenomena leading to internal stresses are the flow of pyrolysis gases through the porous char, thermal gradients in the material, surface shears, and inertia forces. Failure criteria for the char is influenced by basic material strength, and by the filler (reinforcement) strength and orientation.

Aggravating all the factors mentioned previously is the dynamic environment in which the char operates. This dynamic environment is due to the acoustic excitation from the boundary layer and the combustion processes.

PREVIOUS EFFORT

Thermal and chemical aspects of ablation have been studied extensively, both theoretically and experimentally. The structural aspects of ablation, such as mechanical removal of char material, although observed experimentally, has not been pursued theoretically to any great extent.

Experimental observations of mechanical erosion of char material are well documented (refs. 7 to 11). Of particular interest is the quantitative work done at NASA-Ames (ref. 8) with a typical organic charring ablator, low density (microballooned) phenolic nylon. The ablation behavior of this material was evaluated in high velocity streams of arc heated air, nitrogen and argon. The influence of chemical reactions on char removal was determined by the difference in response in the air and in the chemically inert nitrogen and argon streams. The lack* of a chemical erosion mechanism in the nitrogen and argon streams leads to the conclusion that a significant portion of the mass loss is due to mechanical means. Observations of spallation have also been made for the resin impregnated porous ceramics in certain simulation facilities. Strauss (ref. 11) reports that spallation of a phenolic resin impregnated porous zirconia was found in a high mass flow, high temperature gas stream.

Previous theoretical work on mechanical erosion is documented in references 12 to 15. In the study reported by Dhanak, the only contributing factor to the erosion mechanism considered is the surface shear. The analysis assumes a smooth erosion of the surface with no removal of finite pieces of material as in the spallation process. The theoretical study consists of a dimensionalless analysis (using the Buckingham π Theorem) and results in relations between erosion rate and a modified Reynolds number. The stress distribution in the char is not evaluated, rather it is postulated that mechanical loss of material occurs when the local aerodynamic surface shear stress exceeds the ultimate shear strength of the material.

Scala and Gilbert (ref. 13) included some aspects of the mechanical erosion of the char in a comprehensive formulation of the ablation behavior of char forming plastics. The stresses due to flow of pyrolysis gases through the porous char were determined from an approximate equation based on the one-dimensional equilibrium considerations. An estimate of the thermal stresses was obtained for the case of temperature independent material properties. Mechanical failure and removal of material were assumed to occur when the uniaxial strength of the char is equal to the combined pressure and thermal stresses in the thickness direction.

Menkes (ref. 14) presented a theory to describe the structural behavior of the porous char layer of a charring ablator. The effects of variable temperature, pressure and porosity were considered in determining the stress distribution for an axisymmetrically heated circular cylinder.

* C-N reactions become important at elevated temperatures (see ref. 4).

Mathieu (ref. 15) recently presented an improved formulation for the transient thermal response and ablation performance of charring ablators. Two mechanisms are considered as possible contributors to the mechanical erosion. The first mechanism considers the pressure stresses generated by the flow of pyrolysis gases through the porous char.

METHODS OF ANALYSIS

The structural analysis methods presented here are applicable to any heat protection system in which transpiration cooling (passive or active) is realized by the flow of gases through a porous solid. Examples of systems which use passive transpiration cooling are the organic plastics (modified epoxies, phenolics, melamines) which react to depth to form a porous, carbonaceous char. Methods developed here may be applied to the composite materials also, such as the refractory reinforced plastics (graphite phenolic, phenolic carbon) and the resin impregnated porous ceramics (phenolic filled porous zirconia).

These heat protection systems all possess common characteristics which lead to internal stresses and the possibility of spallation failure. These characteristics are the flow of gases through a porous solid, the presence of thermal gradients, and an external shear force applied to the exposed surface. The methods available for predicting the stresses in such a system are based on the principles of mechanics. In particular, the approach adopted here is based on the linear uncoupled quasi-static theory of thermoelasticity as presented by Boley and Weiner (ref. 16) and on elasticity theory for porous media as presented by Biot (ref. 17).

Thermoelasticity of Porous Media

The fundamental equations from the linear uncoupled quasi-static theory of thermoelasticity for a porous solid are the equilibrium equations, the strain-displacement relations, and the stress-strain relations.

Equilibrium

$$\sigma_{i,j} + f_i = (p \varpi)'_i \quad (1)$$

Strain-displacement

$$\epsilon_{ij} = 1/2 \left(u_{i,j} + u_{j,i} \right) \quad (2)$$

Stress-strain

$$\sigma_{ij} = \delta_{ij} \tau + \epsilon_{RR} + 2 \mu \epsilon_{ij} - \delta_{ij} M T \quad (3)$$

The equilibrium equations (1) are the equations of motion of Newtonian mechanics and as such are applicable to any type of material or process. The body forces (f_i) do not contain

inertia terms due to the quasi-static restriction, and thus, no time derivatives appear explicitly in these equations. If the boundary conditions do not involve time derivatives, then the time t enters the problem as a parameter rather than an independent variable. The effect of internal pressure and porosity is reflected in the term $(p \varphi)$. With the proper definition of stress, the equilibrium equation is the only place, aside from the boundary conditions, where porosity effects enter.

Since the strain-displacement relations (2) are purely geometrical or kinematical in nature, they are applicable to any material or process. However, these relations (2) are restricted to small displacements (or more properly small displacement gradients). These relations define the small strain tensor of linear elasticity where the displacement of a material particle is given by a vector $u_i(x_1, x_2, x_3, t)$. The strain components of the fluid or gas contained within the pores of the solid material are written as (ref. 16)

$$E_{ij} = 1/2 \left(U_{y,j} + U_{j,i} \right) \quad (4)$$

where $U_i(x_1, x_2, x_3, t)$ is the vector displacement of a fluid particle.

It is the constitutive relations which determine the specific type of material we are dealing with. For linear thermoelasticity, these are the stress-strain relations show by equation (3). These stress-strain relations define a linear elastic isotropic media with thermal strains $\epsilon_{th} = \delta_{ij} \alpha T$. Any coupling in the stress-strain relations between the porous solid and the contained gas is assumed to be negligibly small (see Biot, refs. 17, 18) for a formulation which includes this coupling. With these equations, the char (and the virgin material) is considered to be an elastic, isotropic, nonhomogeneous porous material.

In the following sections, the solution of the field equations (1, 2, 3) is considered for two particular geometries, a thick composite cylinder and a thin conical shell.

In the first of these approaches a thick composite cylinder is considered to be subjected to axisymmetric temperature, pressure, and porosity distributions. A two-dimensional elasticity formulation based on the assumptions of generalized plain strain is considered, and it is shown that a single governing differential equation is sufficient to determine the stress distribution.

For the second approach a thin conical shell is considered to be subjected to axisymmetric temperature and surface shear distributions. The usual assumptions of thin shell theory are involved, and a set of two governing differential equations is obtained (modified Reissner-Meissner equations) for the stresses.

Thermal stresses are obtained directly from both of these approaches. The combined stresses, which are due to thermal, pressure-porosity, and surface shear stresses, are obtained by superposition of solutions from these two methods. This superposition is valid within the realm of linear elasticity, and for configurations such as small angle cones for which the cylinder solution is approximately valid.

Thick Cylinder

The geometry of a thick, hollow cylinder (figure C3) is a useful model for analytical investigations of the structural behavior of charring ablators. This geometry is, for the case of an external char layer, an idealization of certain types of plug nozzles, and some types of ablation test models. For the case of an internal char layer, this geometry simulates the test model in certain types of ablation simulation facilities, the combustion chamber of most propulsion systems, and also is an approximation to the throat of a space rocket nozzle.

Large temperature gradients, which are invariably present in such geometries under operating conditions, invalidate the assumption of material homogeneity. This is caused by the strong temperature dependence of material properties, which leads to space dependent properties for the structural analysis.

Several previous investigations (refs. 19 to 22) are available which consider temperature dependent properties in a cylinder. Baltrukonis (ref. 19) has given a very general formulation in which the properties E (modulus), ν (Poisson ratio), and α (thermal expansion) are taken to be temperature dependent for a cylinder under plane strain ($\epsilon_{zz} = 0$). Solution of the resulting governing differential equation is performed by numerical methods with a digital computer. Several approximate (temperature independent) formulations amenable to closed form solution, are then compared with the numerical solution.

Hilton (ref. 21) considered the shear modulus G and the thermal expansion α to be temperature dependent for a cylinder under plane strain ($\epsilon_{zz} = 0$) or constant strain (with $F_z = 0$). However, Poisson's ratio was assumed to have a constant value of $1/2$ (i. e., an incompressible material), thus, allowing a closed form solution.

Heap (ref. 21) considered only the thermal expansion α to be temperature dependent for a cylinder under plane strain. Mahig (ref. 22) allowed E to be space dependent and obtained approximate solutions by a perturbation technique.

These investigations are restricted to cylinders under plane strain (except ref. 20 as mentioned previously) and to single layer cylinders. Although not explicitly mentioned, ref. 22 is readily extended to multi-layer cylinders. The present analysis is applicable to a multi-layer cylinder composed of different materials and subjected to an arbitrary axial force (i. e., generalized plain strain since $\epsilon_{zz} = \text{const.}$).

For the cylindrical body of figure 3 with an axisymmetric pressure, porosity, and temperature distribution, the equilibrium equation (1) becomes:

$$\sigma_r' + \left(\sigma_r - \sigma_\theta \right) / r = (P \omega)' \quad (5)$$

where the prime implies differentiation with respect to the radius (r). Under these conditions, the strain-displacement relations (2) become:

$$\epsilon_r = u' \quad (6)$$

$$\epsilon_\theta = u/r \quad (7)$$

with the additional assumption of generalized plane strain, the remaining strain component is:

$$\epsilon_z = \epsilon_o \quad (\text{constant}) \quad (8)$$

Now the compatibility equation is obtained by differentiating equation (5) and substituting into equation (6):

$$\epsilon_r - \left(r \epsilon_\theta \right)' = 0 \quad (9)$$

The stress-strain relations (3) for generalized plane strain become:

$$\begin{aligned} \epsilon_r &= \left(\frac{1+\nu}{E} \right) \left[(1-\nu) \sigma_r - \nu \sigma_\theta \right] - \nu \epsilon_o + \alpha T \\ \epsilon_\theta &= \left(\frac{1+\nu}{E} \right) \left[(1-\nu) \sigma_\theta - \nu \sigma_r \right] - \nu \epsilon_o + \alpha T \end{aligned} \quad (10)$$

Equations 5, 9 and 10 are the four governing equations in terms of the unknowns σ_r , σ_θ , ϵ_r , ϵ_θ .

By suitable elimination of the unknowns σ_θ , ϵ_r , ϵ_θ , the governing differential equation in terms of σ_r may be obtained:

$$Q \sigma_r = F_1(P_o) + F_2(\alpha T) \quad (11)$$

where Q is the second order ordinary differential operator with variable coefficients

$$Q(\) = (\)'' + \left[\frac{3}{r} + E(E-1)' \right] (\)' + (E^{-1})' \left[\frac{E(1-2\nu)}{r(1-\nu)} \right] (\)$$

and the "forcing functions" due to pressure, porosity and thermal expansion are

$$F_1(P_o) = (P_o)'' + \left[E(E^{-1})' + \frac{2+\nu}{r(1-\nu)} \right] (P_o)'$$

$$F_2(\alpha T) = \frac{-E}{r(1-\nu)} (\alpha T)'$$

Thin Conical Shell

One of the parameters affecting the structural behavior of the char and influencing the mechanical erosion is the viscous aerodynamic shear acting at the surface. As shown in figure C2 this surface shear may contribute to mechanical erosion through the surface erosion mechanism or through the spallation mechanism. The present section is devoted to formulating a theory capable of predicting the stresses due to surface shear which influence the spallation mechanism.

The approach used to determine these stresses is based on the shell equations presented in refs. 23 through 26. The equations for small deformations of thin elastic shells of revolution, due to E. Reissner (ref. 23), are modified by DeSilva in ref. 24 to include thermo-elastic effects. In ref. 25 Naghdi has shown the influence of surface shears in the stress-strain relations. In ref. 26, McDonough has included both effects for monotropic materials. However, these theories are restricted to the homogeneous case (constant modulus E). In the present report, the equations are generalized for the inhomogeneous case where E is considered as variable, but Poisson's ratio is still kept as constant..

General Shell Equations

The shell equations presented here may be derived directly from the three dimensional elasticity equations (1, 2, 3). An example of such a derivation is presented in ref. 26. The shell compatibility and equilibrium equations obtained are:

Compatibility

$$r' \epsilon_{\xi}^0 = \left(r \epsilon_{\theta}^0 \right)' - Z' \left(2 \epsilon_{\xi}^0 \zeta - \beta \right) \quad (14)$$

Equilibrium

$$(rV)' = - r \alpha P_V$$

$$(rH)' - \bar{\alpha} N_{\theta} = - r \bar{\alpha} P_H$$

$$\left(rM_{\xi} \right)' - r' M_{\theta} - \bar{\alpha} (rH) \sin \varphi + \bar{\alpha} (rV) \cos \varphi = \bar{\alpha} r d_1 \tau^+ \quad (15)$$

These equations apply to a general shell of revolution, figure C4 whose reference surface is described by the parametric equations:

$$r = r(\xi)$$

$$z = z(\xi)$$

The usual stress-strain relations employed in the classical theory of shells are for homogeneous shells, that is, constant material properties through the thickness of the shell. Thus, when transverse shear (Q) and surface shear (τ^+) are considered in the expression for the transverse shear stress in the homogeneous shell becomes (ref. 25):

$$\sigma_{\xi \zeta} = \frac{3}{2h} Q \left[1 - \left(\frac{\zeta}{h/2} \right)^2 \right] - \frac{1}{4} \tau^+ \left[1 - 2 \left(\frac{\zeta}{h/2} \right) - 3 \left(\frac{\zeta}{h/2} \right)^2 \right] \quad (16)$$

The shell stress-strain relation in terms of the shear stress resultant Q may then be obtained from the stress-displacement relation:

$$\sigma_{\xi \zeta} = G \left[- \frac{u_o}{r_{\xi}} + \beta + \frac{1}{\alpha} w_o' \right] \quad (17)$$

by multiplying eq. (17) by $\left[1 - \left(\frac{\zeta}{h/2} \right)^2 \right]$, substituting $\sigma_{\xi \zeta}$ from eq. (16) into eq. (17) and integrating through the thickness:

$$Q = \frac{5}{6} h G \left[- \frac{u_o}{r_{\xi}} + \beta + \frac{1}{\alpha} w_o' \right] + \frac{1}{6} \left(\frac{h}{2} \right) \tau^+ \quad (18)$$

This procedure for obtaining the shear stress-strain relation is followed since it simulates the algebraic and integration processes involved in the variational approach (ref. 25) for arriving at the shell stress-strain relations.

For the inhomogeneous case considered here, the expression for the transverse shear stress analogous to eq. (16) is obtained by assuming the shear strain may be represented by a quadratic function:

$$\frac{\sigma_{\xi \zeta}}{G} = \frac{Q/h}{G_{AVE}} f_1(\zeta) + \frac{\tau^+}{G^+} f_2(\zeta) \quad (19)$$

where

$$f_1(\zeta) = a_o + a_1 \zeta + a_2 \zeta^2$$

$$f_2(\zeta) = b_o + b_1 \zeta + b_2 \zeta^2$$

$$G_{AVE} = \int G d\zeta / h$$

$$G^+ = G @ \zeta = d_1$$

The function $f_1 (\zeta)$ is evaluated by using the conditions:

$$a) \quad f_1 = 0 \quad @ \quad \zeta = d_1$$

$$b) \quad f_1 = 0 \quad @ \quad \zeta = -d_2$$

$$c) \quad \int \sigma_{\xi \zeta} d\zeta = Q$$

The function $f_2 (\zeta)$ is evaluated by using the conditions:

$$a) \quad f_2 = 1 \quad @ \quad \zeta = d_1$$

$$b) \quad f_2 = 0 \quad @ \quad \zeta = -d_2$$

$$c) \quad \int \sigma_{\xi \zeta} d\zeta = 0$$

Thus,

$$f_1 (\zeta) = (1-\gamma) \left[1 + \left(\frac{d_1 - d_2}{d_1 d_2} \right) \zeta - \frac{\zeta^2}{d_1 d_2} \right] \quad (20)$$

$$f_2 (\zeta) = \left\{ \frac{\gamma d_2}{h} + \left[\gamma + \frac{d_2}{d_1} (1-\gamma) \right] \left(\frac{\zeta}{h} \right) + \left(\frac{1-\gamma}{d_1/h} \right) \left(\frac{\zeta}{h} \right)^2 \right\} \quad (21)$$

where

$$\gamma = \frac{1}{1 - \frac{d_1 d_2 C}{D (1-\nu^2)}} \quad (22)$$

Now the stress-strain relations are obtained by multiplying eq. (17) by $f_1 (\zeta)$:

$$\sigma_{\xi \zeta} f_1 (\zeta) = G f_1 (\zeta) \left[-\frac{u_o}{r_{\xi}} + \beta + \frac{1}{\alpha} w_o' \right] \quad (23)$$

Then substituting for $\sigma_{\xi \zeta}$ (from eq. (19) into eq. (23) and integrating through the thickness of the shell, gives:

$$Q = H_{\xi} \left[-\frac{u_o}{r_{\xi}} + \beta + \frac{1}{\alpha} w_o' \right] - H_{\tau} \tau^+ \quad (24)$$

where the transverse shear stiffness H_{ξ} (shown in figure 5) is

$$H_{\xi} = \frac{\left(\frac{h E_{AVE}}{2(1+\nu)} \right) \left[d_1 d_2 + \frac{1}{2} (d_1 - d_2)^2 - \frac{1}{3} \left(\frac{d_1^3 + d_2^3}{d_1 + d_2} \right) \right]}{(1-\gamma) \left[\left(\frac{d_1 d_2}{d_1 - d_2} \right)^2 + d_1 d_2 + \frac{1}{3} \left\{ 1 - \frac{2d_1 d_2}{(d_1 - d_2)^2} \right\} \left(\frac{d_1^3 + d_2^3}{d_1 + d_2} \right) - \frac{1}{2} (d_1^2 + d_2^2) + \frac{1}{5} \frac{(d_1^5 + d_2^5)}{(d_1 - d_2)^2 (d_1 + d_2)} \right]} \quad (25)$$

which reduces to $\frac{5}{6} Gh$ in the homogeneous case (ref. 25).

The stiffness H_{τ} is:

$$\begin{aligned} H_{\tau} = & \frac{hG_{AVE}}{G^+} \left[\frac{(d_1 d_2)^2}{(d_1 + d_2)(d_1 - d_2)^2} \left(\frac{\gamma d_2}{h} \right) (d_1 + d_2) + \left\{ \frac{\gamma}{h} + \frac{d_2}{d_1} \frac{(1-\gamma)}{h} + \right. \right. \\ & + \left. \left. \frac{(d_1 - d_2)}{d_1 d_2} \right\} \frac{1}{2} (d_1^2 - d_2^2) + \left\{ \frac{(1-\gamma)}{d_1 h} + \left(\frac{d_1 - d_2}{d_1 d_2} \right) \left(\frac{\gamma}{h} + \frac{d_2}{d_1} \frac{(1-\gamma)}{h} \right) - \right. \right. \\ & - \left. \frac{\gamma}{d_1 h} \right\} \frac{1}{3} (d_1^3 - d_2^3) + \left\{ \left(\frac{d_1 - d_2}{d_1 d_2} \right) \left(\frac{(1-\gamma)}{d_1 h} \right) - \frac{1}{d_1 d_2} \left(\frac{\gamma}{h} + \frac{d_2}{d_1} \frac{(1-\gamma)}{h} \right) \right\} \frac{1}{4} (d_1^4 - d_2^4) - \\ & - \left\{ \left(\frac{1}{d_1 d_2} \right) \left(\frac{(1-\gamma)}{d_1 h} \right) \right\} \frac{1}{5} (d_1^5 + d_2^5) \left. \right] / \left[(1-\gamma) \left[\left(\frac{d_1 d_2}{d_1 - d_2} \right)^2 + d_1 d_2 + \right. \right. \\ & + \left. \left. \frac{1}{3} \left\{ 1 - \frac{2d_1 d_2}{(d_1 - d_2)^2} \right\} \left(\frac{d_1^3 + d_2^3}{d_1 + d_2} \right) - \frac{1}{2} (d_1^2 + d_2^2) + \frac{1}{5} \frac{(d_1^5 + d_2^5)}{(d_1 - d_2)^2 (d_1 + d_2)} \right] \right] \quad (26) \end{aligned}$$

which reduces to $-\frac{h}{12}$ in the homogeneous case (ref. 25).

The remaining shell stress-strain relations may be obtained directly and are recorded here as:

$$\begin{aligned}
 N &= \frac{C}{1-\nu^2} \left[\frac{1}{\alpha} \left(u_o' + \nu \frac{r'}{r} u_o \right) + \left(\frac{1}{r_\xi} + \frac{1}{r_\theta} \right) w_o \right] - N_\tau \\
 N_\theta &= \frac{C}{1-\nu^2} \left[\frac{1}{\alpha} \left(u_o' + \frac{r'}{r} U_o \right) + \left(\frac{\nu}{r_\xi} + \frac{1}{r_\theta} \right) w_o \right] - N_\tau \\
 M_\xi &= D \left[\frac{1}{\alpha} \left(\beta' + \nu \frac{r'}{r} \beta \right) \right] - M_T \\
 M_\theta &= D \left[\frac{1}{\alpha} \left(\nu \beta' + \frac{r'}{r} \beta \right) \right] - M_T
 \end{aligned} \tag{27}$$

where

$$\begin{aligned}
 C &= \int E \, d\zeta \\
 D &= \frac{1}{1-\nu^2} \int E \, \zeta^2 \, d\zeta \\
 N_T &= \frac{1}{1-\nu} \int E \, \alpha \, T \, d\zeta \\
 M_T &= \frac{1}{1-\nu} \int E \, \alpha \, T \, \zeta \, d\zeta
 \end{aligned} \tag{28}$$

The compatibility, equilibrium, and constitutive equations may now be combined into two governing differential equations in the basic variables (β) and (rH). Upon proper elimination, these two second order differential equations are obtained:

$$\mathcal{L}_1 [\beta] - \left(\frac{Z\bar{\alpha}}{rD} \right) (rH) = f_{11} + f_{12} + f_{13} \quad (29)$$

$$\mathcal{L}_2 [rH] + \left(\frac{Z'C\bar{\alpha}}{r} \right) \beta = f_{21} + f_{22} + f_{23} \quad (30)$$

where:

$$\mathcal{L}_1 \left[\begin{matrix} \\ \end{matrix} \right] = \left[\begin{matrix} \\ \end{matrix} \right]'' + \frac{(r/\bar{\alpha})'}{(r/\bar{\alpha})} \left[\begin{matrix} \\ \end{matrix} \right]' + \left\{ \frac{(r'/\bar{\alpha})'}{(r'/\bar{\alpha})} v - \left(\frac{r'}{r} \right)^2 \right\} \left[\begin{matrix} \\ \end{matrix} \right]$$

$$\mathcal{L}_2 \left[\begin{matrix} \\ \end{matrix} \right] = \left[\begin{matrix} \\ \end{matrix} \right]'' + \frac{(r/\bar{\alpha})'}{(r/\bar{\alpha})} \left[\begin{matrix} \\ \end{matrix} \right]' - \left(\frac{r'}{r} \right)^2 + v \frac{(r'/\bar{\alpha})'}{(r/\bar{\alpha})} + \left(\frac{z'}{r} \right)^2 \frac{C}{H_{\xi}} \left[\begin{matrix} \\ \end{matrix} \right]$$

$$f_{11} = - \frac{r' \bar{\alpha}}{r D} (rV)$$

$$f_{12} = \frac{\bar{\alpha}}{D} M'_T$$

$$f_{13} = - \frac{\bar{\alpha}^2}{D} d_1 \tau^+$$

$$f_{21} = \left\{ v \frac{(z'/\bar{\alpha})'}{(r/\bar{\alpha})} + \frac{z'r'}{r^2} \left(1 - \frac{C}{H_{\xi}} \right) \right\} (rV) + v \frac{z'}{r} (rV)' - \frac{\left(r'^2 P_H \right)' + v r r' P_u}{(r/\bar{\alpha})}$$

$$f_{22} = - \bar{\alpha} (1-v) N'_T$$

$$f_{23} = \frac{Z'C}{(r/\bar{\alpha})} \left(\frac{H_{\tau}}{H_{\xi}} \right) \tau^+$$

Solution for cone

The governing differential equations for the general shell (eq. 29) and (30) are now specialized to the case of a conical shell. The parametric equations of the reference surface of a conical shell (figure C6) may be written as:

$$r = S \sin \omega$$

$$z = S \cos \omega$$

Now $dS = d\xi$ thus $\bar{\alpha} = 1$ and

$$r' = \sin \omega \quad z' = \cos \omega$$

where primes now denote differentiation with respect to S .

Inserting these parameters into equations (29) and (30) the governing equations for the cone are obtained:

$$L_1 \begin{bmatrix} \beta \end{bmatrix} + \Psi(rH) = F_{11} + F_{12} + F_{13} \quad (31)$$

$$L_2 \begin{bmatrix} (rH) \end{bmatrix} + \theta \beta = F_{21} + F_{22} + F_{23} \quad (32)$$

where

$$L_1 \begin{bmatrix} \quad \end{bmatrix} = \begin{bmatrix} \quad \end{bmatrix}'' + \frac{1}{S} \begin{bmatrix} \quad \end{bmatrix}' - \frac{1}{S^2} \begin{bmatrix} \quad \end{bmatrix}$$

$$L_2 \begin{bmatrix} \quad \end{bmatrix} = \begin{bmatrix} \quad \end{bmatrix}'' + \frac{1}{S} \begin{bmatrix} \quad \end{bmatrix}' - \left\{ \frac{1}{S^2} + \frac{C}{H_\xi} \left(\frac{1}{r^2} - \frac{1}{S^2} \right) \right\} \begin{bmatrix} \quad \end{bmatrix}$$

$$\Psi = -\cos \omega / rD$$

$$\theta = C \cos \omega / r$$

$$F_{11} = \frac{-\sin \omega}{rD} (rV)$$

$$F_{21} = -\frac{1}{r^2} \left(r^2 P_H \right)' + \frac{\nu}{r} P_H \sin \omega + \frac{1}{2} \left(1 - \frac{C}{H_\xi} \right) \sin \omega \cos \omega (rV) + \frac{\nu}{r} \cos \omega (rV)'$$

$$F_{12} = M'_T / D$$

$$F_{22} = - (1-\nu) N'_T$$

$$F_{13} = - d_1 \tau^+ / D$$

$$F_{23} = \frac{Z'C}{r} \quad \frac{H_\tau}{H_\xi} \tau^+$$

An approximate particular solution to these equations may be obtained by following the work of Hildebrand (ref. 27) and De Silva (ref. 24).

Let

$$\beta = \beta_1 + \beta_2 + \beta_3$$

$$(rH)_p = (rH)_1 + (rH)_2 + (rH)_3$$

where β_i and $(rH)_i$ refer to the particular solution for the forcing functions F_{1i} and F_{2i} .

Now β_i and $(rH)_i$ are represented by the sequences $\{\beta_i^{(n)}\}$ and $\{(rH)_i^{(n)}\}$. The convergence of these sequences has been demonstrated by Hildebrand for β_1 and $(rQ)_1$, and by De Silva for β_2 and $(rH)_2$ for the arbitrary shell of revolution. Their method of successive approximations is implemented by setting $\beta_i^{(0)} = 0$ in the equilibrium eq. (31) and thus obtaining $(rH)_i^{(0)}$ directly.

Then $(rH)_i^{(0)}$ is used in the compatibility eq. (32) to obtain $\beta_i^{(1)}$. This procedure is continued, resulting in the recurrence relations:

$$\begin{aligned} (rH)_i^{(n)} &= \frac{1}{\Psi} \left\{ F_{1i} - L_1 \left[\beta_i^{(n)} \right] \right\} \\ \beta_i^{(n)} &= \frac{1}{\theta} \left\{ F_{2i} - L_2 \left[(rH)_i^{(n-1)} \right] \right\} \\ \text{with } \beta_i^{(0)} &= 0 \end{aligned} \tag{33}$$

It may be shown that the successive approximations need be carried only to the point of evaluating $\beta_i^{(1)}$ and $(rH)_i^{(1)}$. This is consistent with assumptions of thin shell theory, and the restriction that distributed loadings may vary appreciably only over a distance comparable with the representative dimension of the shell (such as r).

For the case of negligible axial variation in T , p , and τ^+ , this method yields:

$$\beta_1 = \frac{(rV)}{C S \cos^2 \omega} - \frac{2}{C} \left[\frac{(1-\nu)}{\cos \omega} - \nu \tan^2 \omega \right] S \sin^2 \omega P$$

$$\beta_2 = 0 - \frac{\nu S}{C} \tan \omega \cos 2 \omega \tau^+$$

$$\beta_3 = \left[\left(\frac{H_\tau}{H_\xi} \right) + \frac{d_1}{H_\xi} \right] \tau^+$$

$$(rH)_1 = \left[1 - D/C (S \cos \omega)^2 \right] \tan \omega (rV)$$

$$(rH)_2 = 0$$

$$(rH)_3 = \left[S d_1 - \frac{D}{S} \left(\frac{H_\tau}{H_\xi} \right) - \frac{D}{S} \frac{d_1}{H_\xi} \right] \tan \omega (\tau^+)$$

The stress resultants are now determined from equations 15 and 27 which are written for the conical shell as:

$$(r_V) = \sin \omega \int_0^{\omega} S P_V dS$$

$$N_\theta = S P_H \sin \omega + (rH)'$$

$$N_s = \frac{(rH)}{S} + \frac{(rV)}{S \tan \omega}$$

$$Q = \frac{(rH)}{S \tan \omega} - \frac{(rV)}{S}$$

$$M_{\theta} = D \left[\nu \beta' + \frac{\beta}{S} \right] - M_T$$

$$M_S = D \left[\beta' + \nu \frac{\beta}{S} \right] - M_T$$

From these stress resultants, the stresses are found from: (ref. 28)

$$\sigma_S = \frac{E}{C} \left[N_S + N_T \right] + \frac{E \zeta}{D(1-\nu^2)} \left[M_S + M_T \right] - \frac{E \alpha T}{1-\nu}$$

$$\sigma_{\theta} = \frac{E}{C} \left[N_{\theta} + N_T \right] + \frac{E \zeta}{D(1-\nu^2)} \left[M_{\theta} + M_T \right] - \frac{E \alpha T}{1-\nu}$$

$$\sigma_{s\zeta} = \frac{E}{C} \left[Q \right] f_1(\zeta) + \frac{E}{E^+} \left[\tau^+ \right] f_2(\zeta)$$

where $f_1(\zeta)$ and $f_2(\zeta)$ are given by equations 20 and 21 and E^+ is E at $\zeta = d_1$.

Parametric Studies

The methods developed in the previous section enables one to predict the state of stress in the char and virgin material (treated as a continuum). These stresses (due to thermal gradients, pressure forces, and surface shears) must then be compared to an appropriate failure criteria in order to determine survival or failure of the char material. Before pursuing this matter further, it is worthwhile to inquire about some approximate analysis for prediction of the stresses. If such approximate analysis can be shown to give accurate answers in certain situations, then a considerable savings of effort may be realized.

Approximate Methods

A simplified analysis for the pressure stresses (stresses due to flow of pyrolysis gases through the porous char) and the thermal stresses are obtained by considering the semi-infinite slab of figure C1. The constraints of displacement are chose such that

$$u = u(x) \quad r = w = 0$$

The porous solid is subjected to the pressure and temperature distributions shown in figure C1, and the equations (1 and 2) of the quasi-static* uncoupled theory become:

*See ref (29) for an analysis which includes the inertia effects for thermal stresses in a semi-infinite slab with a moving boundary.

$$\sigma_{xx,x} = (P\phi)_{,x} \quad (34)$$

$$\epsilon_{xx} = u_{,x} \quad (35)$$

$$\sigma_{xx} = (\lambda + 2\mu) \epsilon_{xx} - mT \quad (36)$$

$$\sigma_{YY} = \sigma_{ZZ} = \lambda \epsilon_{xx} - mT \quad (37)$$

The remaining stresses and strains are zero:

$$\sigma_{xY} = \sigma_{YZ} = \sigma_{zx} = 0$$

$$\epsilon_{xY} = \epsilon_{YZ} = \epsilon_{zx} = \epsilon_{YY} = \epsilon_{ZZ} = 0$$

The boundary conditions for this problem are:

$$\sigma_{xx}(0) = -(1-\phi_0) P_0$$

$$\epsilon_{xx}(\infty) = 0$$

By integrating the one-dimensional equilibrium equation (34) and enforcing the boundary condition at $X = 0$, the σ_{xx} stress is found to be:

$$\sigma_{xx} = P\phi - P_0 \quad (38)$$

Note that only the pressure and porosity, and no thermal effects, appear in this equation.

The remaining stresses σ_{YY} and σ_{ZZ} are found from equations (36) and (37) to be:

$$\sigma_{YY} = \sigma_{ZZ} = mT \left(\frac{\lambda}{\lambda + 2\mu} - 1 \right) + \frac{\lambda (P\phi - P_0)}{\lambda + 2\mu} \quad (39)$$

Thus, these stresses contain both pressure, porosity, and thermal effects.

The expression for the pressure and porosity stresses given by equation (38) is quite simple and straightforward. However, it is strictly applicable to the plane slab only and must be used with caution for geometries which contain curvature. For large radius structures, such as large diameter nozzles, equation (38) gives a good estimate of the pressure and porosity stresses. But the utility of this equation becomes more limited as the curvature changes. Thus, it should not be used for small nozzles and cylindrical or conical ablation models. For these cases, the theory presented in the previous section must be applied. This theory includes the effect of temperature dependent material properties, the coupling between the in-plane stresses (σ_{YY} or σ_r) and stresses through the char thickness (σ_{xx} or σ_r), and accounts for composite or layered materials.

NOMENCLATURE

C	extensional stiffness $\int E d\zeta$
D	flexural stiffness
d_1, d_2	distance (fig. C4)
E	elastic modulus
e_{ij}	strain tensor in fluid
F	force
f_i	body forces
G	shear modulus
h	shell thickness
H	stress resultant (fig. C4)
$H_{\xi 1} H_T$	shear stiffness
m	$(3\lambda + \mu)\alpha$
M	moment
N	stress resultant
P	internal pore pressure
Q	transverse shear
r	radial coordinate
s	conical coordinate (fig. C6)
t	time
T	temperature difference from reference state
u_i	displacement vector of solid
v_i	displacement vector of fluid
V	stress resultant (fig. C4)

NOMENCLATURE (Cont'd)

x_i	cartesian coordinate
u, v, w	displacement
\dot{W}	mass loss through ablation
z	axial coordinate
β	rotation
$\bar{\alpha}$	scale factor
α	thermal expansion coefficient
δ_{ij}	Kronecker delta
ϵ_{ij}	strain tensor in solid
λ, μ	Lame's constants
ν	Poisson's ratio
σ_{ij}	stress tensor
φ	porosity
ω	cone angle
λ^+	surface shear

Subscripts

H	perpendicular to shell axis
o	at reference surface
r	radial
s	conical coordinate (fig. C6)
T	thermal
v	parallel to shell axis
x, y, z	coordinate

NOMENCLATURE (Cont'd)

ξ

meridional

θ

circumferential

ζ

normal to surface (thickness)

Superscripts

o

at reference surface (middle surface for a homogeneous shell)

APPENDIX C

REFERENCES

1. D. L. Schmidt, "Ablation of Plastics," ASD Tech. Rpt. No. 61-650, February , 1962.
2. S. Scala, "The Ablation of Graphite in Dissociated Air: Part I, Theory," GE-TIS-R62SD72, September, 1962.
3. N.S. Diaconis, P.D. Gorsuch and R.A. Sheridan, "The Ablation of Graphite in Dissociated Air: Part II, Experimental Investigation," GE-TIS-R62SD86, September, 1962.
4. S.M. Scala and L.M. Gilbert, "Aerothermochemical Behavior of Graphite at Elevated Temperatures," 16th Pacific Coast Regional Meeting of the American Ceramic Society, October, 1963.
5. K.M. Kratsch, L.F. Hearne and H.R. McChesney, "Thermal Performance of Heat Shield Composites During Planetary Entry," Presented at AIAA-NASA National Meeting, Palo Alto, California, September, 1963.
6. L.E. McAllister, J.C. Bolger, E.L. McCaffery - P.J. Roay and A.C. Walker, "Behavior of Pure and Reinforced Charring Polymers During Ablation under Hypervelocity Re-entry Conditions," Chemical Engineering Progress Symposium Series, Vol. 59, No. 40, pp. 17-32, 1963.
7. W.T. Barry and C.A. Gaulin, "A Study of Physical and Chemical Processes Accompanying Ablation of G.E. Century Resins," GE TIS-R62SD2, May, 1962.
8. N.S. Vojvodich and R.B. Pope, "An Investigation of the Effect of Gas Composition on the Ablation Behavior of a Charring Material, " AIAA Pre-print 63-465, AIAA Conference of Physics of Entry into Planetary Atmospheres, MIT, Cambridge Mass., August, 1963.
9. D.L. Robblines, "Thermal Erosion of Ablative Materials, " ASD-TR-61-307 (Aerojet General Corp.), April, 1962
10. D.L. Schmidt, "Behavior of Plastic Materials in Hyperthermal Environments," WADC Tech. Report 59-574, April, 1960.
11. E.L. Strauss, "Heat Transfer and Thermal Exposure Studies of Resin Impregnated Zirconia Foam," Transactions of the Eighth Symposium on Ballistic Missile and Space Tech., Vol. 1, pp. 311-337, October, 1963.
12. A.M. Dhanak, "A Theoretical Study of Mechanical Erosion from a Charred Surface in Boundary Layer Flows," AVCO RAD-7-TM-60-74, December, 1960.
13. S.M. Scala and L.M. Gilbert, "Thermal Degradation of a Char-Forming Plastic During Hypersonic Flight," ARS Journal, Vol. 32, No. 6, June, 1962.
14. E.G. Menkes, "Thermal and Pressure Stresses in a Porous Cylinder under Conditions of Generalized Plane Strain, with Application to Charring Ablators," GE Document No. 63SD589, May, 1963.

15. R.D. Mathier, "Theoretical Analysis for the Mechanical Spallation of a Typical Charring Ablator," GE TIS-R63SD53, December, 1963.
16. B.A. Boley and J.H. Weiner, "Theory of Thermal Stresses," John Wiley & Sons, New York, 1960.
17. M.A. Biot, "Theory of Elasticity and Consolidation for a Porous Anisotropic Solid," J. of Applied Physics, Vol. 26, No. 2, pp. 182-185, February 1955.
18. M.A. Biot, "General Theory of Three-Dimensional Consolidation," J. Of Applied Physics, Vol. 12, pp. 155-164, February, 1941.
19. J.H. Baltrukonis, "Comparison of Approximate Solutions of the Thermoelastic Problem of the Thick-Walled Tube," J. of the Aerospace Sciences, Vol. 26, No. 6, pp 329-334, June, 1959.
20. H.H. Hilton, "Thermal Stresses in Bodies Exhibiting Temperature-Dependent Elastic Properties," J. of Applied Mechanics, Vol. 19, pp. 350-354, September, 1952.
21. J.C. Heap, "Thermal Stresses in Concentrically Heated Hollow Cylinders, " American Society of Mechanical Engineers, Paper No. 62-WA-228, November, 1962.
22. J. Mahig, "Stresses in Nonhomogeneous Elastic Thick-Walled Cylinders," J. of Applied Mechanics, pp. 343-344, June, 1964.
23. E. Reissner, "On the Theory of Thin Elastic Shells," H. Reissner Anniversary Volume, pp. 231-247, Edwards, Ann Arbor, Michigan, 1949.
24. C.H. De Silva, "Thermal Stresses in the Bending of Ogival Shells," J. of the Aerospace Sciences, February, 1962.
25. P.M. Naghdi, "On the Theory of Thin Elastic Shells," Quarterly of Applied Mathematics, Vol. XIV, No. 4, 1957.
26. T.B. McDonough, "Monotropic Shell Theory: Theoretical Development," GE Doc. No. 64SD663, May, 1964.
27. F.B. Hildrebrand, "On Asymptotic Integration in Shell Theory," Proceedings of the Third Symposium in applied Mathematics, Vol. 3, pp. 53-66, McGraw-Hill Book Co., New York, 1950.
28. E.G. Menkes, "Thermoelastic Analysis of Beams, Plates, and Shells Including The Effect of Variable Material Properties:, Structural Mechanics TM-8156-11, August, 1962.

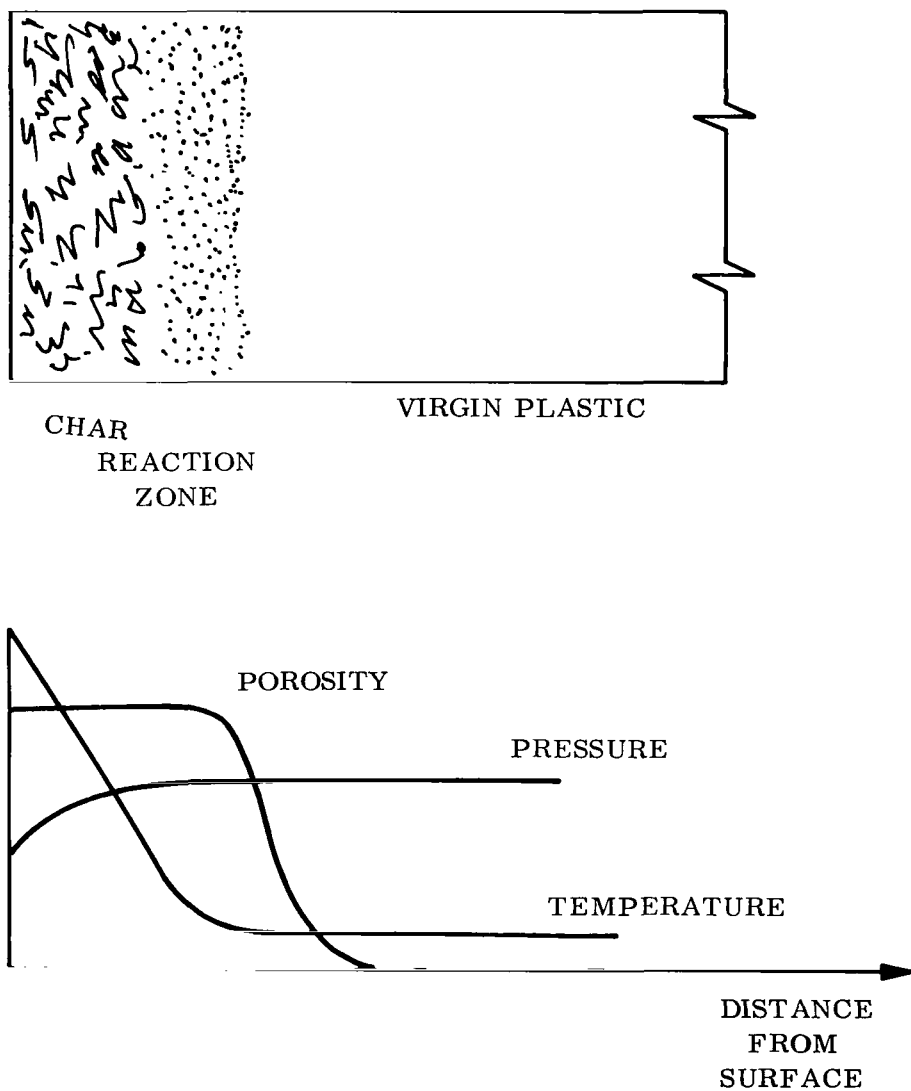


Figure C1. Characteristics of a Charring Ablator

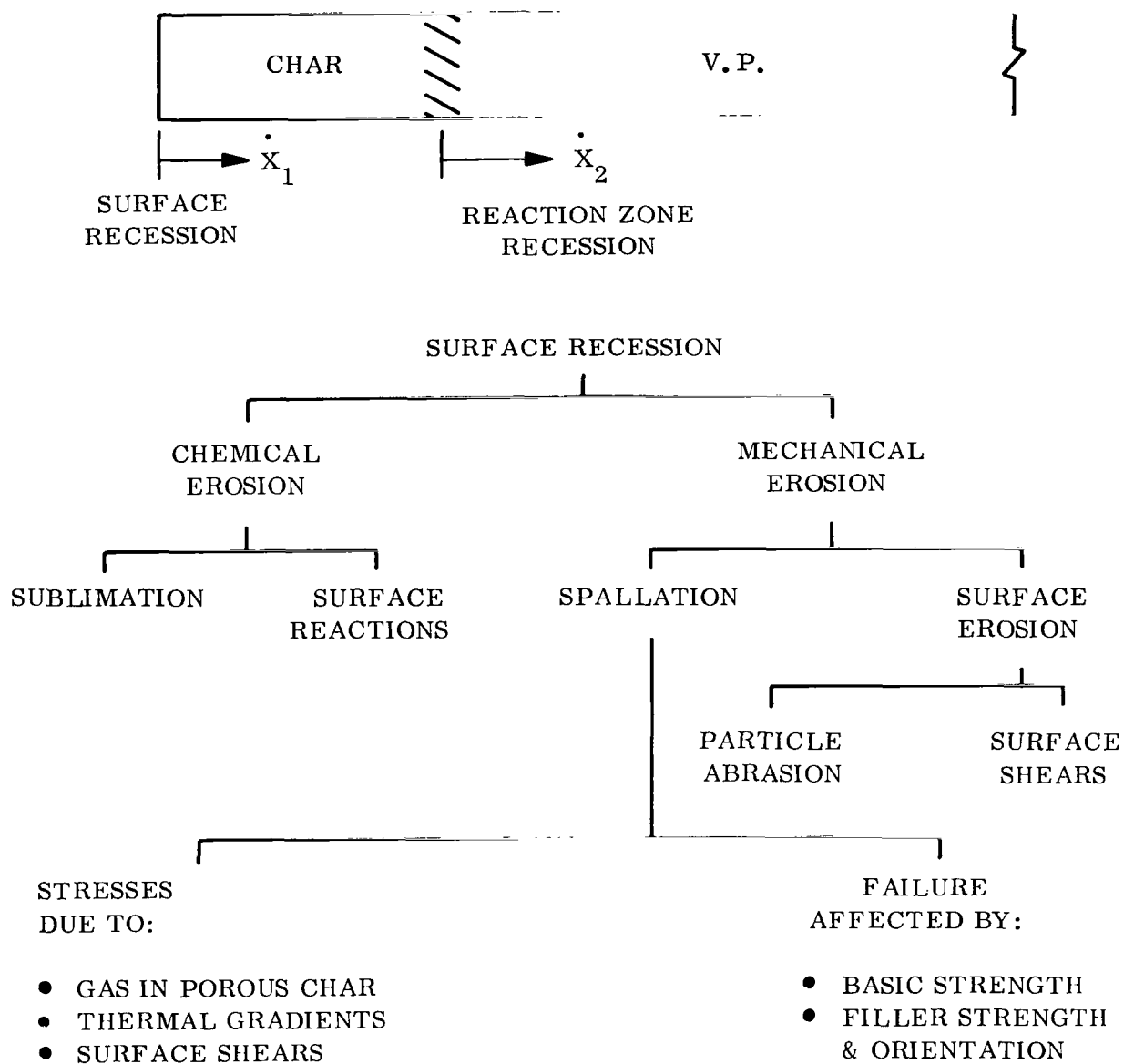
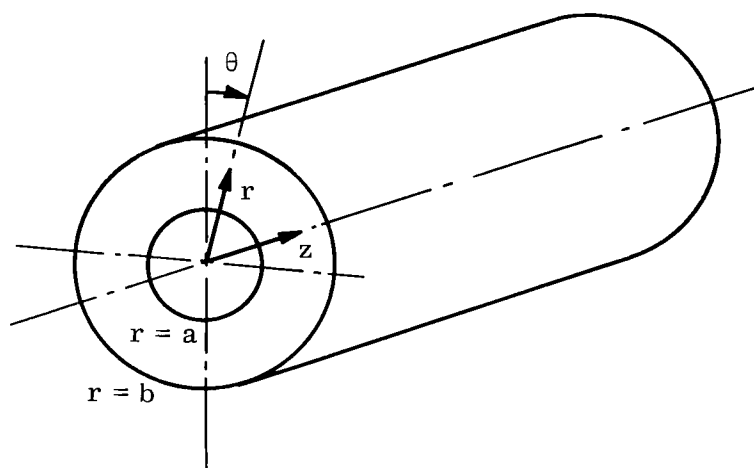
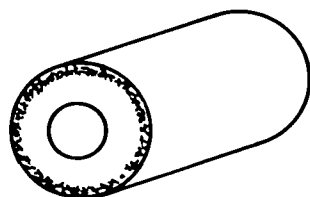


Figure C2. Mechanisms Contributing to the Surface Recession of Charring Ablators

C-24



EXTERNAL
CHAR LAYER



INTERNAL
CHAR LAYER

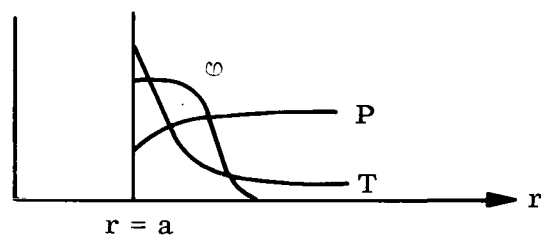
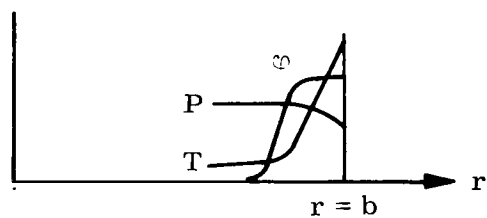
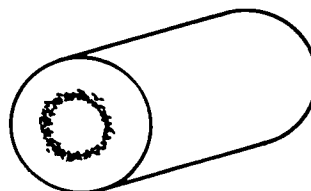
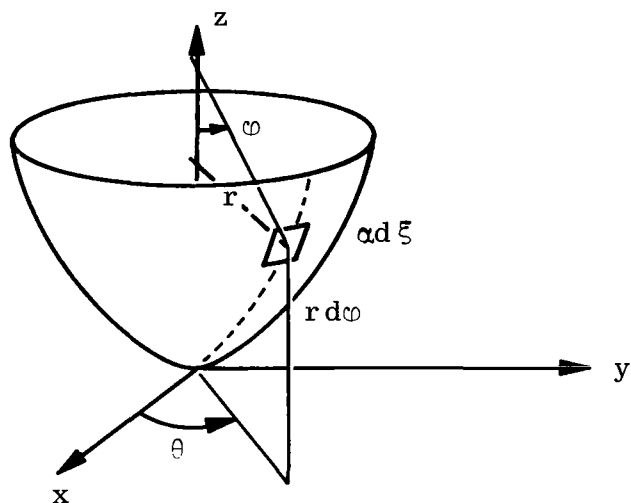
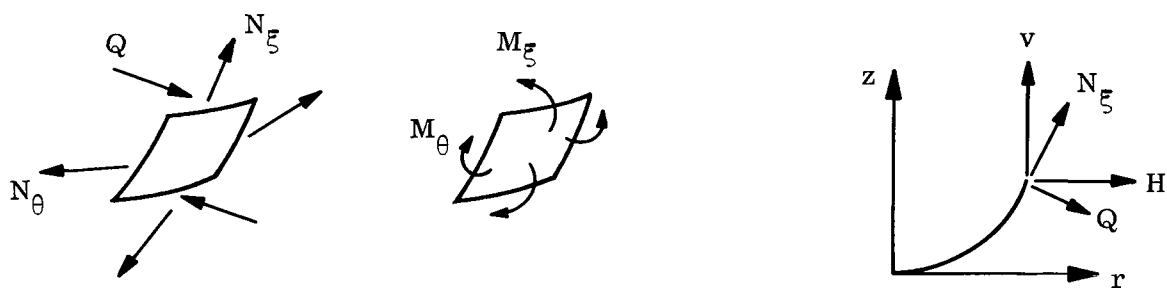


Figure C3. Thick Cylinder Geometry

(a) GEOMETRY



(b) STRESS RESULTANTS



(c) LOADING

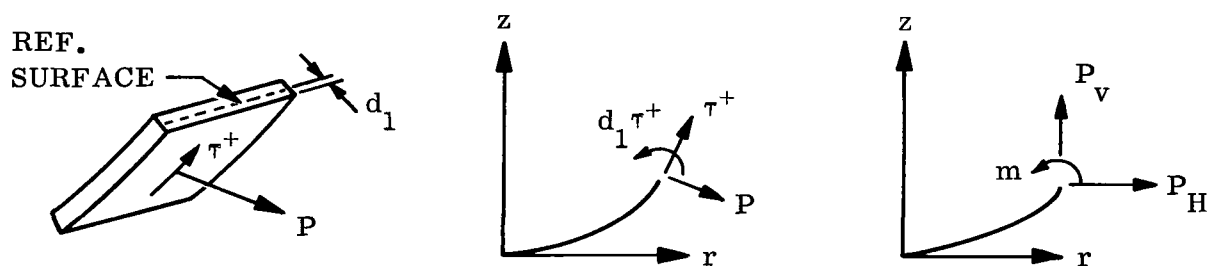


Figure C4. General Shell of Revolution

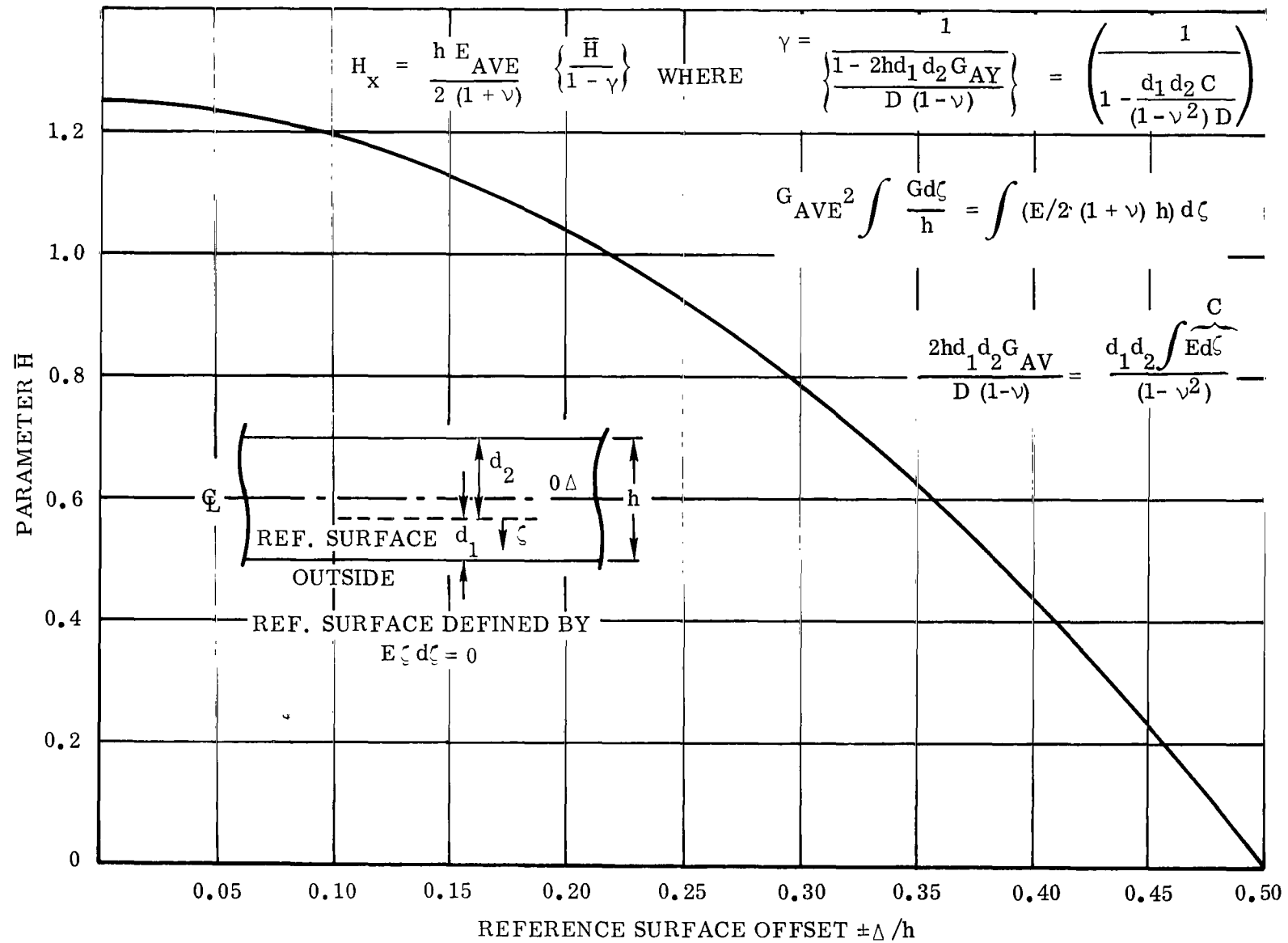
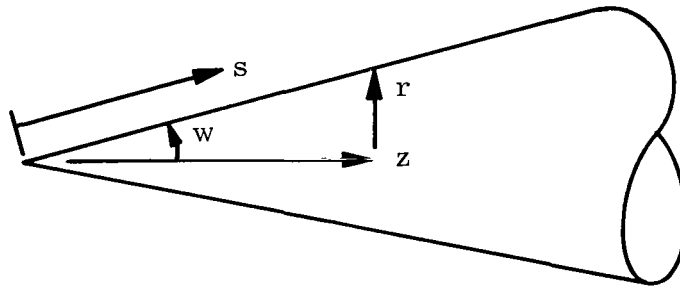


Figure C5. Shear Stiffness of an Inhomogeneous Shell

(a) GEOMETRY



(b) STRESSES

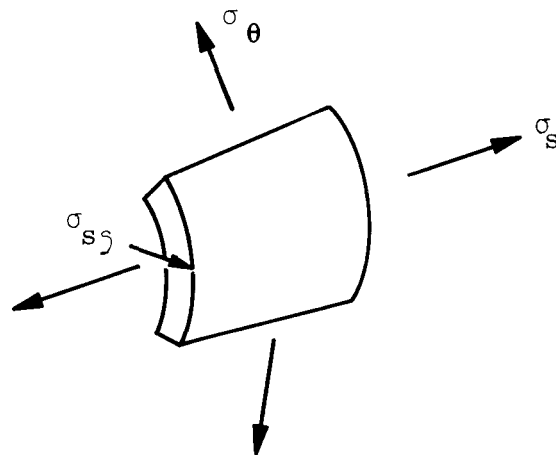


Figure C6. Conical Shell

APPENDIX D
PROGRAM STRUCTURE

This appendix is designed to be a guide for the programmer between Appendix B and the Fortran listing of the program itself. As a result, the manual is very general in its nature and does not contain any specific equations. This allows flexibility without tying the programmer down with modifying the write-up for numerous modifications.

It was decided to reference the equations in the Fortran program by the numbers used in the Appendix B since the numbers assigned to the general equations will not be changed.

Flow charts are generalized also, since ample comments are included within the Fortran program. This may require more effort on the part of a programmer familiarizing himself with the program, but then the results are retained longer.

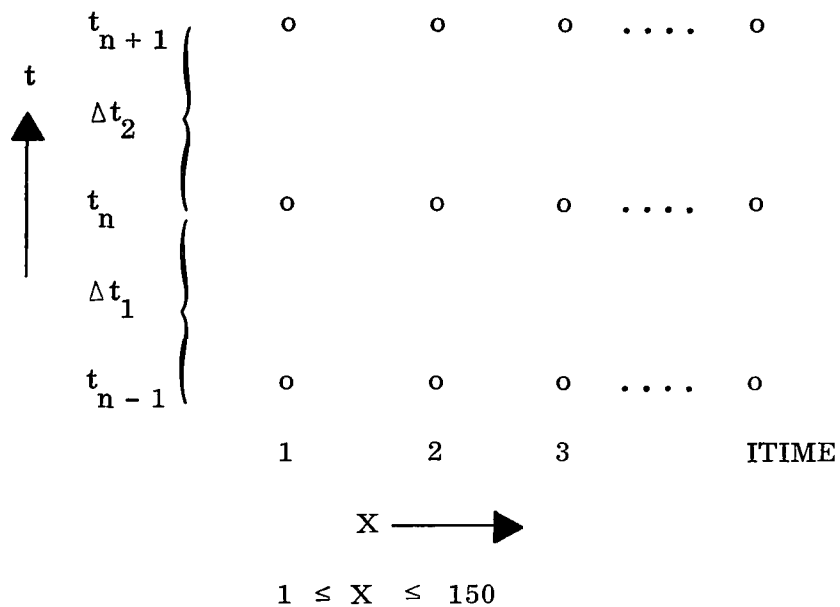
Point Counter Configuration

For the purposes of continuity and consistency in the programs, the following conventions have been used.

1. J is the layer counter. $1 \leq J \leq 10$
2. II is the point counter in the arrays (T, DENS, P) where more than one time step is saved.
3. MN is the point counter in the arrays (e.g. XLOC, ETASBX, ETASBT, ETC.) where only one time stop is saved.
4. JLAYER (J) is an array which gives the last interior point of the (J - 1) layer and where JLAYER91) = 0.
5. KONVAR(1) is the total number of points in the body. This is also referred to as ITIME.
6. KONVAR(2) is the time step counter (i.e. it is a one for the first time step and a two thereafter). This is also referred to as KTIME.

There are presently three arrays which need previously calculated values. These arrays with their dimension are T(450), DENS(450), P(450) or the temperature array, the solid density array and the gas density array. It was found to be convenient to store the previous time step values in the beginning of the array in question.

Let us now look at a chart to illustrate our point.



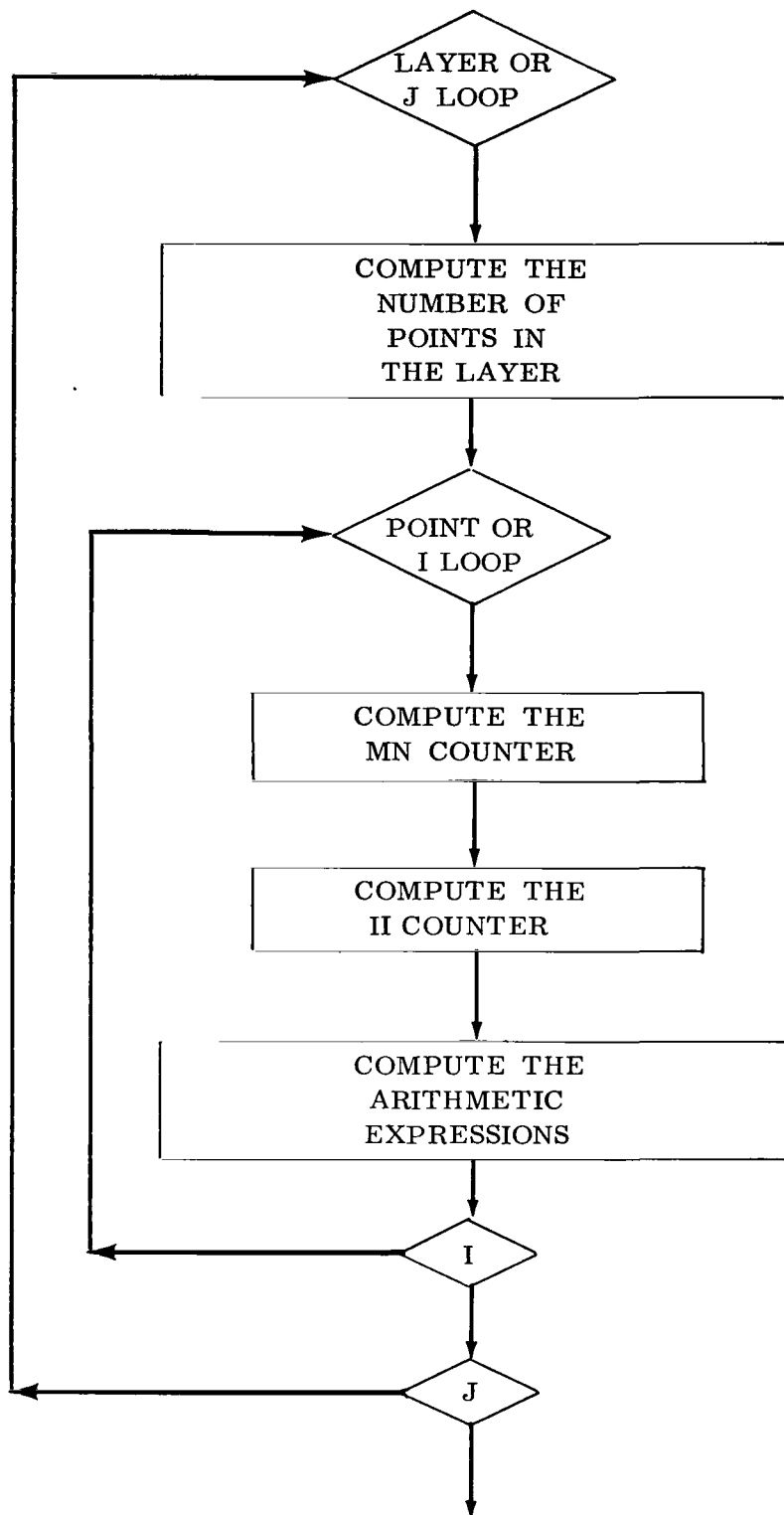
Since the set of points which we are solving are on the t_{R+1} level, we find that it is convenient to compute the Π counter by using the following formula:

$$\Pi = \text{KONVAR}(1) * \text{KONVAR}(6) + \text{MN}$$

MN is computed using the $\text{JLAYER}(J)$ array and the points in the body, I

$$\text{MN} = \text{JLAYER}(J) + I$$

As a result the loops are usually set up as follows:



ABLATE

Calling sequence:

CALL ABLATE (H)

Where if

$H = 0.0$, the rates of melt and char are computed.

$H = \Delta t$, the amounts of melt and char are computed.

Routines in the transfer vector:

TABUP

QBLK

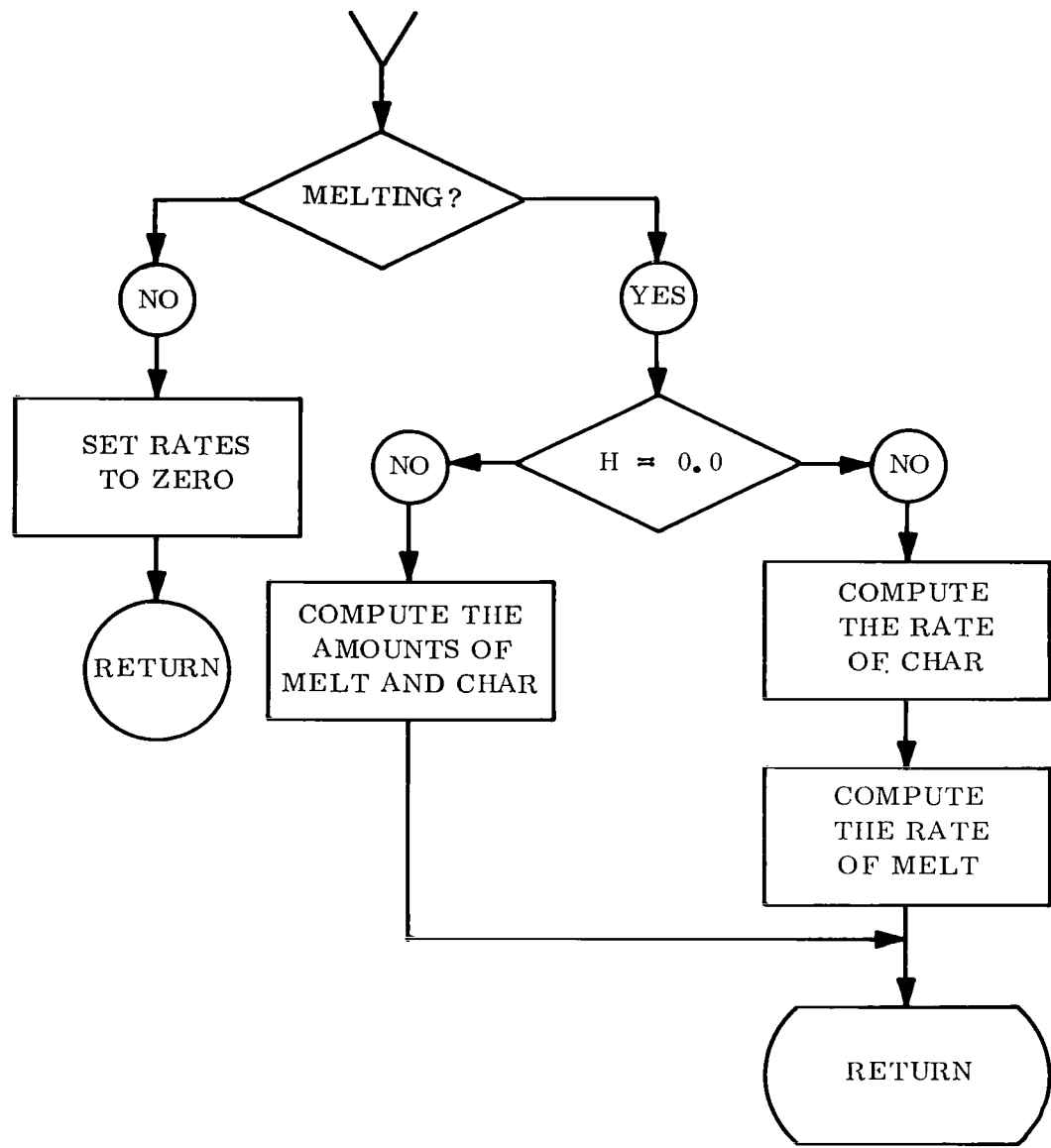
QNET

TNEST

CHARP

Purpose:

This routine computes the rates and amounts of melt and char of an ablating body. The equations for the melting options are described in Section II, part C of the Appendix B.



AIRGAP

Calling sequence:

CALL AIRGAP

Routines in the transfer vector:

TABUP

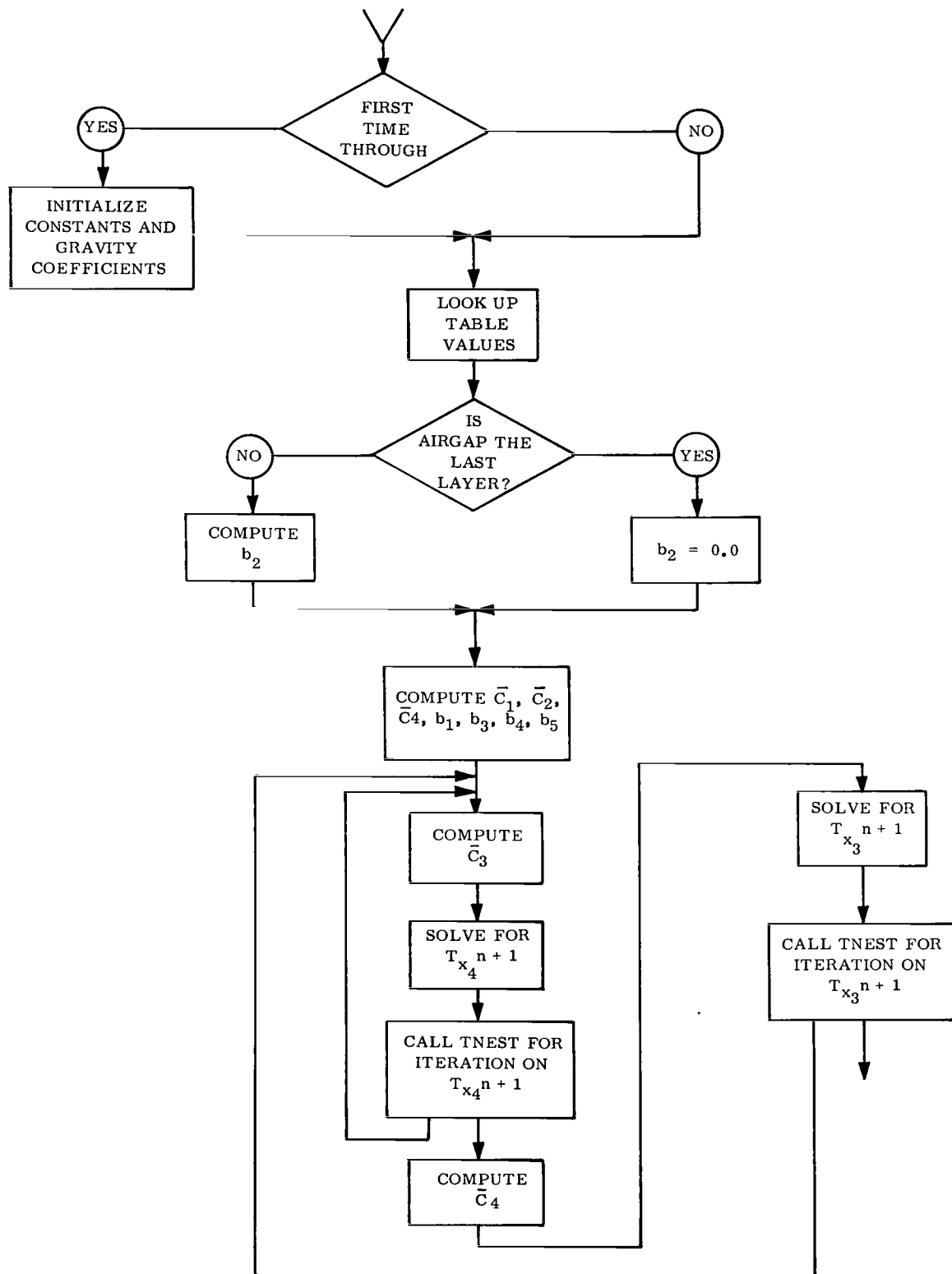
INTPTS

TNEST

Purpose:

This routine solves the air-gap equations discussed in Section IV of the Appendix B.

AIRGAP



BEE

Calling sequence:

CALL BEE (II, MN, J, ITER)

Where

II is the point counter of the arrays which save previous time steps

MN is the point counter of the arrays which do not save previous time steps.

J is the layer counter

ITER is a control which is set in BEE to control the iteration on a point in the subroutine INTPTS.

Routines in the transfer vector:

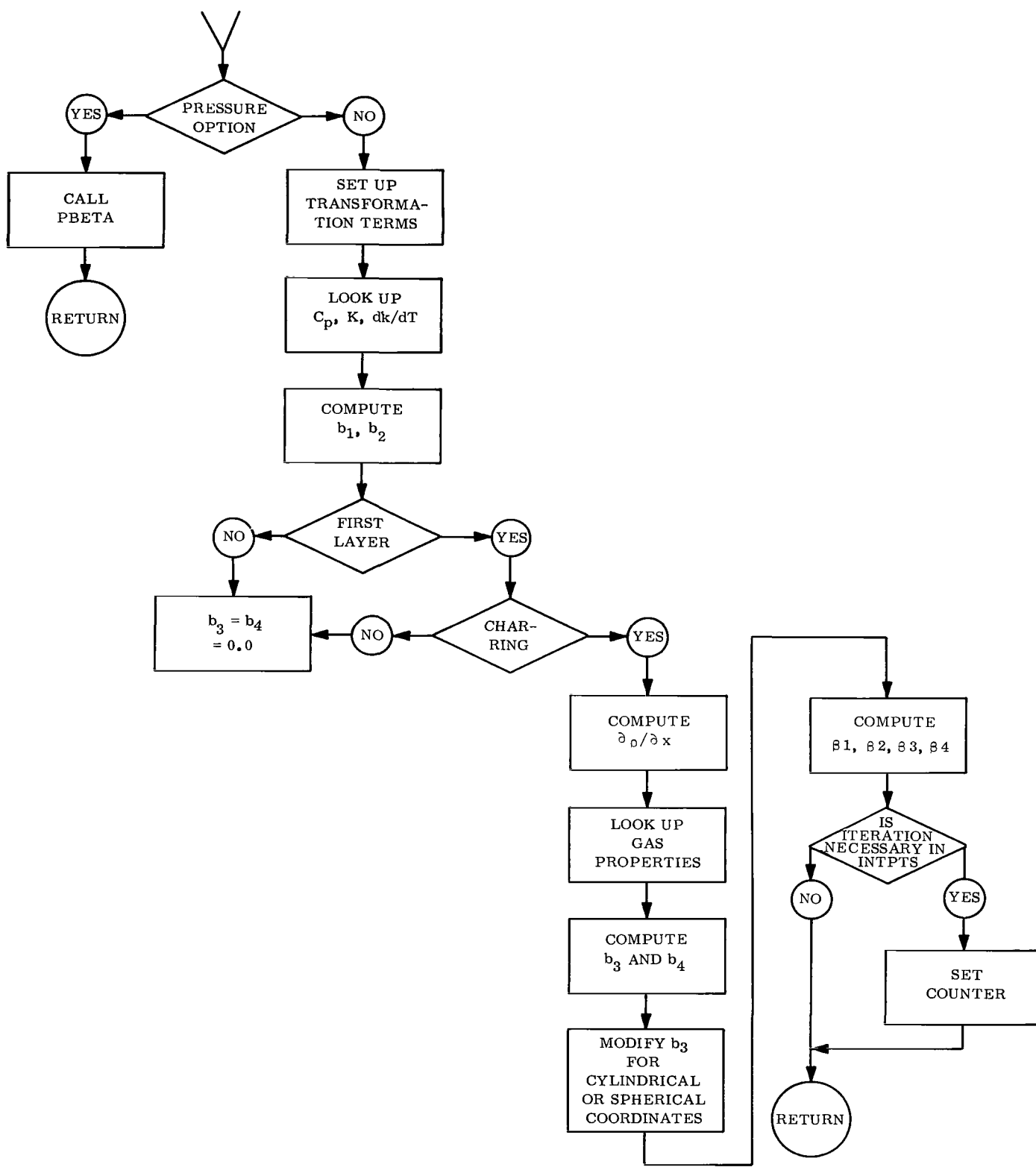
DFINTC PBETA

TABUP

Purpose:

This routine computes the Beta coefficients of the heat transfer equation. The equations are discussed in Section II, part B of Appendix B.

BEE



CHARP

Calling sequence:

CALL CHARP(II, J)

Where:

II is the position counter with respect to time step and η .

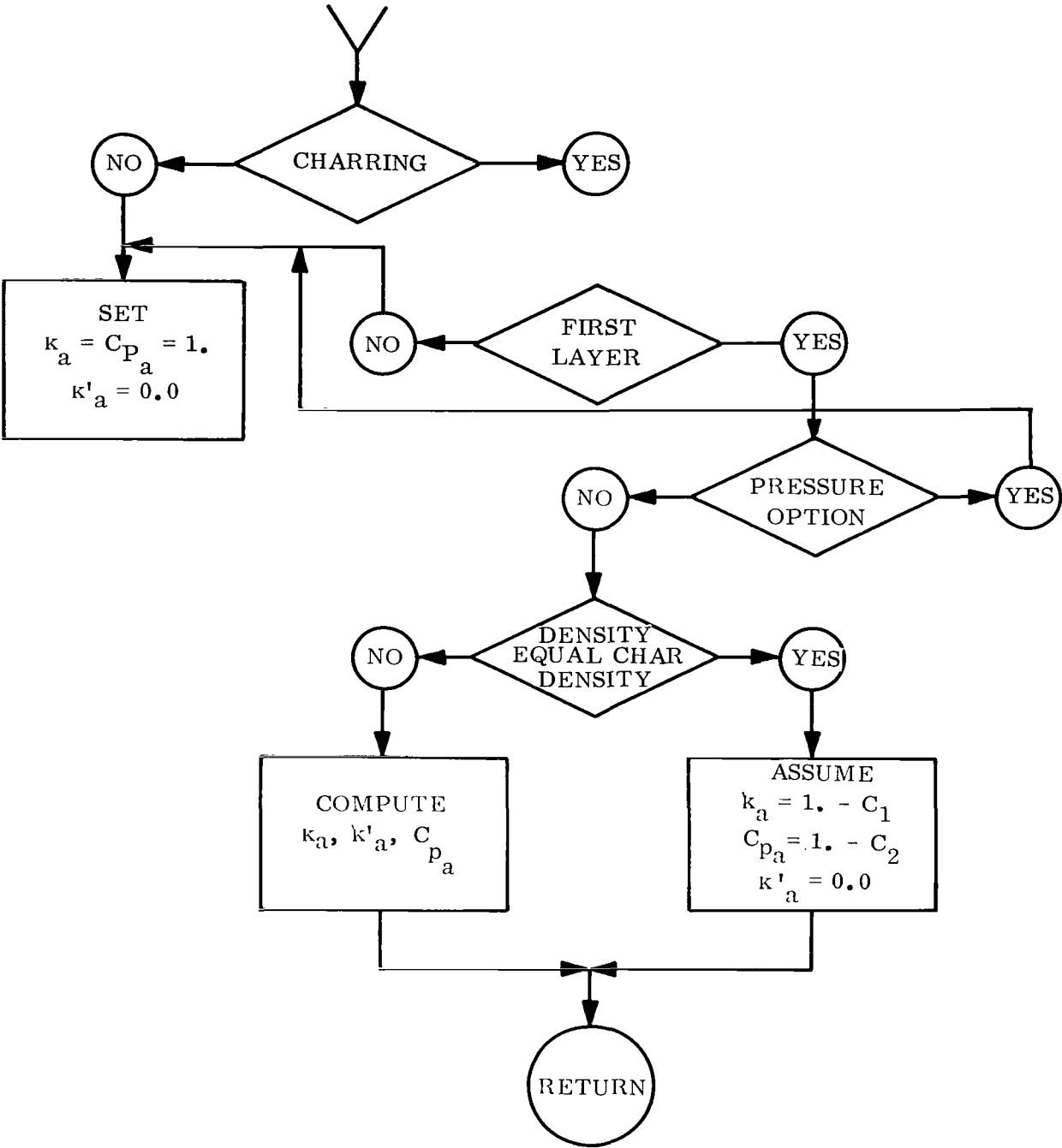
J is the layer counter

Routines in the Transfer Vector:

NONE

Purpose:

The routine computes the k_a , k_a' , and c_{p_a} discussed in Appendix B, Section II, Part 2.



CLCINT

Calling sequence:

A = CLCINT (IND, DX, FX, TEMP)

Where:

A is the value of the integral

IND $\begin{cases} = 0, & \text{Trapezoidal rule} \\ = 1, & \text{Simpson's rule} \end{cases}$

D X $\begin{cases} = 0, & \text{when X.EQ.A} \\ = X(N) - X(N - 1), & \text{when X.NE.A} \end{cases}$

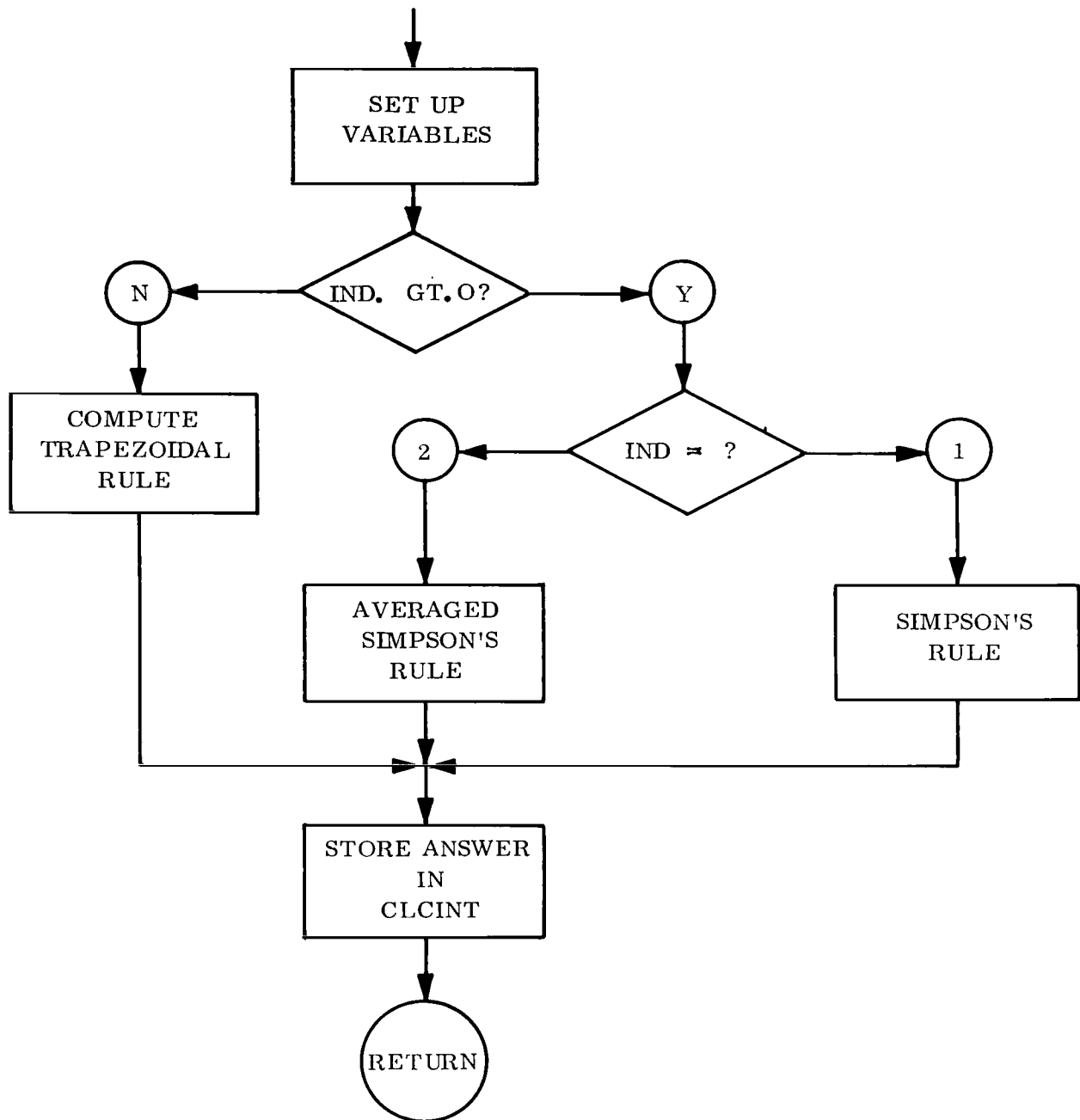
FX is the integrand

TEMP is an array containing 5 cells which must not be used for any other purpose while the integration is being performed

Purpose:

To compute the definite integral of $\int_A^B F(x)dx$ by

0. Trapezoidal rule
1. Simpson's rule



CLPOLY

Calling sequence:

$$Y = \text{CLPOLY}(X, A, N)$$

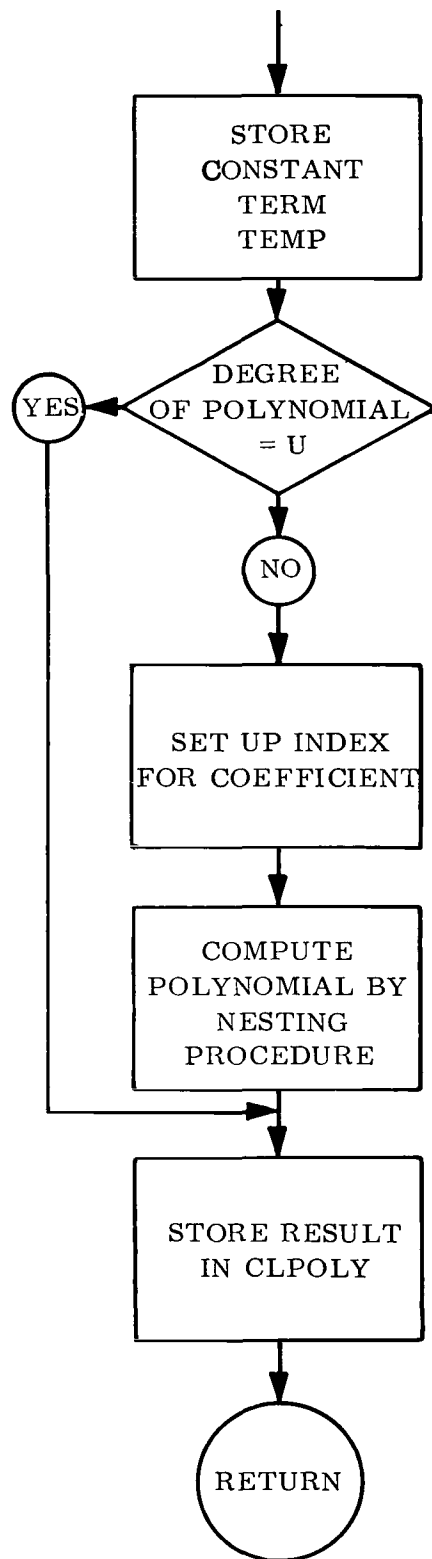
Where: Y is the value of the polynomial
X is the independent variable
A is the name of the array of coefficients
N is the degree of the polynomial

Routines in Transfer vector:

NONE

Purpose:

To evaluate the polynomial $(\text{SUM}(A(I) * X^{(I-1)} \text{ I} = 1, N + 1))$.



DEE

Calling sequence:

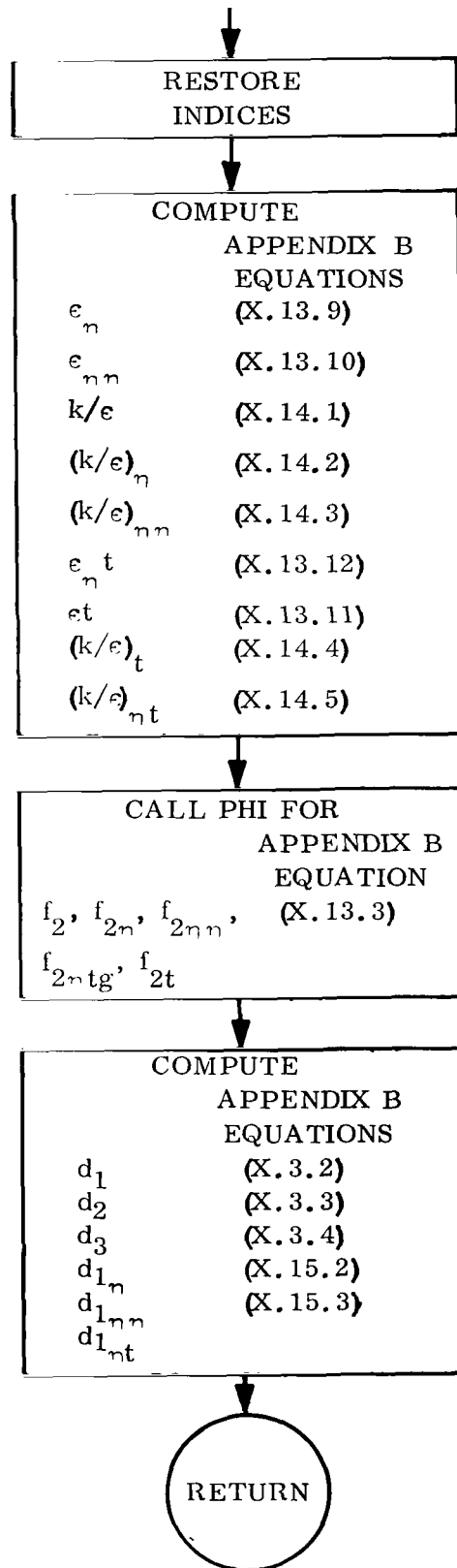
CALL DEE (II, MN)

where II is the point counter in the body and MN is the point counter in the layer.

Routines in transfer vector

Purpose:

This routine computes K/ϵ and its partial derivatives and the d_i coefficients for the pressure difference equation discussed in Appendix B, Section X, Pressure Option.



DFINTC

Calling sequence:

```
CALL DFINTC (DFFC, II, MN, J, FD, SD)
```

where:

DFFC = Array for which the partials are to be computed

II = Point counter on body

MN = point counter in layer

J = layer

FD = First partial derivative

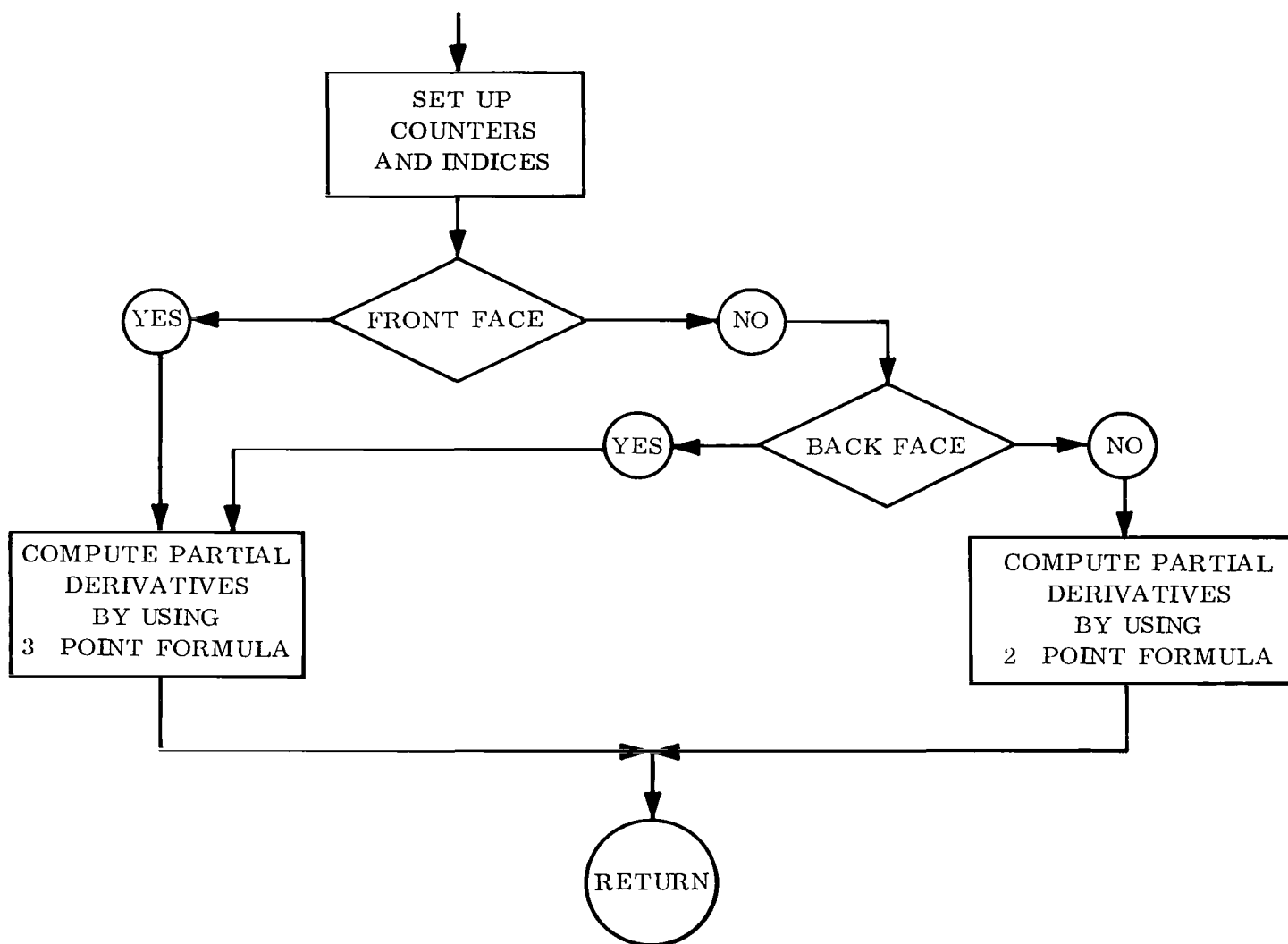
SD = second partial derivative

Routines in transfer vector

NONE

Purpose:

To compute the first and second partial derivatives of an array by using differences.



DELTAT

Calling Sequence:

CALL DELTAT(K)

Where if:

K = -1, Δt is modified since

$$\Delta t < \frac{\Delta \eta}{-\dot{S}_m \eta_x}$$

K = 0, Δt is chosen from the table DTIME

K = 1, Δt is assumed to be the correct magnitude.

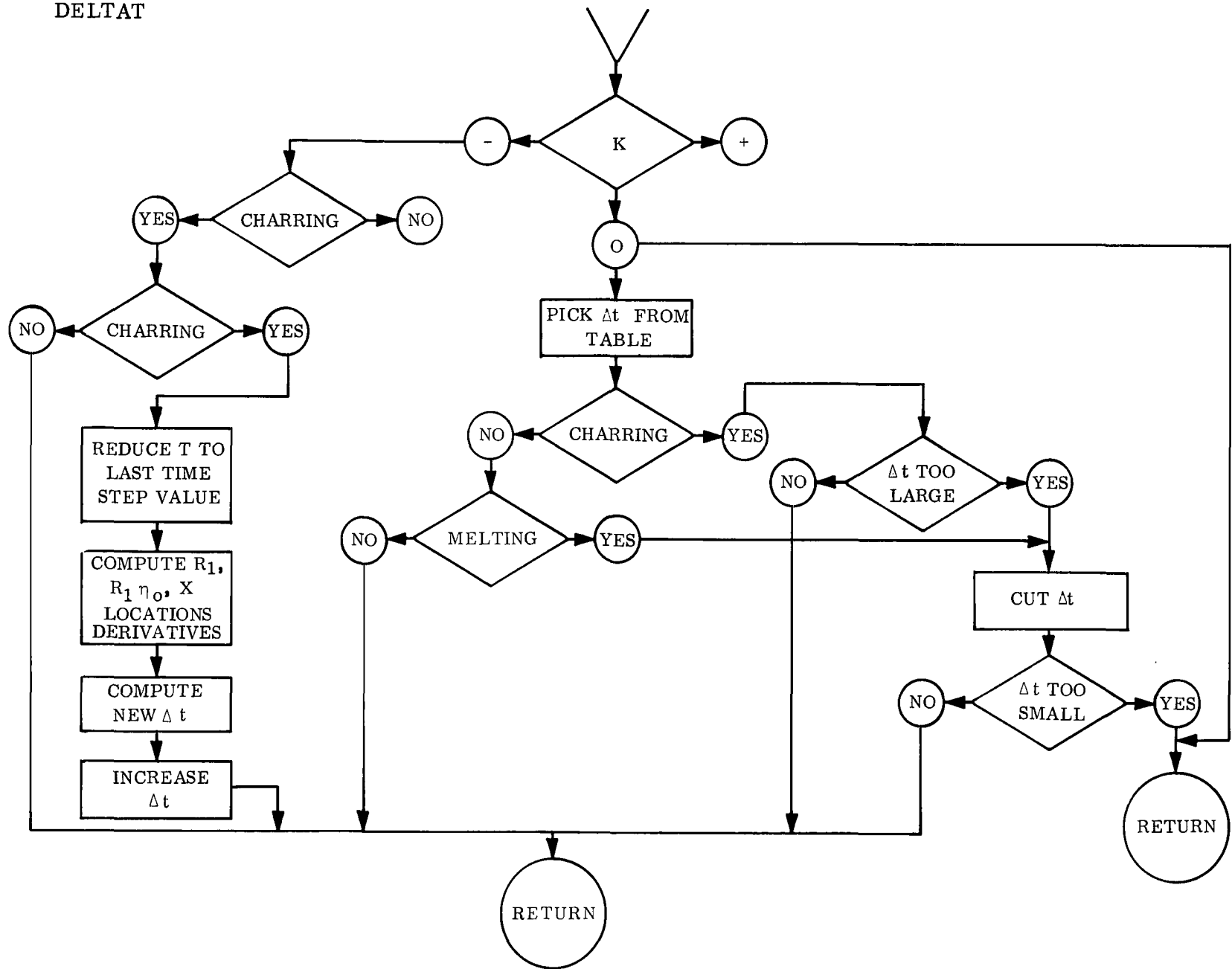
Routines in the Transfer Vector:

RITER

Purpose:

To compute the Δt for the time step.

DELTAT



DENSIT

Calling sequence:

CALL DENSIT (II, MN, K)

Where:

II refers to the point with respect to the time step and η position.

MN refers to the point with respect to the η position.

K refers to an indicator for use of either the explicit ($K = 1$) or implicit ($K = 0$) scheme.

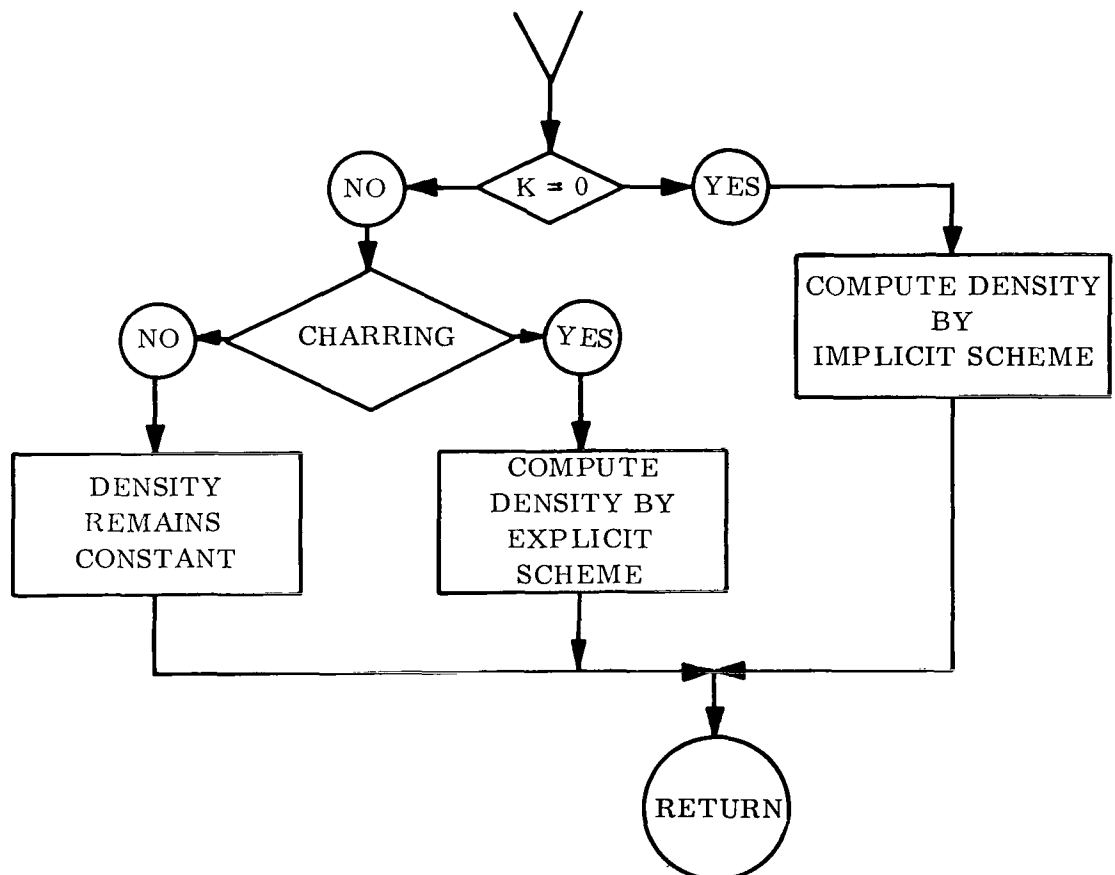
Routines in the Transfer Vector:

WDP

TNEST

Purpose:

This routine computes the densities in the body. Changes in density, due to charring, take place only in the first layer. The equations used in this subroutine are discussed in Appendix B Section V.



DIFTAB

Calling sequence:

CALL DIFTAB (Y, X, DYDX, NX, NL) where:

Y ≡ Dependent table

X ≡ Independent table

DYDX ≡ Derivatives of Y table with respect to X

NX ≡ Independent table length

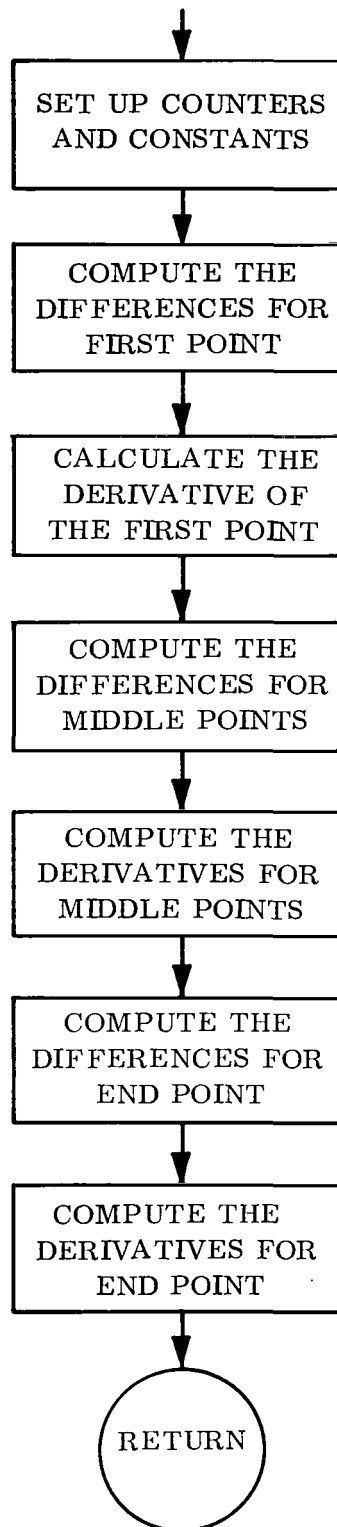
NL ≡ Number of layers

Routines in transfer vector:

NONE

Purpose:

To compute the derivatives by finite differences of tabular arrays. The equations are in Part B, Appendix D.



DPRESS

Calling sequence:

```
CALL DPRESS (II, MN, I)
```

where:

II is the point counter on the body MN is the point counter in the layer

I is the explicit/implicit control

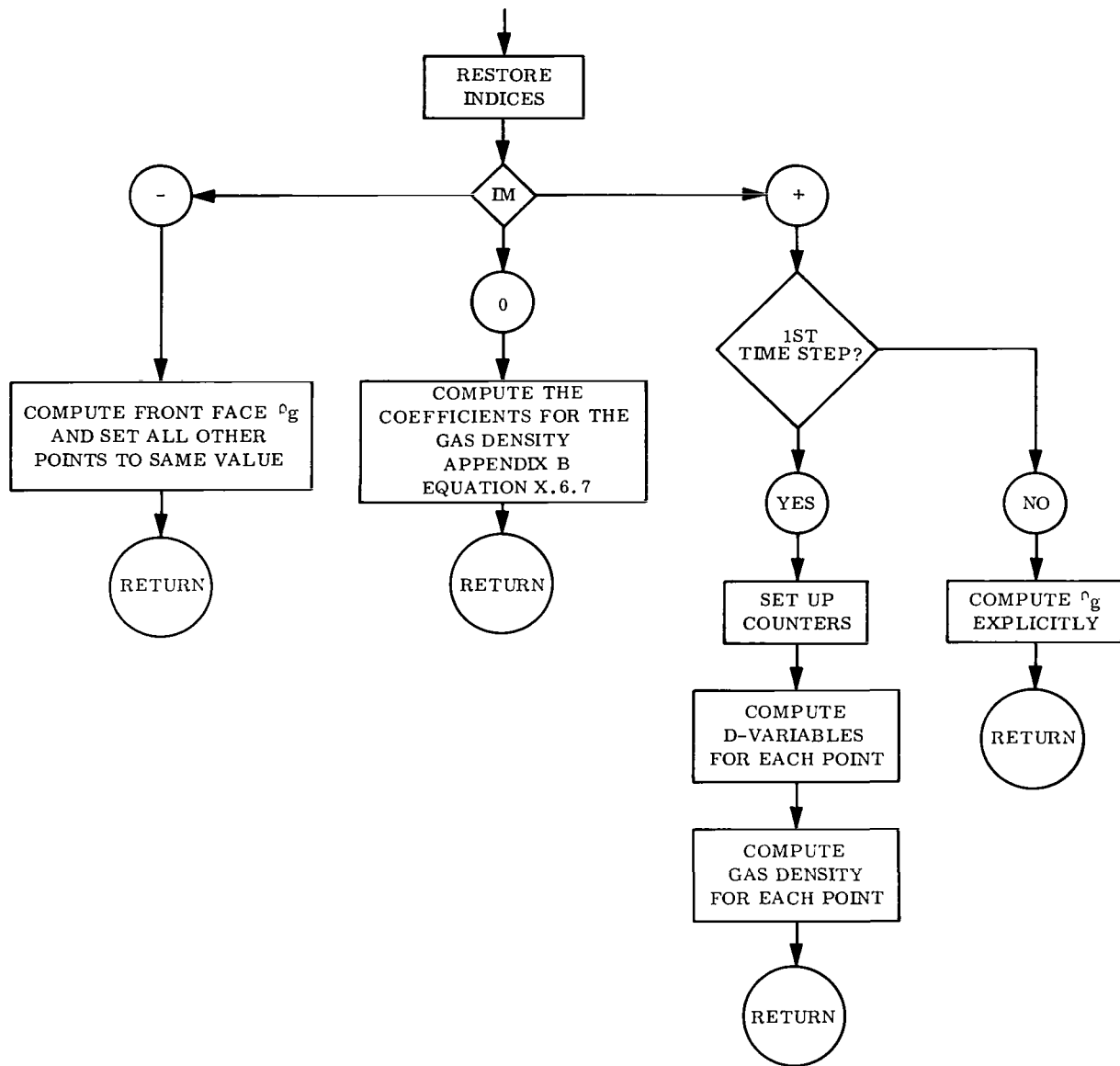
Routines in transfer vector

```
DEE  
RHOFEC  
ERROR
```

Purpose:

The compute the gas densities at each interior point. By either the explicit or implicit scheme. Appendix B, section X, Pressure Option.

DPRESS



EMG

Calling sequence:

CALL EMG (II)

Where:

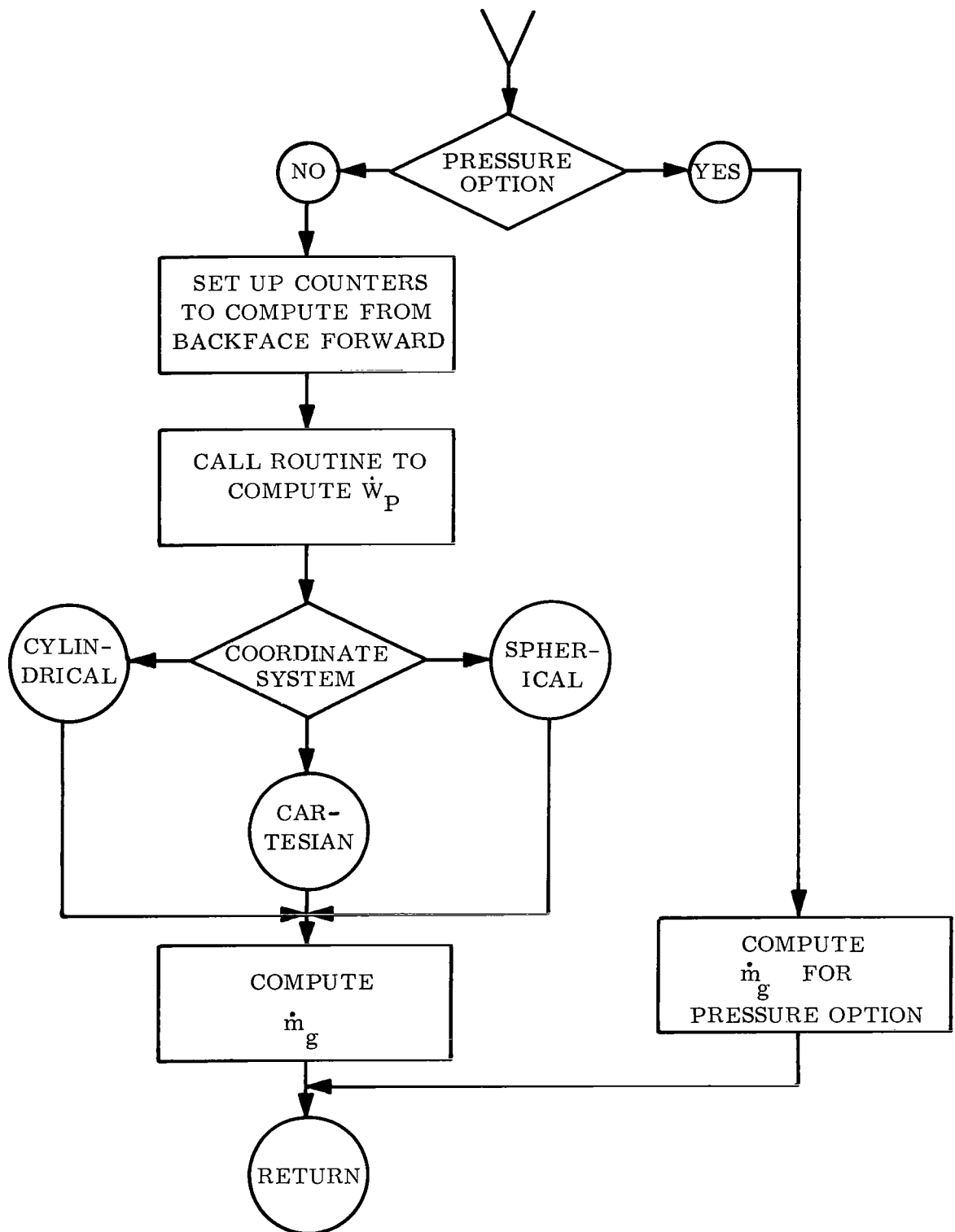
II is the point counter with respect to the time step and η

Routines in the Transfer Vector

WDP

Purpose:

Computes the \dot{m}_g , mass flux of gas, in the first layer. The equation is defined in Appendix B, Section II. B. 2.



ENLARG

Calling Sequence:

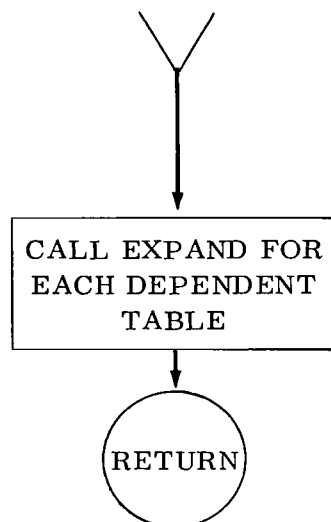
CALL ENLARG

Routines in the Transfer Vector:

EXPAND

Purpose:

The routine calls EXPAND to make all dependent tables the correct length.



EXEC

Calling Sequence:

CALL EXEC

Routines in transfer vector:

DENSIT	PRESSM	STARTT	TABOUT
TNEST	INIT	DELTAT	HTBLNS
PTX1	NSUBT	INTPTS	
PTX12	AIRGAP	RITER	
INPUT	OUTPUT	ABLATE	
INTFC	GAMA	EMG	

Purpose:

To call the subroutines in their proper order. For flow chart see page E-5.

EXPAND ROUTINE

I Title: EXPAND

II Type: Fortran IV Subroutine

III Calling Sequence:

CALL EXPAND (NIND, XTABL, NARAY, ENDTBL, NVLUS, NMTB)

where:

NIND: Number of values in independent table

XTABL: First location of dependent table array

NARAY: Dimension of dependent table array

ENDTBL: First location of independent table

NVLUS: First location of array which contains number of values read as input in each dependent table of the array

NMTB: Maximum number of tables in the array

IV Table Formats:

A. Dependent table array may have

- (1) one value -- constant table
- (2) two values requiring interpolation to expand to NIND values
- (3) NIND values where no expansion would be needed

B. Independent table must be in ascending order

V Method:

The subroutine will test the NVLUS array to count the number of expandable tables. When NVLUS (1) is zero it indicates that there are no more tables.

If there is only one value then the table is constant and the subroutine expands the table to the size of the independent table putting the value given in the input into all the locations. In the NIND + 1 location of the table, the program puts a zero to signify that it is a constant table.

If two values are read into the table, then the subroutine will expand the table to the proper size by linear interpolation using the ratio between the independent table values. In the NIND + 1 location of the table the program puts a "1" to distinguish it as a variable table.

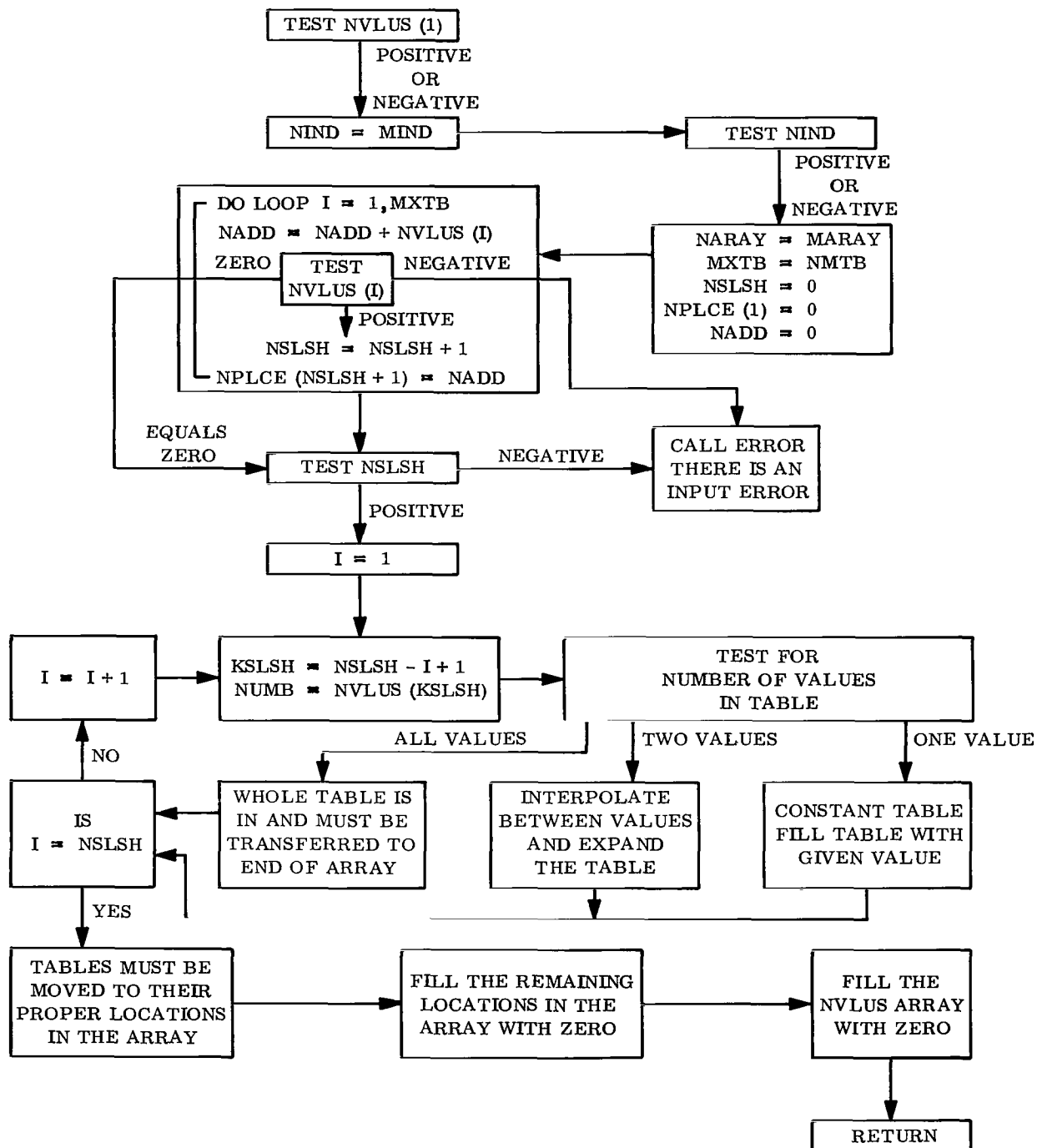
If all the values have been given in the input, then the subroutine will not need to expand the table but will merely put a "1" in the NIND 1 location.

In the event that several cases may be run using the same tables, the program sets all the values in the NVLUS array to the number of independent table values (NIND). This eliminates any further expansion when the EXPAND routine is called for the next case.

VI Error Returns:

- A. A negative value in the NVLUS array causes an error message.
- B. When the number of values in the NVLUS array is greater than two but not equal to the number of independent table values (NIND), an error message is printed.

EXPAND (MIND, XTABL, MARAY, ENDTBL, NVLUS, NMTB)



GAMA

Calling Sequence:

CALL GAMA (H)

Where H is $-\Delta t$

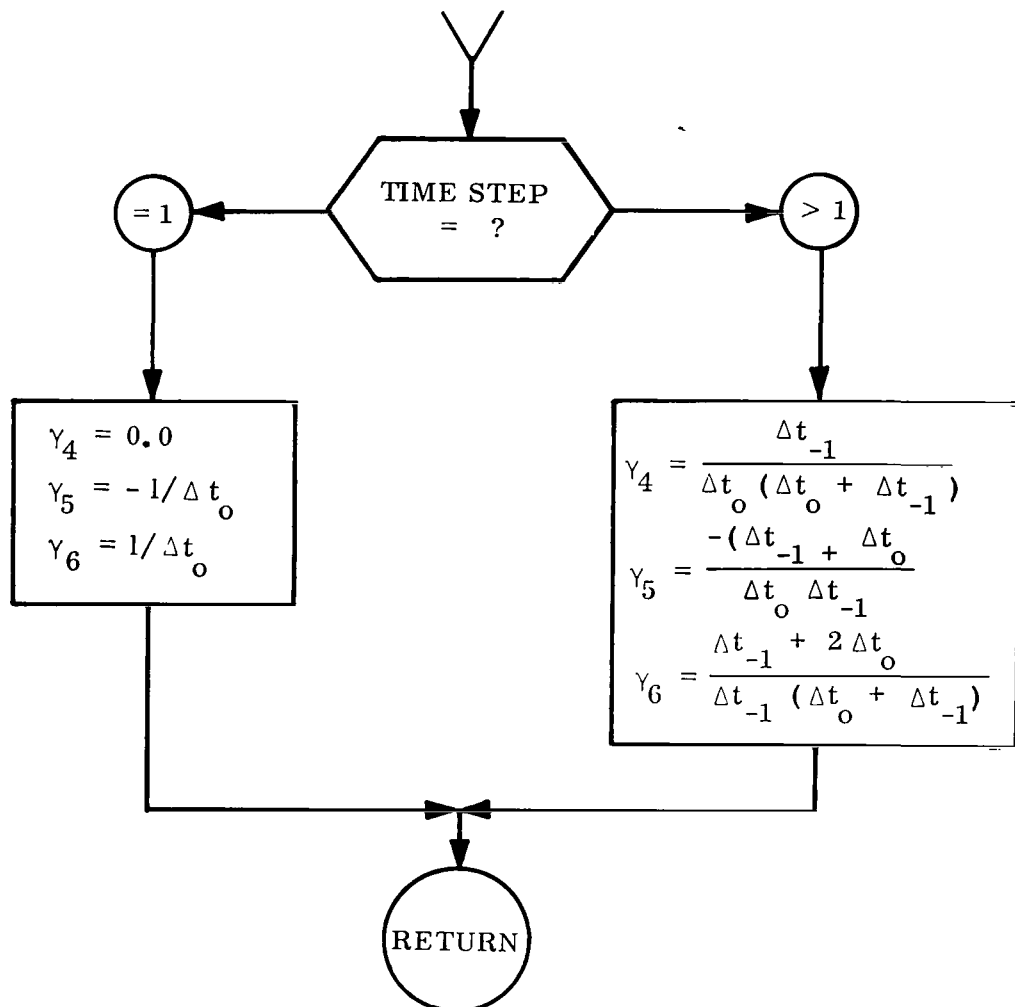
Routines in Transfer Vector:

NONE

Purpose:

This routine computes the gamma coefficients discussed and defined in Appendix B, Section IV, The Interface Equations.

The locations of GAMMA (1 - 3) are available for future modification.



HTBLNS

Calling Sequence:

CALL HTBLNS (IKBLN)

Where:

When IKBLN = 0, means the routine was called from the routine, STARTT and the initialization of variables is done.

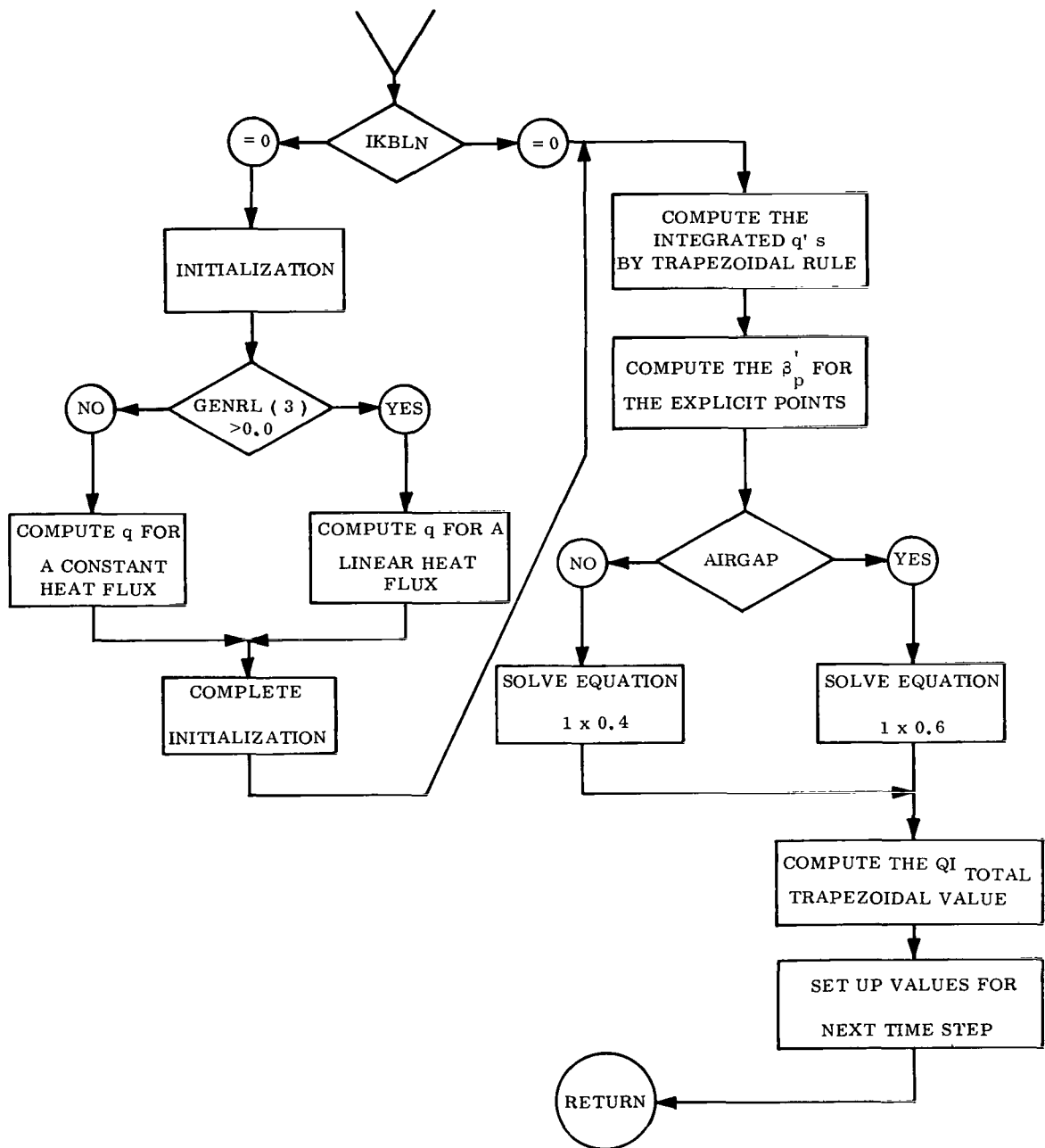
When IKBLN = 1, the initialization is skipped and the best balance equations are computed.

Routines in the Transfer Vector:

NONE

Purpose:

This routine computes the integrated q's and then computes the Q_i as discussed and defined in Appendix B, Section 1X.



KEFFS

Calling Sequence:

CALL KEFFS (II, MN)

Where:

II = Point counter in body

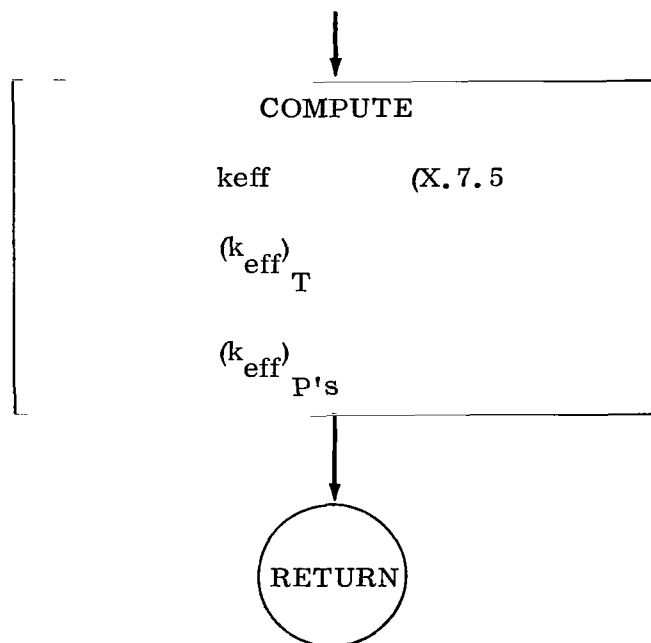
MN = Point counter in layer

Routine in Transfer Vector:

NONE

Purpose:

Computes the K eff and its Partial derivatives.



KFS

Calling Sequence:

CALL KFS (II, MN)

Where:

II is point counter on body

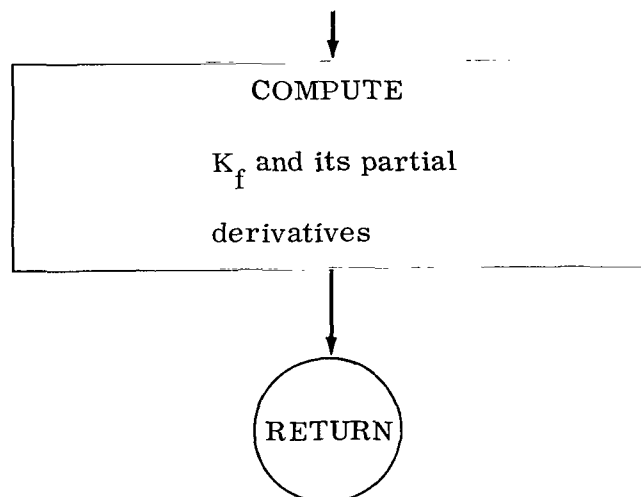
MN is point counter in layer

Routines in Transfer Vector:

NONE

Purpose:

To compute K_f and its derivatives. Appendix B, Section X, Pressure Option



INIT

Calling Sequence:

CALL INIT (K)

While:

K = 1, initialization of tables and constants, construct difference tables and store zeroes in the computed common

K = 2, this block prepares for the next time step, updates the count array, shift the T, P, DENS, DELTO, SMELT and SCHAR arrays.

K = 3, this block prepares for the next case prints the output and stores zeroes in the computed common

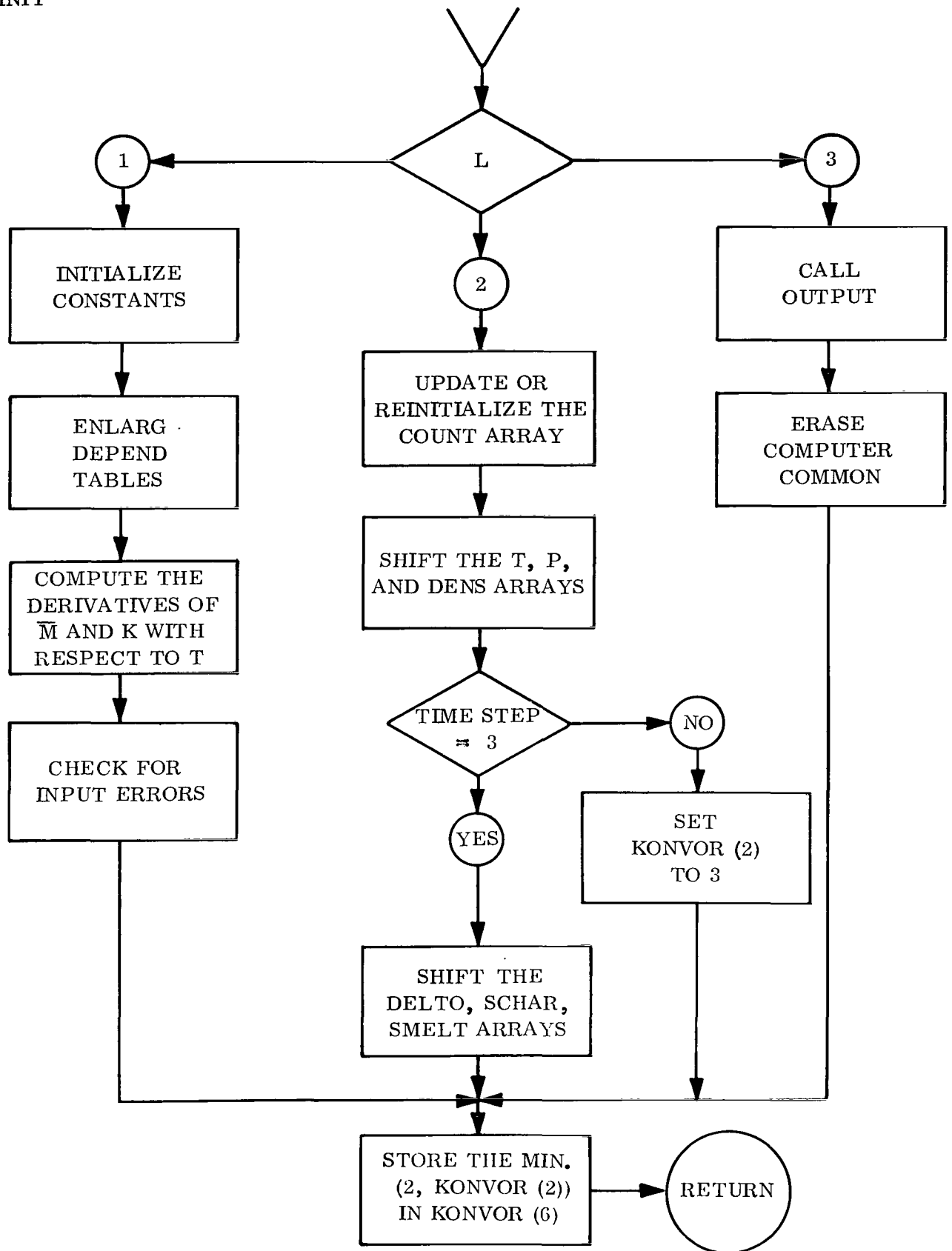
Routines in the Transfer Vector

ENLARG	TNEST
DIFTAB	OUTPUT

Purpose:

This routine initializes the arrays and constants for the first time step, succeeding time steps and for consecutive cases.

INIT



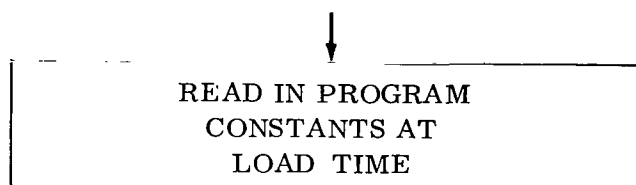
INITB

Calling Sequence:

BLOCK DATA

Purpose:

To read in constants at load time



INTFC

Calling Sequence:

CALL INTFC

Routines in the Transfer Vector

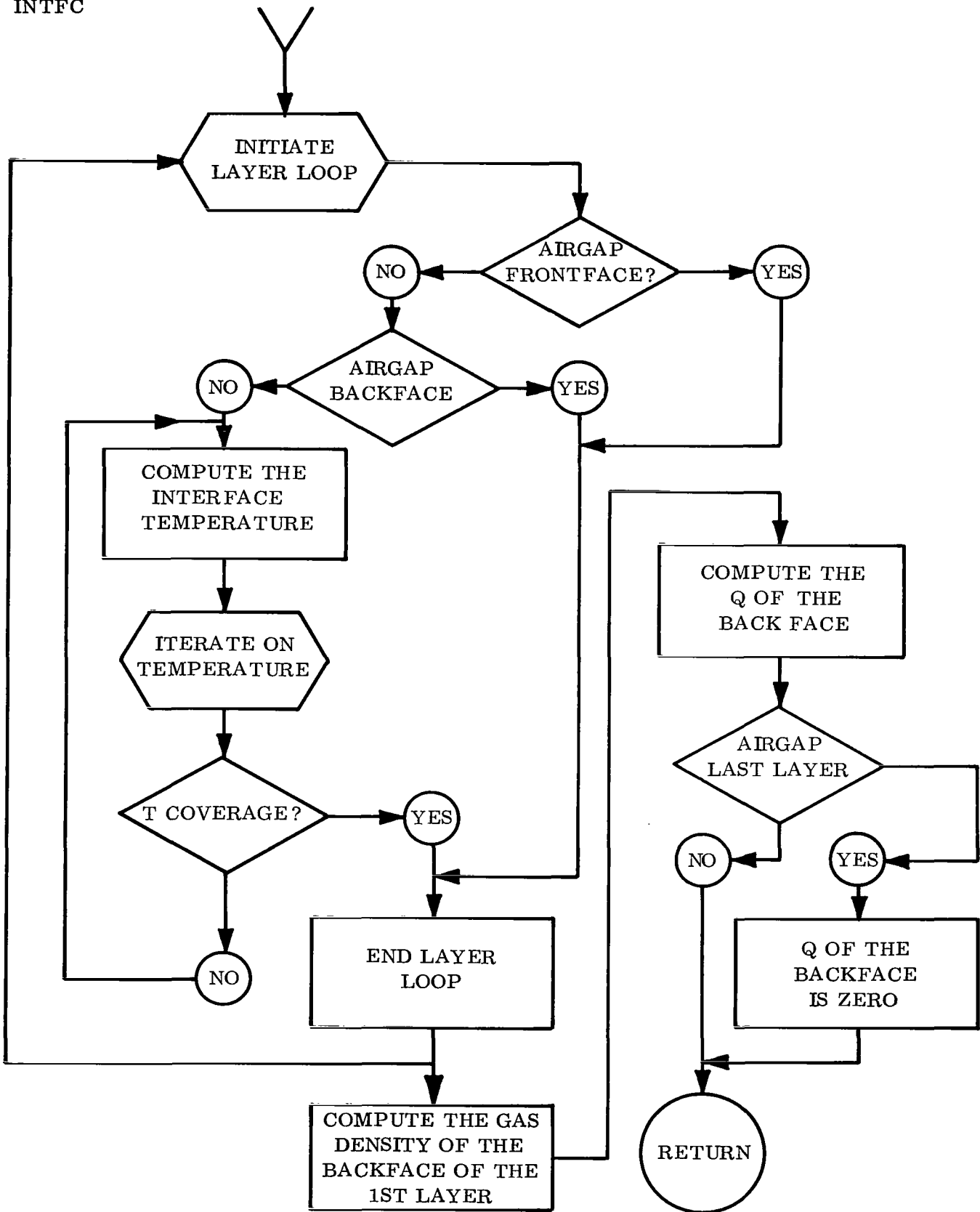
INTPTS DPRESS

TABUP PFFC

TNEST

Purpose:

This routine computes the inter-face and back-face temperatures and pressures as discussed in Appendix B, Section IV, Numerical Solution of Energy equation in Boundary condition.



INTPTS

Calling Sequence:

CALL INTPTS (I, J)

Where:

$$I = \begin{cases} -1, & \text{indicates use the implicit equations} \\ 0, & \text{indicates use the explicit equations} \\ >0, & \text{evaluate a point by the implicit equations} \end{cases}$$

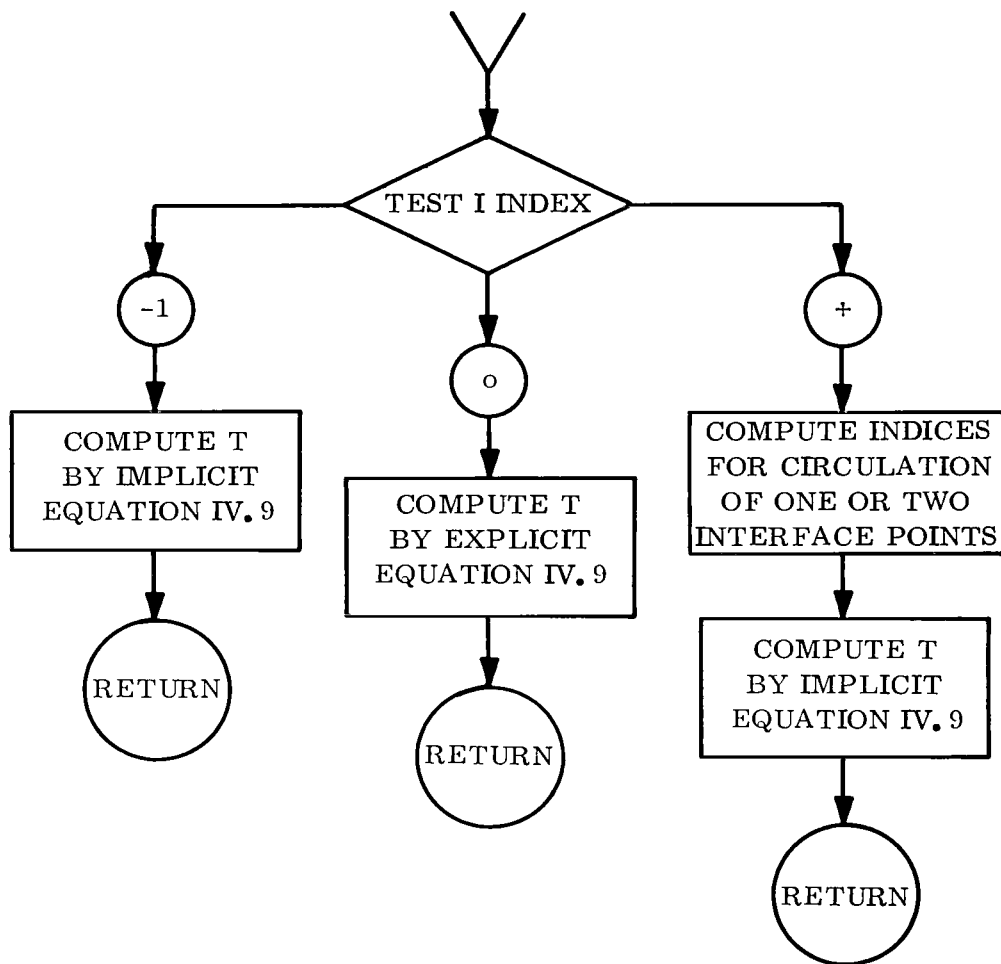
J = Point to be evaluated.

Routines in the Transfer Vector:

BEE	DENSIT
CHARP	PRESSM
EMG	TNEST

Purpose:

This routine evaluates the values of the temperatures for the interior points as discussed in Section IV.



MOMENT

Calling Sequence:

CALL MOMENT (XARAY)

Where:

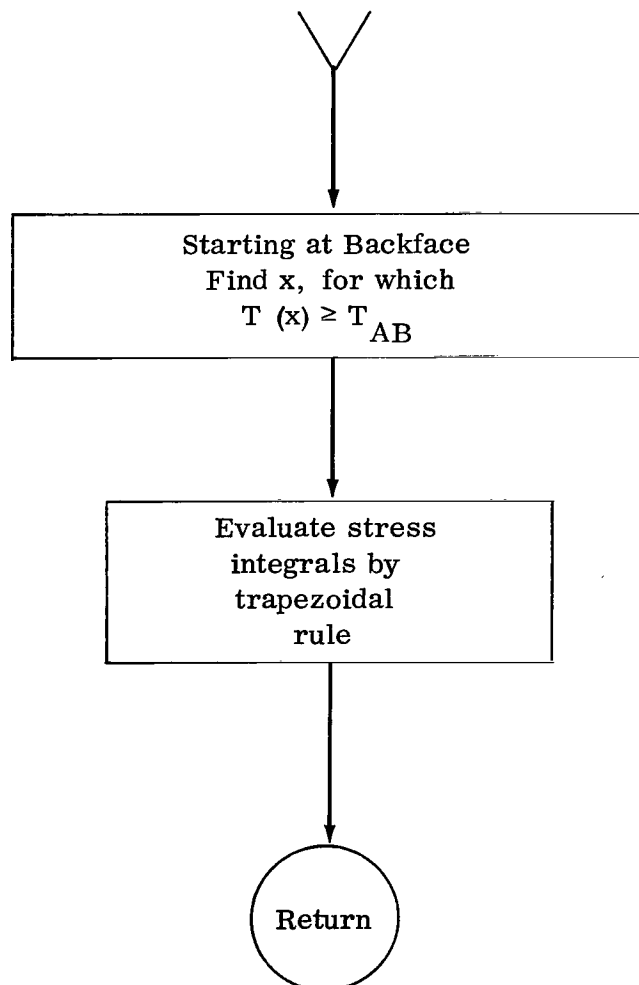
XARAY is the array where the x coordinates are stored in the OUTPUT routine.

Routines in the Transfer Vector:

NONE

Purpose:

The purpose of this routine is to compute the stress calculations discussed in Section II of the analysis.



NSUBT

Calling Sequence:

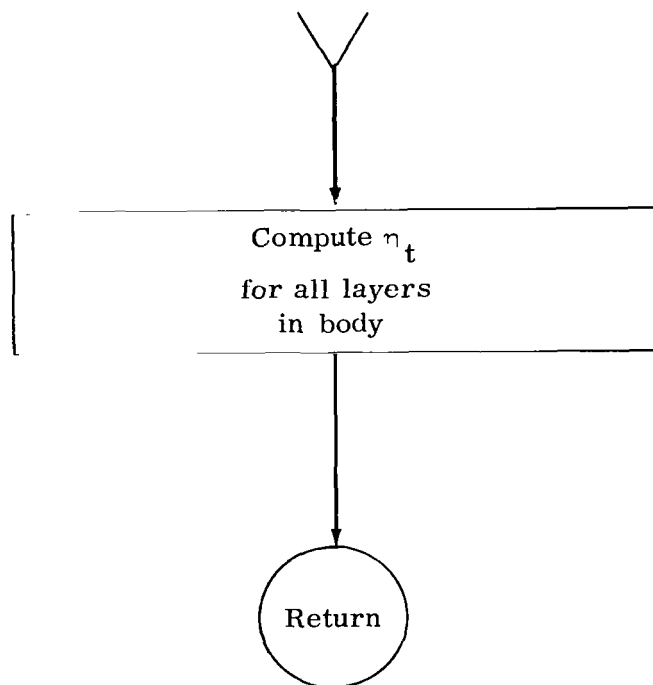
CALL NSUBT

Routines in the Transfer Vector:

NONE

Purpose:

The purpose of this routine is to calculate the partial derivative of η with respect to time. The equation is discussed in Section VII of Appendix B.



OUTPUT

Calling Sequence:

CALL OUTPUT

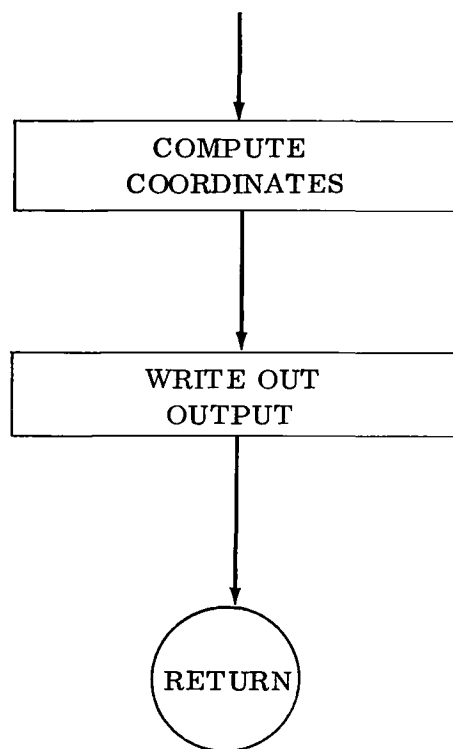
Routines in the Transfer Vector:

TABUP

MOMENT

Purpose:

To print out the computed output.



PBETA

Calling Sequence:

CALL PBETA (II, MN, J, ITM)

Where:

II	=	point counter in body
MN	=	point counter in layer
J	=	layer
ITM	=	iteration control set in PBETA

Routines in Transfer Vector:

TABUP

KEFFS

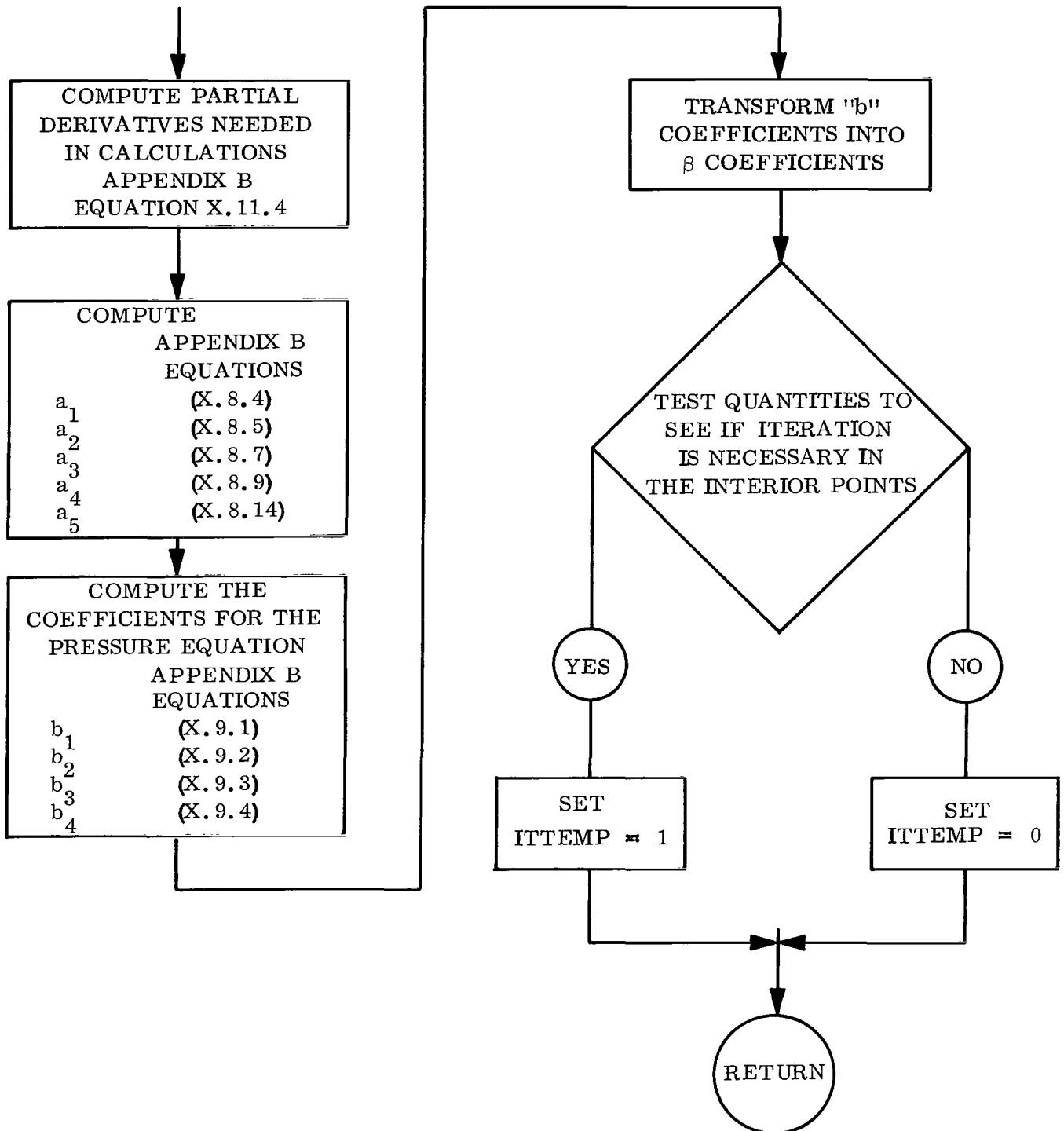
RCPEFS

DFINTC

Purpose:

To compute the Beta coefficients for the temperature equation discussed in Appendix B, Section X, Pressure Option.

PBETA



PEMDG

Calling Sequence:

CALL PEMDG (K)

where:

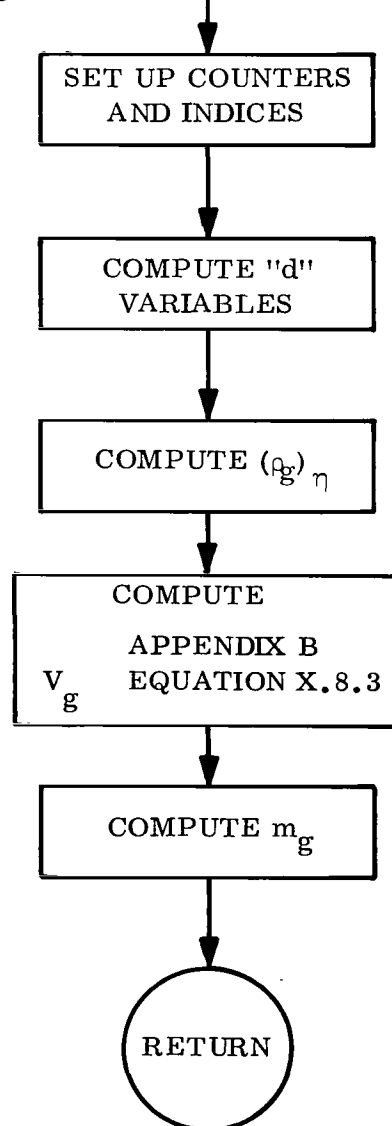
K is a point counter for Front Face determination.

Routines in Transfer Vector

DEE

Purpose:

To compute the mass loss, \dot{m}_g , at the body points



PFFC

Calling Sequence:

This is a dummy subroutine and may be deleted if desired by removing the CALL from INTFC

PMELT

Calling Sequence:

This is a dummy routine and may be deleted if desired by removing the CALL from the ABLATE routine.

PHI

Calling Sequence:

CALL PHI (II, MN)

where:

II is point counter on body

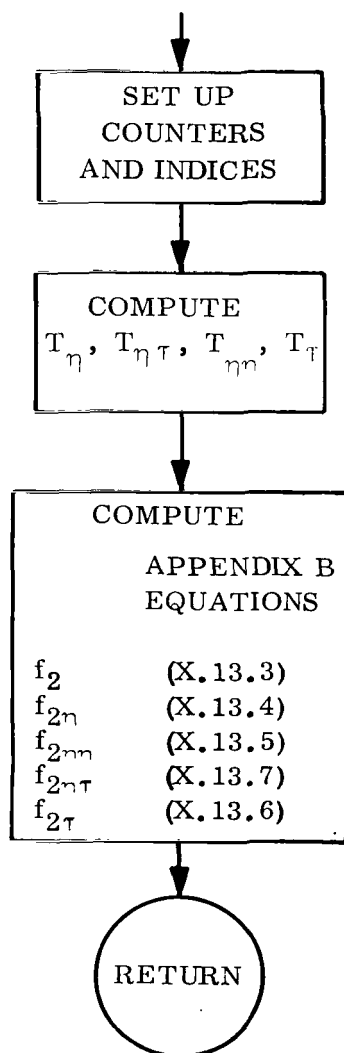
MN is point counter in body

Routines in Transfer Vector:

DFINTC

Purpose:

To compute f_2 and its partial derivatives as discussed in Appendix B, Section X, Pressure Option.



PRESSM

Calling Sequence:

CALL PRESSM (II, J, N, K)

where:

II is the point counter on the body

J is the layer

N is a dummy variable

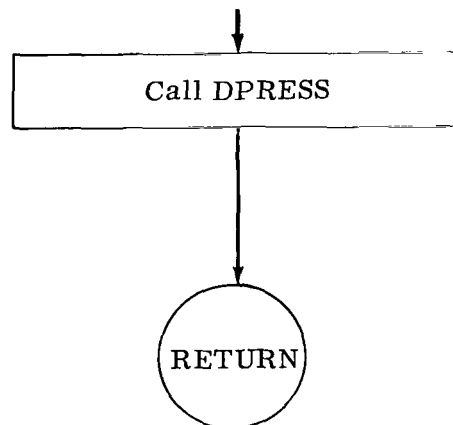
K is implicit/explicit indicator

Routines in Transfer Vector:

DPRESS

Purpose:

Routine calls DPRESS.



PTX1

Calling Sequence:

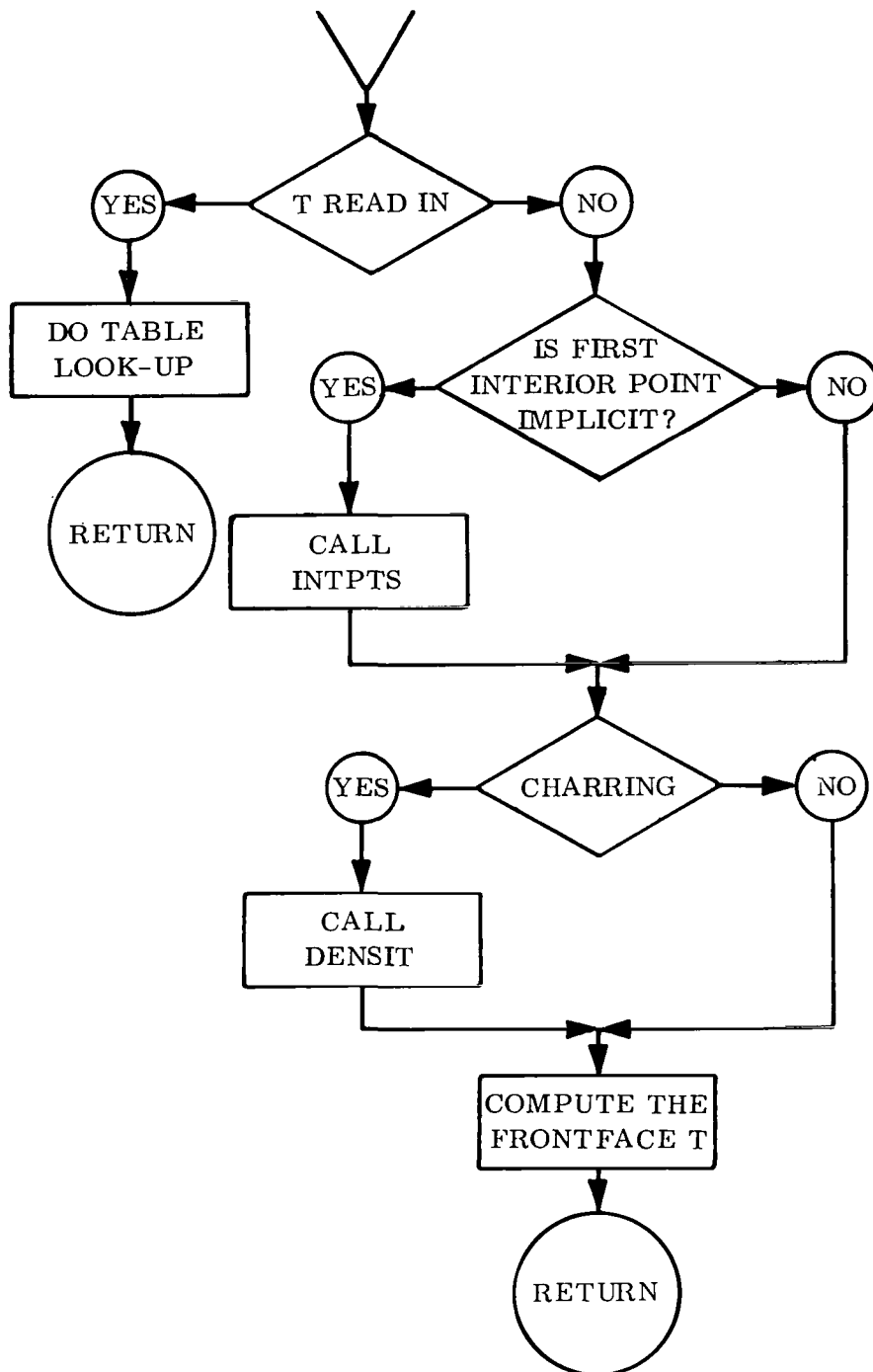
CALL PTX1

Routines in Transfer Vector:

CHARP	INTPTS	DPRESS
BEE	DENSIT	KEFFS
TABUP	EMG	
TNEST	QNET	

Purpose:

The purpose of this routine is to compute the temperature and density of the front face. The equations are discussed in Section IV and V of Appendix B.



PTX12

Calling Sequence:

CALL PTX12

Routines in Transfer Vector:

TNEST

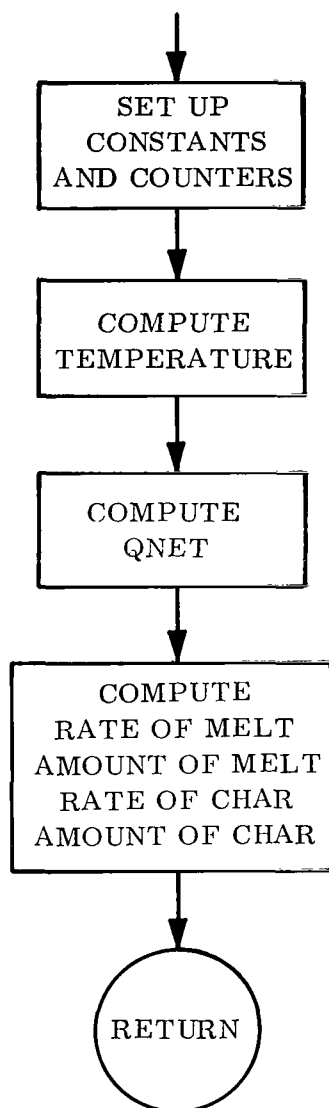
QNET

OUTPUT

TABUP

Purpose:

This subroutine computes the temperature of the body when there would be no distribution of temperatures through the body. This is done if and only if there is one layer and only one interior point. The equations are in Appendix B5.



QBLK

Calling Sequence:

CALL QBLK (QC, HRDHW, QBLOCK, EMV)

where:

QC ≡ convective heat flux

HRDHW ≡ ratio of heat enthalpies

QBLOCK ≡ blocking action heat flux

EMV ≡ mass loss

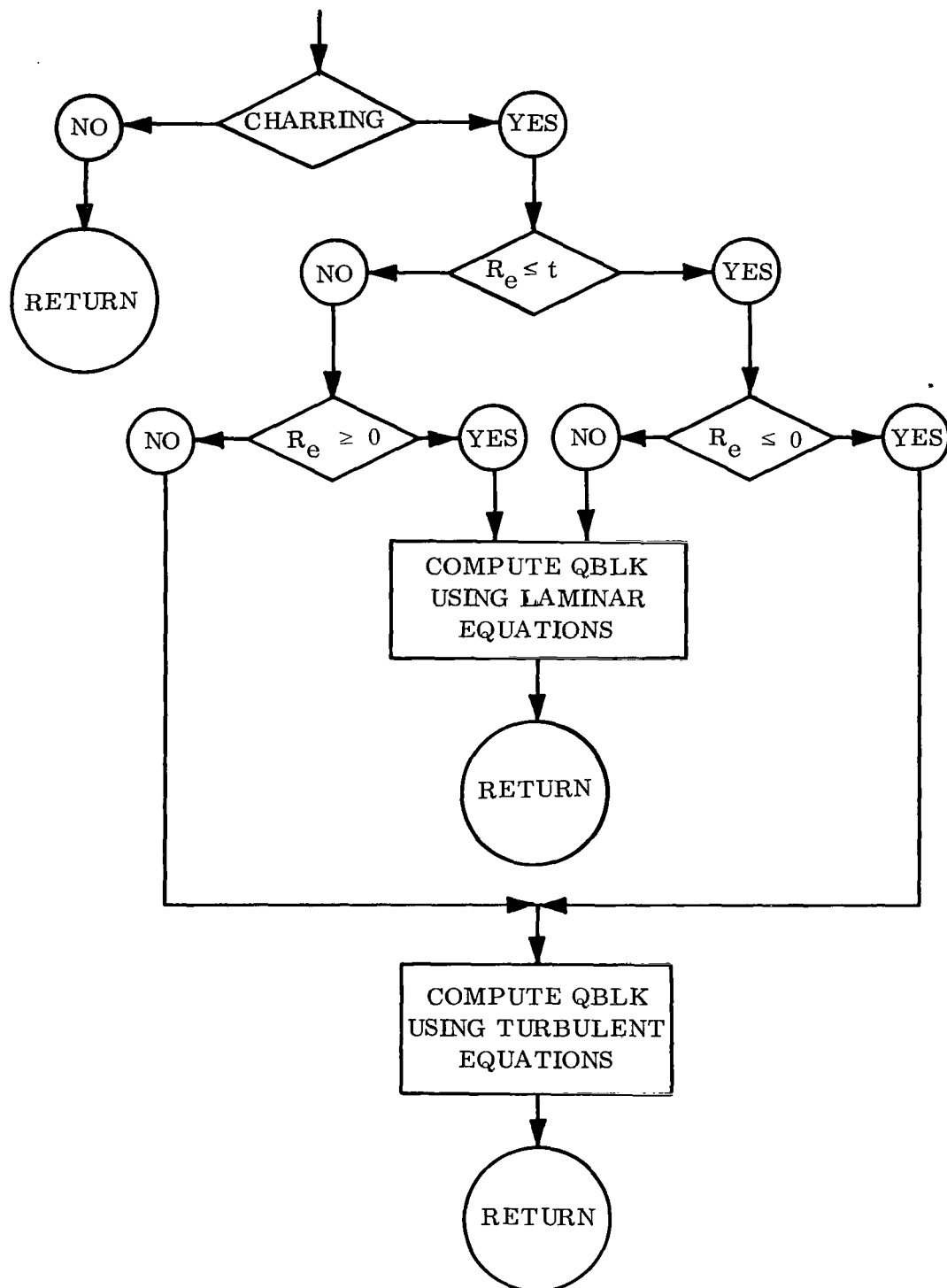
Routines in Transfer Vector:

NONE

Purpose:

This routine computes the heat flux due to the blocking action. The equations are discussed in Appendix B, Section II.

QBLK



QNET

Calling Sequence:

CALL QNET

Routines in the Transfer Vector:

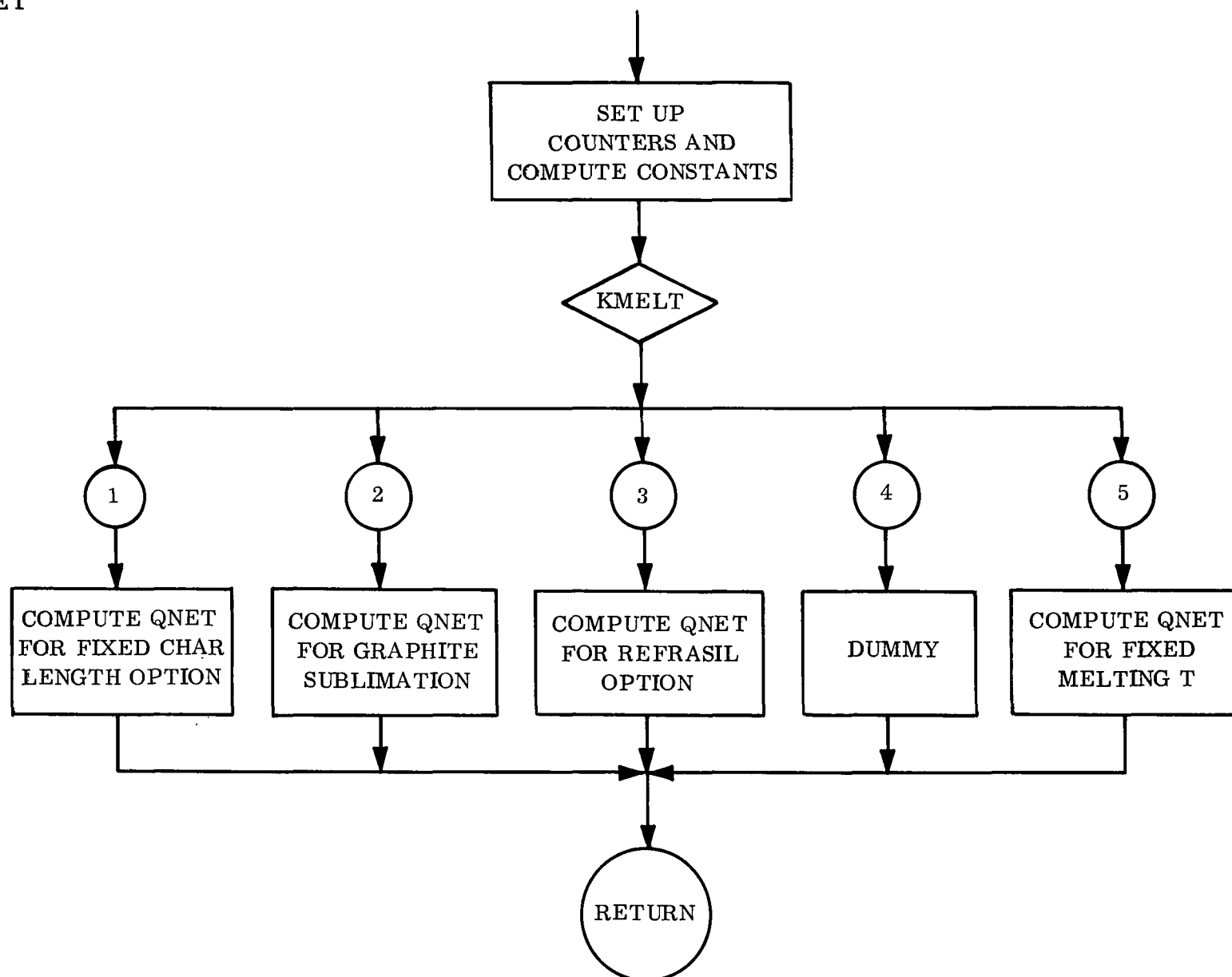
TABUP

QBLK

Purpose:

This routine computes the heat content of the body. The equations are discussed in Appendix B.

QNET



RCPEFS

Calling Sequence:

CALL RCPEFS (II, MN)

where:

II is the point counter on the body

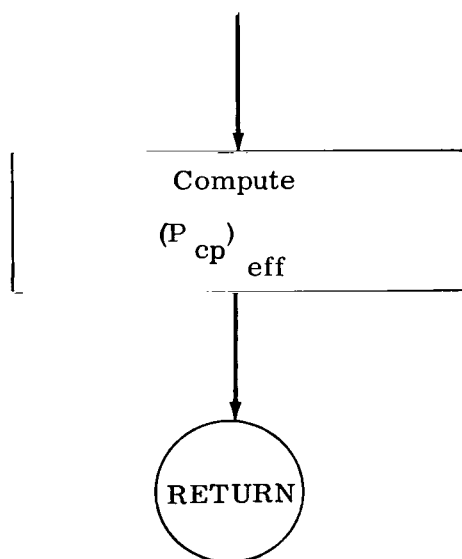
MN is the point counter in the layer

Routines in Transfer Vector

ERROR

Purpose:

The routine computes $(\rho_{cp})_{eff}$ discussed in Appendix B, Section X, Pressure Option



RHOFFC

Calling Sequence:

CALL RHOFFC (II, MN, IM)

where:

II is point counter on body

MN is point counter in layer

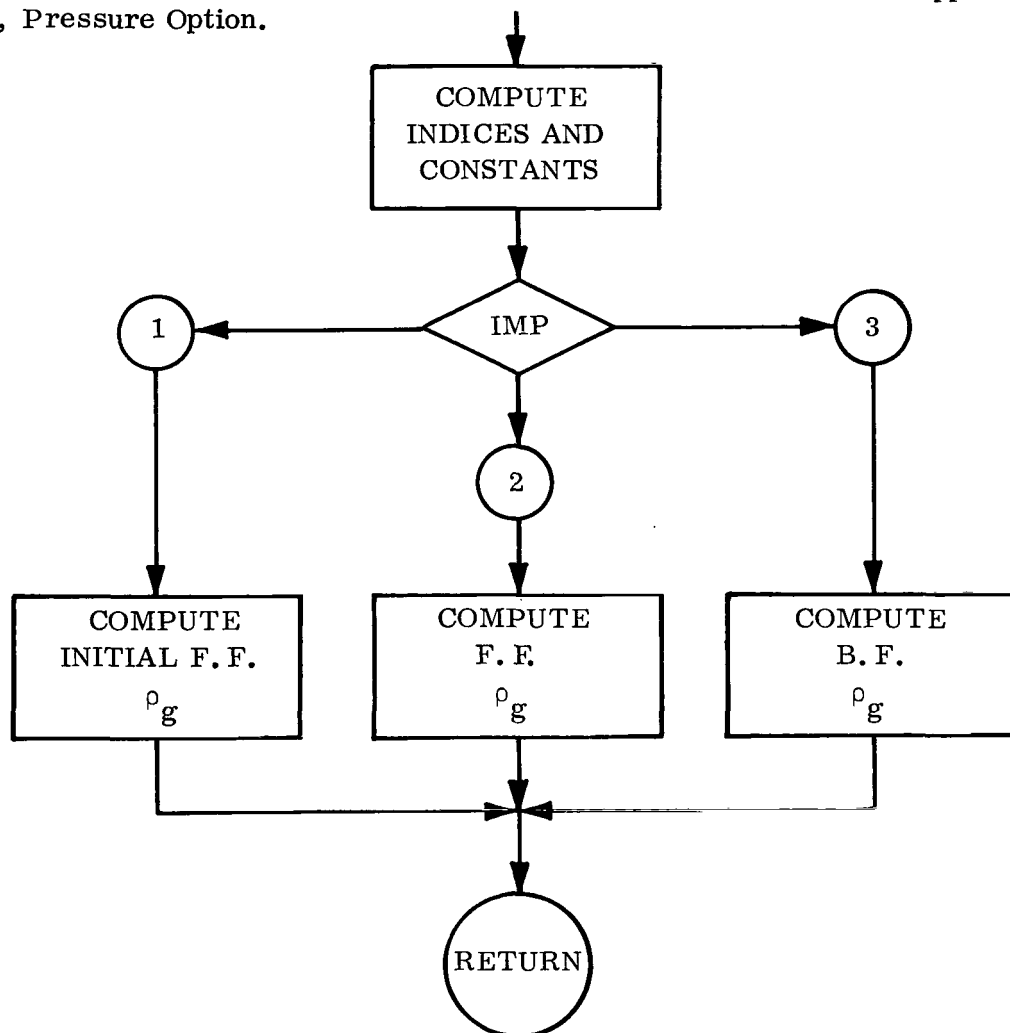
IM control for computed GE TO

Routines in Transfer Vector:

NONE

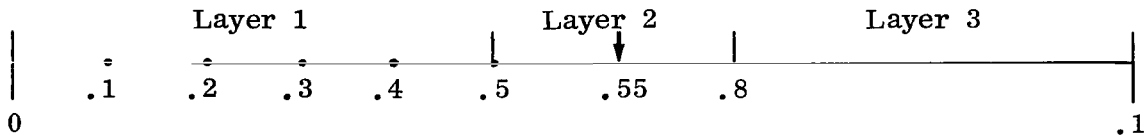
Purpose:

To compute the gas density at the front face, and back-face discussed in Appendix B, Section X, Pressure Option.



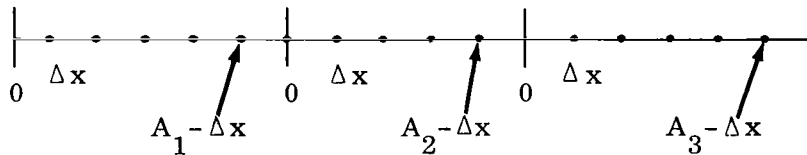
The XLOC array is the array of coordinates and is computed in the routine RITER. If Cylindrical or spherical coordinates are computed, then COORD is also used.

For the Cartesian system the coordinates are consecutively increasing through all layers.



For the cylindrical and spherical the XLOC array represents the actual radial position, consecutive through all layers; increasing or decreasing depending on the direction of the heat flux.

The XRAY in the subroutine OUTPUT is the coordinate of each point in the layer, i.e. $0 \leq \text{XRAY} \leq A_L$ in each layer, A_i .



RITER

Calling Sequence:

CALL RITER (\bar{KON})

where:

$\bar{KON} = 1 \equiv$ Compute the r values, the x values, and the η derivatives

$\bar{KON} = 2 \equiv$ Compute only the r values.

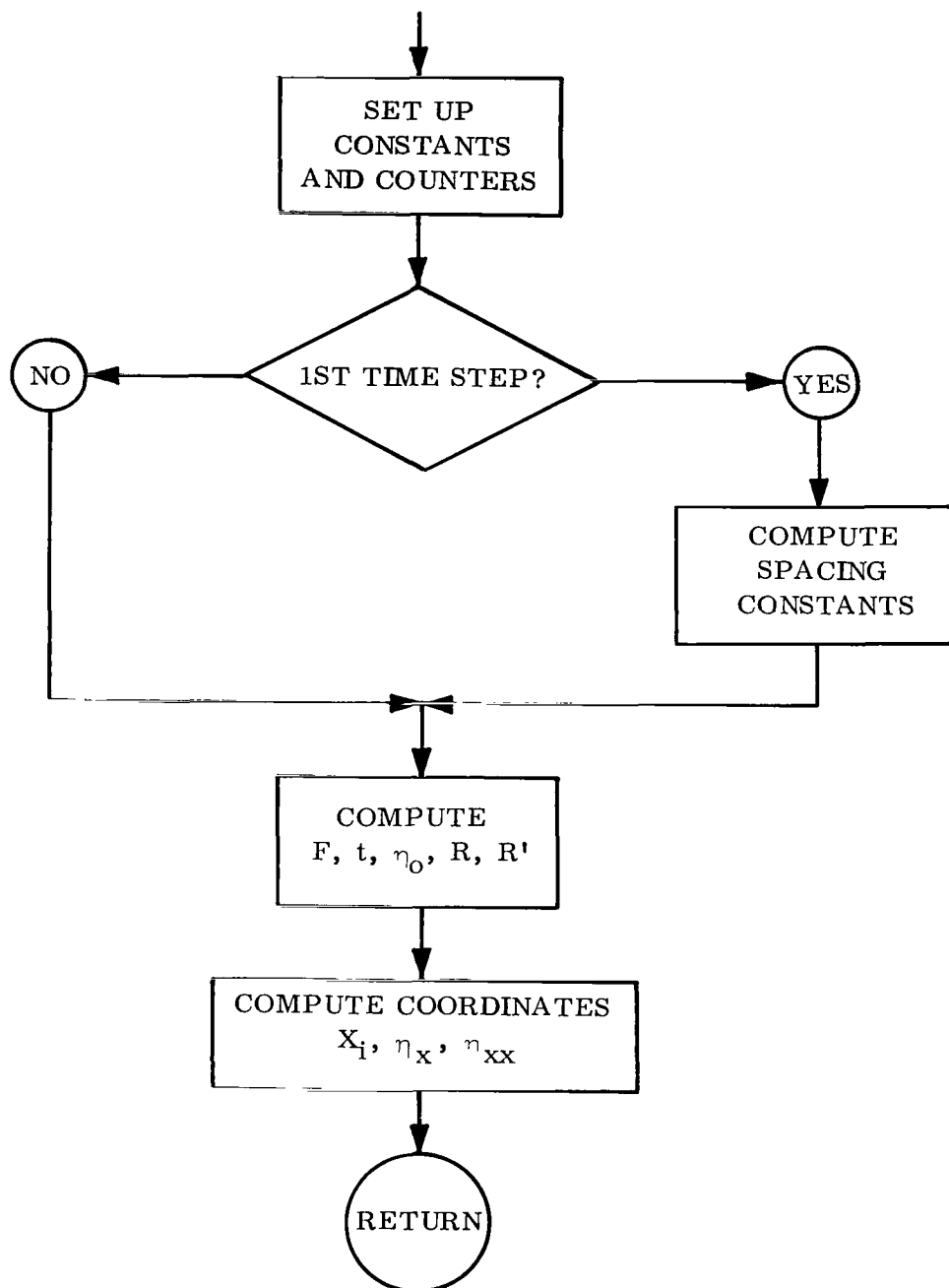
$\bar{KON} = 3 \equiv$ Compute the x values and the η derivatives.

Routines in the Transfer Vector:

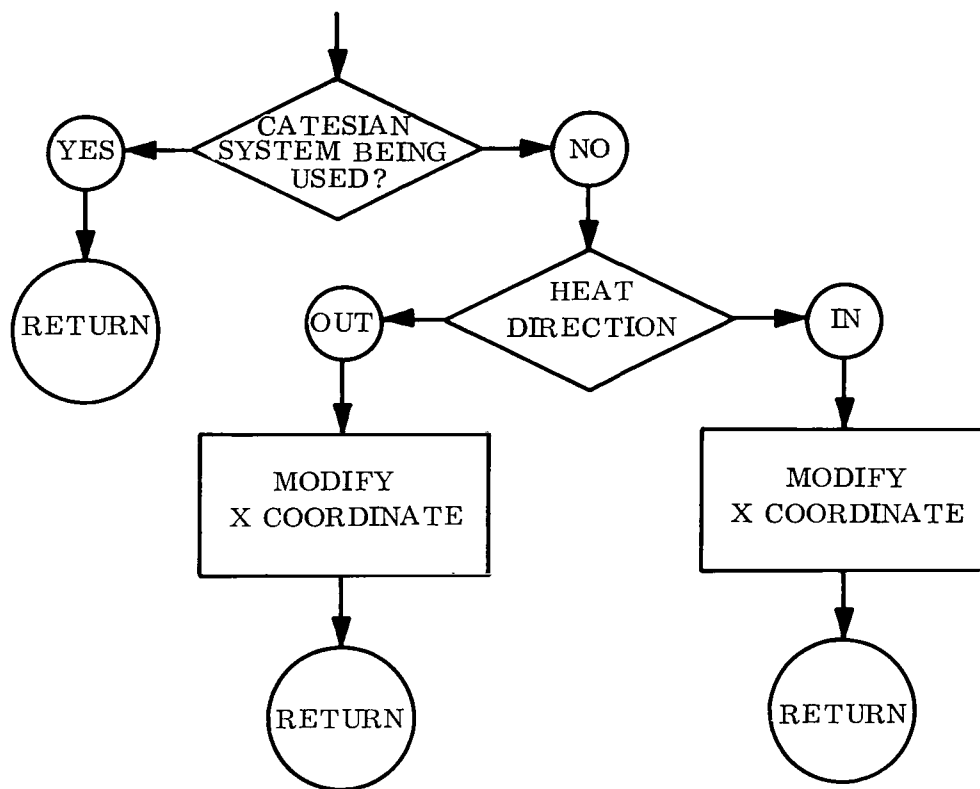
COORD

Purpose:

The purpose of this routine is to compute the r or spacing parameters, the x or coordinates of the body and the η or spacing derivatives. The equations are discussed in Appendix B, Section VII and Appendix B2.



COORD



STARTT

Calling Sequence:

CALL STARTT

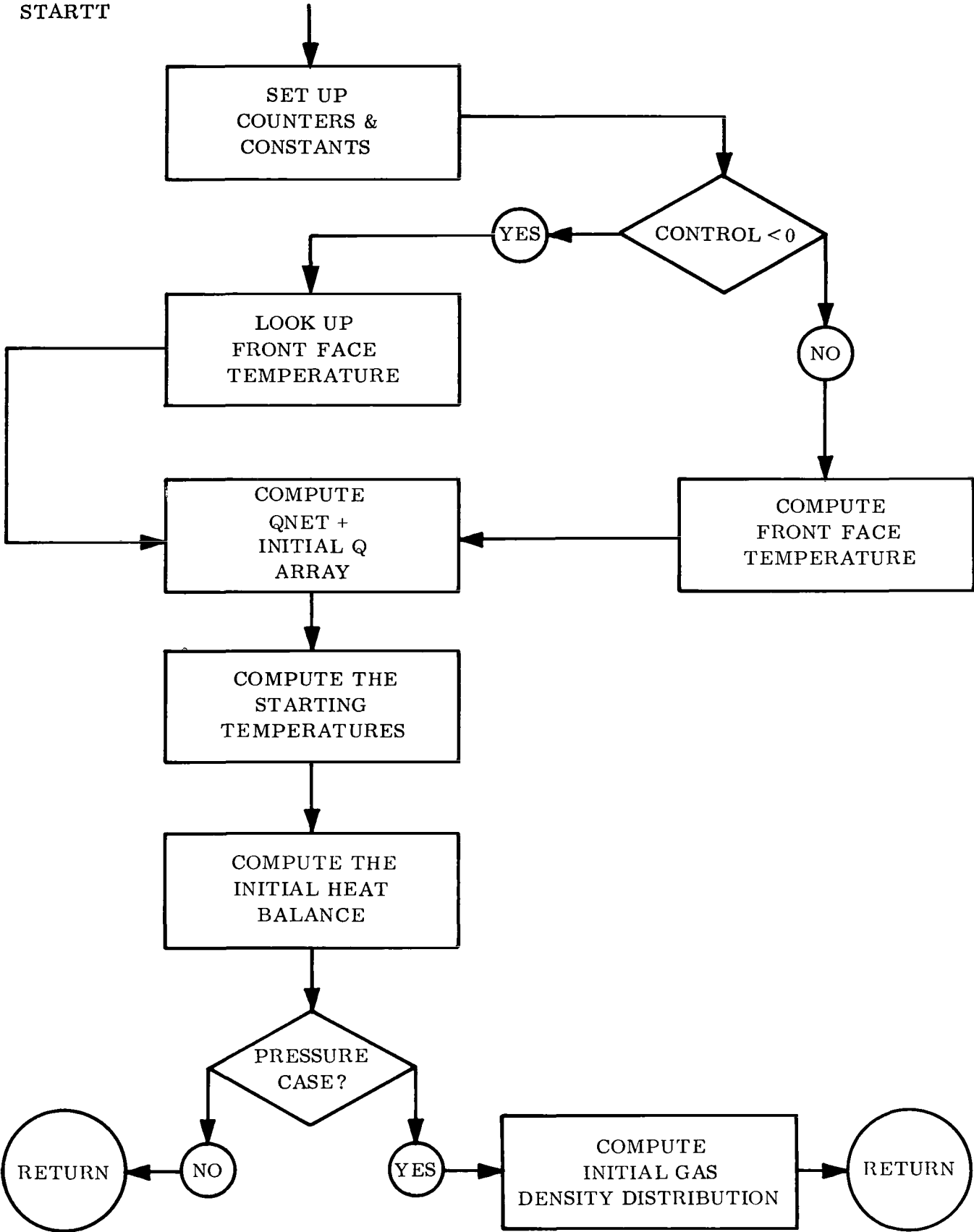
Routines in the Transfer Vector:

QNET	TNEST
DPRESS	CLPOLY
TABUP	CHARP
HTBLNS	

Purpose:

The purpose of this routine is to compute the initial temperature, density, and gas density distributions. The equations are discussed in Appendix B, Sections VI and IV.

STARTT



TABOUT

Calling Sequence:

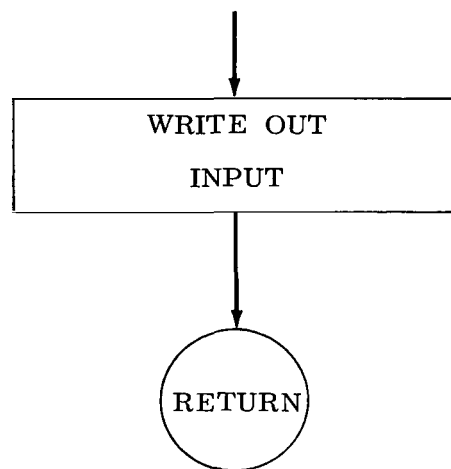
CALL TABOUT

Routines in the Transfer Vector:

NONE

Purpose:

To point out the input tables.



TABUP

I Title: Table look-up

II Type: Subroutine

III Calling Sequence:

CALL TABUP (TABIND, TABDEP, VARIND, VARDEP, NENTRY, KIN)

Where:

TABIND: Location of independent table

TABDEP: Location of dependent table array

VARIND: Location of independent variable

VARDEP: First location of dependent variable answers

NENTRY: Number of values in independent table

KIN: Numerical code for dependent table look-up

1. Positive sign means one table look-up. Numerical value determines number of table in dependent table array from which to obtain dependent variable answer.
2. Negative sign means there may be more than one table look-up. Numerical value determines number of tables starting from the first table in the dependent table array on which to perform a table look-up.

IV Table Formats

A. Dependent Table Format

Each table consists of $NENTRY + 1$ values. The last value in the table ($NENTRY + 1$ element) must be either a zero or 1

0 = means dependent table is constant

1 - means there is a variable dependent table

All the tables are read into the same array using Hench's input formal.

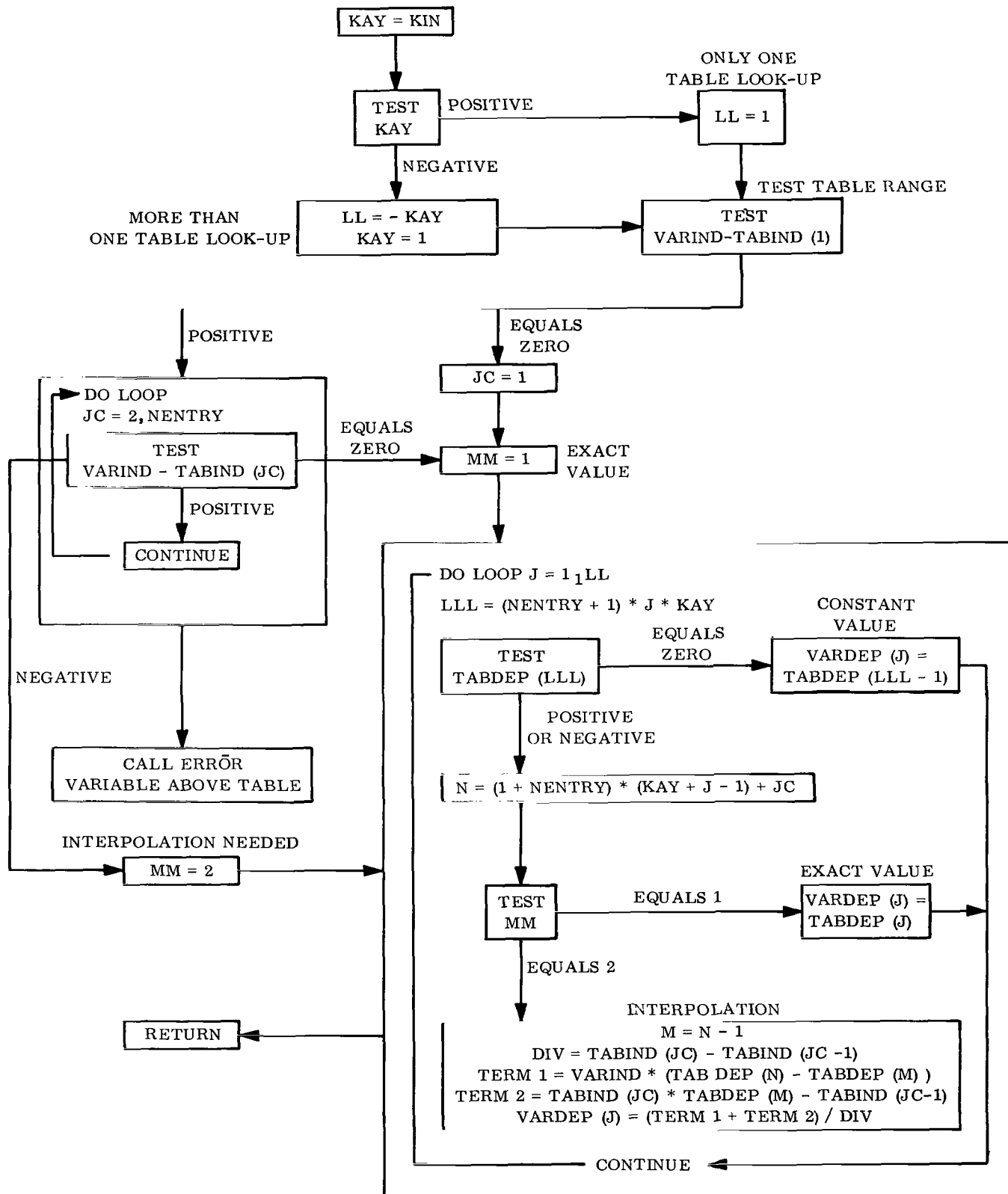
B. Independent Table Format

Array must be in ascending order

V Method: If table is constant, the value in the table is stored immediately in answer array.

For a variable table, the location of the independent variable in the independent table is determined. Linear interpolation is used in the independent table or tables specified by the "KIN" element in the calling sequence. If the independent variable should fall outside the table range, there will be an error print out.

TABUP (TABIND, TABDEP, VARIND, VARDEP, NENTRY, KIN)



TNEST

Calling Sequence:

CALL TNEST (X, Y, E)

Where:

X = Computed guess

Y = The initial guess for the first time through; after this, it is a floating point control to signify convergence or non-convergence

E = The convergence criterion

E = -, Indicates first time through TNEST for any particular iteration

E = +, Indicates after first time through TNEST for any particular iteration.

Routines in the Transfer Vector:

NONE

Remarks: Iteration control for this routine is external. A fixed point Y is interrogated by a computed go to, upon returning from TNEST.

KY = 1, indicates convergence

KY = 2, indicates non-convergence

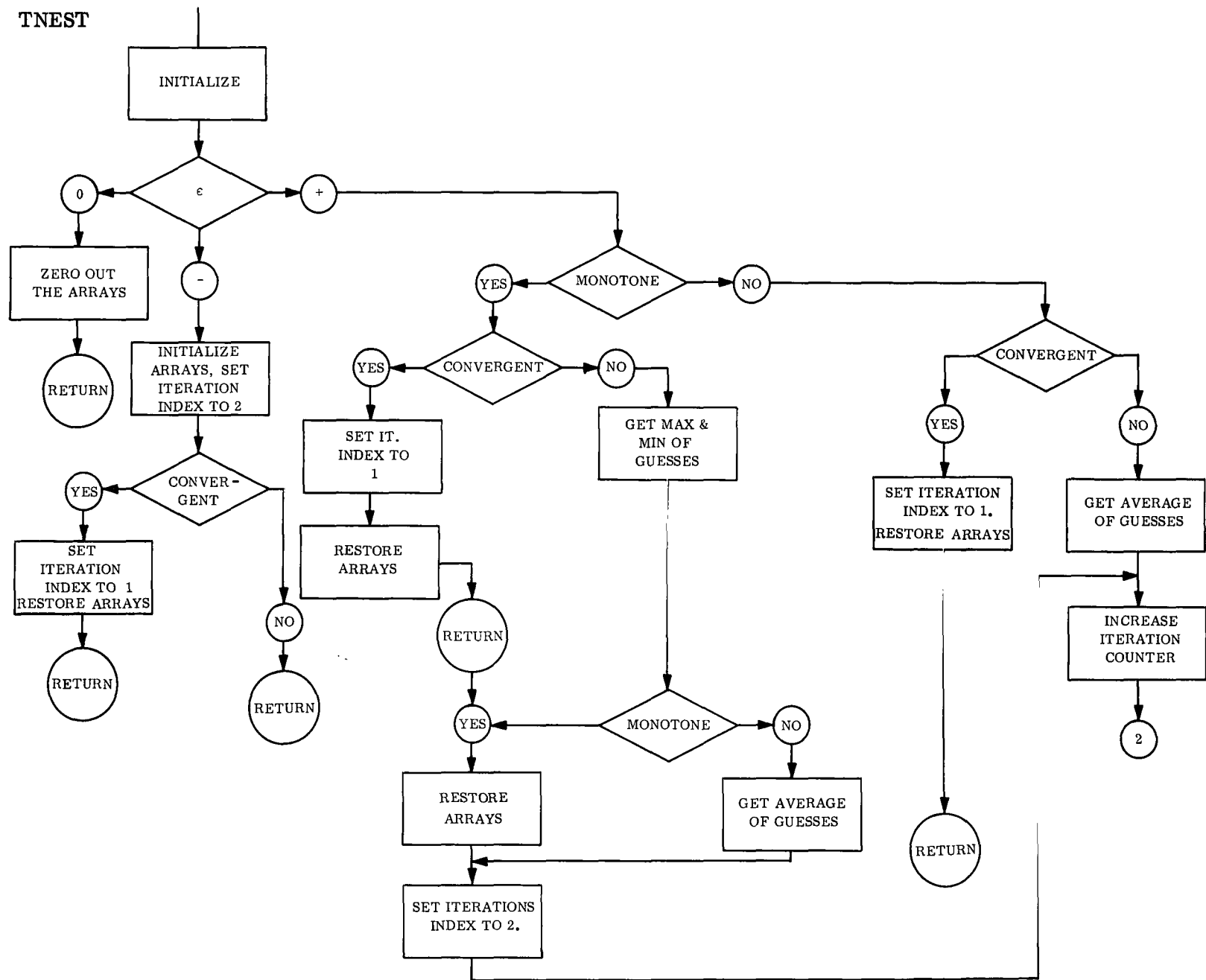
KY = 3, indicates non-convergence for 50 tries and re-try the first 15 attempts.

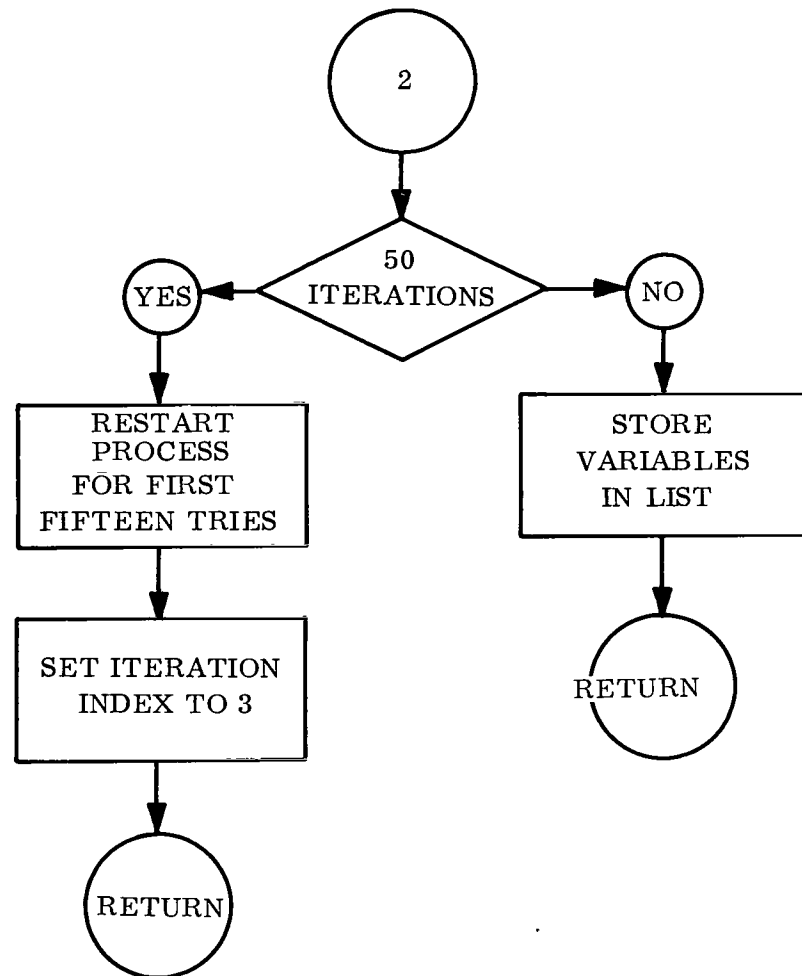
Any printout referring to variables used in computation is external to TNEST.

Purpose:

This routine solves the equation $x - f(x)$ using the equations and methods described in Appendix C3.

TNEST





WDP

Calling Sequence:

CALL WDP (II, L)

Where:

II \equiv the nodal index

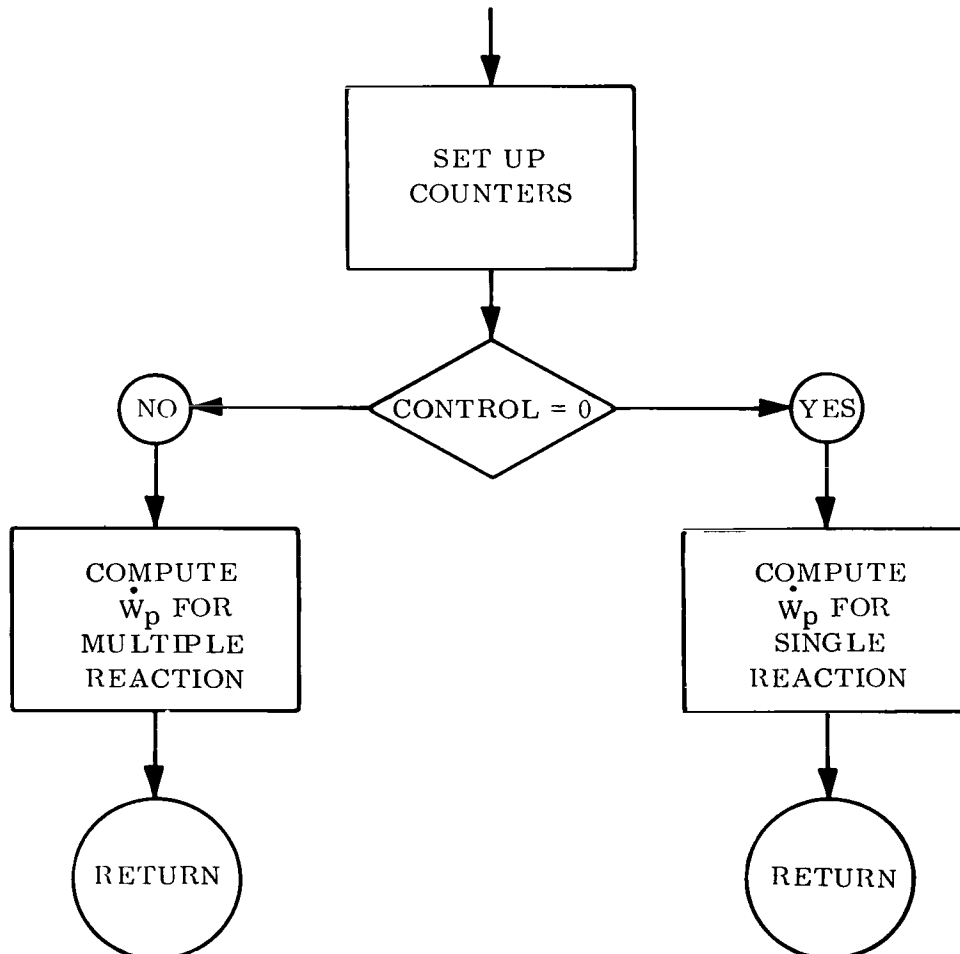
L \equiv the layer

Routines in the Transfer Vector:

TABUP

Purpose:

To compute the \dot{w} of the node. The equations are discussed in Appendix B, Sections II and IV.



APPENDIX E

USER'S MANUAL FOR THE

ONE DIMENSIONAL HEAT CONDUCTION PROGRAM

SECTION I - PROBLEM DESCRIPTION

The "One Dimensional Heat Conduction Program" is programmed in the FORTRAN IV language and for the I. B. M. 7094 digital computer.

The program solves the general parabolic differential equation

$$T_t = B_1 T_{xx} + B_2 (T_x)^2 + B_3 T_x + B_4$$

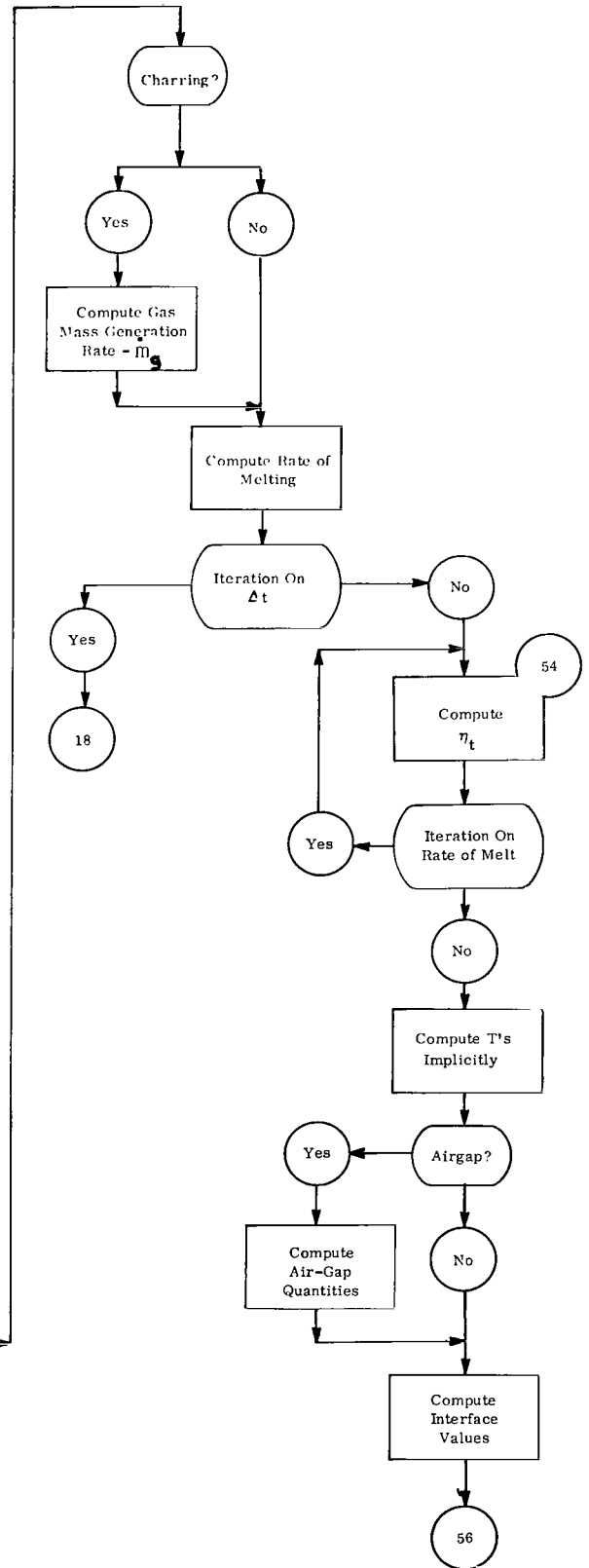
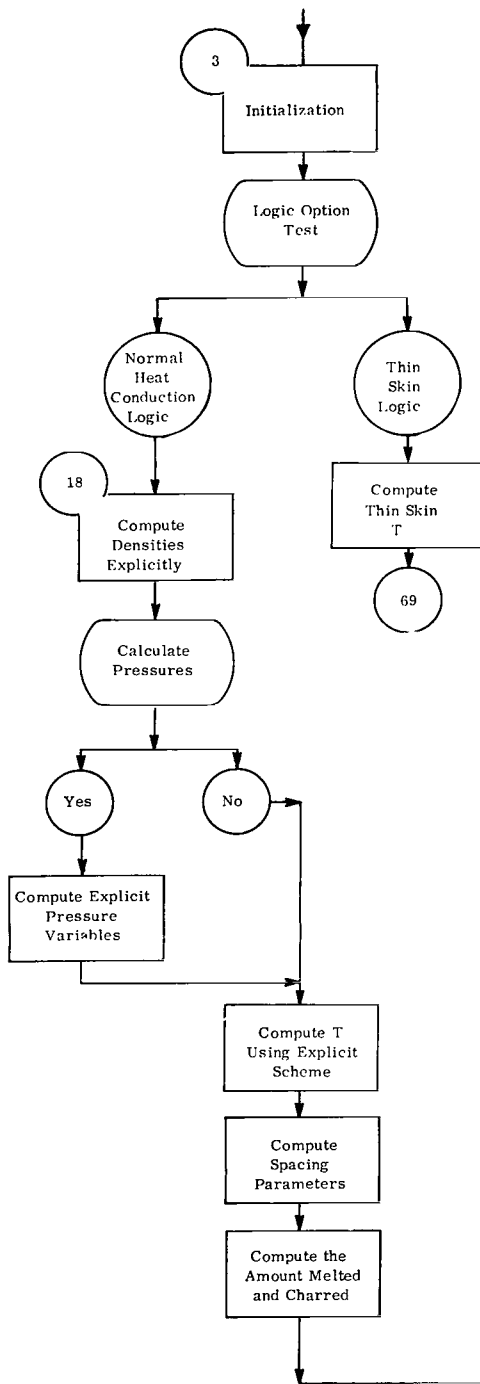
The mathematical derivations are found in the preceding appendices.

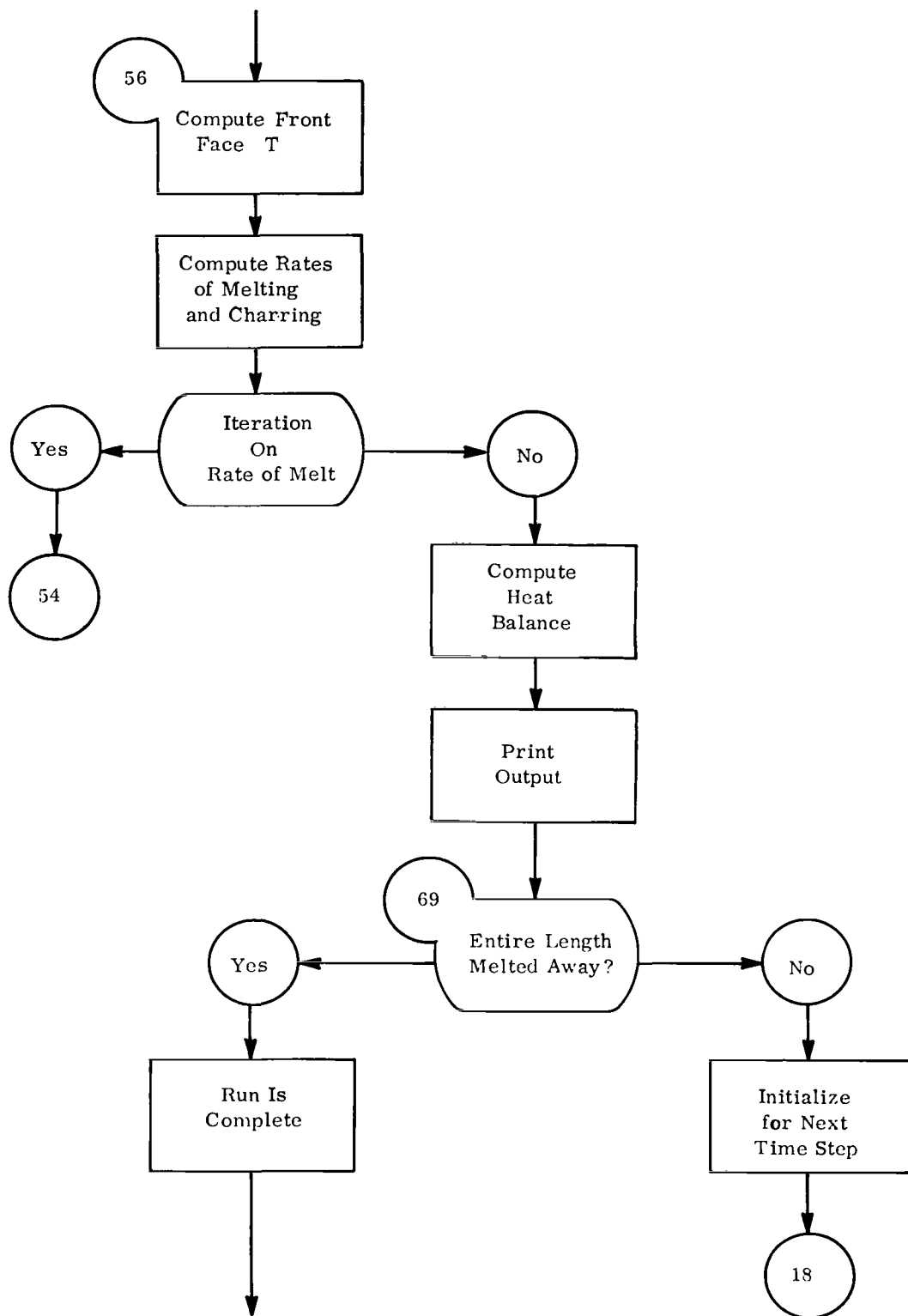
The remaining pages of this section concern themselves with a general flow chart of the program.

FLOW CHART OF THE ONE DIMENSIONAL HEAT CONDUCTION PROGRAM

1. Read in input.
2. Do initialization procedure:
 - a. Expand tables
 - b. Store constants
 - c. Start counters
3. Print out input.
4. Set up initial spacing in the first layer.
5. Compute the η_t 's.
6. Compute the starting T's, ρ 's, and pressures.
7. Compute the Δt .
8. Compute the γ coefficients.
9. Calculate the point to start the explicit computation.
10. Check to see if you are past the stop time:
 - a. YES - Skip to 34
 - b. NO - Continue on
11. Check if this is a thin skin run:
 - a. YES - Call routines for thin skin computations and skip to 32
 - b. NO - Continue on
12. Calculate the densities explicitly.
13. Check for pressure computation:
 - a. YES - Do pressure calculations, and continue on
 - b. No - Continue on
14. Calculate the temperatures of the interior points by using the explicit scheme.
15. Set up the spacing for the time step being computed.
16. Compute the amounts melted and charred.
17. Check if this is a charring run:
 - a. YES - Compute \dot{m}_g and go to 18
 - b. No - Continue on
18. Compute the rates of melting.
19. Set up the constants for iteration on the rate of melt if necessary.
20. Compute the Δt for the iteration.
21. Check to see if there was a change in Δt .
 - a. YES - Compute the γ coefficients and return to 12
 - b. NO - Continue on
22. Compute the η_T 's.
23. Check if iteration of the rate of melt is necessary on the explicit points only:
 - a. YES - Compute the interior points explicitly, calculate the frontface T and the rates of melt and char then return to 22
 - b. NO - Continue on
24. Compute the interior points implicitly.
25. Compute the values for the inter-faces.
26. Compute the values of the air-gap, if there is one.
27. Compute the T, ρ , and pressure of the frontface.
28. Compute the rates of melting and charring.

29. Check to see if iteration is necessary due to rate of melt:
 - a. YES - Return to 22
 - b. NO - Continue on
30. Calculate the heat balance check.
31. Print the output.
32. Check to make sure that the entire length is not charred or melted away:
 - a. YES - Job completed, go to 34
 - b. NO - Continue on
33. Initialize for next time step and return to 7
34. Run is completed. Initialize for new case and return to 1





SECTION II-A

GENERAL DESCRIPTION OF INPUT FOR THIS PROBLEM

For this particular problem, all of the input except the Hollerith identification card is in table form.

Single value inputs are grouped into pseudo tables and the values acquire their identity by storing them in specific locations.

All independent tables must be in ascending order.

The dependent tables may be read into the machine in one of three ways: one value, two values or an entire table. If one value is used, the program assumes the table to be constant and fills it in according to the number of entries in the independent table. If there are two values, the program interpolates to fill in the table. Any amount over two is assumed to be the entire table, so the data items are just stored in core as they are on the input card.

If there are several tables under one table name, as in TTABL, a comma is used to separate them. The comma is also used to separate the tables dependent on layers. The tables are as follows:

ATETB, CTABL, GASPR, HTABL, PROPT, TTABL, ZORET

The tables need not be in any specific order when they are read in, except if the number of input items exceeds one card (then these cards must be in proper order, but not necessarily consecutive), also only the tables that are necessary need be read in.

In running consecutive cases, only the tables that change need be read in, for the cases that follow the first one. When the machine encounters a table name, it stores the new table over the old input. If certain values were numbers in the first case and are to be zero in the second, it is best to read in the zero for the second case.

One must keep in mind if data is to be retained for the second case.

Only the tables that are changes must be read in along with a new I. D. card.

Over thirty tables may be read in as input. Normally, one does not need to use every table, due to one's choice of options.

The next few pages list each table and give brief summaries of their contents.

SECTION II-B

This section indicates what variables are punched or included in each individual table or card. At the NASA-LEWIS Research Center, the input is entered according to the specifications of the input routine by John MacKay described in Section 5 of the NASA-LEWIS Research Center LR94 Monitor Programmer Reference Manual, dated 8/18/64.

The first physical card of the input must be a Hollerith Alpha-numeric identification card. Columns 1 through 72 may be used.

The second group of cards must be the group of cards forming TABLN or the group of cards with the array names.

Immediately before the TABLN cards, a \$D=1 card must follow, the \$ being in column one.

Then the array data cards may follow.

The last physical card of the input deck may either be a \$END or a \$DATA card; either will terminate the reading of input.

GENRL TABLE

The GENRL table includes options, constants, and variables which would not conveniently fit into any other table, hence a general table.

This table has a dimension of 20. However, not all of these locations are used at present.

GENRL (1)	t_o	Initial time to start run.
GENRL (2)	t_s	Time to stop run.
GENRL (3)	Δt	$\left\{ \begin{array}{l} -\Delta t \text{ analytic solution assuming jump heat flux used to time } t_o + \Delta t . \\ +\Delta t \text{ analytic solution assuming linear heat flux used to time } t_o + \Delta t. \end{array} \right.$
GENRL (4)	T	Initial starting temperature.
GENRL (5)		<p>This entry affects the first entry in the TTABL table. For the first TTABL entry to be the:</p> <p>A. <u>Convective Heat Flux</u>: \dot{q}_c -- enter a zero. B. <u>Film coefficient</u>: $\dot{q}_c / \Delta h_c$ -- enter a plus one. C. <u>Frontface T</u>: T_w -- enter minus one.</p>
GENRL (6)	L	Total number of layers.
GENRL (7)		$\left\{ \begin{array}{l} 1. = 5\text{th TTABL table is the backface T.} \\ 0. = 5\text{th TTABL table is the backface } \dot{q}. \end{array} \right.$
GENRL (8)	t_{int}	$\left\{ \begin{array}{l} \text{A zero} \end{array} \right.$
GENRL (9)		$\left\{ \begin{array}{l} +r_L \Rightarrow \text{Cylindrical Coordinates radius in ft.} \\ 0 \Rightarrow \text{Cartesian Coordinates} \\ -r_L \Rightarrow \text{Spherical Coordinates radius in ft.} \end{array} \right.$
GENRL (10)		$\left\{ \begin{array}{l} 0 \dot{q} \text{ direction is the normal one from the outside toward the center} \\ 1.0 \dot{q} \text{ direction is from the center to outside} \end{array} \right.$
GENRL (11)		$\left\{ \begin{array}{l} 0 \text{ output dimensions in ft.} \\ 1.0 \text{ output dimensions in inches.} \end{array} \right.$
GENRL (12)		The number of ordered pairs of Z and E for the multiple reaction equation.

THKN TABLE

This is the table for the thickness of each individual layer. The table has a dimension of ten (10), (i.e., one entry for each layer). All thicknesses should be in feet.

DENSE TABLE

This is the table for the initial density of each layer. The table has a dimension of ten (10), (i.e., one for each layer.) All densities should be in lb/ft^3 .

For an air-gap run, the C_p for the air-gap instead of the density, is entered on this card.

PTSIN TABLE

This is the table for the interior points of each layer. The table has a dimension of ten (10), (i.e., one entry for each layer). The maximum number of points for all ten layers is 149.

The program tests each entry because:

- a. A zero in the appropriate layer entry is used to indicate the air-gap layer. (Please bear in mind that the air-gap may not be the first layer, and that the AGPTB card must be used.)
- b. A one in the first entry, for one layer only, determines the temperature and \dot{q}_{net} for a thin skin with little or no temperature gradient.

RESTRICTIONS AND CHARACTERISTICS OF THIS COMPUTATION

1. There may be only one layer of material.
 2. There is no charring.
 3. The conductivity of the layer does not need to be read in.
 4. This option of the program should be used if the differences in T are in the third to eighth significant digits, otherwise the normal program may be used with appropriate adjustments to Δt , Δx , and the EPTAB table.
 5. All other input is normal.
- c. A number greater than one in the first entry means that the general heat conduction program will be used.

DTIME TABLE

This table enters up to ten (10) Δt_0 , which are chosen by the user and ten (10) cut-off times (i.e., one for each Δt_0). The entries are alternated $\Delta t_0, t_0, \Delta t_1, t_1, \dots, \Delta t_n, t_n$ with the Δt followed by its corresponding cut-off time.

One does not need to use all of the Δt 's. If one or two changes in Δt will do your job, then you only need enter one or two Δt 's. Any entries that are ignored will be assumed to be zero.

DTIME (1)	= Δt_1	= First increment of time used
DTIME (2)	= t_1	= Cut-off time for Δt_1
DTIME (3)	= Δt_2	= Second increment of time used
DTIME (4)	= t_2	= Cut-off time for Δt_2
\vdots	\vdots	
DTIME (n-3)	= Δt_{n-1}	= (N-1) increment of time used
DTIME (n-2)	= t_{n-1}	= Cut-off time for Δt_{n-1}
DTIME (n-1)	= Δt_n	= Final increment of time used
DTIME (n)	= t_n	= Cut-off time for Δt_n

SPACE TABLE

The space table controls the spacing of points in the first layer. If uniform spacing is desired, please leave card out of run. If spacing as a function of time is desired, then space (1) must be a one.

SPACE (1) = Option Space

SPACE (2) = η_1 = Degree of Squeezing at time = 0.

SPACE (3) = η_2 = Degree of Squeezing at t_1 .

SPACE (4) = η_3 = Degree of Squeezing at final time.

SPACE (5) = t_1 = Time for η_2 to take effect.

SPACE (6) = C = Factor to increase squeezing at the backface ($0 \leq C < 8$).

If squeezing is desired, it must be kept in mind that the squeezing is toward the frontface, if η_1 , η_2 and η_3 are greater than 1.0 and toward the backface, if η_1 , η_2 and η_3 are less than 1.0 but greater than zero. Normally, the squeezing is less than 8 to 10. Again, quantities not entered will be assume to be zero.

If constant squeezing is desired for the entire run, just fill in SPACE (1) and SPACE (2).

Please refer to Appendix B for a discussion of the transformation used.

OUTTB TABLE

The OUTTB table controls the frequency of the print-out. The OUTTB table has a dimension of 25. The first 18 locations are taken up by the alternating sequence of time step per print-out, followed by the cut-off time. OUTTB (19) is the option for the heat balance calculation at equally spaced points.

OUTTB (1) = f_1 = Time step per print-out.

OUTTB (2) = t_1 = Cut-off time for f_1 .

OUTTB (3) = f_2 = Second time step per print-out.

OUTTB (4) = t_2 = Cut-off time for f_2 .

\vdots

OUTTB (15) = f_8 = Eighth time step per print-out.

OUTTB (16) = t_8 = Cut-off time for f_8 .

OUTTB (17) = f_9 = Final time step per print-out.

OUTTB (18) = t_9 = Cut-off time for f_9 .

OUTTB (19) = Option for heat balance calculation. The heat balance calculation checks how the T distribution is behaving. It does not have any effect on any computations. If (on the output) "INT QNET" and QI TOTAL" are close to each other, then the T distribution is behaving well. If they are not close, check for oscillations or some other perturbation.

A zero means the program performs the calculation. A one tells the program to skip the computation.

OUTTB (20) = Option to print temperatures at equally spaced points in the first layer. This is helpful, if there is squeezing, or melting.

A zero indicates to the program to print the temperatures.

A one indicates to the program to skip the calculations and this part of the print-out.

HORA TABLE

The HORA table is the independent time table and has room for 50 entries. The only table dependent on the HORA table is the TTABL. The description of the TTABL is on the following page.

TTABL TABLE

The TTABL TABLE is actually one large table made up of several smaller tables, each of which is dependent on time.

One must be sure to check the options in GENRL (5), GENRL (7), and TMELT (1).

1. Dependent on GENRL (5), but whatever option the entry is entered as one table.
 - a. GENRL (5) = 0., then the entry is convective heat flux (\dot{q}_c).
 - b. GENRL (5) = 1., then the entry is the film coefficient ($\dot{q}_c / \Delta h$).
 - c. GENRL (5) = -1., then the entry is the frontface temperature (T_w).
2. h_r (BTU/LB), or T_r (°R) entered as one table. If TTABL 2 is T_r (recovery temperature) then C_{P61} in HTABL must be set equal to 1.0 for all values of temperature.
3. \dot{q}_{hgr} (BTU/ft² sec), entered as one table.
4. If TMELT (1) = 2, this array is P_e (psf) the static pressure at the edge of the boundary layer. For all other values of TMELT, this array is empty.
5. Backface T or \dot{q} if desired, entered as one table. (Check GENRL (7).)
6. Empty array, entered as 0.0, except when the refrasil or the fixed melting "T" option is used. It then is ρL (BTU/ft³)
7. The following are entered here, depending on TMELT (L):
 - a. TMELT (1) = 1, the array is the specified char length (S_{cm})
 - b. TMELT (1) = 2, the array is the K_1 constant for the sublimation equation
 - c. TMELT (1) = r, the array is the Γ^1 (dimensionless) of the fixed melting "T" option.Otherwise, the array is empty and entered as a 0.0.
8. The following is entered here, depending on TMELT (1):
 - a. TMELT (1) = 1, the array is a derivative of TTABL (7). If the array is entered as a zero, the program will compute the S'_{cm}
 - b. TMELT (1) = 2, the array is the K_2 constant for the sublimation equation.
9. An empty array.
10. An empty array.

TMELT(1)	OPTION	TTABL TABLE	TTABL(1)	TTABL(2)	TTABL(3)	TTABL(4)	TTABL(5)	TTABL(6)	TTABL(7)	TTABL(8)	TTABL(9)	TTABL(10)
0	NO MELTING	\dot{q}_c , or $\frac{\dot{q}_c}{\Delta h}$, or T_w	h_r	\dot{q}_{hgr}		T_{BF} or \dot{q}_{BF}						
1	SPECIFIED CHAR LENGTH	\dot{q}_c , or $\frac{\dot{q}_c}{\Delta h}$, or T_w	h_r	\dot{q}_{hgr}		T_{BF} or \dot{q}_{BF}		s_{cm}	s'_{cm}			
2	GRAPHITE SUBLIMATION	\dot{q}_c , or $\frac{\dot{q}_c}{\Delta h}$, or T_w	h_r	\dot{q}_{hgr}	P_e	T_{BF} or \dot{q}_{BF}		K_1	K_2			
3	REFRASIL	\dot{q}_c , or $\frac{\dot{q}_c}{\Delta h}$, or T_w	h_r	\dot{q}_{hgr}		T_{BF} or \dot{q}_{BF}	ρL					
4												
5	FIXED MELTING T	\dot{q}_c , or $\frac{\dot{q}_c}{\Delta h}$, or T_w	h_r	\dot{q}_{hgr}		T_{BF} or \dot{q}_{BF}	ρL	Γ				

WARM TABLE

The WARM table is the independent temperature table for the H_{gf} , C_{pg} , H_{cg} , M , C_p , K , dK/dT , $C_{p_{BL}}$, ϵ_{ff} , C_p L. It allows up to a maximum of twenty (20) entries.

GASPR TABLE

This, too, is a composite table made up of the following individual tables. (Each table is again entered in its entirety, before entering the next table):

1. H_{gf} - Heat of Gas Formation (BTU/LB)
2. C_{pg} - Specific Heat of Gas (BTU/LB °R)
3. H_{cg} - Latent Heat of Cracking (BTU/LB °R)
4. M - Average Molecular Weight

PROPT TABLE

This is also a composite table made up of the following:

1. C_p - Specific Heat (BTU/LB °R)
2. K - Conductivity (BTU/ft sec °R)
3. dK/dT - Derivative of K

Now, since the properties may vary with different layers, one must not only separate the individual tables, but also separate the tables by layers.

For layer 1, read in all the values of the C_p table, then all the values of the K table and all the values of dK/dT and then follow the same procedure for all the layers following.

If one wishes, the dK/dT table can be computed by the machine. This is accomplished by entering a zero for the dK/dT table for each layer.

For an air-gap run, it must be remembered that the ρ of the air-gap as a function of temperature must be read in the part of the table that normally the C_p would go into, and the C_p of the air-gap is entered into the DENSE table in the appropriate location.

CTABL TABLE

This is a temperature dependent table of the boundary condition, $\rho C_p L$ (BTU/ft² °R), for each layer. It can be visualized as a very thin layer of material attached to the previous layer. The ρ is the density of the thin layer, the C_p is the specific heat and L is the thickness of the layer.

HTABL TABLE

This table is a composite, temperature dependent table made up of the table of $C_{p_{bl}}$ specific heat of boundary layers gases and ϵ_{ff} (the product of surface emissivity and configuration factor between the point radiating and the sink).

CHART TABLE (If there is no charring, this table is to be deleted)

This is the table of the char properties. Only the first layer is allowed to char.

The options are as follows:

A. Non-Pressure Dependent

- Chart (1) = 1.
 Chart (2) = ρ_c Density of char
 Chart (3) = η Order of reaction
 Chart (4) = t_t (Trip time for R_e) - time after which boundary layer is turbulent
 Chart (5) = N_1 Parameter for K_a
 Chart (6) = C_1 Parameter for K_r
 Chart (7) = N_2 Parameter for C_{pa}
 Chart (8) = C_2 Parameter for C_{pa}
 Chart (9) = $\frac{m_2}{m_1}$ Constant for laminar flow in \dot{q}_{block} equation
 Chart (10) = P_r Constant for laminar flow in \dot{q}_{block} equation
 Chart (11) = C_T Constant for turbulent flow in \dot{q}_{block} equation
 Chart (12) = δ where:

$$x_t = \int_0^t \frac{t m_g}{(\rho_{vp} - \rho_c)} dt + , x_2 = 1^{st} \text{ point still at } .97 (\rho_{V_p})$$

$$\text{and } S_c = (1-\delta) x_1 + \delta x_2$$

$$0 < \delta < 1$$

Used with the specified char length option.

where: $K_a = (1-C_1) + C_1 \left(\frac{\rho - \rho_c}{\rho_{vp} - \rho_c} \right)^{N_1}$

$$C_{pa} = (1-C_2) + C_2 \left(\frac{\rho - \rho_c}{\rho_{vp} - \rho_c} \right)^{N_2}$$

If it is desirable for the K of the material to be the same as the K for the char, it is recommended that $C_1 = 0$ and $N_1 = 1$.

If it is desirable for the C_{pa} of the material to be the same as the C_{pa} for the char, it is recommended that $C_2 = 0$ and $N_2 = 1$.

The n is used in the following:

$$\dot{W}_p = -Z \rho_{vp} \left(\frac{\rho - \rho_c}{\rho_{vp}} \right)^{(n)} e^{-E/RT}$$

Notice that the quantities Z , E are introduced here. These quantities are entered in the ZORET table.

B. Transient Pressure Option (The previous CHART Table is replaced with the following)

CHART (1)	= 2	
CHART (2)	= ρ_c	Density of char
CHART (3)	= n	Order of reaction
CHART (4)	= t	(Trip time for Re_s : Time after which boundary layer is turbulent).
CHART (5)	= ϵ_f	Final porosity
CHART (6)	= Γ	Gasification factor
CHART (7)	= m	Parameter for k/E $1 < m < 3$
CHART (8)	= $\tilde{\rho}_c$	Density of char based on actual char volume
CHART (9)	= m_2/m_1	Constant for laminar flow in \dot{q}_{block} equation.
CHART (10)	= Pr	Boundary layer gas Prandtl number
CHART (11)	= C_T	Constant for turbulent flow in \dot{q}_{block} equation
CHART (12)	= $\rho_p = \rho_{vp}$	Virgin plastic density

where:

$$\Gamma = 1 - \frac{\rho_c}{\rho_{vp}}$$

$$k/\epsilon = k_f \epsilon^{(m-1)}$$

In addition to the above CHART Table, a PVAT table and a new PROPT Table are required for the pressure option.

PVAR Table

PVAR (1)	= K_g	Average thermal conductivity of the ablation gases
PVAR (2)	= K_c	Average thermal conductivity of the char
PVAR (3)	= K	Average thermal conductivity of the virgin plastic
PVAR (4)	= \bar{C}_p	Average specific heat of the ablation gases
PVAR (5)	= \bar{C}_{vp}	Average specific heat of the virgin plastic
PVAR (6)	= C_{vc}	Average specific heat of the char
PVAR (7)	= k_f	The final permeability constant
PVAR (8)	= $\bar{R} = 1545 \frac{\text{ft} \cdot \text{lb}}{\text{lb} \cdot \text{mo} \cdot ^\circ\text{R}}$	Universal gas constant
PVAR (9)	= \bar{M}	Average molecular weight of ablation gases
PVAR (10)	= μ	Average viscosity of the ablation gases.

PROPT Table

PROPT (1)	= h_g	The enthalpy of the ablation gases
PROPT (2)	= e_c	The internal energy of the char
PROPT (3)	= e_p	The internal energy of the virgin plastic

When utilizing the pressure option, only one layer may be considered.

TDENS Table

This is the independent density table for the collision frequency (Z) and the activation energy (E) used in:

$$\dot{W}_p = -Z \rho_{vp} \left[\frac{\rho - \rho_c}{\rho_{vp}} \right]^{(n_1)} e^{-E/RT}$$

This table is not needed for a multiple reaction case.

ZORET TABLE

This is a density dependent composite table made up of Z (collision frequency in 1/sec.), E (activation energy in BTU/lb. - mole).

Please keep in mind if a temperature is specified in GENRL (4), that the units of T must agree with the units of R in the above equation.

For a multiple reaction case, we change the format of the table and set it up as follows:

ZORET $Z_1, E_1, Z_2, E_2, \dots, Z_N, E_N, 1 \leq N \leq 10$

TABLE FOR AIR-GAP PROPERTIES

AGPTB TABLE

This is the table for the air-gap properties. This table must be included for an air-gap run. The entries are as follows:

AGPTB (1)	= J	= Layer Number ($1 < J < 10$) of the air-gap	
AGPTB (2)	= Fe	= Emissivity factor	
AGPTB (3)	= Fa	= Radiation view factor	
AGPTB (4)	=	Effective area times conductivity of spacer rod	
AGPTB (5)	=	Viscosity	
AGPTB (6)	=	Vertical height	
AGPTB (7)	= G_1	= g at zero	} coefficients for a parabolic curve fit for g
AGPTB (8)	= G_2	= g at mid-point	
AGPTB (9)	= G_3	= g at end point	
AGPTB (10)	=	EM exponent of X/L	= .11
AGPTB (11)	=	Trip Grashof number	= 2.0E5
AGPTB (12)	=	Coefficient for GR trip	= .2
AGPTB (13)	=	Coefficient for GR trip	= .071
AGPTB (14)	=	Exponent for GR trip	= .25
AGPTB (15)	=	Exponent for GR trip	= .33

If your values for the air-gap entries 10 through 15 coincide with those in the table, you only need enter your values for AGPTB entries 1 through 9.

It must be remembered that for the air-gap layer, the density is a function of temperature and should be entered in the PROPT TABLE where the C_p would normally go, and since the C_p of the air-gap is essentially constant, it is put in the appropriate place in the DENSE TABLE. If there is no air-gap, please delete the AGPTB TABLE and ignore the above paragraph.

CRITERIA TABLE

EPTAB TABLE

This is an epsilon or criteria table for various tests:

EPTAB (1) = ϵ to increase Δt	= .2
EPTAB (2) = Inoperative at this time	= .01
EPTAB (3) = ϵ for frontface T	= .0001
EPTAB (4) = ϵ for air-gap T	= .0001
EPTAB (5) = ϵ for interior T's	= .0001
EPTAB (6) = ϵ for rate of melt	= .01
EPTAB (7) = ϵ for density	= .0001
EPTAB (8) = ϵ for maximum S_m per time step	= 0.0

If these values are acceptable to your problem, the table may be deleted since it is read in automatically.

MELTING OPTION TABLE

TMELT TABLE

This is a table of the melting options and parameters.

TMELT (1) = OPTION	0	NO MELTING
	1	SPECIFIED CHAR LENGTH
	2	GRAPHITE SUBLIMATION
	3	REFRASIL
	4	OPEN
	5	FIXED MELTING T

It seems simpler to take each option separately and define the second to eleventh entries for this table. This is done on the following pages.

TMELT SPECIFIED CHAR LENGTH OPTION

ENTRY	SYMBOL	DEFINITION
TMELT (1)	1	OPTION CONTROL

Other entries are entered into the TTABL.

TMELT GRAPHITE SUBLIMATION

ENTRY	SYMBOL	DEFINITION
TMELT (1)	2	OPTION CONTROL

Other entires are entered into the TTABL.

TMELT REFRASIL

ENTRY	SYMBOL	DEFINITION
TMELT (1)	3	Option Control
TMELT (2)	B_1	Factor used in rate of melt
TMELT (3)	B_2	Exponent of wall temperature in rate of melt
TMELT (4)	B_3	Factor in exponential term in rate of melt.
$\text{Rate of melt} = S'_m = B_1 T_w^{B_2} e^{B_3 - B_3/T_w}$		

TMELT FIXED MELTING T

ENTRY	SYMBOL	DEFINITION
TMELT (1)	5	Option Control
TMELT (2)	T _M	Melting Temperature

STVAR TABLE

If the moments and stresses are being calculated, one indicates moments and stresses are to be computed. Zero means skip computation.

Then:

$$\text{STVAR (1)} = 1$$

$$\text{STVAR (2)} = T_{\text{ref}} = \text{Reference temperature for } \alpha T \text{ table}$$

$$\text{STVAR (3)} = T_{\text{ab}} = T \text{ for which } E(T) = \text{zero}$$

DGREE TABLE

This is the independent-temperature table, with a dimension of 20, for the ATETB Table.

ATETB TABLE

This is a composite table made up of the thermal stresses (αT) for each layer, the derivative of the thermal stresses (αT)', The E-modulus (E) and the derivative of the E-modulus, (E').

The table is temperature dependent with the temperatures being stored in the DGREE table.

The table is used for the calculation of the moments and stresses; if you are not computing these, please delete this table.

The input is set up as follows:

$$(\alpha T)_1, (\alpha T)_1', E_1, E_1', (\alpha T)_2, (\alpha T)_2', E_2, E_2', \dots,$$

$$(\alpha T) \quad , \quad (\alpha T)' \quad , \quad E \quad , \quad E'$$

where the subscripts represent layers.

* The last physical card may be either \$DATA or \$END
with the \$ being in Column I.

In order to provide the user with the flexibility, discussed in the beginning of Section IIA, we need to know the number of entries in each independent table, (i. e. WARM, DGREE, HORA AND TDENS) and also the number of entries in each dependent table or the number of entries of each sub-table of the pseudo tables (i. e. PROPT, CTABL, HTABL, GASPR, ATETB, TTABL, ZORET). The following convention is followed: the bookkeeping cell or array is named by prefixing the counted array by the letter N, hence the bookkeeping cell for the independent temperature array, WARM, is NWARM and the bookkeeping array for the dependent PROPT pseudo table is NPROPT. The cells and array are listed below along with the associated table and dimensions.

<u>BOOKKEEPER CELL OR ARRAY</u>	<u>DIMENSION</u>	<u>COUNTABLE ARRAY</u>
NWARM	1	WARM
NPROPT	30	PROPT
NHTABL	2	HTABL
NCTABL	5	CTABL
NGASPR	5	GASPR
NHORA	1	HORA
NTTABL	10	TTABL
NDGREE	1	DGREE
NATETB	20	ATETB
NTDENS	1	TDENS
NZORET	4	ZORET

The arrays need not be entirely filled. Only as many entries are filled as sub-tables used.

Only those arrays that are necessary to solve the particular problem need be read in; i. e., if there is no charring you need not read in the NGASPR, GASPR, NTDENS, TDENS, NZORET or ZORET arrays.

SECTION III-C

On the succeeding pages are examples of input for the jobs mentioned in Section IV.

This input is the card image.

Please note that the input cards are mixed (i.e., if you take the input form as a standard), and that this does not impair the run.

SAMPLE INPUT FORMAT

\$DATA

TEST CASE 1. FRONT AND BACK-FACE T READ IN WITH CHARRING.

\$D=1

\$TABLN,1=CHART,26=GASPR,131=TDENS,151=ZORET,260.=NATETB,280.=NCTABL,
285.=NDGREE,286.=NGASPR,291.=NHORA,292.=VHTABL,294.=NNU,300.=NPROPT,
330.=NTDENS,331.=NTTABL,341.=NWARM,342.=NZORET,346=TMELT,371=TRAJT,
396=AGPTB,421=DENSE,431=DTIME,456=EPTAB,466=GENRL,491=OUTTB,516=PTSIN,
526=SPACE,536=THIKN,546=PVAR,596=CTABL,806=HTABL,848=PROPT,1478=WARM,
1498=HORA,1548=TTABL,2208=ATE TB,2778=DGREE,3098=NU,3808=STVAR
DENSE=62,

DTIME=.1,10,.2,100,

GENRL=0,60,.1,530,-1,1,1,

OUTTB=.01,1,1,100,

PTSIN=13,

THIKN=.0078,

HTABL=.24,.8,

NHTABL=1,1,

NPROPT=1,1,1,

NWARM=2,

PROPT=.4,.3E-4,0,

WARM =529,7000.,

HORA =0,.25,.5,.8,2,10,20,30,37,50,60,

NHORA=11,

NTTABL=11,1,1,1,11,1,1,

TTABL=530,632,690,727,790,833,874,931,971,961,952,0,0,0,

530,530,530,530,530,562,597,624,642,665,581,

0.,.0025,

CHART=1,12,4,1,0,1,0,1,0,1,.72,1,

GASPR=500,.60,0,30,0,

NGASPR=1,1,1,1,1,

NTDENS=2,

NZORET=1,1,

TDENS=1,1000,

ZORET=.106E13,.463E5,

TMELT=1,

\$END

\$DATA

TEST CASE 2 FRONT AND BACK-FACE T CALCULATED WITH CHARRING.

\$D=1
\$TABLN,1=CHART,26=GASPR,131=TDENS,151=ZORET,260.=NATETB,280.=NCTABL,
285.=NDGREE,286.=NGASPR,291.=NHORA,292.=NHTABL,294.=NNU,300.=NPROPT,
330.=NTDENS,331.=NTTABL,341.=NWARM,342.=NZORET,346=TMELT,371=TRAJT,
396=AGPTB,421=DENSE,431=DTIME,456=EPTAB,466=GENRL,491=OUTTB,516=PTSIN,
526=SPACE,536=THIKN,546=PVAR,596=CTABL,806=HTABL,848=PROPT,1478=WARM,
1498=HORA,1548=TTABL,2208=ATE TB,2778=DGREE,3098=NU,3808=STVAR
DENSE=62,
DTIME=.1,10,.2,100,
GENRL=0,60,-.1,530,0,1,
OUTTB=1,80,.19,90,1,100,
0,0,0,0,0,0,0,0,0,0,0,0,0,0,0,0,19.6,3,
PTSIN=25,
THIKN=.015,
HTABL=.24,.8,
NHTABL=1,1,
NPROPT=1,1,1,
NWARM=2,
PROPT=.4,.3E-4,0,
WARM =529,7000,
HORA =0,37.8,100,
NHORA=3,
TTABL=5.5,1000,0,0,0,0,.0025,
CHART=1,12.4,1,20,0,0,0,0,0,1,.72,1,
GASPR=500,.6,0,30,0,
NGASPR=1,1,1,1,1,
NTDENS=2,
NZORET=1,1,
TDENS=1,1000,
ZORET=.106E13,.463E5,
TMELT=1,
NTTABL=1,1,1,1,1,1,1,0,
\$END

```

$DATA TEST CASE 3 AIR-GAP WITH CONSTANT MELTING T AND NO CHARRING.
$TABLN,1=CHART,26=GASPR,131=TDENS,151=ZORET,260.=NATETB,280.=NCTABL,
285.=NDGREE,286.=NGASPR,291.=NHORA,292.=VHTABL,294.=NNU,300.=NPROPT,
330.=NTDENS,331.=NTTABL,341.=NWARM,342.=VZORET,346=TMELT,371=TRAJT,
396=AGPTB,421=DENSE,431=DTIME,456=EPTAB,466=GENRL,491=OUTTB,516=PTSIN,
526=SPACE,536=THIKN,546=PVAR,596=CTABL,806=HTABL,848=PROPT,1478=WARM,
1498=HORA,1548=TTABL,2208=ATE TB,2778=DGREE,3098=NU,3808=STVAR
$D=1
GENRL=0,280,1,560,0,3,
TMELT=5,1100,
THIKN=.0165,.00833,.1,
PTSIN=19,9.,0.,
DENSE=71.2,38.5,.24,
DTIME=1,225,.125,235,1,280,
OUTTB=10,100,20,280,
HORA= 0,30,60,90,120,140,160,180,200,210,215,220,225,230,235,245,250,
260.,275.,280.,
NHORA=20,
TTABL=0.,0.,0.,1.19,2.35,5.10,11.9,19.8,27.4,38.1,48.3,53.1,54.3,55.2,
ITABL=53.3,51.2,140,102,76.6,35.6,1.79,0,
53.3,51.2,140,102,76.6,35.6,1.79,0,
0.,0.,435000.,
NTTABL=1,1,20,1,1,1,
CHART=0.,1.E-5,
WARM=460,960,1960,5000,
NWARM=4,
PROPT=.4,.4E-4,0.,.4,.196E-4,0.,.09,.04,.021,.021,.3E-5,.6E-5,.12E-4,
.12E-4,0.,
NPROPT=1,1,1,1,1,1,4,4,1,
CTABL=0.,.0257,.0257,
NCTABL=1,1,1,
AGPTB=3.,.66,1.,.00000738,0.,1,
$END

```

SECTION IV - TIMING

For a program with as many options as this one, estimating a running time for production runs could very easily degenerate into a guessing game.

A few jobs are outlined below with their running times so that at least an educated estimate may be made.

<u>JOB NO.</u>	<u>DESCRIPTION</u>	<u>RUNNING TIME</u>
1	Temperature Dependent Properties were Constant. Front and Backface Temperatures were read in. Charring 1 Layer with 13 Interior Points Thickness = .015' $\Delta t_1 = .1$ up to 10: $\Delta t_2 = .2$ up to 100. $t_{STOP} = 60$	2 min.
2	Same as job 1 except Front and Backface Temperatures are calculated.	4 min.
3	Three layers. Layer 2 was Air Gap. C_p and K for Layer 1 are constant C_p and K for Air Gap are Variable C_p and K for Layer 3 are constant H_{gf} is Variable. Q_{HGR} is Variable. Layer 1 has 19 interior points and a Thickness of .0165' Layer 2 is Air Gap of Thickness .01' Layer 3 has 9 interior points and a thickness of .01 Melting but no Char $\Delta t_1 = 1$ up to 280 $t_{STOP} = 280$.	2.6 min.

SECTION V - RESTRICTIONS

INPUT

1. The body may only have 10 layers, including any air gap.
2. The body may only have a total of 150 points.
3. There may be only one air gap in the body.
4. The independent "T" table has a maximum of twenty (20) entries.
5. The independent time table has a maximum of 50 entries.
6. All directions on the input data form should be noted and followed closely.

INPUT DATA FORM - One Dimensional Heat Flow in a Decomposing Plastic

1. One input in table denotes a constant value.
2. Two inputs in table denotes linear values between first and last independent variables.
3. If table requires more than one card, just continue onto the next card. (You may not split numbers at the end of a card)
4. First card is the Hollerith ID. card.
5. Last card is either \$END or \$DATA.
6. Data starts in Column 1.
7. Data may be punched up to and including Column 80.
8. If two cards are read in with the same table name, the data on the second card will be in core, since it will be read in on the top of the first card's data.

GENERAL CONSIDERATIONS

1. It is strongly recommended when running an entirely new case, that it be planned to make at least one short run before the production run. The reason for this is the sensitivity of the program to the choice of the Δt and Δx . It should be kept in mind that picking a reasonable value of Δt is important. If there is a large change in the properties of the material, a small Δt should be chosen for this interval. The preliminary run could indicate this along with the possible need for the squeezing of or for additional interior points.
2. Due to the space transformation, which results in the squeezing of points rather than dropping them, a large rate of melt can result in a too rapid moving of points. Normally it is corrected by cutting Δt .

3. Lists of tables needed for various types of runs.

A. Tables needed for all options:

GENRL	OUTTB	HTABL
THIKN	HORA	
PTSIN	TTABL	
DENSE	WARM	
DTIME	PROPT	

B. Tables which may be used with all options:

CTABL
SPACE
EPTAB
AGPTB (Must be used for any air gap).

C. Additional tables needed for the Charring Options:

CHART
GASPR
TDENS
ZORET

D. Additional tables needed for the Melting Options:

TMELT

TABLE STORAGE OF INDIVIDUAL ITEMS

INDTL

1. NTDENS	Number of entries in TDENS table
2. NDGREE	Number of entries in DGREE table
3.	Empty
4. NTEMP = NWARM	Number of entries in WARM table
5. NTIME = NHORA	Number of entries in HORA table

DIMENSION

KONVAR

1. ITIME	Total number of points or nodes in body
2. KTIME	Time step counter 1 KTIME 3
3. NZERO	Starting Node for Implicit scheme
4. LAYER	Number of LAYERS of material
5. JGAP	The layer of the Airgap
6. N3	
7. CHART (1)	Charring Option cell
8. TMELT (1)	Melting Option cell
9. Q_c^* Control	Determines if Q_c^* should be computed in Q_{net}

HTCONV

1. $R = 1.9858$	Universal Gas Constant
2. $\sigma = .476E-12$	Stefan - Boltzmann Constant
3. $.0174532925$	Radian Conversion Factor
4. S'_c	Rate of Char
5. S'_m	Rate of Melt
6. Q_c (from Q_{net} for graphite sublimation)	
7. S_m	Amount of Melt
8. S_c	Amount of Char
9. ALNTH	Length of First Layer
10. Q^* (from q_{net} for graphite sublimation)	

SPACVR

- | | |
|-----------|-------------------------------------|
| 1. R_1 | Parameter for squeezing computation |
| 2. R_1' | Parameter for squeezing computation |
| 3. ϕ | Parameter for squeezing computation |
| 4. Empty | |
| 5. Empty | |

CHARV

- | | |
|----------------------------------|------------------------------------|
| 1. AK | Density Dependent Portion of K |
| 2. AKP | Density |
| 3. CPA | Density Dependent Portion of C_p |
| $Q(1, 13) = Q_{\text{var}}$ | Q of vaporization |
| $Q(2, 13) = S_m' L$ | Rate of Melt Times the L of Body |
| $Q(3, 13) = Q_{\text{ablation}}$ | Q of ablation |
| $Q(4, 13) = QI(\text{LAYER})$ | Computed Q of Body |
| THIKIN (11) = ALNTH | Original length of Layer 1 |

SPECIAL STORAGE ALLOCATIONS FOR THE PRESSURE OPTION

TABLD (1) d_1	SCDTB (1) k_{eff}
TABLD (2) d_2	SCDTB (2) $(k_{eff})_\tau$
TABLD (3) d_3	SCDTB (3) $(k_{eff}) \rho'_s$
TABLD (4) d_4	SCDTB (4) $(\rho_{cp})_{eff}$
TABLD (5) $d_{1\eta}$	SCDTB (5)
TABLD (6) $d_{1\eta\eta}$	SCDTB (6) f_2
TABLD (7) $d_{1\eta\tau}$	SCDTB (7) $f_{2\eta}$
TABLD (8) $d_{1\tau}$	SCDTB (8) $f_{2\eta\eta}$
TABLD (9) e	SCDTB (9) $f_{2\eta\tau}$
TABLD (10) e_η	SCDTB (10) $f_{2\tau}$
TABLD (11) $e_{\eta\eta}$	SCDTB (11)
TABLD (12) $e_{\eta\tau}$	SCDTB (12) k_f
TABLD (13) e_τ	SCDTB (13) $(k_f)_\eta / k_f$
TABLD (14) ρ'_{cf}	SCDTB (14) $(k_f)_{\eta\eta} / k_f$
TABLD (15) k/ϵ	SCDTB (15) $(k_f)_\tau / k_f$
TABLD (16) $(k/\epsilon)_\eta$	SCDTB (16) $(k_f)_{\eta\tau} / k_f$
TABLD (17) $(k/\epsilon)_{\eta\tau}$	SCDTB (17)
TABLD (18) $(k/\epsilon)_\tau$	SCDTB (18) $(\epsilon_{zw} V_g)$
TABLD (19) $(k/\epsilon)_{\eta\eta}$	SCDTB (19)
TABLD (20)	SCDTB (20)

SPECIAL STORAGE ALLOCATIONS FOR THE PRESSURE OPTION (Cont)

CHART (1)	z	GRAPH OR PVAR (1)	K'_g	PROPT (1)	H_g
CHART (2)	ρ'_c	GRAPH OR PVAR (2)	K_C	PROPT (2)	e_c
CHART (3)	η	GRAPH OR PVAR (3)	K	PROPT (3)	e_p
CHART (4)	R_e	GRAPH OR PVAR (4)	C_p		
CHART (5)	ϵ_f	GRAPH OR PVAR (5)	C_{vp}		
CHART (6)	Γ	GRAPH OR PVAR (6)	C_{vc}		
CHART (7)	n	GRAPH OR PVAR (7)	k_f		
CHART (8)	$\tilde{\rho}_c$	GRAPH OR PVAR (8)	R		
CHART (9)	Ma/Mt	GRAPH OR PVAR (9)	M		
CHART (10)	P_i	GRAPH OR PVAR (10)	μ		
CHART (11)	C_t	GRAPH OR PVAR (11)	M_T		
CHART (12)	ζ	GRAPH OR PVAR (12)	M_{TT}		
CHART (13)	ρ_p	GRAPH OR PVAR (13)			

ERROR MESSAGES

I. INPUT

A. KEY PUNCH ERROR

Check input for misspelled table name.

B. THERE IS A COMMA ERROR

Check the number of entries of the dependent tables against the number of entries of the independent table. (The arguments listed in the error return will help to identify the tables in question.)

INDEPENDENT	DEPENDENT
WARM	GASPR
	CTABL
	EMOD
	HTABL
	PROPT
HORA	TTABL
TDENS	ZORET
DGREE	ATETB

II. PROGRAM

A. DIVIDED BY ZERO

This is in every arithmetic subroutine of the program, so one must refer to the trace-back given you when the error occurred.

Sometimes one can diagnose quickly what the problem is, by noting the subroutine where the error message was called.

EXAMPLES

1. ERROR IN BEE

BEE	IN	INTPTS
INTPTS	IN	PTX1
PTX1	IN	EXEC
EXEC	IN	MAIN

For this particular combination, most of the time, it means that C_{pa} in the chart table is zero.

2. ERROR IN INTPTS

INPTS	IN	PTX1
PTX1	IN	EXEC
EXEC	IN	MAIN

This combination could mean that the K_a referred to in the chart table is zero.

Again, most of the time this error return is triggered by an error in input.

B. TOO MANY ITERATIONS IN TEST

It is difficult to diagnose a non-convergence error in TNEST from the trace-back. Since this is a computational error message, rather than an input error, we try to diagnose the problem through more data. The routine (TNEST) will now print out the first 15 iterations.

C. There are runs in which the \dot{q}_{net} is greater than the Q_i total. This situation may possibly be corrected by a judicious cutting of Δt , although it must be understood that this may not be the only answer to the problem.

D. If Q_{net} is increasing and T_{ff} is decreasing, check K_a or C_{pa} computations, since K_a or C_{pa} may be negative.

E. ERROR IN QNET

QNET	IN	PTX1
PTX1	IN	EXEC
EXEC	IN	MAIN

Indicates either CHART (10) is zero or the $\dot{q}_c/\Delta h$ is zero for the turbulent option.

SECTION OUTPUT

Output is off-line and consists of a printout of the input tables and the computed values which are defined on the following pages.

PRINTED NAME	SYMBOL	DEFINITION
TIME	t	Time
DELTA TIME	Δt	Increment of Time
AMT. CHAR	$S_c(t)$	Total amount of material charred
RATE CHAR	$\dot{S}_c(t)$	Rate of Charring
AMT. MELT	$S_m(t)$	Total amount of material melted
RATE MELT	$\dot{S}_m(t)$	Rate of Melting
EMDG (1)	\dot{m}_{g1}	Mass flux of gas at the frontface
AR1 (1)	r	Spacing Parameters
AR1P (1)	dr/dt	Derivatives of spacing parameter w/r to time
ETA0 (1)	n_{01}	Amount of squeezing of points toward frontface

TIME TABLE ENTRIES

1 These are the interpolated values for the
2 T table (see input data form).
3
4
5

.

INT QNET	$\int \dot{q}_{net} dt$	Integrated value of q_{net} with respect to t
INT QRR	$\int \dot{q}_{rr} dt$	Integrated value of q_{rr} with respect to t
INT QG HR	$\int \dot{q}_{hgr} dt$	Integrated value of q_{hgr} with respect to t
INT QC	$\int \dot{q}_c dt$	Integrated value of q_c with respect to t
INT QBLK	$\int \dot{q}_{block} dt$	Integrated value of q_{blk} with respect to t
INT QBKFAC	$\int \dot{q}_{backface} dt$	Integrated value of q_{bkfac} with respect to t
QI TOTAL		Amount of heat stored in body
QDNET	\dot{q}_{net}	Heat flux entering body
QDRR	\dot{q}_{rr}	Radiative heat flux

<u>PRINTED NAME</u>	<u>SYMBOL</u>	<u>DEFINITION</u>
QHGR	\dot{q}_{hgr}	Hot gas heat flux
QC	\dot{q}_c	Convective heat flux
QDBLK	$\dot{q}_{blocked}$	Heat flux blocked by mass injection into boundary layer
QBKFAC	$\dot{q}_{backface}$	Heat flux at backface
Q*		Q* Computed in sublimation option
QABL	\dot{q}_{abla}	The heat due to ablation
COORDINATES VALUES		Position of nodes in real space
TEMPERATURES	$T_{(i)}$	Temperature at each point layer
COUNT LIST		See page E - 42

OPTIONAL OUTPUT

<u>OPTIONAL OUTPUT</u>		
DENSITIES	$\rho_{(i)}$	Density of material at each point of layer
EQUALLY SPACED	T	Temperatures at equally spaced points of layer
GAS DENSITIES	ρ'_g	Gas density at each point of layer
QHGR		In the graphite option the heat of sublimation is printed out as \dot{q}_{hgr}
STRESSES		Results of stress equations are printed out.

SAMPLE OUTPUT FORMAT

IDENTIFICATION OF RUN

t = x. xxxxxxxx Δt = x. xxxxxxxx

$S_c(t)$	$\dot{S}_c(t)$	$S_m(t)$	$\dot{S}_m(t)$	\dot{m}_g	r_1	dr_1/dt	η_0
x. xxxxExx	x. xxxxExx	x. xxxxExx	x. xxxxExx	x. xxxxExx	x. xxxxExx	x. xxxxExx	x. xxxxExx

TIME TABLE ENTRIES 1 THROUGH 10

x. xxxxExx	x. xxxxExx	x. xxxxExx	x. xxxxExx	x. xxxxExx	x. xxxxExx		
$\int \dot{q}_{net} dt$	$\int \dot{q}_{rr} dt$	$\int \dot{q}_{hgr} dt$	$\int \dot{q}_c dt$	$\int \dot{q}_{blocked} dt$	$\int \dot{q}_{backface} dt$	Q	
x. xxxxExx	x. xxxxExx	x. xxxxExx	x. xxxxExx	x. xxxxExx	x. xxxxExx	x. xxxxExx	
\dot{q}_{net}	\dot{q}_{rr}	\dot{q}_{hgr}	\dot{q}_c	$\dot{q}_{blocked}$	$\dot{q}_{backface}$	$\dot{q}_{vaporization}$	\dot{q}^*
x. xxxxExx	x. xxxxExx	x. xxxxExx	x. xxxxExx	x. xxxxExx	x. xxxxExx	x. xxxxExx	x. xxxxExx

COORDINATE VALUES LAYER = 1

TEMPERATURES LAYER = 1

DENSITIES LAYER = 1 (If computed)

GAS DENSITY LAYER = 1 (If computed)

(Repeat distributions of coordinate values, temperatures, and densities until the total number of layers are printed out.)

EQUALLY SPACED TEMPERATURE FIRST LAYER

COUNT =

STRESS ANSWERS

COUNT LIST

- COUNT (1): Total number of time steps.
- COUNT (2): Total number of iterations for run on rate of melt.
- COUNT (3): Iterations on rate of melt/time step.
- COUNT (4): Total number of iterations in PTX1.
- COUNT (5): Iterations in PTX1/time step.
- COUNT (6): Total number of iterations in INTPTS
- COUNT (7): Iterations in INTPTS/time step.
- COUNT (8): Total number of iterations at interface.
- COUNT (9): Iterations at interface/time step.
- COUNT (10): Total number of iterations in DENSIT.
- COUNT (11): Iterations in DENSIT/time step.
- COUNT (12): Total number of iterations in air-gap.
- COUNT (13): Iterations in air-gap/time step.
- COUNT (14): Number of times Δt is cut by density criterion.
- COUNT (15): Number of times $\alpha_3 < 1/2$.
- COUNT (16): Number of times Δt is cut due to s_m .
- COUNT (17): Number of times Δt is cut by density criterion after explicit calculations.

APPENDIX F

MATERIAL PROPERTIES

Material Properties

The material properties required for application of the Reaction Kinetics Ablation Program (REKAP) are given within this Appendix. The materials for which the properties are given are phenolic nylon, phenolic refrasil, phenolic graphite, phenolic carbon and pyrolytic graphite. The material properties of concern here are those thermal and chemical kinetic properties which are required to calculate the thermal degradation and the surface recession. At the present time all the parameters required for the operation of the pressure and stress option are not available and some of those which are available are in considerable question at the high char temperatures. It will be necessary to conduct an experimental program to determine their values. Prior to the determination of these high temperature properties, extrapolations from low temperature values are necessary for parametric study purposes.

A tabulation of the material properties is given in Table F1 and the thermal conductivity and the specific heat for typical compositions of the various materials are given in Figures F1 to F5. The property values given here should be considered to be approximate and a check should be made each time a new material is to be analyzed for a comparison of the properties. The variation of properties of a similar material can be seen in Figures F2 and F5. It is particularly important that the thermal conductivity of the material to be analyzed is correct since it has been found that it has a major influence on the performance of a material. The rather large variations in thermal conductivities can be observed in Figure F2.

The activation energy, collision frequency and the order of the reaction were determined for phenolic nylon, phenolic refrasil and phenolic graphite on this contract through thermogravimetric analysis methods. The materials evaluated were:

Phenolic Nylon:	Mfgr.: Wellington-Sears #SM19 Resin Type: CTL 91LD Resin Content: $45\% \pm 5\%$
Phenolic Refrasil:	Mfgr.: Fiberite #MXS75 Resin Content: $31\% \pm 2\%$ Silica Powder Filler Content: $8\% \pm 1\%$
Phenolic Graphite:	Mfgr.: H. I. Thompson - 5014 Resin Content: 39%

The thermogravimetric analysis curves are shown in Figures F6 to F8. Figure F6 shows that the major weight loss for phenolic nylon to occur between 300 and 500°C. The steepness of the thermogram between 350 and 450°C indicates a relatively rapid decomposition mechanism. The ash amounted to approximately 25% of the initial sample weight.

The degradation (Figure F7) of phenolic refrasil occurs between 350 and 500°C and it loses only about 18% of its initial weight when heated to 1000°C.

The degradation as shown in Figure F8 for phenolic graphite took place over the temperature range of 350°C to 650°C. After heating the sample to 1000°C, the weight reduction amounted to only 17% of its initial weight.

TABLE F1

APPROXIMATE MATERIAL PROPERTIES FOR USE WITH REKAP FOR ROCKET MOZZLES

Material Properties	Phenolic Nylon	Phenolic Refrasil	Phenolic Graphite	Phenolic Carbon	Pyrolytic Graphite
Plastic Density (lb/ft ³)	71	104	90.4	90.4	137
Char Density (lb/ft ³)	17.75	87.5	77.1	74.0	0
Heat of Gas Formation (Btu/lb)	1000	400	300	300	-
Specific Heat of Gas (Btu/lb°R)	0.60	0.60	0.40	0.4	-
Latent Heat of Cracking (Btu/lb°R)	0	0	0	0	0
Average Molecular Weight	20	20	34	34	0
Specific Heat of Plastic (Btu/lb°R)	Fig. F1	Fig. F2	Fig. F3	Fig. F4	Fig. F5
Thermal Conductivity Plastic (Btu/ft-sec°R)	Fig. F1	Fig. F2	Fig. F3	Fig. F4	Fig. F5
Latent Heat of Melting (Btu/lb)	-	0	-	-	-
Graphite Sublimation Constants					
K ₁	-	-	4240	4240	4240
K ₂	-	-	5.77	5.77	5.77
Order of Reaction	3	2	2	2	-
Charring Constants					
N ₁	1	1	1	1	-
C ₁	0	-1.70	0.10	0.1915	-
N ₂	1	1	1	1	-
C ₂	0	.40	0.360	0.744	-
Collision Frequency (1/sec)	44.5 x 10 ⁶	1300	83.4	83.4	-
Activation Energy (Btu/lb mole)	57.0 x 10 ³	33.5 x 10 ³	25.2 x 10 ³	25.2 x 10 ³	-

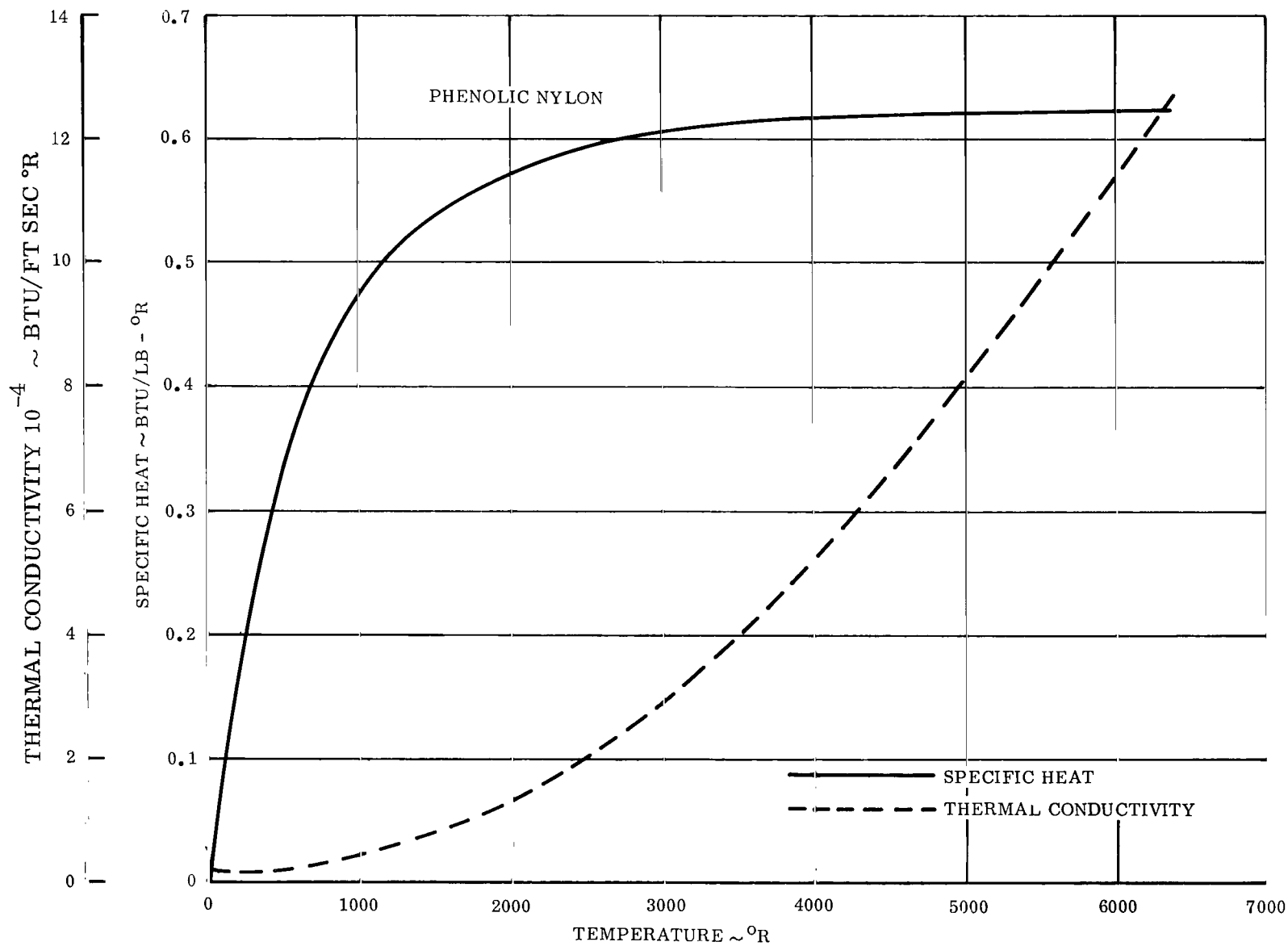
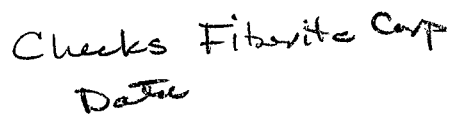


Figure F1. Phenolic Nylon


$$\frac{Btu}{ft^2 hr^{\circ}F/in}$$

2.8 → 2.9 300 °F
2.5 500 °F

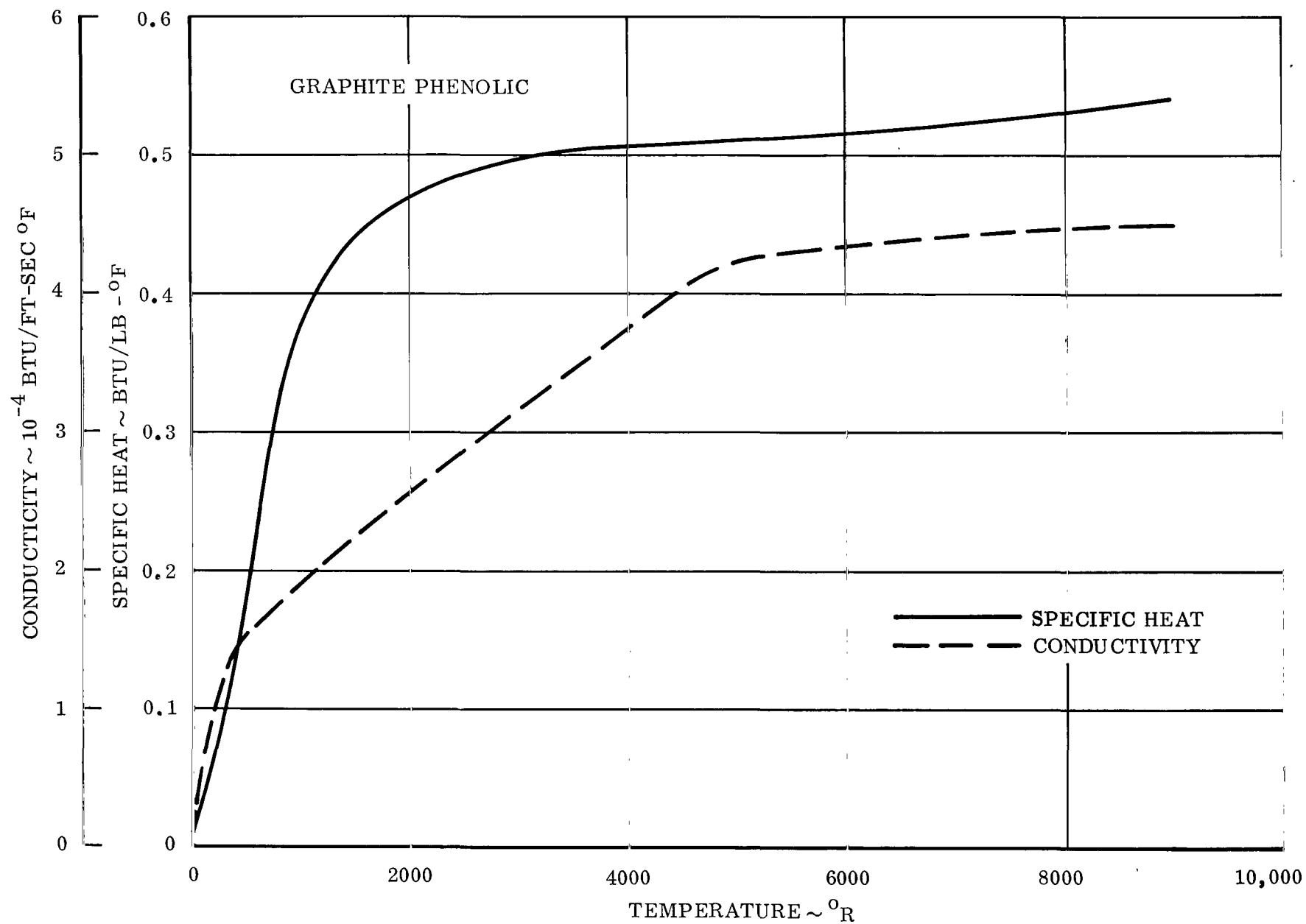


Figure F2 Graphite Phenolic

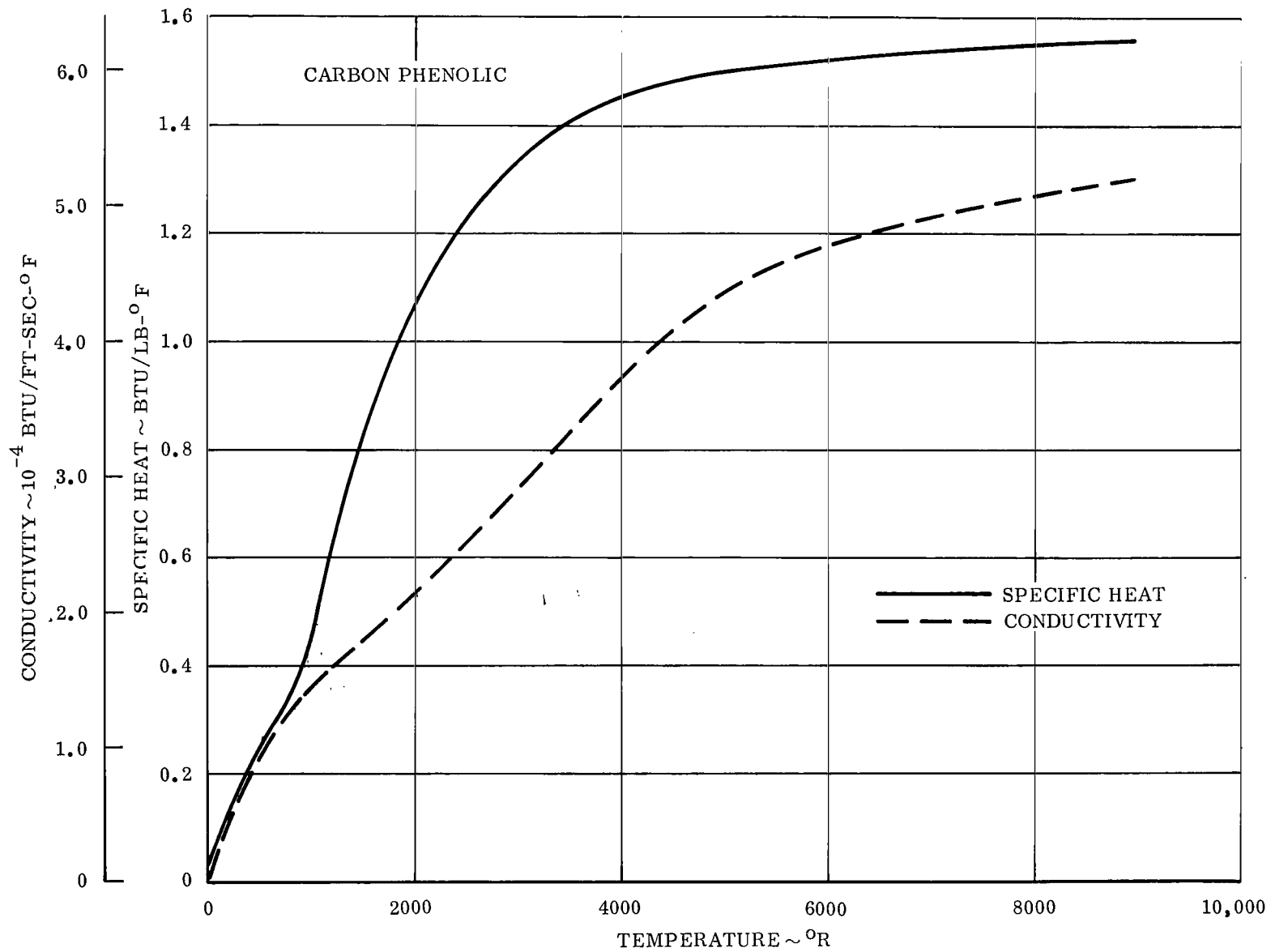
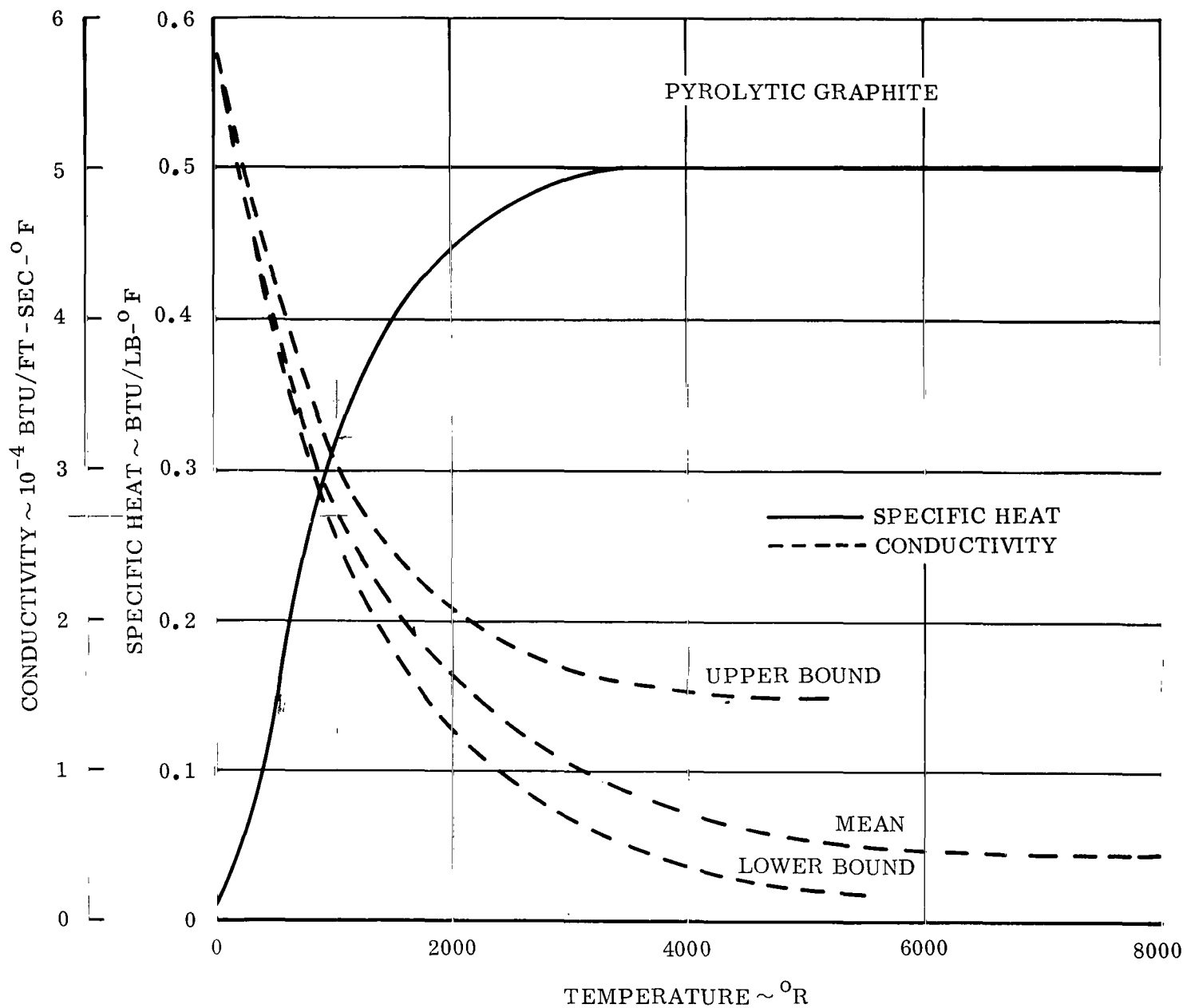


Figure F4. Carbon Phenolic



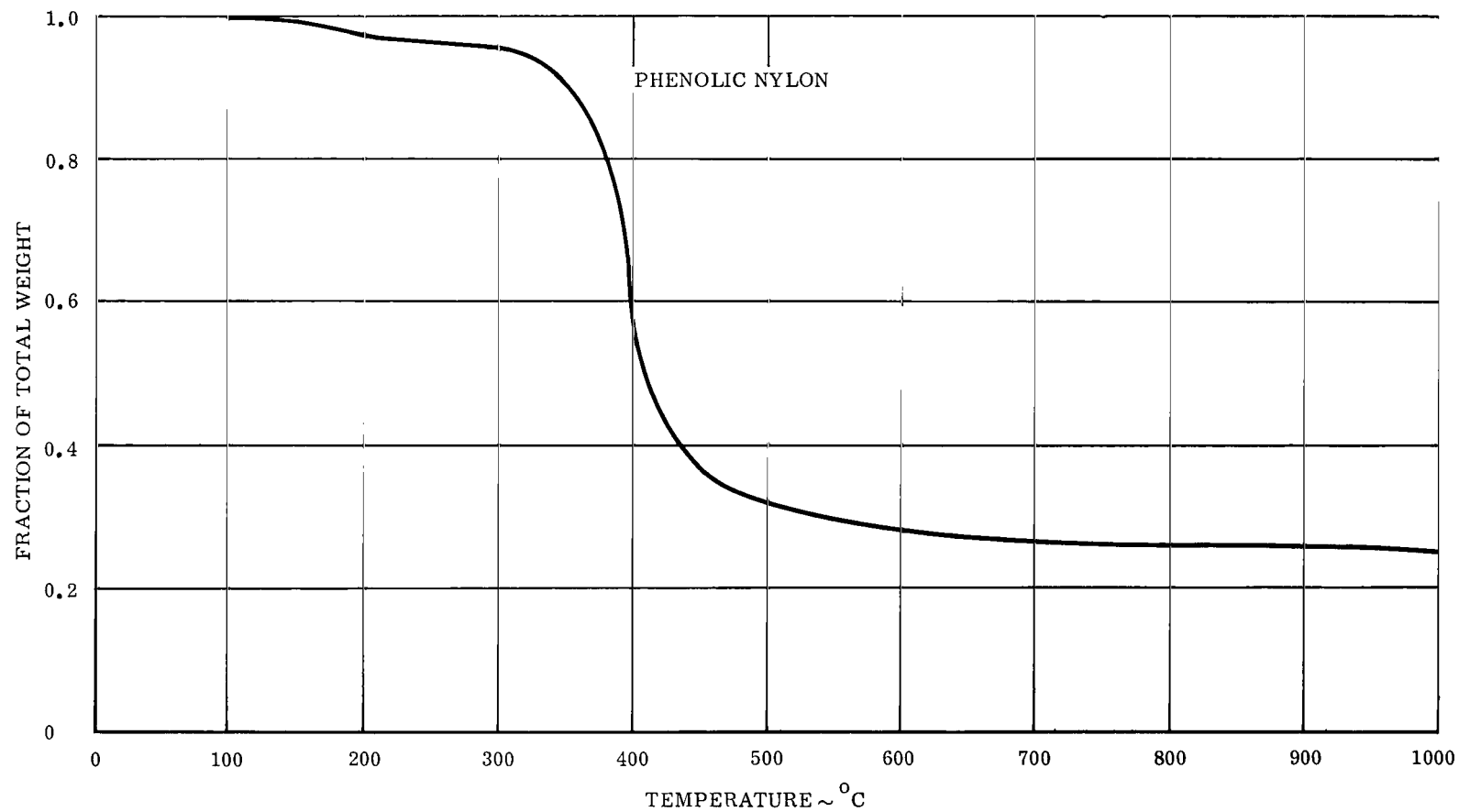


Figure F6. Phenolic Nylon

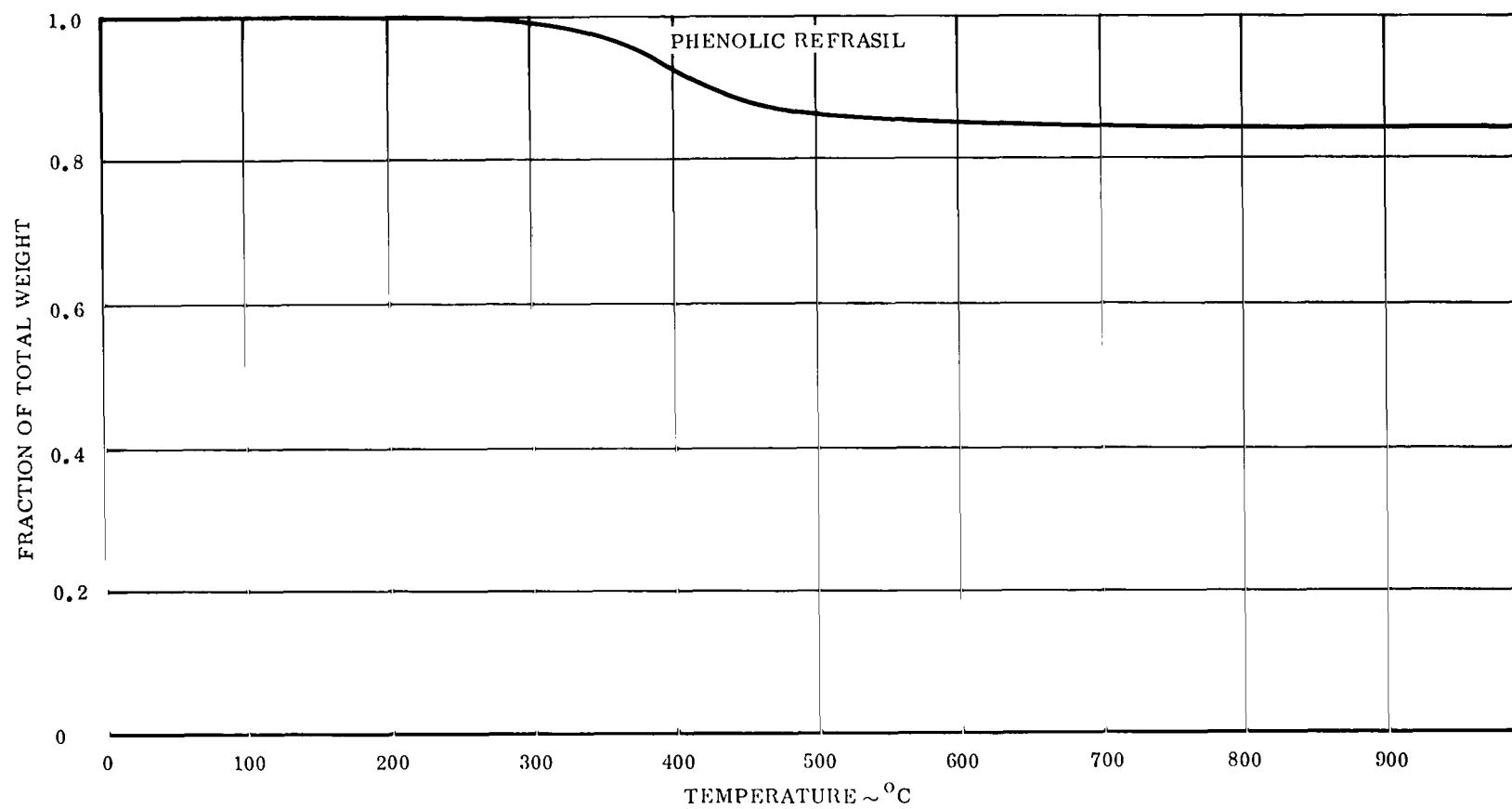


Figure F7. Phenolic Refrasil

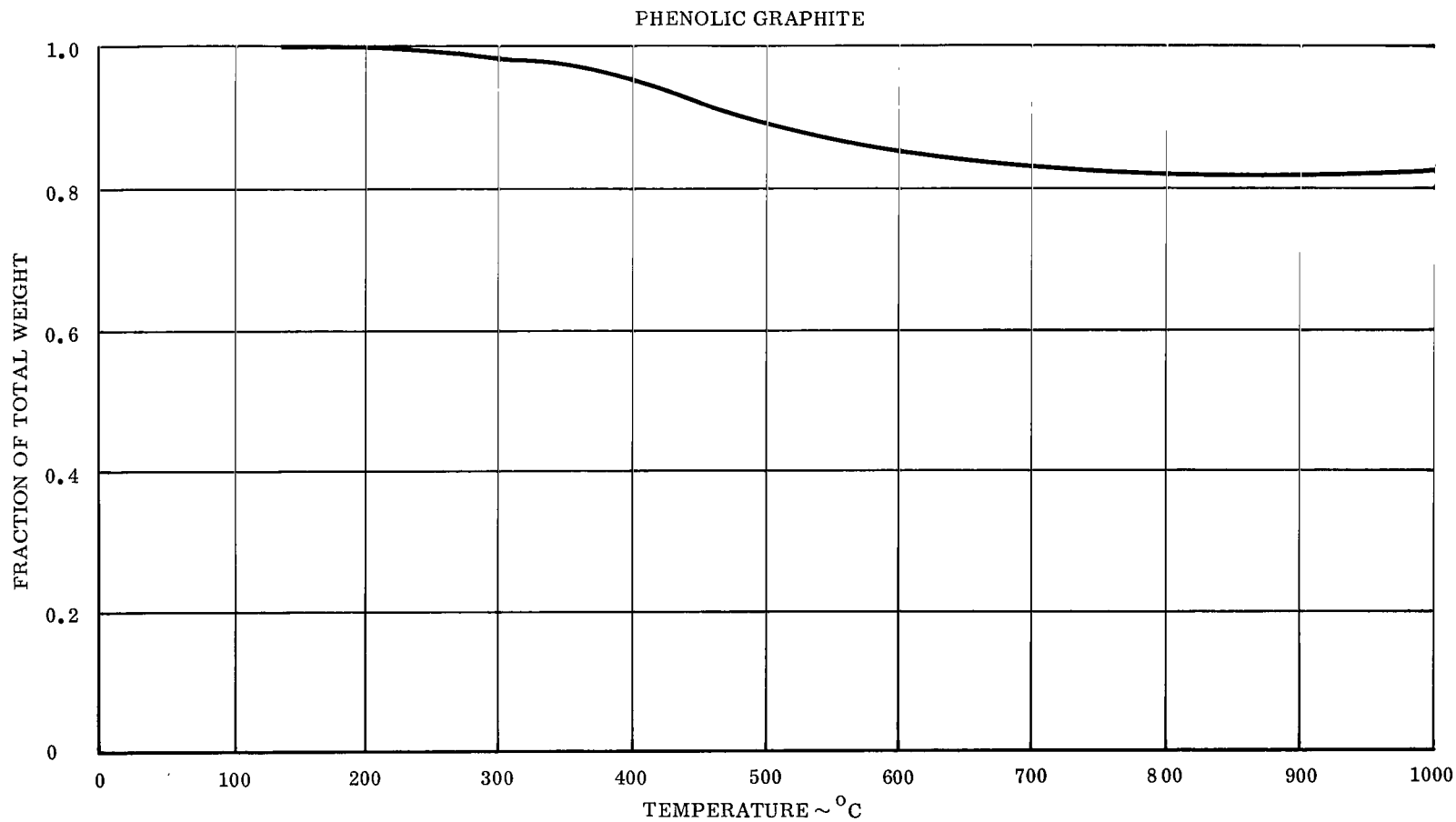


Figure F8. Phenolic Graphite

APPENDIX G
APPLICATIONS AND RESULTS

Application and Results

The nozzle dimensions used for the analysis were those supplied by NASA Lewis for their small 1.2 inch throat diameter test nozzles. The propellant combinations were hydrogen/oxygen and $\text{N}_2\text{O}_4/\text{UDMH} - \text{N}_2\text{H}_4$ (50-50) having a fuel to oxidizer ratio of 6.5 and 2.0 respectively. The nominal chamber pressure was 95 psia. The rocket nozzle flow fields including the boundary layer edge conditions and thermodynamic and transport properties were provided by NASA Lewis. These conditions and properties were used to calculate the convective film coefficient at the throat of the nozzle. The film coefficients were calculated using Bartz (Ref. 1) method with no corrections. The calculated convective film coefficients for the hydrogen/oxygen and the $\text{N}_2\text{O}_4/\text{UDMH} - \text{N}_2\text{H}_4$ (50-50) at the 1.2 inch throat of the NASA Lewis rocket nozzles were $0.76 \text{ BTU/ft}^2 \text{ sec } ^\circ\text{F}$ and $0.342 \text{ BTU/ft}^2 \text{ sec } ^\circ\text{F}$ respectively. The corresponding recovery temperatures were $4300 ^\circ\text{F}$ for the hydrogen/oxygen propellant combination and $4420 ^\circ\text{F}$ and $4730 ^\circ\text{F}$ for the $\text{N}_2\text{O}_4/\text{UDMH} - \text{N}_2\text{H}_4$ propellant combination. The combination of the recovery temperature and the convective heat transfer coefficient determined using the above methods resulted in predicted values that were considerably higher than the experimentally obtained values. This was later shown to be the result of a lower recovery or boundary layer edge temperature. A calorimeter configuration and temperature data was supplied by NASA Lewis. An analysis was made using a transient heat transfer computer program and thus the temperature response for a number of environmental conditions was determined. The results of this analysis is shown in Figure G1. It was concluded from these results that the actual driving temperature to which the local material was exposed was approximately $3100 ^\circ\text{F}$. The results shown in Figures G2 and G4 confirm the fact that $3100 ^\circ\text{F}$ is a more realistic boundary layer edge temperature than was the recovery temperature.

The temperature responses shown in Figures G2 to G4 show the effects of the different temperature conditions. They also clearly identify the effect of curtain cooling as an important parameter in material system evaluation, as well as the importance of measuring the local heat rate as a boundary condition for the thermal analysis. This lower driving temperature could have resulted from a fuel curtain produced by the injector which protected the nozzle walls from the higher temperature combustion gases.

From the results given in Tables G1 and G2 and shown in Figures G2 to G7 it is possible to evaluate the relative performance of the various materials for two different propellants. The analytical results reported here were calculated assuming constant values for film coefficients and recovery or boundary layer edge temperatures where the REKAP program has the capability of including time varying parameters, they were not utilized for the six cases studies here since their primary purpose was to investigate the application of the program to several materials with widely different properties and to determine their relative performance as rocket nozzle heat protection materials.

The material properties used in this analysis are tabulated in Table F1 of Appendix F. The surface recession control mechanism used for the phenolic graphite calculations was a graphite oxidation and sublimation option, since the char formed is essentially carbon or graphite. The constants K_1 and K_2 used in the diffusion mass loss equations are the turbulent values which were determined for oxygen reactions. The surface recession for both

the phenolic nylon and the phenolic refrasil was the specified char thickness option. Based on the experimental data reported by Rollbukler (Ref. 2), the maximum char thickness for a phenolic-silica fiber re-inforced material exposed to the exhaust products of hydrogen/oxygen should be approximately 0.25 inches thick. This value was used as a maximum specified char thickness. Included in the developed REKAP program are two other options which have produced excellent agreement with experimental results for phenolic refrasil. These are the Refrasil option and the Fixed Melting Temperature option. The Refrasil option is explained in detail in Appendix A including the constants recommended for use within the equations. The fixed Melting Temperature option is the most straight-forward of all the options since the melting temperature, the latent heat of fusion and the char density can be determined in a laboratory and does not require previous rocket nozzle tests. However, the factor Γ must be established from previous experimental work. Γ has been defined as the gasification factor; however, as stated in Appendix A, the rocket nozzle wall temperatures for most propellant combinations do not reach sufficiently high values for the material to be vaporized, therefore, Γ is actually the ratio of the amount of char melted to the total char lost.

The surface recession of the phenolic nylon can also be controlled by the graphite oxidation or sublimation routine since its char is primarily a carbon material.

References

1. Bartz, D.R. , "A Simple Equation for Rapid Estimation of Rocket Nozzle Convective Heat Transfer Coefficients," Jet Propulsion, January, 1956, pp 49-51.
2. Rollbukler, R. J. , "Experimental Investigation of Rocket-Engine Ablative Material Performance After Post Run Cooling at Altitude Pressures," NASA TN D-1726, June 1963.

TABLE G1 - SUMMARY OF MATERIAL PERFORMANCE

Run No.	Nozzle Mat.	Propellant Comb.	* Convective Film Coefficient (BTU/ft ² sec ⁰ F)	Recovery Temp. (°F)	Boundary Layer Edge Temp. (°F)	Firing Time (sec)	**** Computed Surface Recession (in)	Exper. Surface Recession (in)	** Computed Char Thickness (in)	Exper. Char Thickness (in)
2219	Phenolic Graphite	Hydrogen Oxygen	0.50	4300	3100	127.9	**** 0.0217	0.0215	0.578	N/A
2220	Phenolic Nylon	Hydrogen Oxygen	0.50	4300	3100	17.3	0.108	0.133	0.114	N/A
2062	Phenolic Refrasil	Hydrogen Oxygen	0.50	4300	3100	29.7	0.0	0.0	0.12	0.157
338	Phenolic Graphite	N ₂ O ₄ UDMH-N ₂ H ₄	0.342	4420	----	32	0.038	0.042	0.327	0.393
----	Phenolic Nylon	N ₂ O ₄ UDMH-N ₂ H ₄	0.342	4420	----	17.3	0.0173	N/A	0.0754	N/A
			0.342	4420	----	50	0.128	N/A	0.0801	N/A
257	Phenolic Silica	N ₂ O ₄ UDMH-N ₂ H ₄	0.342	4730	----	33	0.0	0.002	0.180	0.201

* The convective film coefficient was calculated using the Bartz method for a 1.2 inch throat diameter.

** The char depth is determined by the point where the local density has decreased from the virgin plastic by an amount of 5% of the density difference between virgin plastic and char.

*** The constants in the equation describing the oxidation mass loss rate were corrected for the boundary layer gases.

**** The computed surface recession and char thickness for the runs having the oxygen and hydrogen propellant combination were computed using the boundary layer edge temperature rather than the recovery temperature as the driving temperature.

N/A - Not Available

TABLE G2 - SUMMARY OF TEMPERATURE RESPONSE

Run No.	Nozzle Material	Propellant Combination	Time (sec)	*Initial Thermocouple Location (in)	Experi- mental	**Computed Temperatures	
					Tempera- tures (°F)	1 (°F)	2 (°F)
2219	Phenolic Graphite	Hydrogen Oxygen	0	0.375	37	43	43
			1		46	43	43
			5		46	47	46
			10		89	125	81
			30		319	940	396
			50		887	1768	729
			70		1108		967
			90		1285		1162
			110		1466		1322
			End of Run		1557		1468
			0	0.575	43	43	43
			1		43	43	43
			5		43	43	43
			10		51	45	44
			30		157	235	140
			50		279	632	337
			70		450		532
			90		764		728
			110		948		909
			End of Run		1174		1057
2220	Phenolic Nylon	Hydrogen Oxygen	0	0.275	37	37	37
			1		37	37	37
			5		37	37	37
			10		45	48	39
			End of Run		72	1516	47
			30		141	—	87

* The initial thermocouple location is the radial distance from the front or inner surface before the run.

**The temperature response given in column 1 is that calculated using the recovery temperature and that in column 2 is calculated using the boundary layer edge temperature.

TABLE G2 - SUMMARY OF TEMPERATURE RESPONSE (Cont)

Run No.	Nozzle Material	Propellant Combination	Time (sec)	*Initial Thermocouple Location (in)	Experi- mental Tempera- tures (^o F)	**Computed Temperatures	
						1	2
						(^o F)	(^o F)
2062	Phenolic Refrasil	Hydrogen Oxygen	0	0.216	44	44	44
			5		44	45	45
			10		66	77	63
			20		207	275	173
		End of Run	29.7		NA	—	337
			30		271	—	341
338	Phenolic Graphite	N ₂ O ₄ UDMH-N ₂ H ₄	0	0.375	Not Available	43	
			1			43	
			5			46	
			10			110	
			20			410	
			32			1362	
	Phenolic Nylon	N ₂ O ₄ UDMH-N ₂ H ₄	0	0.575	Not Available	43	
			1			43	
			5			43	
			10			44	
			20			90	
			32			237	
			0		Not Available	37	
			1			37	
			5			37	
			10			37	
			17.3			47	

* The initial thermocouple location is the radial distance from the front or inner surface before the run.

**The temperature response given in column 1 is that calculated using the recovery temperature and that in column 2 is calculated using the boundary layer edge temperature.

TABLE G2 - SUMMARY OF TEMPERATURE RESPONSE (Cont)

Run No.	Nozzle Material	Propellant Combination	Time (sec)	*Initial Thermocouple Location (in)	Experi- mental Tempera- tures (°F)	**Computed Temperatures	
						1 (°F)	2 (°F)
			20			54	
			30			103	
			40			185	
			50			325	
257	Phenolic Silica	N ₂ O ₄ UDMH-N ₂ H ₄	0	0.216	Not Available	43	
			5			44	
			10			65	
			20			228	
			30			414	
			33			456	

* The initial thermocouple location is the radial distance from the front or inner surface before the run.

**The temperature response given in column 1 is that calculated using the recovery temperature and that in column 2 is calculated using the boundary layer edge temperature.

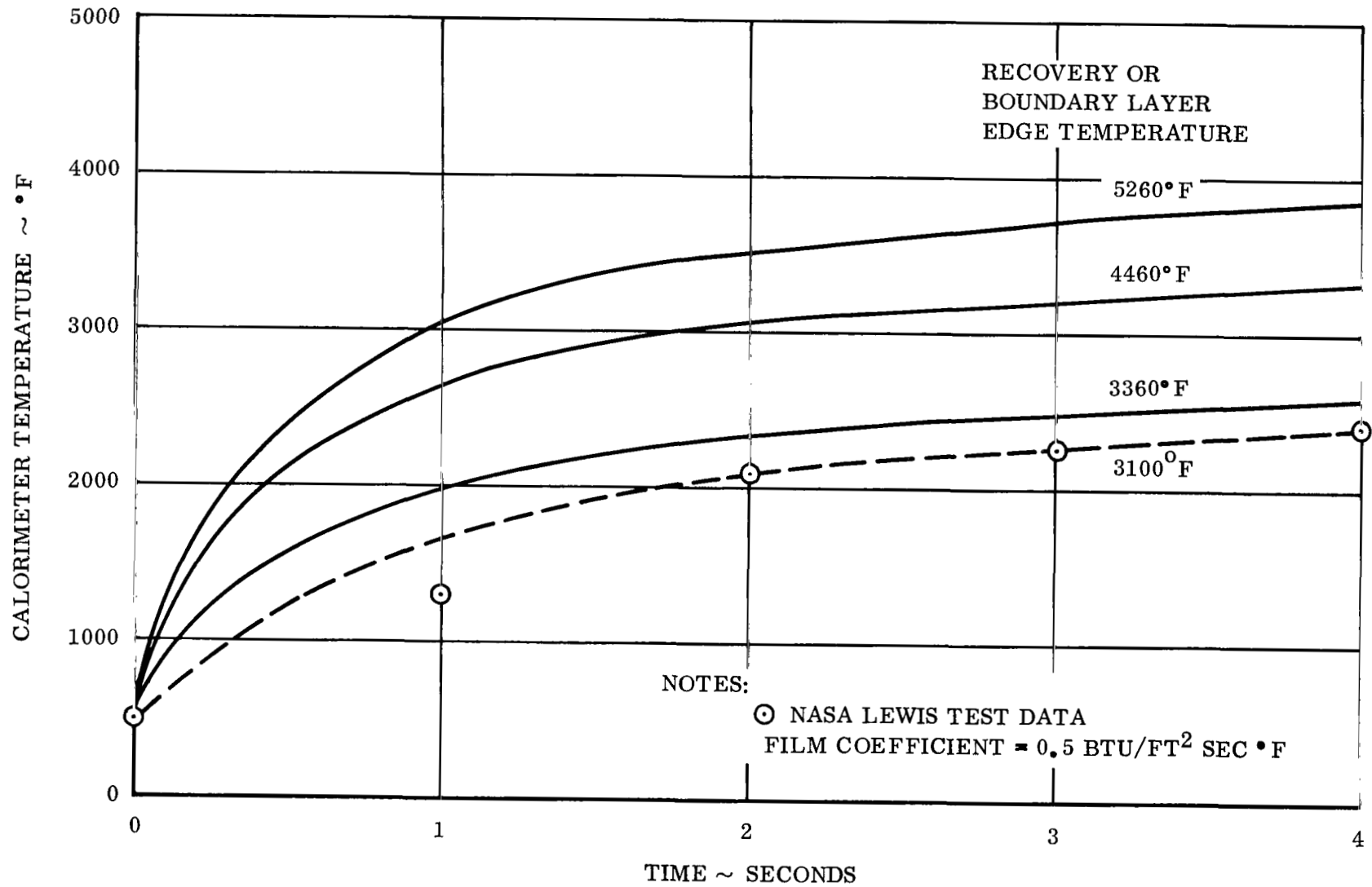


Figure G1. Temperature Response of Tungsten Calorimeter
Within Small NASA Lewis Test Nozzle

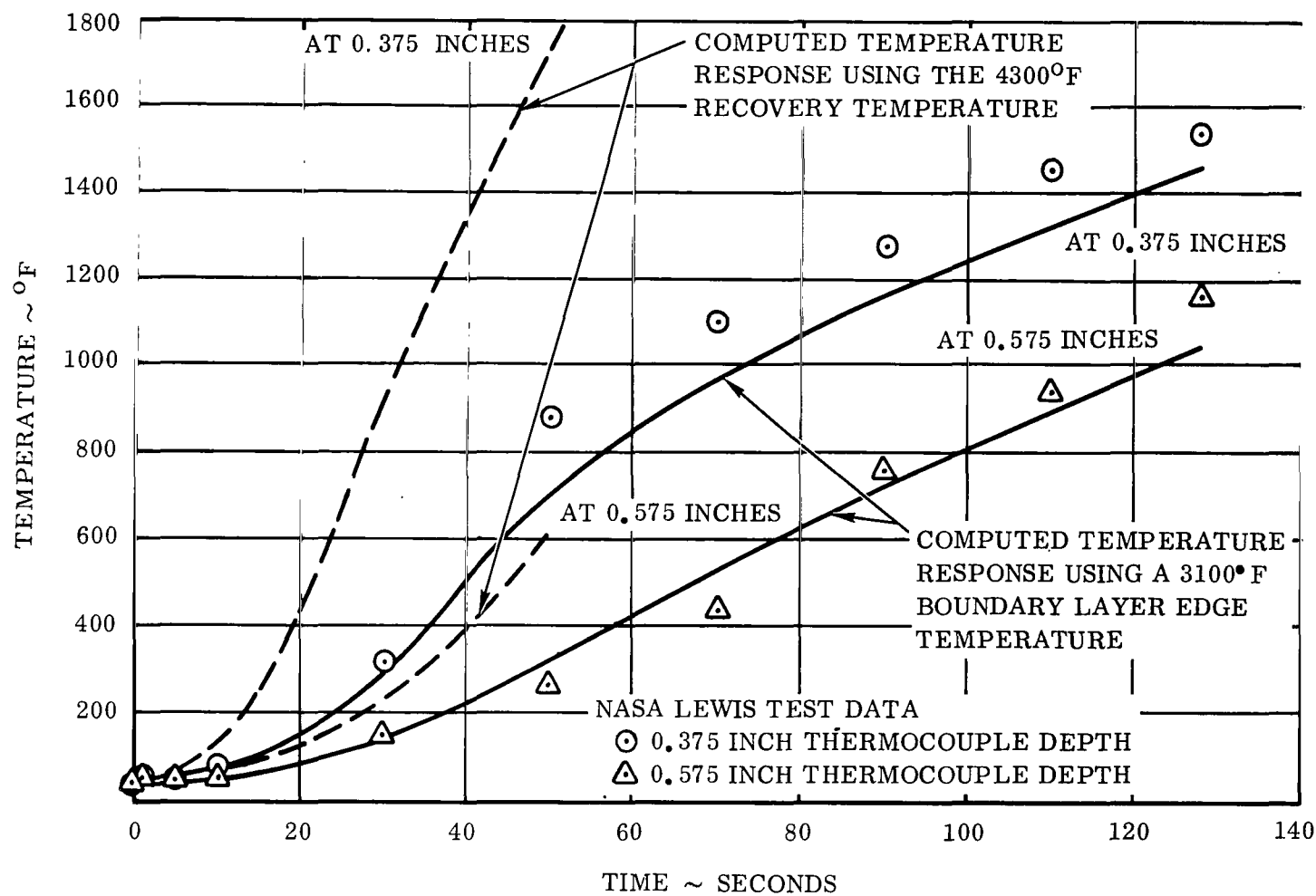


Figure G2. Temperature Response of Phenolic Graphite

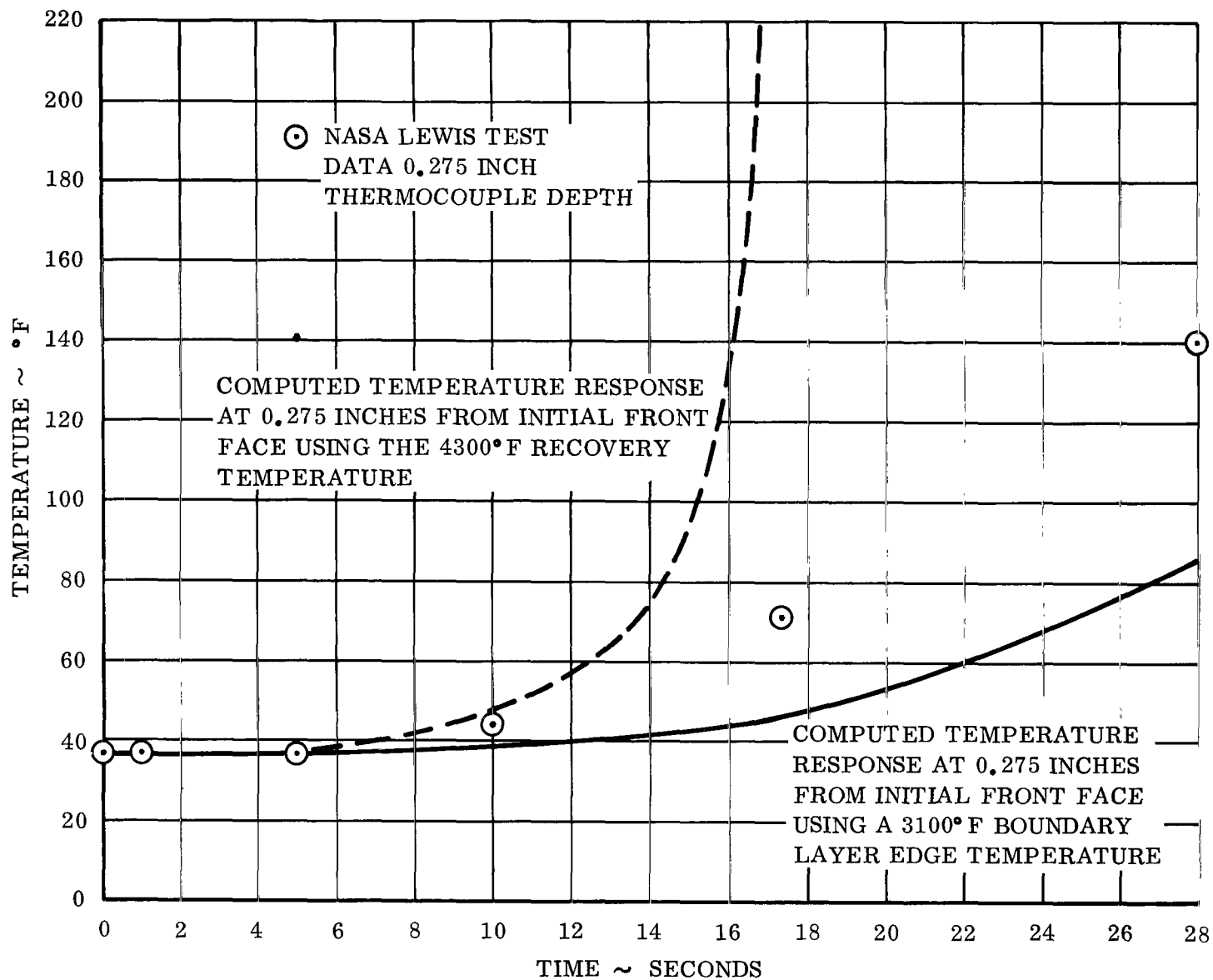


Figure G3. Temperature Response of Phenolic Nylon
PROPELLANT: HYDROGEN-OXYGEN

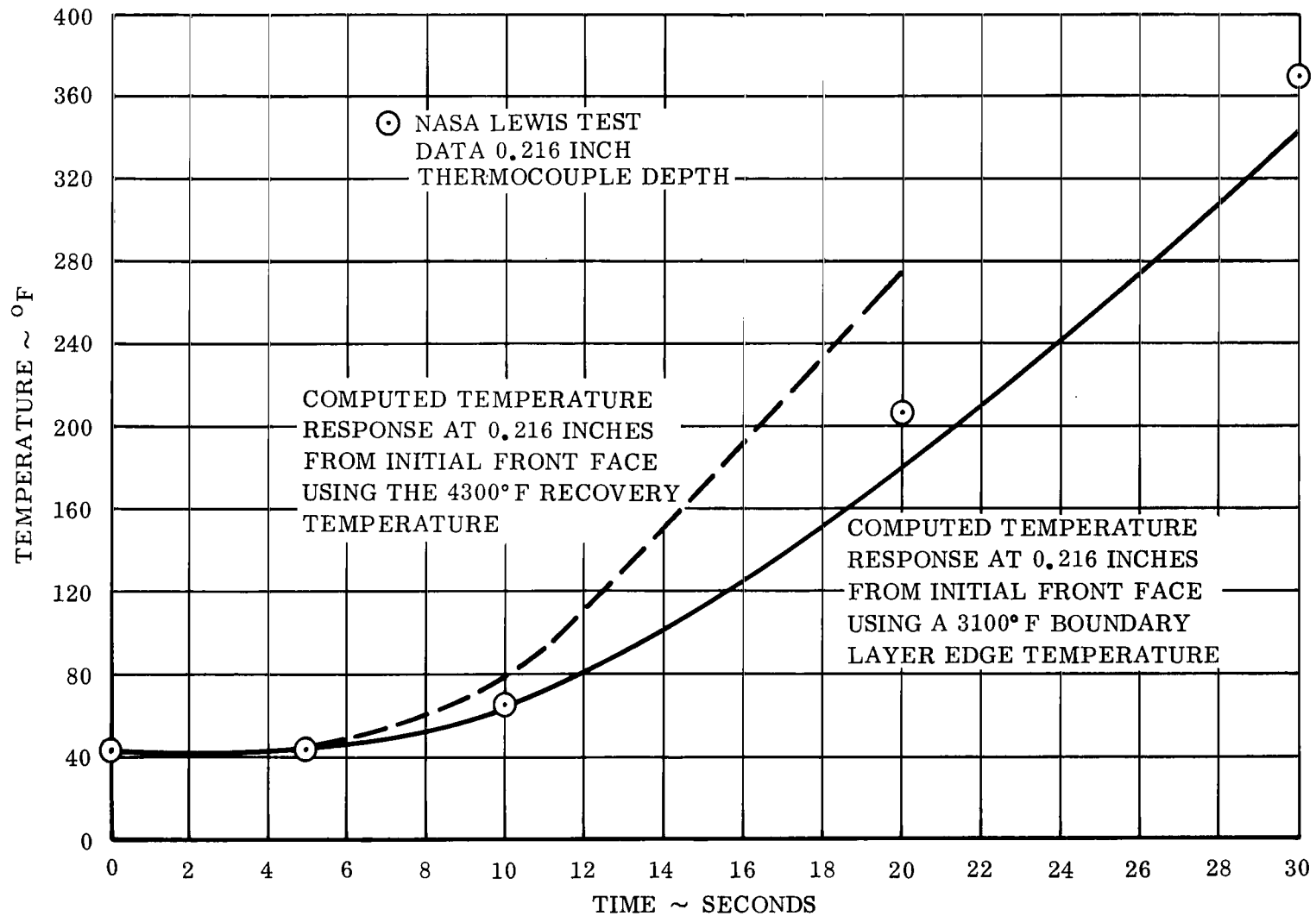


Figure G4. Temperature Response of Phenolic Refrasil
PROPELLENT: HYDROGEN-OXYGEN

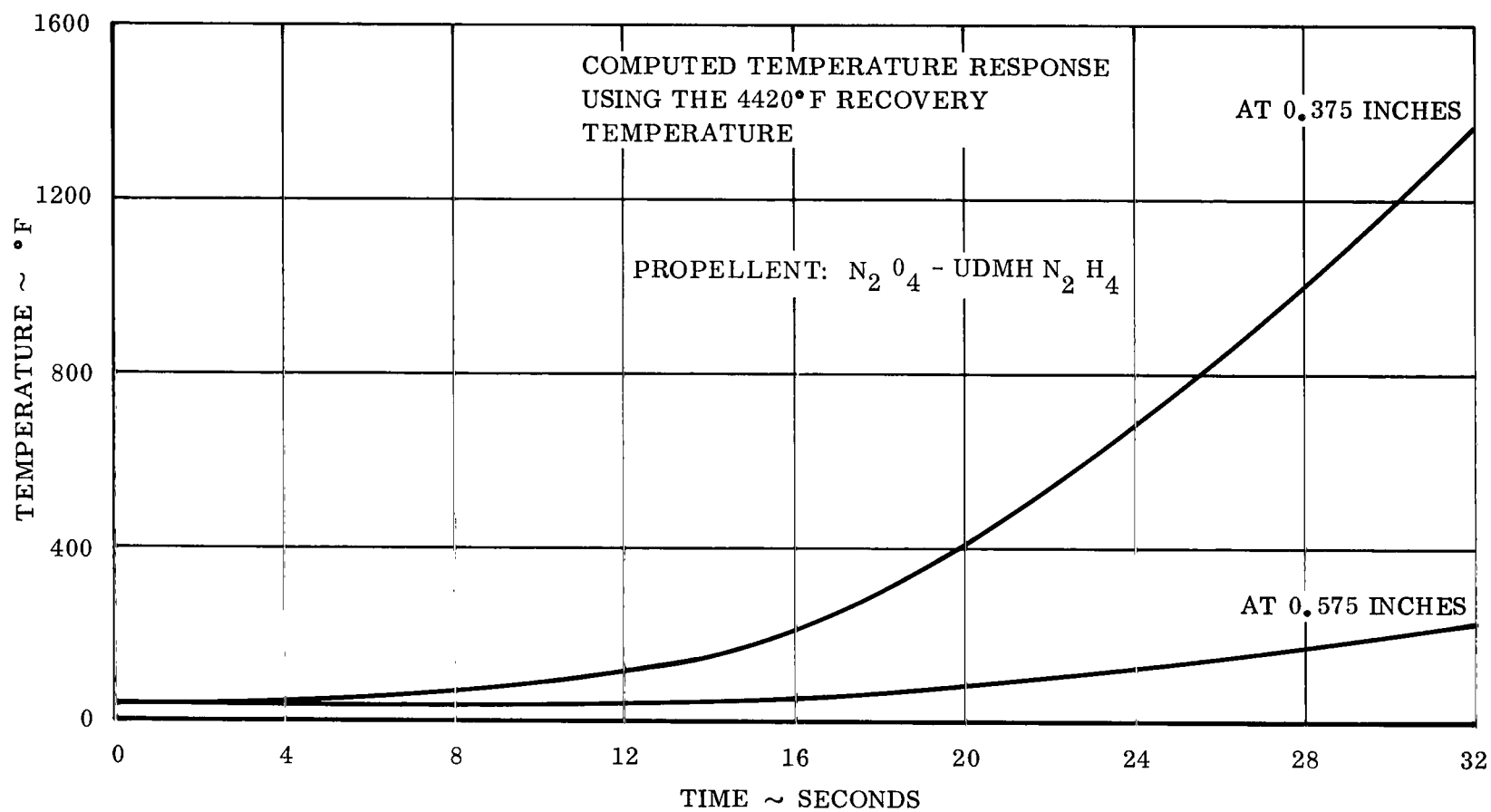


Figure G5. Temperature Response within Phenolic Nylon

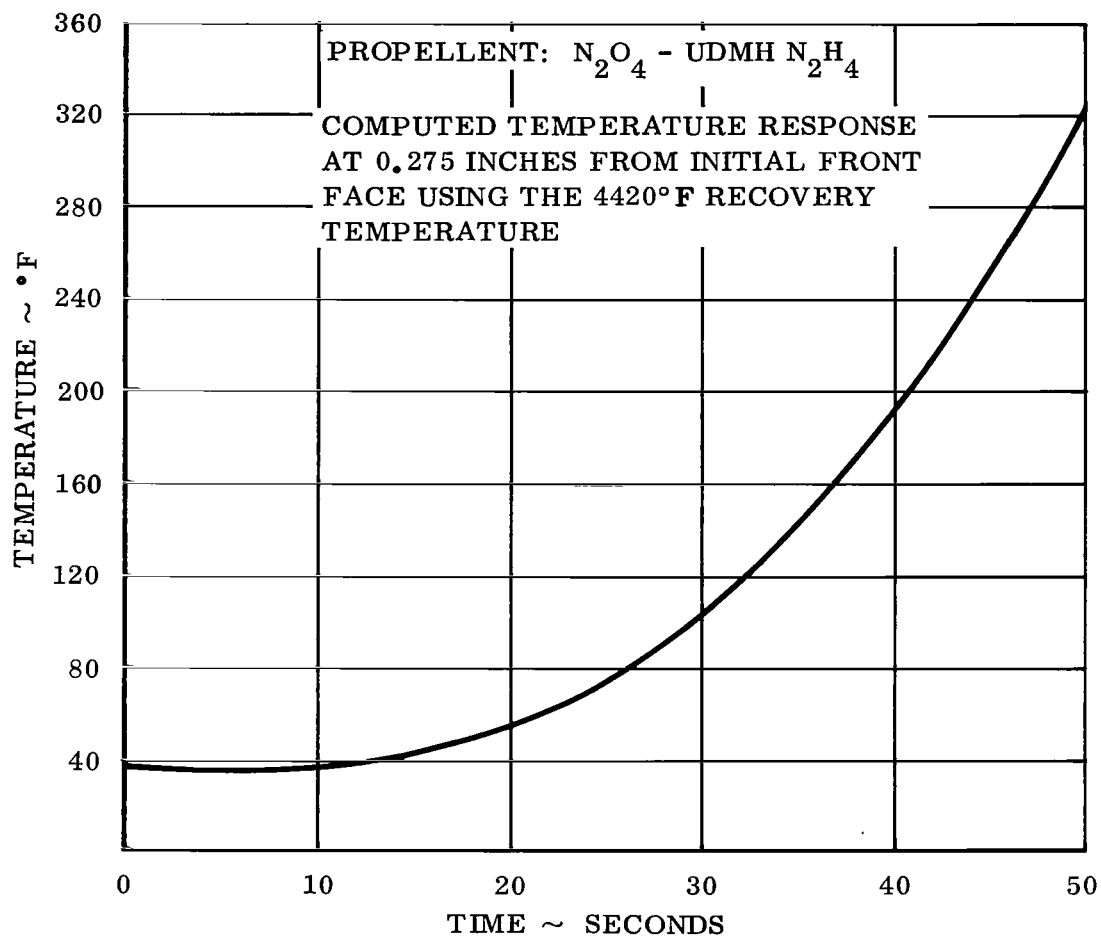


Figure G6. Temperature Response of Phenolic Nylon

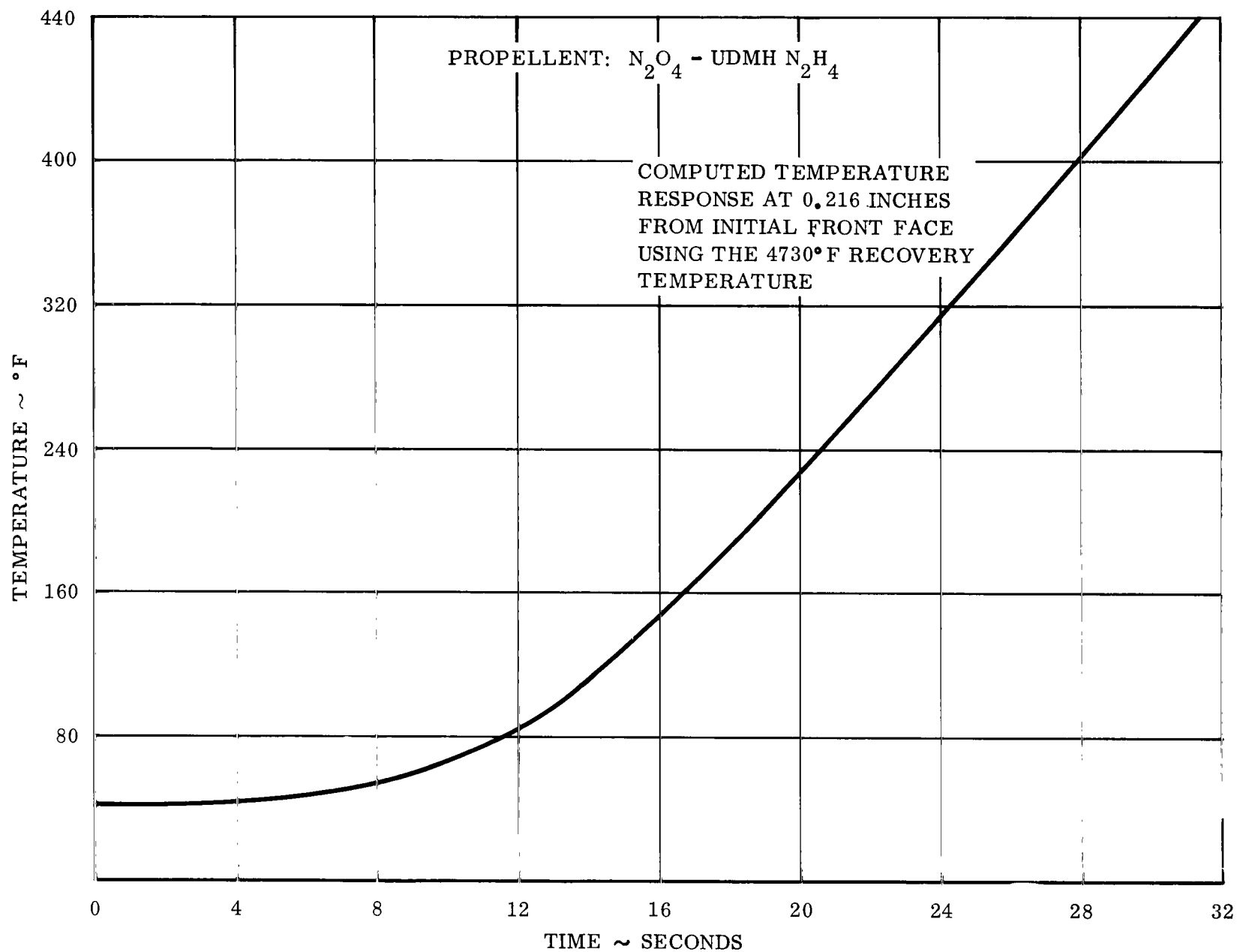


Figure G7. Temperature Response of Phenolic Silica

DISTRIBUTION LIST FOR FINAL REPORT, CR-54,257

Contract NAS 3-2566

"Ablative Materials Study for Rocket Engines"

General Electric Company

COPIES

National Aeronautics and Space Administration
Lewis Research Center
21000 Brookpark Road
Cleveland, Ohio 44135

Attn: Contracting Officer	1
Mail Stop 500-210	
Liquid Rocket Technology Branch	8
Mail Stop 500-209	
Technical Report Control Office	1
Mail Stop 5-5	
Technology Utilization Office	1
Mail Stop 3-16	
AFSC Liaison Office	2
Mail Stop 4-1	
Library	2

National Aeronautics and Space Administration
Headquarters
Washington, D.C. 20546

Attn: Henry Burlage, Jr.	4
--------------------------	---

Scientific and Technical Information Facility	25
NASA Representative, Code CRT	
P. O. Box 5700	
Bethesda, Maryland 20014	

Ames Research Center
Moffett Field, California 94035

Attn: Harold Hornby	2
Mission Analysis Division	

Goddard Space Flight Center
Greenbelt, Maryland 20771

Attn: Merland L. Moseson	2
Code 623	

Distribution List (Cont)

COPIES

Jet Propulsion Laboratory
California Institute of Technology
4800 Oak Grove Drive
Pasadena, California 91103

Attn: Robert F. Rose
Propulsion Div., 38

2

Langley Research Center
Langley Station
Hampton, Virginia 23365

Attn: Floyd L. Thompson
Director

2

Marshall Space Flight Center
Huntsville, Alabama 35812

Attn: Hans G. Paul
Code R-P&VED

2

Manned Spacecraft Center
Houston, Texas 77001

Attn: Robert R. Gilruth
Director (Code D)

2

Western Operations Office
150 Pico Boulevard
Santa Monica, California 90406

Attn: Robert W. Kamm
Director

2

Aeronautical Systems Division
Air Force System Command
Wright-Patterson Air Force Base
Dayton, Ohio 45433

Attn: D. L. Schmidt
Code ASRCNC-2

1

Distribution List (Cont)

COPIES

Air Force Missile Development Center
Holloman Air Force Base, New Mexico

Attn: Maj. R. E. Bracken
Code MDGRT

1

Air Force Missile Test Center
Patrick Air Force Base, Florida

Attn: L. J. Ullian

1

Air Force Systems Command, Dyna-Soar
Air Force Unit Post Office
Los Angeles 45, California

Attn: Col. Clark
Technical Data Center

1

Arnold Engineering Development Center
Arnold Air Force Station
Tullahoma, Tennessee

Attn: Dr. H. K. Doetsch

1

Bureau of Naval Weapons
Department of the Navy
Washington 25, D. C.

Attn: J. Kay
Code RTMS-41

1

Defense Documentation Center Headquarters
Cameron Station, Building 5
5010 Duke Street
Alexandria, Virginia 22314

Attn: TISIA

1

Headquarters, U. S. Air Force
Washington 25, D. C.

Attn: Col. C. K. Stambaugh
Code AFRST

1

Distribution List (Cont)

COPIES

Picatinny Arsenal
Dover, New Jersey 07801

Attn: I. Forsten, Chief
Liquid Propulsion Laboratory

1

Rocket Propulsion Laboratories
Edwards Air Force Base
Edwards, California 93523

Attn: Colonel J. Silk

1

U. S. Atomic Energy Commission
Technical Information Services
Box 62
Oak Ridge, Tennessee

Attn: A. P. Huber
Oak Ridge
Gaseous Diffusion Plant
(ORGDP) P. O. Box P

1

U. S. Army Missile Command
Redstone Arsenal, Alabama 35809

Attn: Dr. Walter Wharton

1

U. S. Naval Ordnance Test Station
China Lake
California 93557

Attn: W. F. Thorn
Code 4562
Chief, Missile Propulsion Division

1

Chemical Propulsion Information Agency
Applied Physics Laboratory
8621 Georgia Avenue
Silver Spring, Maryland 20910

Attn: Neil Safeer

1

Distribution List (Cont)

COPIES

Aerojet-General Corporation
P. O. Box 296
Azusa, California

Attn: L. F. Kohrs

1

Aerojet-General Corporation
P. O. Box 1947
Technical Library, Bldg. 2015, Dept. 2410
Sacramento, California 95809

Attn: R. Stiff

1

Aeronutronic
A Division of Ford Motor Company
Ford Road
Newport Beach, California

Attn: D. A. Carrison

1

Aerospace Corporation
2400 East El Segundo Boulevard
P. O. Box 95085
Los Angeles, California 90045

Attn: John G. Wilder
MS-2293
Propulsion Dept.

1

Arthur D. Little, Inc.
Acorn Park
Cambridge 40, Massachusetts

Attn: A. C. Tobey

1

Astropower, Inc., Subsidiary of
Douglas Aircraft Company
2968 Randolph Avenue
Costa Mesa, California

Attn: Dr. George Moc
Director, Research

1

Distribution List (Cont)

COPIES

Astrosystems, Inc.
1275 Bloomfield Avenue
Caldwell Township, New Jersey

Attn: A. Mendenhall

1

Atlantic Research Corporation
Edsall Road and Shirley Highway
Alexandria, Virginia

Attn: A. Scurlock

1

Beech Aircraft Corporation
Boulder Facility
Box 631
Boulder, Colorado

Attn: J. H. Rodgers

1

Bell Aerosystems Company
P. O. Box 1
Buffalo 5, New York

Attn: W. M. Smith

1

Bendix Systems Division
Bendix Corporation
Ann Arbor, Michigan

Attn: John M. Brueger

1

Boeing Company
P. O. Box 3707
Seattle 24, Washington

Attn: J. D. Alexander

1

Chrysler Corporation
Missile Division
Warren, Michigan

Attn: John Gates

1

Distribution List (Cont)

COPIES

Curtiss-Wright Corporation
Wright Aeronautical Division
Wood-ridge, New Jersey

Attn: G. Kelley

1

Douglas Aircraft Company, Inc.
Missile and Space Systems Division
3000 Ocean Park Boulevard
Santa Monica, California 90406

Attn: R. W. Hallet
Chief Engineer
Advanced Space Tech.

1

Fairchild Stratos Corporation
Aircraft Missiles Division
Hagerstown, Maryland

Attn: J. S. Kerr

1

General Dynamics/Astronautics
Library & Information Services (128-00)
P. O. Box 1128
San Diego, California 92112

Attn: Frank Dore

1

General Electric Company
Re-Entry Systems Department
P. O. Box 8555
Philadelphia, Pennsylvania 19101

Attn: F. E. Schultz

1

General Electric Company
Flight Propulsion Lab Department
Cincinnati 15, Ohio

Attn: D. Suichu

1

Grumman Aircraft Engineering Corp.
Bethpage
Long Island, New York

Attn: Joseph Gavin

1

Distribution List (Cont)

COPIES

Kidde Aero-Space Division
Walter Kidde and Company, Inc.
675 Main Street
Belleville 9, New Jersey

Attn: R. J. Hanville
Director of Research Engineering

1

Lockheed California Company
10445 Glen Oaks Boulevard
Pacoima, California

Attn: G. D. Brewer

1

Lockheed Missiles and Space Company
Attn: Technical Information Center
P. O. Box 504
Sunnyvale, California

Attn: Y. C. Lee

1

Lockheed Propulsion Company
P. O. Box 111
Redlands, California

Attn: H. L. Thackwell

1

The Marquardt Corporation
16555 Saticoy Street
Box 2013 - South Annex
Van Nuys, California 91409

Attn: Warren P. Boardman, Jr.

1

Martin Division
Martin Marietta Corporation
Baltimore 3, Maryland

Attn: John Calathes (3214)

1

Martin Denver Division
Martin Marietta Corporation
P. O. Box 179
Denver, Colorado 80201

Attn: J. D. Goodlette
Mail A-241

1

Distribution List (Cont)

COPIES

McDonnell Aircraft Corporation
P. O. Box 6101
Lambert Field, Missouri

Attn: R. A. Herzmark

1

North American Aviation, Inc.
Space & Information Systems Division
Downey, California

Attn: H. Storms

1

Northrop Space Laboratories
1001 East Broadway
Hawthorne, California

Attn: Dr. William Howard

1

Pratt & Whitney Aircraft Corp.
Florida Research and Development Center
P. O. Box 2691
West Palm Beach, Florida 33402

Attn: R. J. Coar

1

Radio Corporation of America
Astro-Electronics Division
Defense Electronic Products
Princeton, New Jersey

Attn: S. Fairweather

1

Reaction Motors Division
Thiokol Chemical Corporation
Denville, New Jersey 07832

Attn: Arthur Sherman

1

Republic Aviation Corporation
Farmingdale
Long Island, New York

Attn: Dr. William O'Donnell

1

Distribution List (Cont)

COPIES

Rocketdyne (Library Dept. 586-306)
Division of North American Aviation
6633 Canoga Avenue
Canoga Park, California 91304

Attn: E. B. Monteath

1

Space General Corporation
9200 Flair Avenue
El Monte, California

Attn: C. E. Roth

1

Space Technology Laboratories
Subsidiary of Thompson-Ramo-Wooldridge
One Space Park
Redondo Beach, California

Attn: G. W. Elverum

1

Stanford Research Institute
333 Ravenswood Avenue
Menlo Park, California 94025

Attn: Thor Smith

1

TAPCO Division
Thompson-Ramo-Wooldridge, Inc.
23555 Euclid Avenue
Cleveland 17, Ohio

Attn: P. T. Angell

1

Thiokol Chemical Corporation
Redstone Division
Huntsville, Alabama

Attn: John Goodloe

1

Distribution List (Cont)

COPIES

United Aircraft Corporation
Research Laboratories
400 Main Street
East Hartford, Connecticut 06108

Attn: Erle Martin

1

United Technology Center
587 Methilda Avenue
P. O. Box 358
Sunnyvale, California

Attn: B. Abelman

1

Vought Astronautics
Box 5907
Dallas 22, Texas

1

Itek Corporation
Vidya Division
1450 Page Mall Road
Palo Alto, California

Attn: R. Rindal

1



**GENERAL
ELECTRIC**

RE-ENTRY SYSTEMS DEPARTMENT

A Department of the Missile and Space Division

3198 CHESTNUT STREET, PHILADELPHIA 4, PA.